

**MULTIVALENT CYCLODEXTRIN RECEPTORS
IN SOLUTION AND AT SURFACES**

This research has been financially supported by the Council for Chemical Sciences of the Netherlands Organization for Scientific Research (NWO-CW), grant number 700.98.305. The research was carried out within the Supramolecular Chemistry and Technology group (SMCT), MESA⁺ Institute for Nanotechnology, University of Twente.

Publisher: Print Partners Ipskamp, Postbus 333, 7500 AH Enschede, the Netherlands,
<http://www.ppi.nl>

© Alart Mulder, Enschede, 2004

No part of this work may be reproduced by print, photocopy or any other means without permission in writing from the publisher.

ISBN 90-365-2042-8

MULTIVALENT CYCLODEXTRIN RECEPTORS IN SOLUTION AND AT SURFACES

PROEFSCHRIFT

ter verkrijging van
de graad van doctor aan de Universiteit Twente,
op gezag van de rector magnificus,
prof. dr. F. A. van Vught,
volgens besluit van het College voor Promoties
in het openbaar te verdedigen
op donderdag 6 mei om 15.00 uur

door

Alart Mulder

geboren op 15 september 1976
te Meppel

Dit proefschrift is goedgekeurd door:

Promotor: prof. dr. ir. D. N. Reinhoudt

Assistent-promotor: dr. ir. J. Huskens

Aan mijn ouders

Contents

Chapter 1

General introduction	1
1.1 References.....	3

Chapter 2

Multivalency and its role in cyclodextrin systems	5
2.1 Introduction	5
2.2 Multivalency	7
2.2.1 Definitions, nomenclature, and model systems	7
2.2.2 Intra- versus intermolecular binding	10
2.2.3 Effective concentration	12
2.2.3.1 Effective concentration and the mode of binding	12
2.2.3.2 Effective concentration and effective molarity	13
2.2.3.3 Effective concentration from probability functions	14
2.2.3.4 Effective concentration from geometric considerations	15
2.2.4 Thermodynamic aspects of intramolecular multivalency	18
2.2.4.1 Tether length and flexibility	18
2.2.4.2 Valency of the complexes	20
2.2.4.3 Examples of intramolecular multivalent interactions	21
2.2.5 Multivalency and cooperativity	22
2.2.6 Kinetic aspects of multivalent interactions	24
2.2.7 Multivalent interactions at surfaces	25
2.3 Multivalent cyclodextrin systems	27
2.3.1 Structure, physical properties, and complexation behavior of cyclodextrins	27
2.3.2 Cyclodextrin multimers	29
2.3.3 Cyclodextrin polymers	34
2.3.4 Cyclodextrin vesicles	35
2.3.5 Cyclodextrin particles	37
2.3.6 Cyclodextrin self-assembled monolayers	38
2.4 Conclusions	41
2.5 References and notes	42

Chapter 3

Photocontrolled release and uptake of a porphyrin guest by dithienylethene-tethered β -cyclodextrin host dimers..... 55

3.1 Introduction	55
3.2 Results and discussion	58
3.2.1 Synthesis and characterization of the CD dimers	58
3.2.2 Switching behavior of the CD dimers	61
3.2.3 UV-vis modeling	63
3.2.4 Complexation studies	65
3.2.5 Molecular modeling	70
3.2.6 Photo-triggered release and uptake	72
3.3 Conclusions	74
3.4 Experimental section	75
3.5 References and notes	80

Chapter 4

Bis(phenylthienyl)ethene-tethered β -cyclodextrin dimers as photo-switchable hosts 83

4.1 Introduction	83
4.2 Results and discussion	84
4.2.1 Synthesis and characterization of the CD dimers	84
4.2.2 Switching behavior of the CD dimers	87
4.2.3 Complexation studies	90
4.2.4 Photo-triggered release and uptake	94
4.3 Conclusions	95
4.4 Experimental section	96
4.5 References and notes	100

Chapter 5**Complexation of charged porphyrins by charged and metal-chelated EDTA-tethered β -cyclodextrin dimers: a thermodynamic study on the influence of tether charge and flexibility on binding affinity 103**

5.1 Introduction	103
5.2 Results and discussion	104
5.2.1 Synthesis and characterization of the CD dimers	105
5.2.2 Charged and metal-chelated CD dimers	106
5.2.3 Complexation studies	108
5.3 Conclusions	117
5.4 Acknowledgements	118
5.5 Experimental section	118
5.6 References and notes	120

Chapter 6**Divalent binding of a bis(adamantyl)-functionalized calix[4]arene to β -cyclodextrin-based hosts: an experimental and theoretical study on multivalent binding in solution and at self-assembled monolayers ... 123**

6.1 Introduction	123
6.2 Results and discussion	124
6.2.1 Design of the model system	124
6.2.2 Binding to CD substrates in solution	126
6.2.3 Binding at CD SAMs	132
6.2.4 Patterning of surfaces	139
6.3 Conclusions	141
6.4 Experimental section	142
6.5 References and notes	143

Chapter 7

Multivalent host-guest interactions at β -cyclodextrin monolayers on silicon oxide 147

7.1 Introduction 147

7.2 Results and discussion 148

7.2.1 Monolayer preparation 148

7.2.2 Synthesis of fluorescent guest molecules 150

7.2.3 Binding of the fluorescent wedges at the CD monolayers 154

7.2.4 Patterning of surfaces 156

7.3 Conclusions 161

7.4 Acknowledgement 162

7.5 Experimental section 162

7.6 References and notes 170

Summary 175

Samenvatting 181

Dankwoord 187

curriculum vitae 191

General introduction

The drive for miniaturization has pushed research to the nanometer scale, and nowadays a great deal of effort, time, and funding is devoted to nanotechnology. Nanotechnology involves the construction of devices with nanometer dimensions (1 - 100 nm) having specific functions that can be individually addressed and manipulated, and is expected to play a key role in for example future electronic devices¹ and high-density data storage.²

The discipline of supramolecular chemistry takes a unique place among the various research fields active in nanotechnology. Whereas most research areas use the concept of miniaturization of known, working devices to achieve operation at nanometer scales, supramolecular chemistry practices the opposite strategy as it exploits molecules - the world's smallest, defined species with characteristic features and functions - as building blocks for the construction of molecular devices. The past years have seen the first steps towards molecular machines,³ molecular motors,⁴ molecular wires,⁵ and molecular computers.⁶

Nature has billions of years of experience in the design and optimization of molecular machinery, and is a source of inspiration for supramolecular chemists. A clear example is the extensive use of self-assembly which, in analogy to Nature, is widely exploited in supramolecular chemistry for the design of defined and functional nanostructured multicomponent systems.⁷ One especially powerful self-assembly pathway that is common in Nature, but less purposefully applied in supramolecular chemistry, is multivalency. Multivalency denotes the use of multiple interactions between two molecules, which can result in very strong, yet reversible, binding.⁸

The research described in this thesis is aimed at the use of multivalent host-guest interactions in molecular devices and nanotechnological applications. The host-guest motifs employed in this research are based on cyclodextrin host-guest

interactions. Cyclodextrins constitute a family of host molecules that are able to complex a variety of hydrophobic guest molecules in aqueous media.⁹ The cyclodextrins are commercially available and synthetically versatile,¹⁰ and therefore readily implemented in molecular devices.¹¹ The utility of multivalent cyclodextrin host-guest interactions both in solution and at interfaces has been explored.

Chapter 2 presents a general overview on the characteristic features of multivalency. Particular attention is devoted to the role of multivalency in cyclodextrin-based assemblies.

In Chapters 3 to 5, the utility of multivalent cyclodextrin host-guest interactions in solution is described. Switchable tethers are used to link two cyclodextrin cavities in order to achieve tunable receptor molecules, the binding properties of which can be controlled by external stimuli. The switchable tethers are used to control the possible relative orientations of the two cyclodextrin cavities of the dimers and therewith the possible cooperation of the cavities in the multivalent binding of guest molecules.

In Chapter 3, photoswitchable dithienylethene tethers are employed to access cyclodextrin dimers, the binding properties of which can be tuned by irradiation with light. The photoswitching properties of these dimers are discussed together with the binding properties of the various accessible forms of the dimers, which have been studied with isothermal titration microcalorimetry and UV-vis spectroscopy.

Chapter 4 describes cyclodextrin dimers similar to those reported in Chapter 3 but with a larger photoswitchable bis(phenylthienyl)ethene tether. This larger tether has been used to achieve a more complete switching and to obtain larger differences in binding properties between the two forms of the dimers. The binding and photoswitching behavior of these dimers is compared to those of the dimers described in Chapter 3, and the role of the tether in binding guest molecules is discussed.

In Chapter 5, an ethylenediaminetetraacetate (EDTA) tether is used to access cyclodextrin dimers of which the binding properties can be tuned by metal coordination or protonation. The EDTA tether allows switching between four forms of a single dimer having different tether charges and flexibilities. Isothermal titration microcalorimetry studies with charged porphyrin guests have been performed to assess the influence of tether charge and flexibility on the binding properties of the dimers.

Chapters 6 and 7 describe the use of multivalent cyclodextrin host-guest interactions at interfaces. By means of multivalency, complexes of guest molecules at

cyclodextrin monolayers are formed that are sufficiently stable to be employed in supramolecular surface patterning. The cyclodextrin monolayers are used as molecular printboards at which patterns of assemblies can be created with the use of microcontact printing or dip-pen nanolithography.

In Chapter 6, the divalent binding of a guest molecule to cyclodextrin self-assembled monolayers on gold is compared to the divalent binding with a cyclodextrin dimer in solution in order to get a fundamental understanding of multivalent interactions at interfaces. A theoretical model is presented to explain the significant differences in binding strength found for these interactions. Microcontact printing and dip-pen nanolithography have been employed to create patterns of multivalent guests at these cyclodextrin monolayers. These patterns have been subjected to various rinsing procedures in order to demonstrate the concept of molecular printboards.

Chapter 7 describes cyclodextrin monolayers on silicon oxide, which have been developed to enable the use of fluorescence microscopy for the study of multivalent interactions at these interfaces. Various monolayer characterization techniques and binding studies with multivalent fluorescent guests have been employed to elucidate the packing and orientation of the cyclodextrin cavities at the monolayers, and these results have been used for correlation with the cyclodextrin self-assembled monolayers on gold. Several fluorescent multivalent guests have been used in patterning experiments to demonstrate the versatility of the molecular printboard.

1.1 References

¹ a) Service, R. F. *Science* **2001**, *294*, 2442-2443. b) Gittins, D. I.; Bethell, D.; Schiffrin, D. J.; Nichols, R. J. *Nature* **2000**, *408*, 67-69. c) Collier, C. P.; Mattersteig, G.; Wong, E. W.; Luo, Y.; Beverly, K.; Sampaio, J.; Raymo, F. M.; Stoddart, J. F.; Heath, J. R. *Science* **2000**, *289*, 1172-1175.

² a) Irie, M.; Kobatake, S.; Horichi, M. *Science* **2001**, *291*, 1769-1772. b) Lutwyche, M. I.; Despont, M.; Drechsler, U.; Dürig, U.; Häberle, W.; Rothuizen, H.; Stutz, R.; Widmer, R.; Binnig, G. K.; Vettiger, P. *Appl. Phys. Lett.* **2000**, *77*, 3299-3301. c) Mizutani, W.; Ishida, T.; Tokumoto, H. *Langmuir* **1998**, *14*, 7197-7202.

³ Balzani, V.; Credi, A.; Raymo, F. M.; Stoddart, J. F. *Angew. Chem. Int. Ed.* **2000**, *39*, 3348-3391.

⁴ Feringa, B. L. *Acc. Chem. Res.* **2001**, *34*, 504-513.

⁵ a) Cacialli, F.; Wilson, J. S.; Michels, J. J.; Daniel, C.; Silva, C.; Friend, R. H.; Severin, N.; Samori, P.; Rabe, J. P.; O'Connell, M. J.; Taylor, P. N.; Anderson, H. L. *Nature Mat.* **2002**, *1*, 160-164. b) Joachim, C.; Gimzewski, J. K.; Aviram, A. *Nature* **2000**, *408*, 541-548.

⁶ a) Clarck, S. M.; Konermann, L. *Biophys. J.* **2000**, *78*, 257. b) Dirk, S. M.; Price, D. W.; Chanteau, S.; Konsynkin, D. V.; Tour, J. M. *Tetrahedron* **2001**, *57*, 5109-5121. c) Ji, S. *Biosystems* **1999**, *52*, 123-133.

⁷ a) Kerckhoffs, J. M. C. A.; Van Leeuwen, F. W. B.; Spek, A. L.; Kooijman, H.; Crego-Calama, M.; Reinhoudt, D. N. *Angew. Chem. Int. Ed.* **2003**, *42*, 5717-5722. b) Kusukawa, T.; Fujita, M. *J. Am. Chem. Soc.* **2002**, *124*, 13576-13582. c) Special Issue "Supramolecular Chemistry and Self-Assembly": *Science* **2002**, *295*, 2400-2421. d) Special Issue "Nanostructures": Chandross, E. A.; Miller, R. D. *Chem. Rev.* **1999**, *99*, 1644-1990. e) Philp, D.; Stoddart, J. F. *Angew. Chem. Int. Ed. Engl.* **1996**, *35*, 1155-1196.

⁸ Mammen, M.; Choi, S.-K.; Whitesides, G. M. *Angew. Chem. Int. Ed.* **1998**, *37*, 2754-2794.

⁹ a) Special Issue "Cyclodextrins": D'Souza, V. T.; Lipkowitz, K. B. *Chem. Rev.* **1998**, *98*, 1741-2076. b) Szejtli, J. *Cyclodextrin Technology*, Kluwer Academic Publisher: Dordrecht, the Netherlands, **1988**.

¹⁰ a) Easton, C. J.; Lincoln, S. F. *Modified Cyclodextrins*, 1st ed., Imperial College Press: London, **1999**. b) Kahn, A. R.; Forgo, R.; Stine, K. J.; D'Souza, V. T. *Chem. Rev.* **1998**, *98*, 1977-1996.

¹¹ Harada, A. *Acc. Chem. Res.* **2001**, *34*, 456-464.

Multivalency and its role in cyclodextrin systems

2.1 Introduction

The combination of multiple interactions between two non-covalently interacting species can result in an overall interaction strength that is much stronger than that of a monovalent, i.e. single, interaction. This phenomenon is generally referred to as multivalency and is widely applied to overcome the inherently low binding affinities associated with monovalent interactions.¹ Some striking examples^{2,3} are given in Figure 2.1.

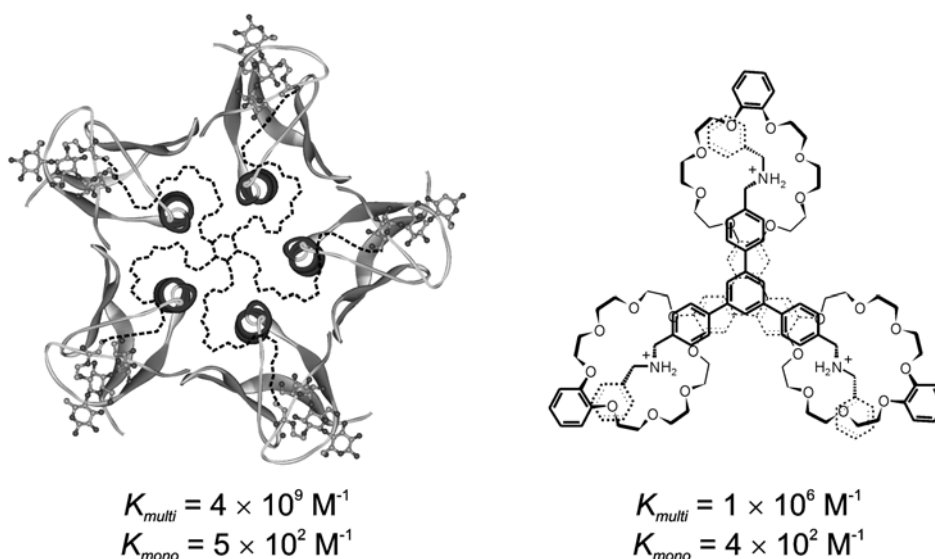


Figure 2.1 Multivalent and corresponding monovalent association constants: crystal structure of the pentavalent complex of cholera toxin and a synthetic inhibitor (left),² and a trivalent complex formed between a trivalent crown ether and a matching trivalent ammonium guest (right).³

Multivalent interactions are ubiquitous in biological processes⁴ and play a crucial role in events that determine microbial virulence,⁵ inflammation,^{6,7} and host immune responses.^{8,9} In analogy with Nature, multivalent interactions are used within the field of biochemistry to inhibit (antagonize) undesired biological processes and promote or effect (agonize) desired ones.¹ A variety of multivalent inhibitors has been synthesized for various lectins and viruses, including for example the influenza virus,^{10,11,12} and the cholera^{2,13,14} and anthrax toxin.¹⁵

In supramolecular chemistry, multivalency is employed for the self-assembly of defined multi-component architectures with high stability,¹⁶ for nano-construction,¹⁷ and for the strong, highly selective binding of guest molecules by multivalent hosts. Several representative examples of multivalency applied in supramolecular chemistry are depicted in Figure 2.2.

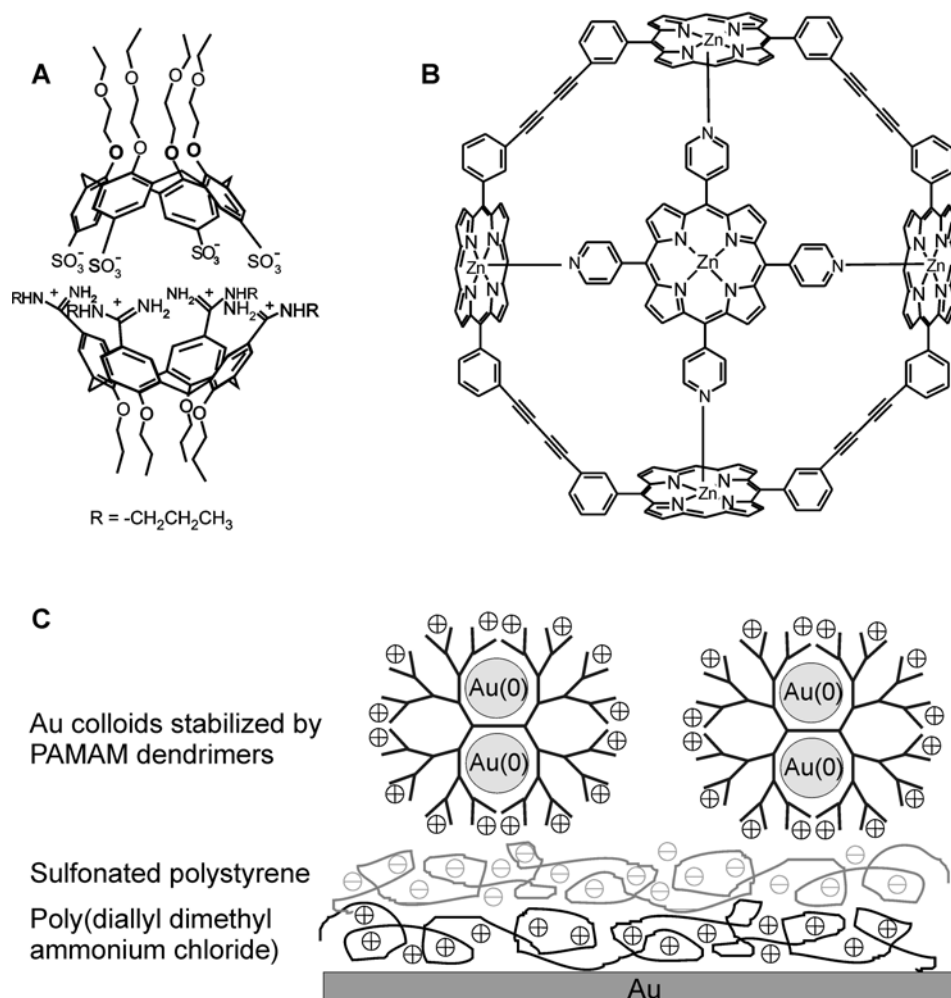


Figure 2.2 Multivalency applied in supramolecular chemistry: molecular capsule formed by multivalent ionic interactions (A),¹⁸ high affinity tetravalent complex (B),¹⁹ and nanoconstruction using layer-by-layer deposition (C).²⁰

The extensive application of multivalency arises from the thermodynamic and kinetic characteristics associated with multivalent interactions. However, despite the general use of multivalency, multivalent interactions and the thermodynamic and kinetic aspects governing them are poorly understood. The first part of this chapter reviews the fundamental aspects and characteristic features of multivalent interactions. The second part is devoted to recent examples of multivalent cyclodextrin assemblies and discusses studies exemplifying functional applications of multivalent hydrophobic interactions, including (tunable) cyclodextrin-based receptors and the positioning of molecules at cyclodextrin surfaces, the two main topics of this thesis.

2.2 Multivalency

2.2.1 Definitions, nomenclature, and model systems

Multivalency denotes the simultaneous binding of multiple functionalities on one entity, which can be anything from a molecule to a surface, with multiple complementary functionalities on a second entity. In biochemistry, the two functionalities participating in the multivalent interaction are generally referred to as receptor and ligand. In supramolecular chemistry the terms host and guest are generally used, and these terms will also be used when possible throughout this chapter to denote the interacting functionalities. The interaction between a host and a guest leads to the formation of a complex.

The valency of an entity is the number of separate connections of the same kind that it can form through host-guest interactions with entities bearing the complementary functionality. The number of shared interactions between two entities defines the valency of the complex (see Figure 2.3). The term monovalent refers to a single functionality or interaction. All interactions involving more than one host-guest interaction are generally considered to be multivalent. Polyvalency is used for higher-order species and interactions.

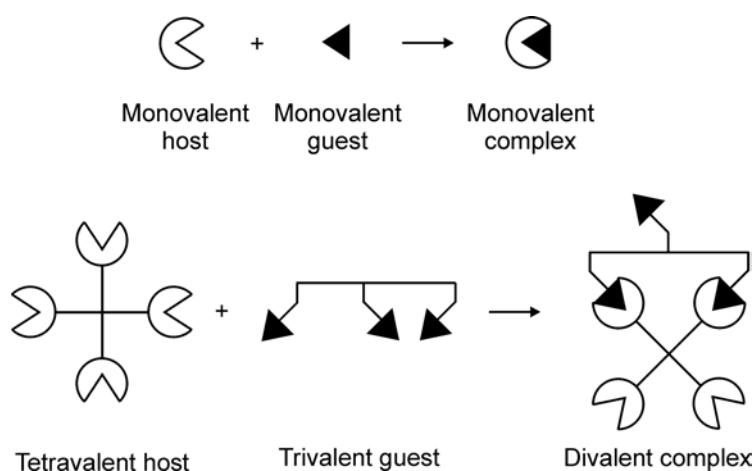


Figure 2.3 Terminology of valencies.

Multivalency is a widely studied topic, especially within the field of biochemistry, where numerous model systems with varying guest topologies have been studied.²¹⁻²⁷ Figure 2.4 gives an overview of the type of scaffolds used to study multivalency. The enormous amount of work on multivalent interactions conducted within the field of biochemistry offers a wealth of information. These biochemical studies generally involve synthetic multivalent guests in combination with naturally occurring multivalent hosts. The guest moiety in these studies is typically a saccharide unit, which is specifically recognized by a naturally occurring multivalent host, mostly proteins. Extensively studied systems include the influenza virus,¹⁰⁻¹² toxins,^{2,13,14} lectins,^{28,29} and selectins.³⁰ In the following sections several examples of these model systems, together with a number of supramolecular systems specifically designed to study multivalency, will be reviewed to illustrate the characteristic features of multivalent interactions.

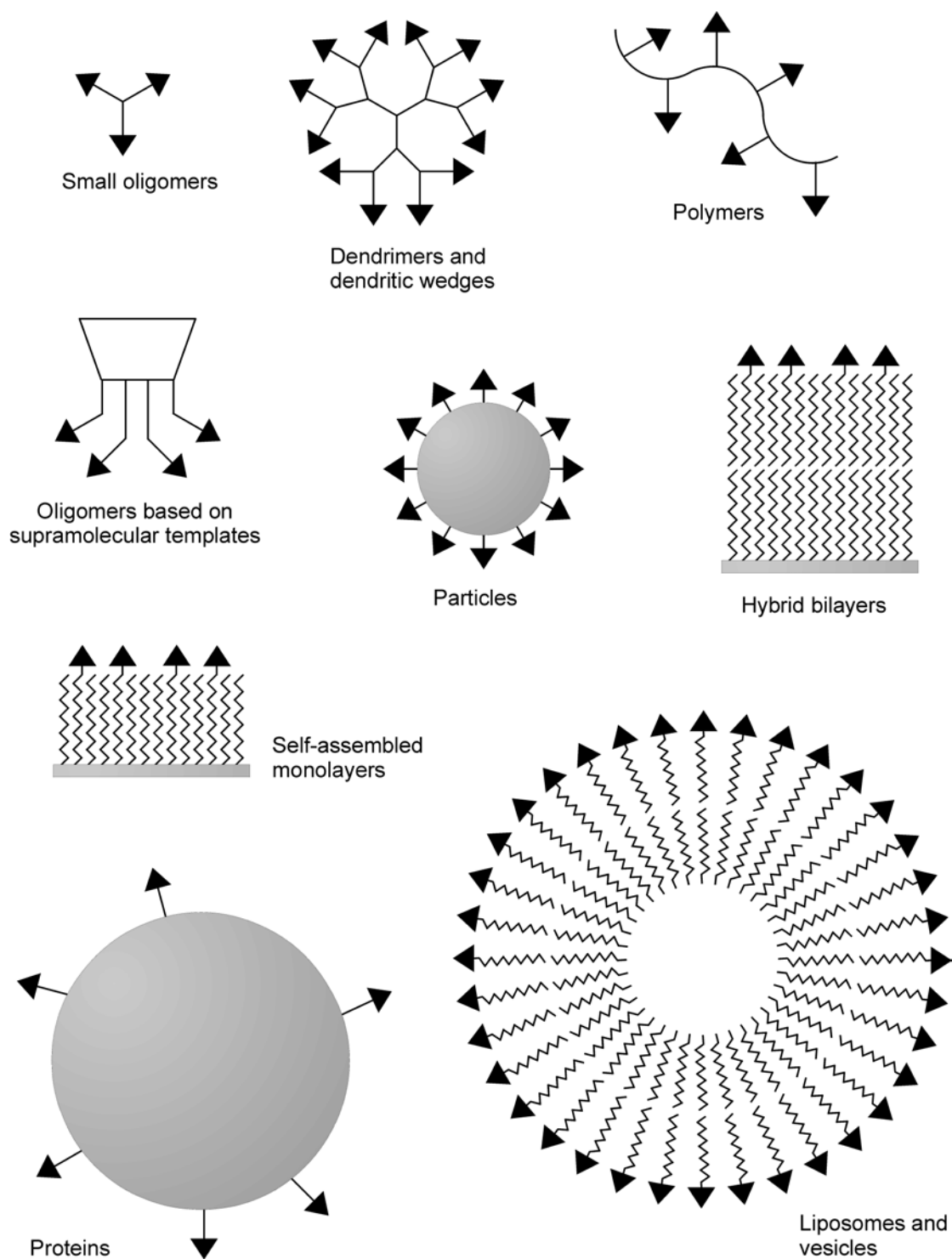


Figure 2.4 Overview of model systems used to study multivalency: small oligomers,^{27,31,32} dendrimers^{33,34} and dendritic wedges,^{33,35,36} polymers,³⁷ supramolecular oligomers,^{38,39,40} particles,^{41,42,43} hybrid bilayers,^{44,45} self-assembled monolayers,^{46,47} proteins,^{25,48} and liposomes.^{49,50,51}

2.2.2 Intra- versus intermolecular binding

There are many ways in which a multivalent guest can bind a multivalent host. Besides intramolecular binding, multivalent guests can also bind multivalent hosts in an *intermolecular* fashion (see Figure 2.5). Intermolecular binding potentially leads to the formation of large aggregates that often precipitate from solution.⁵² Binding does not necessarily have to follow a single pathway, i.e. combinations of intra- and intermolecular binding are also possible.

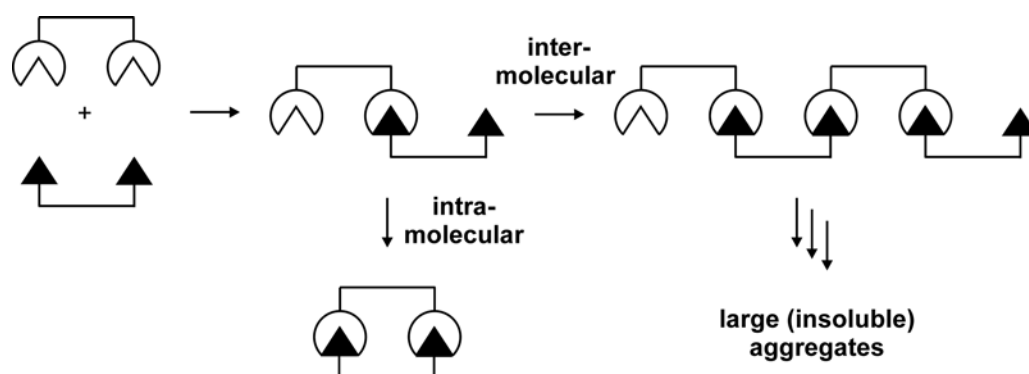


Figure 2.5 Intra- and intermolecular binding.

It is not always straightforward to discriminate between intra- and intermolecular binding, and great care should be taken when interpreting multivalent binding studies. As mentioned above, intramolecular binding typically leads to relatively high association constants with respect to monovalent binding. This is in contrast to intermolecular binding for which association constants can be expected to be comparable to those of the corresponding monovalent interactions. However, precipitation and aggregation have a strong influence on the outcome of the binding affinity. Extensive cross-linking leads to decreased dissociation rates and consequently to apparent binding enhancement. Furthermore, a diminished solubility of the complex also contributes to the overall equilibrium, and kinetic effects arising from irreversible precipitation are coupled to apparent binding energies. As a consequence, intermolecular binding can also give relatively high apparent association constants.⁵³

The groups of Toone and Brewer have demonstrated that calorimetric experiments can give an indication of the mode of binding for the interaction of Concanavalin A and multivalent small oligovalent saccharide guests.^{54,55} Calorimetry

allows the direct determination of the association constant and the enthalpy of binding (ΔH°) from which the entropy of binding (ΔS°) can be calculated, thus providing a complete thermodynamic picture of the interactions. Intramolecular binding generally showed additivity for the enthalpy term, whereas intermolecular interactions generally led to substantially diminished binding enthalpies and large positive entropy values.⁵⁵ Whether this is a general phenomenon for multivalent interactions remains questionable (for more information on the thermodynamics of multivalent interactions, see section 2.2.4).

Several factors determine whether binding occurs intra- or intermolecularly. One of these is the architecture, i.e. the size and shape, of the multivalent entities.⁵⁶ Self-assembled and hybrid monolayers, systems in which the host or guest functionalities are arranged in a two-dimensional plane, are prone to intramolecular binding. On the other hand, combinations of small, relatively rigid, three-dimensional entities such as particles and dendrimers are susceptible to intermolecular binding.^{57,58} The same holds for many biological hosts. Concanavalin A, for example, is a small protein with potentially four binding sites in four opposite directions and is typically bound intermolecularly by multivalent guests.^{54,55,59,60} In contrast, bacterial toxins are particularly suited for binding guests intramolecularly. Unlike most lectins, the bacterial toxins direct all five binding sites along a single axis. Additionally, specific toxins, such as the Shiga-like toxin, are unusually small, with intersite distances between host domains as small as 10 Å.⁶¹

Compatible spacing between guests on one side and hosts on the other is another important aspect that governs the mode of binding. Sufficient tether length between the binding functionalities is of paramount importance, particularly if one of the two is scaffolded on a rigid platform. The vast majority of multivalent guests studied for multivalent interactions with biological host molecules, which are typically relatively rigid structures with host sites spaced at demanding distances, have an insufficient spacer length and therefore bind intermolecularly.⁵³

Besides these obvious geometrical factors, the mode of binding is strongly dependent on the concentration of the two entities. An illustrative example is the concentration dependent self-assembly of pseudorotaxanes reported by Gibson and co-workers.⁶² The pseudorotaxanes in this study consisted of bis(crown ethers) and divalent cationic guest molecules, both with variable tether lengths between the

binding functionalities. At low concentrations and at a stoichiometric ratio of the two molecules, mainly intramolecular binding was observed, whereas at higher concentrations linear polymers were formed as a result of intermolecular binding. This concentration-dependent mode of binding is a well-known phenomenon for multivalent interactions and can be explained in terms of effective concentration, a term that will be discussed in more detail in the following section.

2.2.3 Effective concentration

2.2.3.1 Effective concentration and the mode of binding

The effective concentration represents a probability of interaction between two reactive or complementary interlinked entities and symbolizes a “physically real” concentration of one of the reacting or interacting functionalities as experienced by its complementary counterpart. The first interaction of a multivalent guest with a multivalent host alters the guest site concentration as experienced by the neighboring host site. If this so-called effective concentration is higher than the actual guest site concentration in solution, intramolecular (multivalent) binding is favored (see Figure 2.6). If the guest site concentration in solution is higher than the effective concentration experienced by the host site the binding will most likely proceed in an intermolecular fashion.

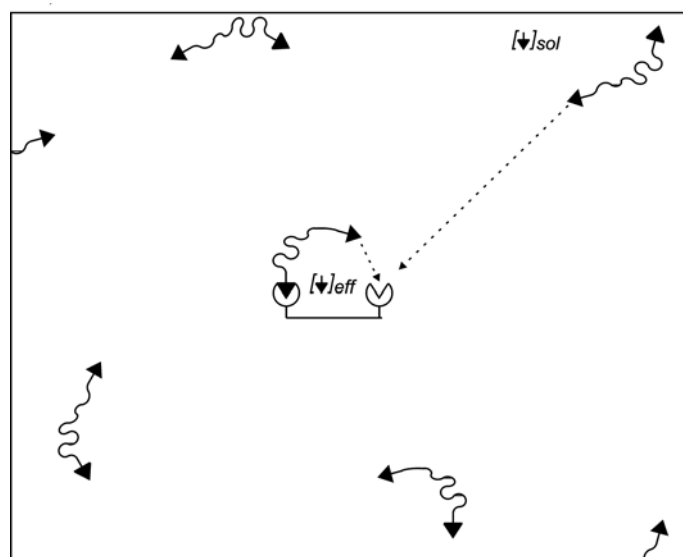


Figure 2.6 Schematical representation of the effective guest site concentration $[\blacktriangledown]_{\text{eff}}$ in a solution with guest site concentration $[\blacktriangledown]_{\text{sol}}$, demonstrating the increased probability of interaction for intramolecular binding events and the concept of effective concentration.

The concept of effective concentration gives rise to a concentration-dependent binding mode for multivalent interactions and this phenomenon has been observed for several multivalent systems, the study of Gibson on pseudorotaxanes discussed above being one of them.^{62,63} Similar reasoning might also explain the concentration-dependent aggregation behavior for the interaction between an oligo(ethylene glycol)-tethered divalent sialoside guest and hemagglutinin, one of the host sites of the influenza virus, observed by Knowles and co-workers.^{64,65} Light-scattering indicated that the guest bound hemagglutinin intramolecularly below 2.0 mM, whereas above this concentration aggregation was observed. This value of 2.0 mM coincides with the effective concentration for the divalent interaction for this specific guest (for calculation of the effective concentration, see below).

2.2.3.2 *Effective concentration and effective molarity*

Effective concentration is conceptually similar to the more generally used *effective molarity*.⁶⁶ Whereas effective concentration is based on concentrations calculated from physical geometries of complexes, effective molarity denotes the ratio of intra- and intermolecular rate or association constants.⁶⁶ The use of the latter term is well-established, and effective molarity has been applied to indicate the ease of cyclization reactions,^{67,68} feasibility of the self-assembly of defined multi-component systems,^{69,70} and as a measure for affinity enhancement using multivalent interactions.^{19,71,72} For an intramolecular n -valent interaction with an association constant K_n , the effective molarity (EM) is given by Equation 1.

$$EM = \left(\frac{K_n}{(K_{mono})^n} \right)^{1/(n-1)} \quad (1)$$

In contrast to the generally used effective molarity, effective concentration is used only scarcely. This is inherent to the difficulties associated with the correct determination of the latter term. Recently, several approaches for the approximation of effective concentrations have been published, and these are discussed in the remainder of this section.

2.2.3.3 Effective concentration from probability functions

One way of calculating the effective concentration (C_{eff}) is by using probability functions. This approach originates from the field of polymer chemistry. In 1934 Kuhn reported a formula for the cyclization probability of two intramolecularly linked chain ends based on random walk statistics and probability functions.⁷³ From this formula, Winnik derived an expression for the effective concentration (Equations 2 and 3), which denotes the presence of two chain ends within an infinitely small volume.⁷⁴

$$C_{eff} = \frac{\beta^3}{N_{AV}\pi^{3/2}} \quad (2)$$

with:

$$\beta = \left(\frac{3}{2nl^2} \right)^{1/2} \quad (3)$$

In these expressions, N_{AV} is Avogadro's number, n the number of repeating segments in the chain, and l the length of the repeating segment.

Recently, Lees and co-workers expanded this methodology of effective concentration to the use in multivalent interactions.¹⁴ Equation 2 was modified to account for host sites spaced at a specific distance, d , to give the expression given in Equation 4.

$$C_{eff}(d) = \frac{\beta^3}{N_{AV}\pi^{3/2}} e^{-\beta^2 d^2} \quad (4)$$

From Equation 4, in combination with Equation 3, optimized values for C_{eff} were calculated, i.e. assuming that the guests are spaced by a tether of optimum length equal to the distance spacing the host sites. Subsequently, these values for C_{eff} were used to approximate the association constant of multivalent interactions. It was shown that this methodology gave a good correlation between experimental and theoretical results for the binding affinity of a trisaccharide-modified polymer with Shiga-like toxins, and a variety of other examples taken from literature.¹⁴ Although the model developed by Lees is suitable for an approximation of the effective concentration and

association constant of multivalent interactions, it is restricted to systems with equivalent host sites spaced at a fixed distance in combination with guests tethered by flexible linkers having an optimal linker length.

It is evident that the empirical rules discussed above are less applicable to short tethers of irregular structure. In order to evaluate the effective concentrations for systems with relatively small numbers of atoms, Kitov and co-workers developed a straightforward method based on molecular dynamics simulations.⁷⁵ Their study involved a single host unit of a Shiga-like toxin, which has multiple binding sites, and a series of divalent guest molecules with different tether lengths and flexibilities. By conformational analysis of monovalently bound guest species, radial probability functions were generated, which gave the probability that the pendent guest site is situated at a specific distance range from the bound guest site. The radial probabilities of the pendent guest site being located at a distance equal to the spacing of the two host sites at the toxin sub-binding site were used to compare the binding efficiencies of the different guest molecules. The divalent guest molecules that gave the highest theoretical binding probability, i.e. the highest effective concentration, calculated by this model were found to bind the toxin sub-unit with the highest affinity.

This computational approach probably gives an accurate estimation of the effective concentration. However, the application of this methodology requires detailed structural information on the multivalent entities involved and demands considerable computing time.

2.2.3.4 Effective concentration from geometric considerations

An alternative approach for the calculation of the effective concentration considers the physically real concentration of the host or guest functionality within the probing volume of its complementary counterpart (Figure 2.7).^{66,76} This methodology for the calculation of the effective concentration is readily applicable. However, the calculated value for the effective concentration is again a crude estimate of the actual effective concentration as the model assumes that the probability of an interaction is uniformly distributed within the probing volume of the uncomplexed functionality. Nevertheless, in several studies this approach has been successfully used to support experimental data.^{13,76}

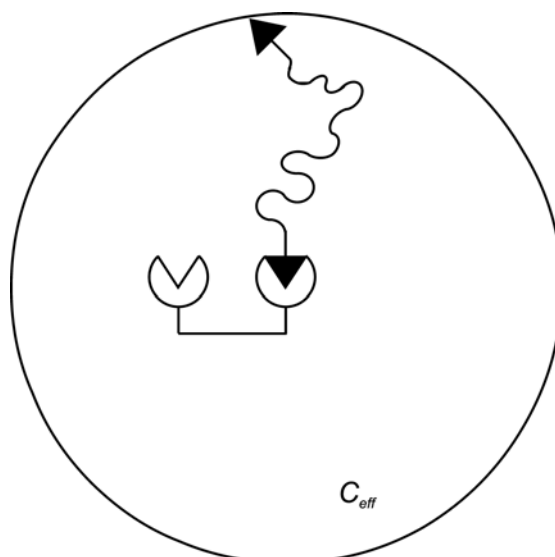


Figure 2.7 Effective concentration for a rigid divalent host and a flexible divalent guest based on geometrical considerations. The pendent guest site is able to probe available host sites within a sphere from which it can not escape.

Kramer and Karpen showed that the methodology is useful both as a descriptive and predictive tool.⁷⁶ By systematically changing the linker length of a divalent, poly(ethylene glycol)-linked guest molecule containing two cyclic nucleotides (cGMP), they determined a chain-length dependent response enhancement for cyclic-nucleotide-gated channels situated at protein surfaces. The maximum enhancement was obtained for a divalent guest spaced by a polymer chain for which the effective length, i.e. the average end-to-end distance between the two guest sites (\bar{r}_0), coincided with the spacing of two host sites. Both shorter and longer chains gave less strong responses, consistent with the concept of effective concentration (Figure 2.8). Effective concentrations were calculated using Equation 5.⁷⁷

$$C_{eff} = \frac{3}{2\pi\bar{r}_0^3 N_{AV}} \quad (5)$$

Additionally, Kramer and Karpen used the set of divalent guests and the concept of effective concentration for the approximation of the spacing between two cGMP host sites on cGMP-dependent protein kinase, a protein the crystal structure of which had not been determined at that moment. The spacing between two host sites,

determined from the effective tether length of the strongest binding divalent guest molecule, was in line with estimates given in previous publications.⁷⁶

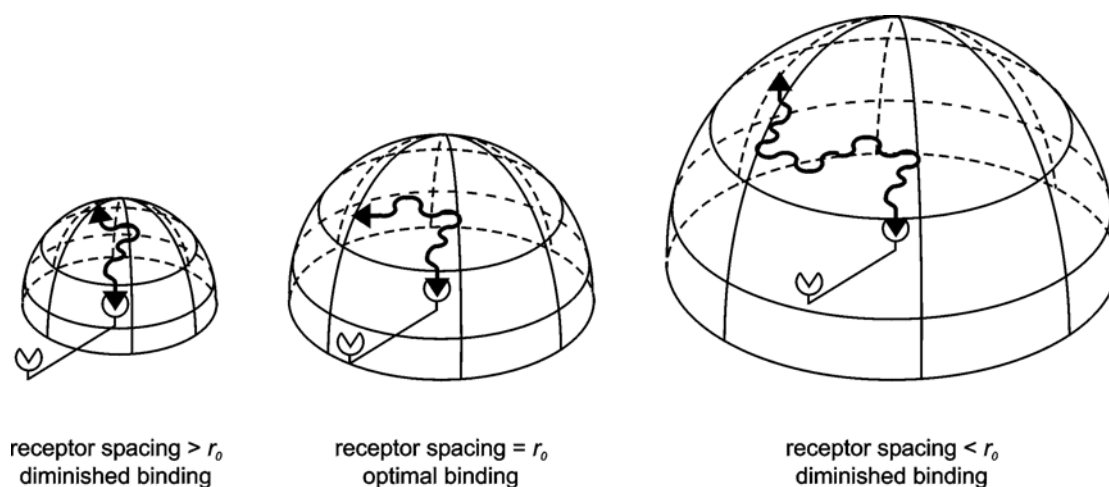


Figure 2.8 Relation between effective concentration and binding affinities as proposed by Kramer and Karpen.⁷⁶ Probing volumes constitute only half a sphere as the interactions take place at a protein surface.

A similar methodology has been followed by Fan and co-workers for the development of penta- and decaivalent inhibitors for the *Escherichia coli* heat-labile toxin, a close relative of the cholera toxin.¹³ Increasing binding affinities were found with increasing tether lengths between the saccharide guest sites. Unfortunately, solubility problems with intermediates in the synthesis of inhibitors with longer spacers limited the number of tether lengths studied and prevented the validation of the optimal spacer length.

Although the use of effective concentration in multivalent interactions has not been applied extensively (yet), the studies outlined above illustrate its efficacy. Effective concentration governs the efficiency of an intramolecular interaction and therewith the mode of binding, i.e. intra- versus intermolecular binding. High effective concentrations give rise to intramolecular multivalent interactions, and lead to the formation of well-defined complexes and structures. Low effective concentrations cause intermolecular binding and polymerization of host and guest species. The following sections are devoted to true multivalency, i.e. intramolecular multivalent interactions, the type of interaction of interest for the work described in this thesis.

2.2.4 Thermodynamic aspects of intramolecular multivalency

As discussed in the previous section, exclusive intramolecular binding can be achieved by proper design of the multivalent entities (architecture and tether compatibility) and experimental setup (concentration). This section will discuss the thermodynamic aspects of intramolecular multivalency in more detail.

The efficiency and strength of an intramolecular interaction is reflected by the free energy of binding, ΔG° . The free energy of binding is constituted of the enthalpy and entropy of binding. The enthalpy of binding, ΔH° , reflects the heat effect of interaction between guest and host and is typically proportional to the number of interactions between two multivalent entities. The entropy of binding, ΔS° , reflects the changes in degrees of freedom upon complex formation and is often divided into a number of terms such as conformational entropy, translational entropy, and rotational entropy. Hereafter the most important parameters governing intramolecular multivalent interactions will be discussed in terms of ΔH° and ΔS° .

2.2.4.1 Tether length and flexibility

The importance of tether length and flexibility has been addressed on several occasions in the previous sections with respect to the binding mode, i.e. inter- versus intramolecular binding. Tether length and flexibility also strongly influence the efficiency of intramolecular binding. Figure 2.9 illustrates the effects of tether length and flexibility on the enthalpy and entropy of binding for a divalent interaction.

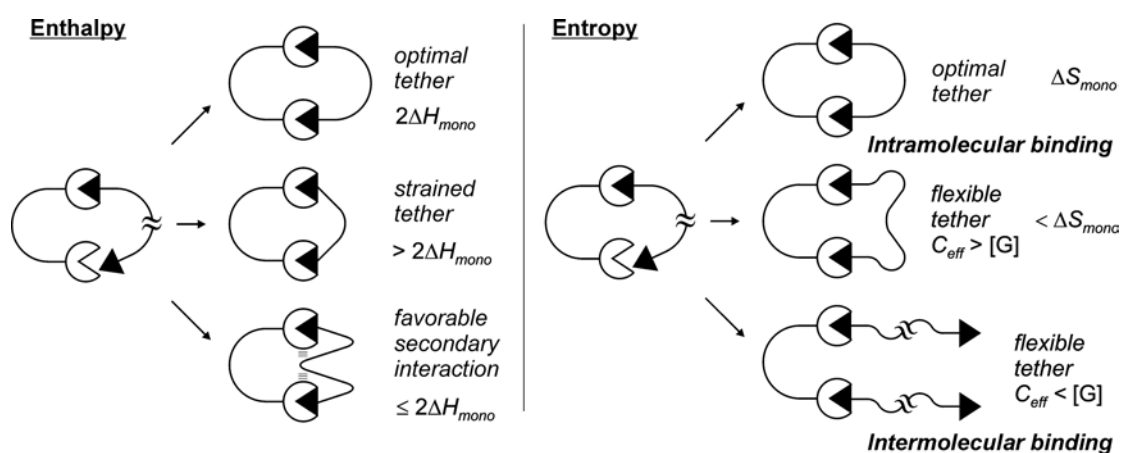


Figure 2.9 The role of tether length and rigidity with respect to the thermodynamics of multivalent interactions.

For many interactions, ΔH° is the main contributor to ΔG° . For this reason it is of the utmost importance that the flexibility and length of the tether enable unhindered binding of the guest sites by the host sites. Too short tethers may result in non-optimal conformations and tether strain giving rise to less favorable ΔH° values. The same holds for too rigid spacers. The use of conformationally rigid tethers is prone to give enthalpically diminished binding, unless the geometric fit between guests and hosts is accurate at a picometer scale, which is exceedingly rare. Knowles et al. synthesized a series of divalent sialoside acid guests linked via tethers of different length and conformational flexibility for the interaction with hemagglutinin.^{64,65} None of the guests tethered via rigid piperazine-based spacers showed enhanced binding affinity over the corresponding monovalent guests, whereas the guests tethered via conformationally flexible ethylene glycol or glycine units showed enhanced binding dependent on the length of the tether.

Secondary interactions between (the tethers of) two entities also contribute to the enthalpy of binding. Favorable van der Waals interactions, for example, may lead to more exothermic enthalpies. These secondary interactions can hamper the attribution of individual contributions to the enthalpy of binding for the complexes involved and may mask indications for strained binding.

When only considering the contribution of the enthalpy of binding for multivalent interactions, it would be most favorable to use long flexible linkers that would allow unstrained complex formation. However, such long flexible tethers are generally avoided for entropic reasons. The entropy term is extremely complex. The individual contributions of the entropy terms to multivalent binding are poorly understood and especially the role of the entropy of conformation, which is often considered most important with respect to binding enhancement through multivalency, is fraught with uncertainty and subject to debate.^{78,79} In classical interpretations it is reasoned that the longer the flexible tethers, the higher the conformational entropy penalty paid upon intramolecular binding. In fact it is often stated that long flexible tethers are guaranteed to fail in multivalent intramolecular interactions for entropic reasons, simply because the conformational entropy penalty paid upon intramolecular binding outweighs the rotational and translational entropy gained.^{1,80} However, these theories do not take into account the concept of effective concentration. Many studies on intramolecular binding involving multivalent guests

tethered by long flexible spacers indicate that entropic concerns should not be taken too severe.^{14,62,63,75,81} In this sense the use of effective concentration provides a more understandable relation between tether flexibility and the energy of binding. Indeed, the lower the effective concentration, the weaker the intramolecular interaction. For this thesis it suffices to note that in the most ideal case the entropy of binding for a multivalent interaction is equal to that of the corresponding monovalent interaction.^{1,80} Typically, however, intramolecular multivalent interactions are characterized by less favorable entropies of binding.

2.2.4.2 Valency of the complexes

An obvious parameter enabling control over the binding strength of multivalent interactions is the valency of the complex, i.e. the number of interactions between the interacting entities. For properly spaced functionalities, the enthalpy of binding is proportional to the number of interactions between two multivalent entities. In general, gains in enthalpy are partially counteracted by more negative entropy values. This is a well-known phenomenon that is referred to as enthalpy-entropy compensation.⁸² This behavior is explained by reasoning that as the enthalpy gets more favorable, indicating stronger interactions, the motions of the host and guest are restricted and consequently the entropy becomes less favorable. Nevertheless, impressive gains in binding affinity have been achieved by increasing the valency of the complex. A particularly illustrative example with respect to valency is a study by Hunter and co-workers who systematically increased the number of hydrogen bonds between two complementary oligovalent strands.⁸³ A stepwise increase in complexation constants was observed for each additional contributing hydrogen bond, going from $K = 20 \text{ M}^{-1}$ for two shared hydrogen bonds to $K = 5.5 \times 10^4 \text{ M}^{-1}$ for two strands complexed via a total of six hydrogen bonds. It is evident that the extent to which additivity leads to an increased binding affinity is strongly dependent on the tether (see above).

2.2.4.3 Examples of intramolecular multivalent interactions

As commented above, the thermodynamic parameters associated with multivalent intramolecular interactions enable a detailed insight into complex formation. Unfortunately, studies giving enthalpy and entropy values for intramolecular multivalent interactions are scarce. Most of the multivalent interactions studied with calorimetry involve cyclodextrin multimers, and this class of multivalent interactions will be discussed in section 2.3. Another particularly well-studied example of multivalency is the interaction between multivalent vancomycin and multivalent D-alanine-D-alanine (DADA) or D-alanine-lactate (DALac), reported by Whitesides and Rao in a series of papers (Figure 2.10).^{72,84-88}

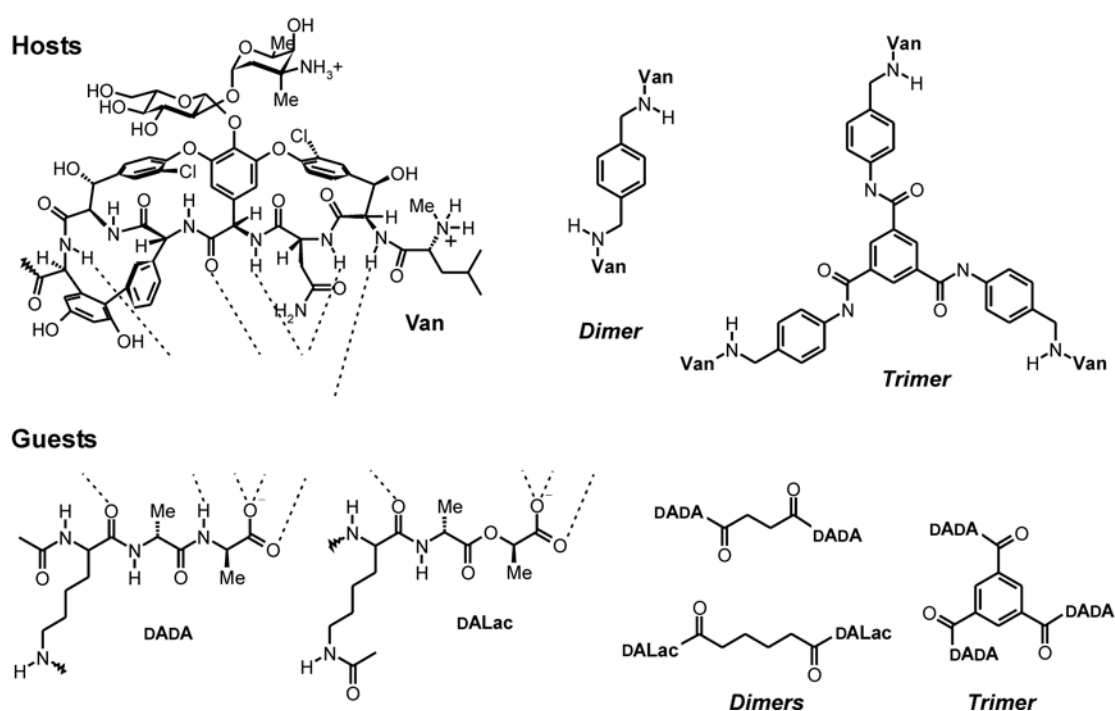


Figure 2.10 Multivalent host (vancomycin) and guest (DADA, and DALac) entities used by Rao and Whitesides.^{72,84-88} Hydrogen bonding patterns involved in the binding of the guests by vancomycin are illustrated by the dotted lines.

A vancomycin dimer was shown to bind a DALac dimer with an association constant, K , of $2.3 \times 10^4 \text{ M}^{-1}$, a factor of 40 stronger than the corresponding monovalent DALac, which bound vancomycin with a K of $5.6 \times 10^2 \text{ M}^{-1}$.⁸⁷ The enthalpy of binding for the divalent interaction, $-6.5 \text{ kcal mol}^{-1}$, was less than twice

that of the monovalent interaction, $-3.7 \text{ kcal mol}^{-1}$, indicating that the tether of the divalent guest is probably too short.⁸⁷

In a later study the corresponding trivalent vancomycin-DADA interaction was investigated. DADA binds vancomycin with higher affinity than DALac as a result of an additional hydrogen bond (Figure 2.10), and binds with an association constant of $6.3 \times 10^5 \text{ M}^{-1}$. The vancomycin trimer binds the DADA trimer with $K = 2.5 \times 10^{16} \text{ M}^{-1}$, a factor of 40 billion more strongly than the corresponding monovalent interaction.^{72,88} The association constant for the formation of the trivalent complex was determined using competition experiments monitored with HPLC and is one of the largest quantified association constants in literature. Such strong association constants are difficult to determine by microcalorimetry. The enthalpy of binding for this trivalent system, $-40 \text{ kcal mol}^{-1}$, was approximately three times that of the monovalent binding, $-12.0 \text{ kcal mol}^{-1}$.^{72,88} Strongly negative entropy values partially compensated the gain in free energy of binding obtained by this enhanced enthalpy of binding.

2.2.5 Multivalency and cooperativity

Enthalpy and entropy values also provide information on possible cooperativity. The assessment of cooperativity in multivalent interactions is notoriously difficult,^{1,89} and there are numerous examples in the literature where multivalent binding is incorrectly declared negatively or positively cooperative simply based on mono- and multivalent association constants.⁸⁹ Before any conclusions can be drawn regarding cooperativity in multivalent interactions a thorough deconvolution of the effects of multivalency and cooperativity is required.

Cooperativity is a rigorously defined term, well suited for consecutive monovalent interactions at a multivalent platform.⁹⁰ The degree of cooperativity is generally given by the parameter α , which is defined by Equation 6:

$$\Delta G_{mono,avg} = \alpha \Delta G_i \quad (6)$$

Here $\Delta G_{mono,avg}$ is the average free binding energy of the monovalent interaction at the multivalent platform, and ΔG_i is the intrinsic free energy of binding. Depending on the ratio of these two energies, values of α are either less than, equal to, or greater

than unity, and the binding is respectively called negatively cooperative (interfering), non-cooperative (statistical), or positively cooperative (synergistic). A classical example of positively cooperative binding is the interaction of dioxygen with hemoglobin.⁹¹ Positive cooperativity also applies to the binding of monovalent GM₁, a portion of a toxin guest site displayed at cell surfaces, to pentavalent cholera toxin.⁹² Defining the extent of cooperativity in these systems is relatively straightforward as they are well defined and the overall binding is easily dissected into the contributing binding energies of the monovalent interactions.

Multivalent systems are often less well defined. The number of interactions in multivalent complexes involving polyvalent entities such as polymers, dendrimers etc. is often unknown. Additionally, for the majority of multivalent interactions, the individual contribution of the monovalent host-guest interactions to the overall multivalent binding is difficult, if not impossible, to interpret. For this reason Whitesides and co-workers introduced a parameter β , which represents a binding enhancement factor for multivalent interactions over their monovalent analogue:

$$K_{multi} = \beta K_{mono} \quad (7)$$

Here K_{multi} is the association constant of the multivalent interaction and K_{mono} the monovalent association constant. The quantity β does not conclude the extent of cooperativity, but simply gives the binding enhancement of the multivalent interaction over the intrinsic interaction.

In order to assess cooperativity for multivalent interactions, the inter- and intramolecular processes should be considered separately and independently. That is, cooperativity can only be assessed if the compared equilibrium constants have the same dimensions. In a recent paper on cooperativity in self-assembled systems Ercolani stated that comparison of experimental and statistical association constants for intramolecular interactions can give an indication of the extent of cooperativity.⁸⁹ If the former exceeds the latter, there is positive cooperativity, whereas if the opposite occurs negative cooperativity is involved. Alternatively this can be translated in terms of effective concentration (C_{eff} , see section 2.2.3) and effective molarity (EM , see section 2.2.3). Large deviations between the two parameters can be indicative of a negatively ($EM < C_{eff}$) or positively cooperative binding mode ($EM > C_{eff}$). The

majority of (synthetic) multivalent systems reported in the literature can be analyzed using a statistical, non-cooperative binding mode, i.e. in terms of pure multivalency and effective concentration.^{13,14,72-76,84-88} In these cases, the effective concentration is more or less equal to the effective molarity. One example of positive cooperativity in a multivalent system might be the self-assembly of a DNA double helix.⁹³

2.2.6 Kinetic aspects of multivalent interactions

The previous sections have emphasized that multiple interactions give rise to strong binding, or in other words thermodynamic stability. As a result, the kinetics of multivalent interactions are typically characterized by (extremely) slow dissociation. However, dissociation rates can be remarkably increased with the use of monovalent competing guests. This kinetic aspect of multivalent interactions has been elegantly demonstrated by Whitesides and Rao in their study on the trivalent interaction of a vancomycin trimer and a DADA trimer. Extremely slow dissociation was found for the trivalent vancomycin-DADA system, which showed no sign of decomplexation in HPLC for time spans over 45 minutes.^{72,88} However, dissociation of the high affinity trivalent interaction could be achieved by competition with monovalent DADA.^{72,88} This is characteristic for multivalent interactions and indicates that dissociated guest sites quickly rebind because of the high effective concentration. Low dissociation rates that can be increased by competition are a hallmark of multivalent interactions and indicate a stepwise dissociation scheme (Figure 2.11).⁷²

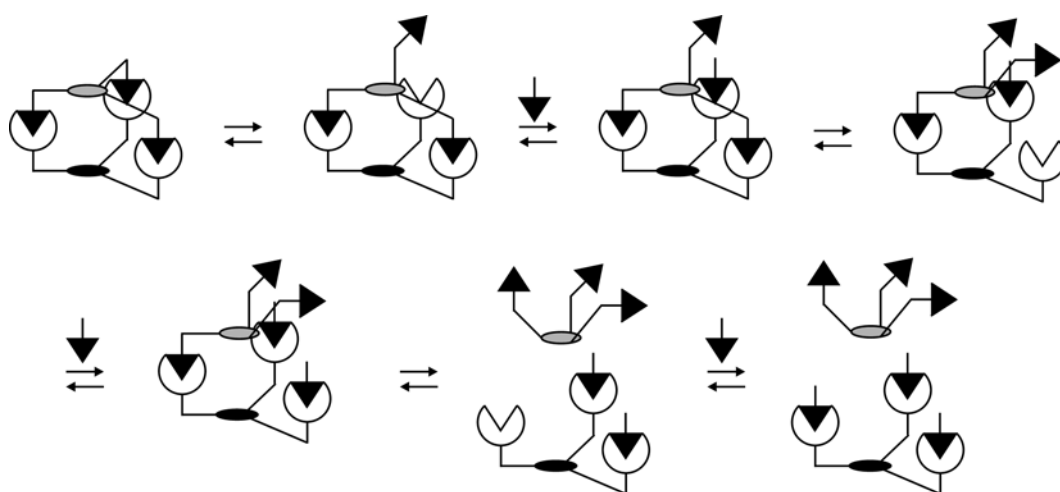


Figure 2.11 Stepwise dissociation of a multivalent interaction by competition with a monovalent analogue.

More examples demonstrating this characteristic feature of multivalency can be found for multivalent complexes at surfaces, which are particularly suited for studying the kinetic aspect of multivalent interactions. These will be discussed in the following section.

2.2.7 Multivalent interactions at surfaces

For mechanistic studies of multivalent interactions, monolayers offer a number of advantages over the solution model systems discussed above. Conducting layers, such as gold, are compatible with surface plasmon resonance spectroscopy, potentially enabling the characterization of the kinetic behavior of multivalent interactions. Most interestingly, the structure, density, and environment of the immobilized functionalities are easily varied, enabling systematic studies concerning multivalency and effective concentration.

The majority of studied multivalent interactions at surfaces involve divalent interactions between divalent antibodies and surface-immobilized hapten moieties.^{94,95} Unfortunately, most of these studies have been performed using a single or only a few different hapten concentrations, making it difficult to draw conclusions on multivalency versus cooperativity and the relation with monovalent binding at surfaces. There are a few studies in which the guest concentration at the surface has been systematically varied. Cremer and co-workers prepared a series of hybrid layers with different hapten concentrations.⁹⁵ The binding of labeled antibodies at these layers could be monitored simultaneously by the combination of confocal microscopy and microfluidic channels. Decreasing binding affinities with decreasing hapten concentrations at the surface exemplified the role of effective molarity. Based on the comparison of determined inter- and intramolecular association constants, $K_{inter} = 4.0 \times 10^4 \text{ M}^{-1}$ and $K_{intra} = 7.1 \times 10^7 \text{ m}^2/\text{mol}$, the authors mistakenly concluded that the antibody was bound in a positively cooperative fashion.⁹⁶

Williams et al. systematically varied the concentration of metal chelating guests at lipid bilayer membrane surfaces and found an extraordinary 4:1 receptor:copper(II) complex at high concentrations of guest.⁹⁷ The formation of this complex that has not been observed in solution was ascribed to the extremely high concentration of guests in the lipid membrane.

A study of particular interest concerns the binding of multivalent vancomycin derivatives at surfaces presenting DALac or DADA functionalities (for the structure of the guest see Figure 2.10) performed by Whitesides and Rao.^{84,87} This study allows comparison of the binding at the surface with the analogous multivalent binding in solution. The binding of a vancomycin dimer at a DALac SAM ($\chi_L = 0.50$) gave a binding constant of $3.0 \times 10^6 \text{ M}^{-1}$.⁸⁷ This increased binding affinity compared to the divalent interaction in solution (see section 2.2.5) can probably be attributed to a less strained binding of the vancomycin dimer and, additionally, to a larger effective concentration of DALac at the SAM (see also Chapter 6 of this thesis). A similar study with the vancomycin dimer at a SAM with a lower DADA concentration ($\chi_L = 0.05$) gave a binding constant, $K = 2 \times 10^9 \text{ M}^{-1}$,⁸⁶ that was only slightly higher than the corresponding divalent interaction in solution, $K = 9 \times 10^8 \text{ M}^{-1}$.⁸⁵

In another study, Whitesides and co-workers employed a bifunctional polymer presenting vancomycin and fluorescein groups for the direction of anti-fluorescein antibodies to self-assembled monolayers containing DADA moieties.⁹⁸ The vancomycin moieties of the bifunctional polymer were shown to interact in a multivalent fashion with the DADA SAM. The dissociation rate of the polymer could be controlled using competing monovalent DADA guests in the supernatant solution, a characteristic feature of multivalency (see section 2.2.6). The pendent fluorescein groups were available for successive interaction with the antibody. Inhibition of the latter interaction in the presence of soluble fluorescein allowed the determination of both mono- and divalent association constants, $1.3 \times 10^5 \text{ M}^{-1}$ and $5 \times 10^8 \text{ M}^{-1}$, respectively. Dissociation sensograms indicated that the rate of dissociation increased with increasing fluorescein concentration.

Kahne and co-workers demonstrated that multivalent binding at self-assembled monolayers might be surface coverage-dependent.⁹⁹ The study involved the multivalent binding of *B. purpura* lectin to two different immobilized carbohydrates, a natural and a synthetic one. For both interactions, the amounts of bound lectin decreased with increasing monovalent competing guests in solution, and low dissociation rates were observed, indicative of multivalent binding. Interestingly, a surface-coverage dependent selectivity switch was observed for the binding of the lectin to the carbohydrates. At low carbohydrate densities ($\chi_L = 0.1$) the immobilized natural guest interacted most strongly, while at higher densities ($\chi_L = 0.6$) the

synthetic guest gave the strongest binding. These findings possibly give a first insight into density-regulated cellular interactions.

2.3 Multivalent cyclodextrin systems

Cyclodextrins are probably among the most abundantly used host molecules in science and industry. This popularity primarily stems from the enormous variety of guest molecules that can be complexed by cyclodextrins.¹⁰⁰ This, combined with the ease of synthetic modification¹⁰¹ and the large quantities available at low prices, has led to an average of over 1000 publications per year and the application of cyclodextrins in pharmaceuticals, food products, cosmetics, and a variety of chemical and biochemical processes.^{102,103}

Although the majority of research on cyclodextrins involves the monovalent derivatives, there are a considerable number of publications devoted to cyclodextrin multimers, in which most of the types of multivalent systems listed in

Figure 2.4 have been employed. After a general introduction on cyclodextrins, the different multivalent architectures of cyclodextrin reported in the literature will be discussed, with an emphasis on multivalent interactions.

2.3.1 Structure, physical properties, and complexation behavior of cyclodextrins

Cyclodextrins are water-soluble cyclic oligosaccharides of α -D-glucopyranose moieties connected via α -1,4-glycosidic linkages. The cyclodextrins are naturally occurring products obtained from the degradation of starch by microorganisms.¹⁰² The most commonly used and commercially available cyclodextrins are α -, β -, and γ -cyclodextrin, consisting of 6, 7, and 8 glucose units, respectively. The primary and secondary hydroxyl groups, situated at the rims of the cyclodextrins, dominate the exterior of the cyclodextrins and render the molecules water-soluble. Additionally, a ring of intramolecular hydrogen bonds between the secondary hydroxyl groups (C2-OH and C3-OH, Figure 2.12) of neighboring α -D-glucopyranose units makes the structures of these cyclodextrins relatively rigid, giving rise to a well-defined central cavity. The interior of the cavity is shaped by the C3 and C5 hydrogens and the glycosidic oxygens, making it relatively apolar. This hydrophobic environment

enables the encapsulation of a variety of hydrophobic organic molecules in aqueous solution.¹⁰⁰ Higher analogues of the cyclodextrins with up to 31 glucose moieties have been isolated, but due to an increased flexibility these molecules tend to adopt an elliptic shape and therefore lack the presence of a persistent cavity.¹⁰⁴

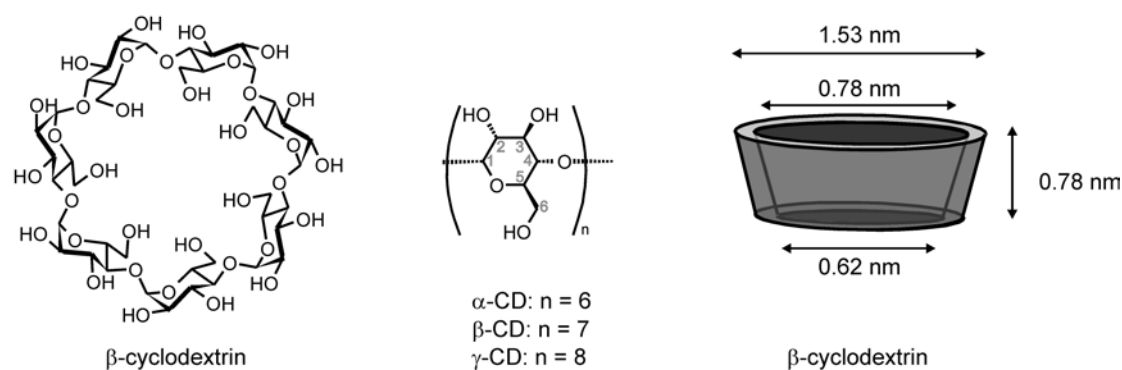


Figure 2.12 Several representations of the structure of cyclodextrins.

The driving force for inclusion is often referred to as “the hydrophobic effect”. In a sense this term is misleading as the complexation of guest molecules in the cyclodextrin cavity is governed by the interplay of hydrophobic interactions and release of water molecules combined with additional factors, of which the most important are the Van der Waals interactions, conformational changes or strain release upon guest complexation, electrostatic interactions, and hydrogen bonding. In contrast to the classical hydrophobic effect, the complexation of guest molecules by cyclodextrins is generally enthalpy-driven, with slightly positive or negative entropies of binding.¹⁰⁰ Guest inclusion is usually a rapid, diffusion-limited process,¹⁰⁵ and thermodynamic equilibrium is readily achieved.¹⁰⁶

Synthetic modification of the cyclodextrins typically involves the hydroxyl groups, each of which has its own reactivity. The primary hydroxyl groups (C6-OH, Figure 2.12) are the most nucleophilic and best accessible, and can be easily functionalized by nucleophilic substitution reactions. The secondary hydroxyls at C2 are the most acidic due to intramolecular hydrogen bonding to C3-OH and the electron withdrawing acetal moiety at C1. Selective deprotonation of C2-OH can be achieved using strong bases such as LiH and NaH. The C3 hydroxyls are the least reactive, and selective functionalization at this position is typically achieved indirectly by using protecting group strategies.

2.3.2 Cyclodextrin multimers

The majority of multivalent cyclodextrin systems involve covalently linked cyclodextrins, and many of these concern cyclodextrin dimers. Apart from a few reports on the synthesis and binding studies of so-called heterodimers, i.e. dimers consisting of two types of cyclodextrin,^{107,108,109,110} most cyclodextrin clusters involve cyclodextrins of the same kind. Cyclodextrin trimers^{111,112,113,114} and tetramers^{112,115,116,117} are relatively rare, inherent to the size of guest molecules that are generally studied and the synthetic effort associated with the preparation of these multimers. Nolte and co-workers have cleverly circumvented the difficulties encountered with the synthesis of higher order cyclodextrin multimers by chelating three cyclodextrin dimers at a ruthenium center.¹¹⁸ Ease of synthesis is also the reason for the relative large number of primary side-linked cyclodextrin multimers. For these multimers, multivalent binding of guest molecules proceeds via the shallower primary sides of the cyclodextrin cavities. However, the binding of guest molecules to cyclodextrins usually takes place via their wider secondary side and in this respect it is more logical to connect the cyclodextrin cavities via their secondary sides, though this typically requires more synthetic effort. The superiority in binding ability for the secondary-linked cyclodextrin dimers over the primary side-linked cyclodextrin dimers has been confirmed experimentally by the groups of Breslow¹⁰⁸ and Shen¹¹⁹, which showed that larger guest molecules are more effectively bound by secondary side-linked cyclodextrin dimers compared to the corresponding primary side-linked cyclodextrin dimers.

Cyclodextrin multimers have been applied in catalysis,^{107,112,120,121} templating reactions,^{122,123,124} and as sensor systems.^{118,125,126} Typically, cyclodextrin multimers bind guest molecules in an intramolecular fashion. Intermolecular binding is restricted to a few cases where incompatibility of host and guest molecules leads to the formation of aggregates.^{127,128,129} Many of the multivalent cyclodextrin multimers show enhanced affinity and selectivity for hydrophobic substrates, characteristic of multivalent binding. Table 2.1 lists the effective molarities (*EM*) for a number of β -cyclodextrin dimers.

Table 2.1 Effective molarity (EM) values for β -cyclodextrin dimers. Effective molarities were calculated using Equation 1 (section 2.2.3) using binding affinities determined for the dimer (K_2) and the corresponding monovalent interactions (K_{mono}). Only studies in which the divalent and both monovalent K_s were determined with one single technique have been used for the calculations of EM. The attachment point of the tether to the cyclodextrin is given in parenthesis.

Entry	Guest	Host	EM (M)	Ref.
1			0.2	130
2			0.01	131
3			0.02	130
4			0.002	130
5			0.01	130
6			1.0	132
7			0.17	133
8			0.12	133
9			0.04	133
10			0.06	133

Table 2.1 Continued.

Entry	Guest	Host	EM (M)	Ref.
11			0.05	133
12			0.21	134
13			0.10	134
14			0.02	135
15			1.25	136
16			0.64	137

Effective molarities found for cyclodextrin dimers are typically in the range of 0.01 to 0.2 M, and in many cases these values are within the same range as the effective concentration, indicating that guest molecules are generally bound in a non-cooperative, statistical fashion. An illustrative example is given by the work published by Petter and co-workers who studied the binding of toluidino-2-naphthalene sulfonate (TNS) by a range of β -cyclodextrin dimers tethered by spacers with variable length (Figure 2.13). The authors determined a linear relation between the energy of complexation (ΔG°) and the number of carbon atoms in the β -cyclodextrin dimer tether. However, no fundamental explanation for this ratio was given. Figure 2.13 shows a plot of the complexation constant (K), taken from the publication of Petter, versus a calculated inverse cubic tether length (based on a maximum extension of the

chain, assuming an average bond length of 0.154 nm and an average bond angle of 109.5°). The linear relation between binding affinity and inverse cubic tether length implies that this difference might be explained in terms of effective concentration.

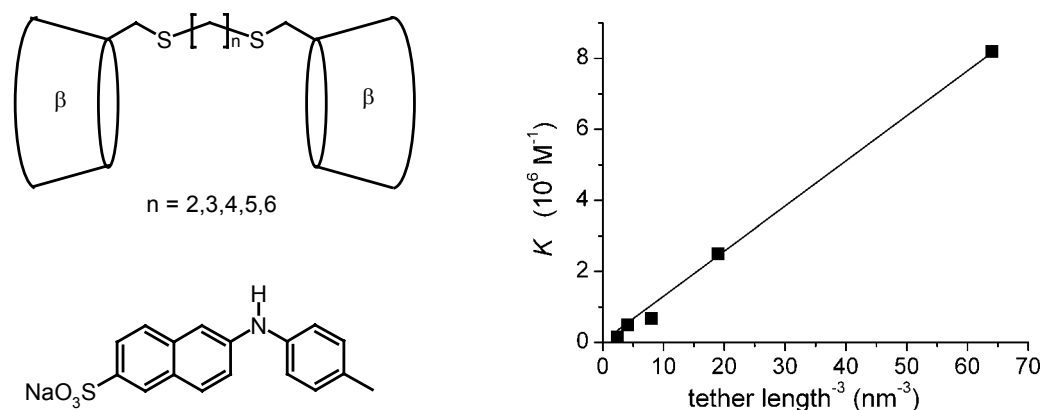


Figure 2.13 Plot of binding affinity versus inverse cubic tether length for complexation of TNS by β -cyclodextrin dimers with variable tether length.

Trends of spacer length versus binding affinity for a specific guest molecule are a general phenomenon. For many systems linear relations between binding affinity and inverse cubic tether length, similar to the plot in Figure 2.13, have been determined.^{138,139}

Secondary interactions between tether and guest molecule may lead to higher binding affinities and consequently give rise to relatively high values of EM . A clear example is entry 6 of Table 2.1, in which ligation of the phosphate moiety of the guest molecule to the metal-ion complexed at the tether results in an EM of 1.0 M. Similar effects have been observed for other metal-chelated cyclodextrin dimers and charged guest molecules,¹⁴⁰ and for intramolecular chelation of the tether to metal-containing guest molecules.¹⁴¹

Rigidity, in both host and guest, can lead to tight binding. Illustrative in this respect are doubly linked cyclodextrin dimers, which display extremely high affinities compared to their mono-linked analogues.¹⁴² The drawback of these dimers is again the inherent difficulties encountered in synthesis. Recently Sinaÿ and co-workers developed a synthesis route for the selective A-D deprotection of benzylated and methylated cyclodextrins,^{143,144} which opens possibilities for the facile synthesis of doubly linked dimers.¹⁴⁵ Extremely tight binding is only obtained when host and guest

structures are compatible, and care should be taken as mismatches cannot be compensated for. As discussed in section 2.3.1, the enthalpy of binding is often the major contributor to the free energy of binding, and ineffective binding results in binding affinities that are only marginally larger than that of the corresponding monovalent interaction. Illustrative is entry 4 in Table 2.1. On the other hand, guest binding affinities of dimers having long flexible spacers can be diminished by self-inclusion of the spacer in the cyclodextrin cavity.^{109,146}

Several groups have attempted to gain control over binding affinities of β -cyclodextrin dimers by tethering β -cyclodextrin cavities with linkers that are able to change their conformation, and therewith the extent of cooperativity, upon an external input.¹⁴⁷⁻¹⁵⁰ Ueno et al. were the first to report such a tunable system. They synthesized a photoswitchable β -cyclodextrin dimer by tethering two β -cyclodextrin cavities via their primary sides with an azobenzene linker.¹⁴⁷ Despite the photoswitchable properties of the dimer, no guest species were found that displayed selectivity for one of the two configurations of the dimer.

The groups of Wu¹⁴⁸ and Liu¹⁴⁹ synthesized several β -cyclodextrin dimers containing oligo(ethylenediamine) tethers. Upon coordination of metal ions the tether flexibility of these dimers is altered which results in a change in binding affinity. For the guest molecules studied thus far, however, these primary side-linked dimers displayed only marginal differences in binding properties. Differences in binding affinity upon metal complexation were limited to a factor of 5 or smaller.¹⁴⁹

A successful approach towards cyclodextrin dimers able to release guest molecules was reported by Breslow et al. The dimers consisted of two cyclodextrin cavities tethered via a photocleavable linker.¹⁵⁰ Both secondary and primary side-linked dimers were synthesized. Upon irradiation of the dimer-guest complexes, the linkers are cleaved and the guest molecules precipitate. This system in principle gives the largest possible difference in affinity between two states, i.e. it is switched from di- to monovalent. The drawback of this approach is that photocleavage results in the irreversible destruction of the dimer.

2.3.3 Cyclodextrin polymers

There are numerous reports on β -cyclodextrin in polyvalent architectures. In the majority of these studies, cyclodextrins have been randomly cross-linked to give cyclodextrin networks, an approach often applied in molecular imprinting.¹⁵¹ Well-defined polymers have been synthesized by coupling cyclodextrins to side chains,¹⁵² reaction of mono-deprotonated cyclodextrin with reactive poly(maleic anhydride) polymers,¹⁵³ bis-modification of cyclodextrin with polymerizable groups,¹⁵⁴ and cross-linking of templated rotaxanes to give nanotubes.¹⁵⁵

Concerning multivalency, there are three studies that are of particular interest. Brown et al. studied the interaction of an adamantane end-capped poly(ethylene glycol) polymer ($M_w = 10^4$ g/mol) with a β -cyclodextrin polymer, synthesized by random linking with epichlorohydrin (Figure 2.14A).¹⁵⁶ The interaction between the two polymers was studied at various concentrations of the guest polymer and two limiting cases were observed. At low concentration, the adamantane end-capped polymer was shown to bind the β -cyclodextrin polymer intramolecularly, whereas at high concentration the cyclodextrin polymers were saturated with monovalently bound guest polymer.

Wenz et al. studied the interaction of a 4-*tert*-butylphenyl-modified polymer with a β -cyclodextrin-modified polymer (Figure 2.14B).¹⁵⁷ The polymers were synthesized by reacting poly(maleic anhydride) polymers with β -cyclodextrin and 4-*tert*-butylaniline, respectively, giving polymers with a 10 % substitution degree and 90 % free carboxylic acid groups, rendering the polymers water-soluble. The interaction between the host and guest polymers led to gel formation and consequently to an extreme increase in viscosity. Calorimetry experiments gave an enthalpy of binding similar to those found for the interaction of the guest polymer with native β -cyclodextrin.

Another type of multivalent interaction was described by Yui and co-workers who studied the complexation of a poly(ethylene oxide)-block-poly(tetrahydrofuran)-block-poly(ethylene oxide) triblockcopolymer by an α -cyclodextrin-based nanotube composed of 4 to 9 interlinked α -cyclodextrins (Figure 2.14C).¹⁵⁸ The hydrophilic poly(ethylene oxide) blocks (45 ethylene glycol units) adjoining the hydrophobic poly(tetrahydrofuran) block (9 THF units) of the polymer improve the water-solubility of the triblockcopolymer. Strong exothermic heat effects were observed for

the titration of the α -cyclodextrin nanotube to the triblock copolymer, indicative of the complexation of the polymer by the nanotube. The stoichiometry of the interaction was dependent on the length of the nanotube and varied from 2:1 (nanotube:polymer) for the low molecular weight nanotubes to 1:2 for the higher molecular weight nanotubes. The latter stoichiometry indicates that the nanotube might feature several kink points allowing two polymers to be bound by a single nanotube. The enthalpy of binding increased with the length of the nanotube and was largely compensated by the reduced entropy of binding to give moderate enhancements in binding affinity with increasing tube length.

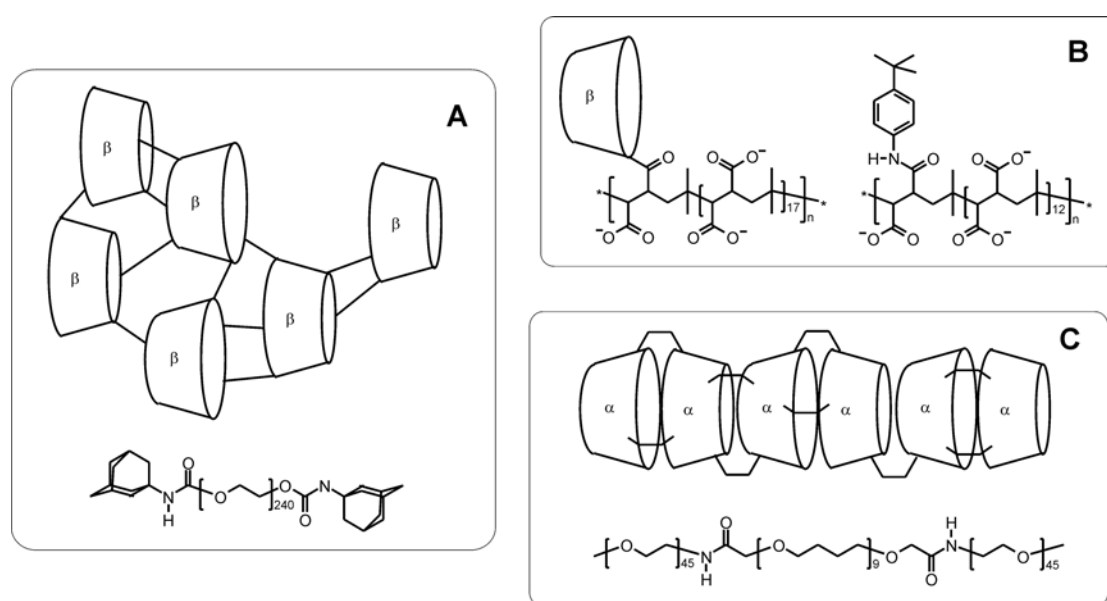


Figure 2.14 Multivalent interactions involving multivalent β -cyclodextrin polymers.

2.3.4 Cyclodextrin vesicles

A particularly interesting type of multivalent display of cyclodextrins concerns cyclodextrin vesicles.¹⁵⁹ The cyclodextrins are three-dimensionally organized in a non-covalent fashion and attain a certain extent of lateral mobility. Typically, cyclodextrin vesicles consist of bilayers of cyclodextrins modified with hydrophobic tails, in which the hydrophobic tails are directed inwards and the hydrophilic cyclodextrin cavities face the aqueous environment (Figure 2.15). The size of the vesicles can be tuned by varying the length of the hydrophobic tails,¹⁶⁰ sonication,¹⁶¹ mixing with other amphiphilic compounds,¹⁶² and size extrusion.¹⁶³ Vesicle sizes

varying from 30 to 350 nm have been reported. One of the characteristic features of the vesicles is that guest molecules can be encapsulated in the vesicles' interior.¹⁶⁴ Controllable release of guest molecules from the vesicles' interior was achieved by linking the hydrophobic tails to the cyclodextrin by a labile disulfide bond.¹⁶⁵ Treatment of the vesicles with a reducing agent led to cleavage of the disulfide bond and disintegration of the vesicles.

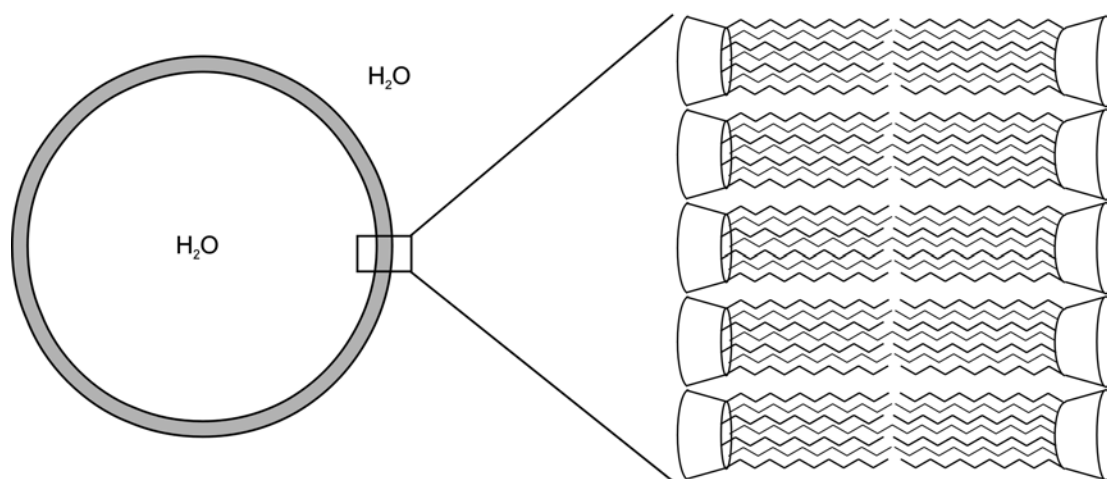


Figure 2.15 Schematic representation of cyclodextrin vesicles.

Ravoo and co-workers studied the multivalent interaction between cyclodextrin vesicles and poly(isobutylmaleic acid) polymers (see Figure 2.14B for the structure of the polymer) modified with adamantane or *tert*-butylphenyl groups.¹⁶³ The association of vesicles and polymers was studied by capillary electrophoresis, which revealed that the interaction between vesicles and *tert*-butylphenyl-modified polymers with a 10% substitution degree was three orders of magnitude stronger than the interaction of the vesicles with *tert*-butylaniline. Interestingly, analogous polymers with a 42% substitution degree gave a less strong binding enhancement, only two orders of magnitude. Adamantane-modified polymers showed almost no increase in binding affinity. Similar trends were observed for the interaction of these polymers with native β -cyclodextrin. The reduced affinities found for the more hydrophobic polymers were attributed to intramolecular association of the hydrophobic endgroups, i.e. coiling of the polymers, resulting in a diminished probability and strength of interaction. Dynamic light scattering studies did not show aggregation of vesicles, indicating intramolecular multivalency.

2.3.5 Cyclodextrin particles

Several approaches for the synthesis of cyclodextrin-covered nanoparticles have been published, either using native β -cyclodextrin^{166,167} or per-6-thio- β -cyclodextrin.^{168,169} Cyclodextrin nanoparticles have mainly been used for catalysis on monovalently binding substrates.^{170,171} Kaifer and co-workers studied the interactions of β -cyclodextrin gold nanoparticles with a divalent bis(ferrocene) (Figure 2.16).¹⁶⁹ Addition of the bis(ferrocene) to a solution of β -cyclodextrin nanoparticles led to the formation of a red precipitate, which was shown to consist of aggregated bis(ferrocene) and β -cyclodextrin nanoparticles. The authors postulated that the intermolecular binding is due to the rigidity of the linker, although it is more likely that the length between the two ferrocene units is insufficient to bind two β -cyclodextrin at a single nanoparticle. By addition of ferrocene methanol the precipitated aggregates could be resolubilized. Similar aggregation behavior was observed with γ -cyclodextrin-capped gold nanoparticles and C₆₀ fullerene molecules.¹⁷²

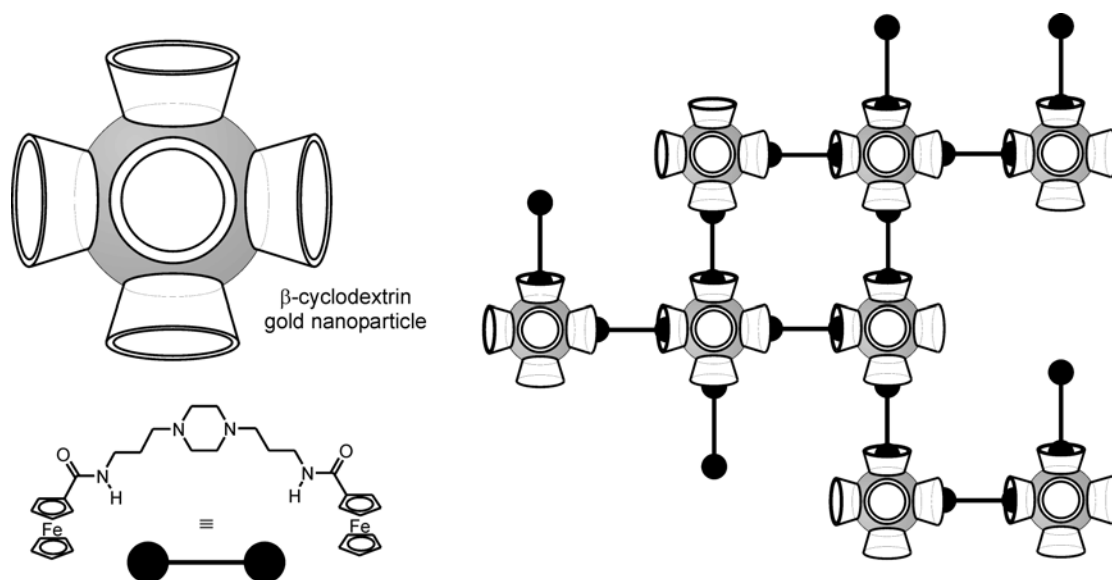


Figure 2.16 The interaction of a bis(ferrocene) guest with β -cyclodextrin gold nanoparticles leading to the formation of large aggregates owing to intermolecular cross-linking.¹⁶⁹

2.3.6 Cyclodextrin self-assembled monolayers

Apart from the covalently linked cyclodextrin multimers, the most extensively studied multivalent cyclodextrin systems are the self-assembled cyclodextrin monolayers (CD SAMs). Various routes for the immobilization of cyclodextrins on surfaces have been developed, with most of the work concentrated on gold surfaces.¹⁷³ Cyclodextrins have been mono-,^{174,175} oligo-,^{176,177} and per-6-functionalized¹⁷⁸⁻¹⁸⁴ with sulfur containing moieties. Mono-functionalized cyclodextrins may be subject to the formation of quasi-two-layer systems, rendering only half of the cyclodextrin cavities available for complexation of guest molecules.¹⁷⁵ Oligo- and per-6-functionalized cyclodextrins form CD SAMs in which the cyclodextrin cavities are fixated upwards with their wider secondary face towards the solution. The most often used per-6-functionalized cyclodextrin adsorbates are the per-6-thiol cyclodextrins (Figure 2.17B&D), first reported by Kaifer et al. and readily synthesized from native cyclodextrin.¹⁷⁸ The limited lateral mobility of these cyclodextrin adsorbates causes the formation of imperfect, disordered monolayers, and successive treatment is required to fill the resulting defects.^{178,179} The lateral mobility of thiol-functionalized cyclodextrin adsorbates was systematically investigated by Mittler-Neher and co-workers who studied the immobilization kinetics of a number of cyclodextrin adsorbates with different substitution numbers and chain lengths.¹⁷⁴

Well-ordered, densely packed cyclodextrin monolayers are readily obtained when using per-6-thioether-modified cyclodextrins (Figure 2.17C).^{180,181} The function of the thioether chains is twofold: the thioether functionalities, which independently bind relatively weakly to gold, but combined give rise to stable assemblies, assure some lateral mobility of the adsorbate molecules at low coverages and elevated temperatures. The alkyl chains, two per cyclodextrin glucose unit, completely fill the space underneath the cyclodextrin headgroup and therewith govern the packing of the adsorbate molecule. High-resolution atomic force microscopy revealed that these per-6-thioether-modified cyclodextrin adsorbates form dense, hexagonally-packed monolayers.¹⁸² Binding studies at such CD SAMs, performed with a variety of small hydrophobic guest molecules using surface plasmon resonance and single molecule force spectroscopy, indicated that the complexation properties of the immobilized β -cyclodextrins are comparable to those of native β -cyclodextrin.^{182,183,184}

For a long time, the use of CD SAMs was restricted to the detection of small monovalently binding guest molecules. Only in the last three years have CD SAMs been applied to multivalent interactions.

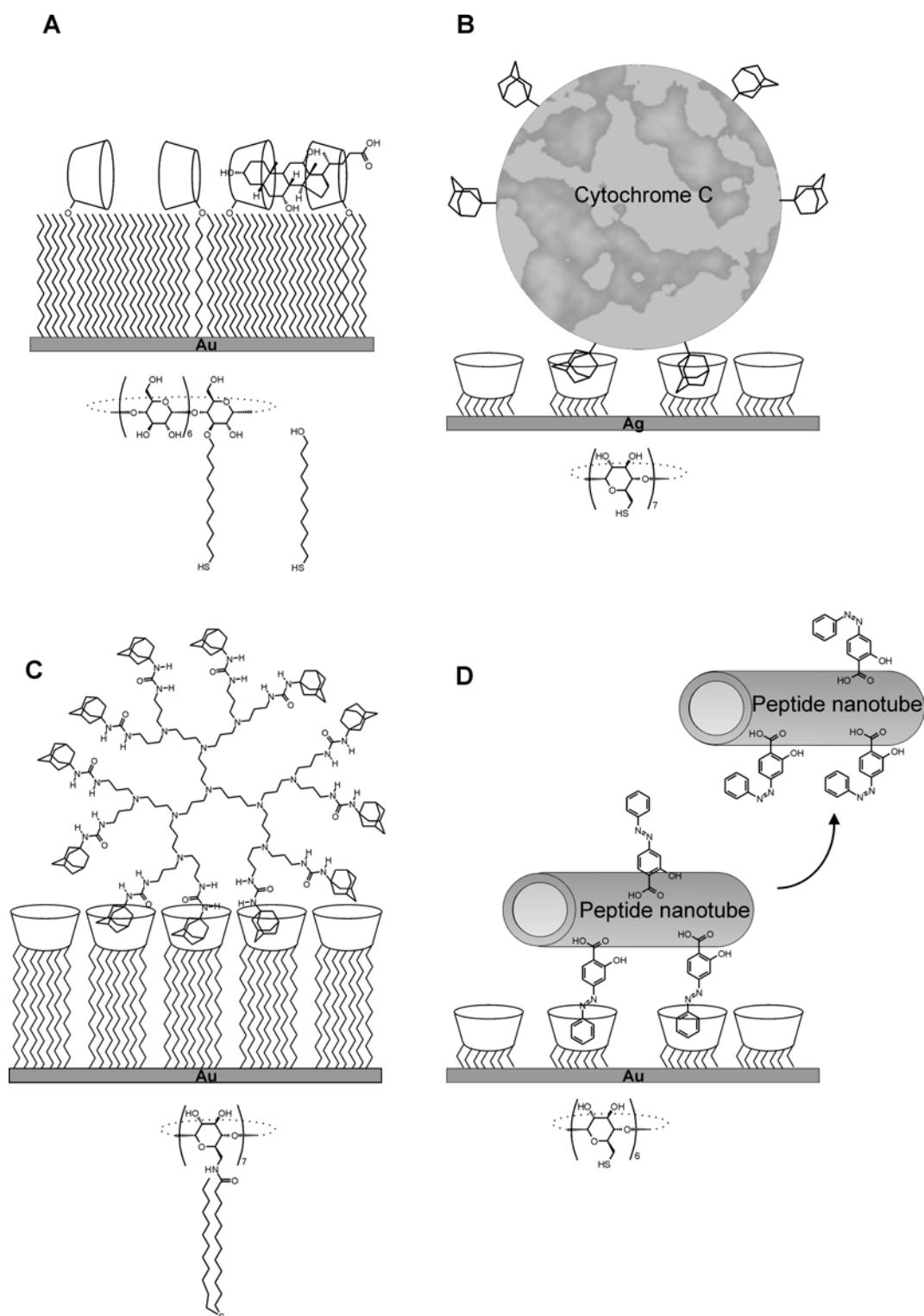


Figure 2.17 Multivalent interactions at CD SAMs: divalent binding of steroids (A),¹⁸³ immobilization of cytochrome C at electrodes (B),¹⁸⁵ multivalent binding of dendrimers (C),¹⁸⁶ and the positioning of peptide nanotubes (D).¹⁸⁷

Our group has employed mixed monolayers of a β -cyclodextrin monofunctionalized with a thiol chain and mercaptoundecanol for the detection of steroids at gold surfaces by means of surface plasmon resonance spectroscopy.¹⁸³ The mixed monolayers were shown to bind the steroids cholate and deoxycholate in a divalent fashion (Figure 2.17A). The steroids chenodeoxycholate, ursodeoxycholate, and lithocholate displayed both mono- and divalent binding at the CD SAMs, dependent on the fraction of the β -cyclodextrin adsorbate used in the monolayer formation. These findings are in accordance with complexation studies performed with this set of steroids and a β -cyclodextrin dimer.¹²⁵

Cao and co-workers used multivalency to immobilize an adamantyl-modified cytochrome C at silver electrode surfaces coated with per-6-thiol- β -cyclodextrin (Figure 2.17B).¹⁸⁵ Cytochrome C was synthetically modified with adamantyl moieties, yielding an average of about 9 adamantyls per protein. The CD SAMs were shown to have both an anchoring and a protective function. Compared to cytochrome C physisorbed at bare electrode surfaces, the supramolecularly immobilized cytochrome C was electrochemically stable for longer periods of time. Surface coverages were slightly lower than the theoretically calculated values. This was attributed to defective, disordered monolayers. No quantification or competition studies were performed to determine the thermodynamic and kinetic character of the multivalent interaction.

Around the same time, our group published a systematic study on the kinetic and thermodynamic issues related to the use of multivalent hydrophobic interactions for the attachment of molecules at surfaces.¹⁸⁶ The complexation of three different generations of adamantyl-terminated dendrimers (generation two, three, and four poly(propylene imine) dendrimers, having 8, 16, and 32 adamantyl endgroups respectively) at CD SAMs (Figure 2.17C) was studied with the use of surface plasmon resonance and atomic force microscopy. None of the three assemblies at the CD SAMs showed appreciable desorption in pure water, indicating that the assemblies were kinetically stable. Partial desorption could be achieved for the lower generation adamantyl-terminated dendrimers by washing with an 8 mM β -cyclodextrin solution. SPR and AFM measurements showed that the assemblies with the highest generation adamantyl-terminated dendrimer were stable even under these

conditions. Partial removal of the higher generation dendrimers found for the AFM experiments indicated thermodynamically rather than kinetically stable assemblies.

Matsui et al. employed azobenzene as a linking unit for the hydrophobic immobilization of peptide nanotubes at gold surfaces (Figure 2.17D).¹⁸⁷ The procedure involved hydrogen bonding of hydroxy azobenzene carboxylic acid to amide functionalities in an ethanol-water mixture and interaction of the trans-form of these azobenzene moieties with per-6-thiol- α -cyclodextrin adsorbed at gold surfaces. UV-irradiation led to the switching of the azobenzenes to the cis-form, which have a lower affinity for α -cyclodextrin, and consequently to desorption of the nanotubes from the surface. The lack of control experiments for this complex system implies that the results reported in this communication should be met with considerable skepticism.

2.4 Conclusions

Multivalency constitutes a powerful tool for the construction of high affinity non-covalent assemblies based on relatively weak interactions. The stability of the assembly formation is strongly dependent on the number of host-guest interactions between the entities that form the assembly and the connection between the interacting functionalities. The rigidity and length of the tethers with which the functionalities are connected determine the efficiency of assembly formation. By carefully tuning the number of shared interactions between two interacting species, control over the thermodynamic and kinetic aspects of the multivalent interaction can be accomplished.

With respect to host molecules, the cyclodextrins are of particular interest for application in multivalent interactions. They are readily modified, and moderate binding strengths and low selectivity associated with the interaction of guest molecules with monovalent cyclodextrin can be dramatically increased using the concept of multivalency. This pronounced difference in guest binding affinity between mono- and multivalent cyclodextrins has been employed for the synthesis of tunable cyclodextrin dimers, discussed in Chapters 3, 4, and 5 of this thesis. Chapters 6 and 7 describe the use of multivalency for the positioning of molecules at CD SAMs.

2.5 References and notes

- ¹ Mammen, M.; Choi, S.-K.; Whitesides, G. M. *Angew. Chem. Int. Ed.* **1998**, *37*, 2754-2794.
- ² Kitov, P. I.; Sadowska, J. M.; Mulvey, G.; Armstrong, G. D.; Ling, H. Pannu, N. S.; Read, R. J.; Bundle, D. R. *Nature* **2000**, *403*, 669-672.
- ³ Balzani, V.; Clemente-Leon, M.; Credi, A.; Lowe, J. N.; Badjic, J. D.; Stoddart, J. F.; Williams, D. J. *Chem. Eur. J.* **2003**, *9*, 5348-5360.
- ⁴ Varki, A. *Glycobiology* **1993**, *3*, 97-130.
- ⁵ Sharon, N.; Lis, H. *Essays Biochem.* **1995**, *30*, 59-63.
- ⁶ Lasky, L. A. *Annu. Rev. Biochem.* **1995**, *64*, 113-139.
- ⁷ Weis, W. I.; Drickamer, K. *Annu. Rev. Biochem.* **1996**, *65*, 441-473.
- ⁸ Dwek, R. A. *Chem. Rev.* **1996**, *96*, 683-720.
- ⁹ Rudd, P. M.; Elliot, T.; Creswell, P.; Wilson, I. A.; Dwek, R. A. *Science* **2001**, *291*, 2370-2376.
- ¹⁰ a) Spaltenstein, A.; Whitesides, G. M. *J. Am. Chem. Soc.* **1991**, *113*, 686-687. b) Lees, W. J.; Spaltenstein, A.; Kingery-Wood, J. E.; Whitesides, G. M. *J. Med. Chem.* **1994**, *37*, 3419-3433. c) Mammen, M.; Dahmann, G.; Whitesides, G. M. *J. Med. Chem.* **1995**, *38*, 4179-4190. d) Sigal, G. B.; Mammen, M.; Dahmann, G.; Whitesides, G. M. *J. Am. Chem. Soc.* **1996**, *118*, 3789-3800. e) Choi, S.-K.; Mammen, M.; Whitesides, G. M. *J. Am. Chem. Soc.* **1997**, *119*, 4103-4111.
- ¹¹ Sabesan, S.; Duus, J. Ø.; Neira, S.; Domaille, P.; Kelm, S.; Paulson, J. C.; Bock, K. *J. Am. Chem. Soc.* **1992**, *114*, 8363-8375.
- ¹² Mastrovich, M.; Klenk, H.-D. *Rev. Med. Virology* **2003**, *13*, 85-97.
- ¹³ a) Fan, E.; Zhang, Z.; Minke, W. E.; Hou, Z.; Verlinde, C. L. M. J.; Hol, W. G. J. *J. Am. Chem. Soc.* **2000**, *122*, 2663-2664. b) Merrit, E. A.; Zhang, Z.; Pickens, J. C.; Ahn, M.; Hol, W. G. J.; Fan, E. *J. Am. Chem. Soc.* **2002**, *124*, 8818-8824. c) Zhang, Z.; Merrit, E. A.; Ahn, M.; Roach, C.; Hou, Z.; Verlinde, C. L. M. J.; Hol, W. G. J.; Fan, E. *J. Am. Chem. Soc.* **2002**, *124*, 12991-12998.
- ¹⁴ Gargano, J. M.; Ngo, T.; Kim, J. Y.; Acheson, D. W. K.; Lees, W. J. *J. Am. Chem. Soc.* **2001**, 12909-12910.
- ¹⁵ Mourez, M.; Kane, R. S.; Mogridge, J.; Metallo, S.; Deschatelets, P.; Sellman, B. R.; Whitesides, G. M.; Collier, R. J. *Nat. Biotechnol.* **2001**, *19*, 958-961.

- ¹⁶ a) Hof, F.; Craig, S. L.; Nuckolls, C.; Rebek Jr., J. *Angew. Chem. Int. Ed.* **2002**, *41*, 1488-1508. b) de Mendoza, J. *Angew. Chem. Int. Ed.* **1998**, *4*, 1373-1377. c) Conn, M. M.; Rebek, Jr., J. *Chem. Rev.* **1997**, *97*, 1647-1668.
- ¹⁷ a) Hammond, P. T. *Curr. Opin. Colloid Interface Sci.* **2000**, *4*, 430-442. b) Decher, G. *Science* **1997**, *277*, 1232-1237. c) Knoll, W. *Curr. Opin. Colloid Interface Sci.* **1996**, *1*, 137-143.
- ¹⁸ Corbellini, F.; Fiammengo, R.; Timmerman, P.; Crego-Calama, M.; Versluis, K.; Heck, A. J. R.; Luyten, I.; Reinhoudt, D. N. *J. Am. Chem. Soc.* **2002**, *124*, 6569-6575.
- ¹⁹ Anderson, H. L.; Anderson, S.; Sanders, J. K. M. *J. Chem. Soc., Perkin Trans. 1* **1995**, 2231-2245.
- ²⁰ He, J.-A.; Valluzi, R.; Yang, K.; Dolukhanyan, T.; Sung, C.; Kumar, J.; Tripathy, S. K. *Chem. Mater.* **1999**, *11*, 3268-3274.
- ²¹ Houseman, B. T.; Mrksich, M. *Top. Curr. Chem.* **2002**, *218*, 1-44.
- ²² Rojo, J.; Morales, J. C.; Pandalés, S. *Top. Curr. Chem.* **2002**, *218*, 46-92.
- ²³ Lindhorst, T. K. *Top. Curr. Chem.* **2002**, *218*, 201-235.
- ²⁴ Kiessling, L. L.; Strong, L. E.; Gestwicki, J. E. *Annu. Rep. Med. Chem.* **2000**, *35*, 321-330.
- ²⁵ Davis, B. G. *J. Chem. Soc., Perkin Trans. 1* **1999**, 3215-3237.
- ²⁶ Roy, R. *Curr. Opin. Struct. Biol.* **1996**, *6*, 692-702.
- ²⁷ Roy, R. *Top. Curr. Chem.* **1997**, *187*, 242-274.
- ²⁸ Dam, T. K.; Brewer, F. *Chem. Rev.* **2002**, *102*, 387-429.
- ²⁹ Lis, H.; Sharon, N. *Chem. Rev.* **1998**, *98*, 637-674.
- ³⁰ Simanek, E. E.; McGarvey, G. J.; Jablonowski, J. A.; Wong, C.-H. *Chem. Rev.* **1998**, *98*, 833-862.
- ³¹ Lee, Y. C.; Lee, R. T. *Acc. Chem. Res.* **1995**, *28*, 321-327.
- ³² Herzner, H.; Reipen, T.; Schultz, M.; Kunz, H. *Chem. Rev.* **2000**, *100*, 4495-4537.
- ³³ Röckendorf, N.; Lindhorst, T. K. *Top. Curr. Chem.* **2001**, *217*, 210-238.
- ³⁴ Esfand, R.; Tomalia, D. A. *Drug Discovery Today* **2001**, *6*, 427-436.
- ³⁵ Roy, R.; Zanini, D.; Meunier, S. J.; Romanowska, A. *J. Chem. Soc., Chem. Commun.* **1993**, 1869-1872.
- ³⁶ Vrasidas, I.; André, S.; Valentini, P.; Böck, C.; Lensch, M.; Kaltner, H.; Liskamp, R. M. J.; Gabius, H.-J.; Pieters, R. *J. Org. Biomol. Chem.* **2003**, *1*, 803-810.
- ³⁷ Bovin, N. V. *Glycoconjugate J.* **1998**, *15*, 431-446.

- ³⁸ Fulton, D. A.; Stoddart, J. F. *Bioconjugate Chem.* **2001**, *12*, 655-672.
- ³⁹ Fujimoto, T.; Miyata, T.; Aoyama, Y. *J. Am. Chem. Soc.* **2000**, *122*, 3558-3559.
- ⁴⁰ Aoyama, Y.; Matsuda, Y.; Chuleerarak, J.; Mishiyama, K.; Fujimoto, K.; Fujimoto, T.; Shimizu, T.; Jayashida, O. *Pure Appl. Chem.* **1998**, *70*, 3279-2384.
- ⁴¹ a) Liang, R.; Yan, L.; Loebach, J.; Ge, M.; Uozumi, Y.; Sekanina, K.; Horan, N.; Gildersleeve, J.; Thompson, C.; Smith, A.; Biswas, K.; Still, W. C.; Kahne, D. *Science* **1996**, *274*, 1520-1522. b) Liang, R.; Loebach, J.; Horan, N.; Ge, M.; Thompson, C.; Yan, L.; Kahne, D. *Proc. Natl. Acad. Sci. USA* **1997**, *94*, 10554-10559.
- ⁴² a) Lin, C.-C.; Yeh, Y.-C.; Yang, C.-Y.; Chen, C.-L.; Chen, G.-F.; Chen, C.-C.; Wu, Y.-C. *J. Am. Chem. Soc.* **2002**, *124*, 3508-3509. b) Lin, C.-C.; Yeh, Y.-C.; Yang, C.-Y.; Chen, G.-F.; Chen, Y.-C.; Wu, Y.-C.; Chen, C.-C. *Chem. Commun.* **2003**, 2920-2921.
- ⁴³ Gu, H.; Ho, P. L.; Tong, E.; Wang, L.; Xu, B. *Org. Lett.* **2003**, *3*, 1261-1263.
- ⁴⁴ a) Charych, D.; Cheng, Q.; Reichert, A.; Kuziemko, G.; Stroh, M.; Nagy, J. O.; Spevak, W.; Stevens, R. C. *Chem. Biol.* **1996**, *3*, 113-120. b) Vogel, J.; Bendas, G.; Bakowsky, U.; Hummel, G.; Schmidt, R. R.; Kettman, U.; Rothe, U. *Biochem. Biophys. Acta* **1998**, *1372*, 205-215. c) Gege, C.; Vogel, J.; Bendas, G.; Rothe, U.; Schmidt, R. R. *Chem. Eur. J.* **2000**, *6*, 111-122.
- ⁴⁵ Mann, D. A.; Kanai, M.; Maly, D. J.; Kiessling, L. L. *J. Am. Chem. Soc.* **1998**, *120*, 10575-10582.
- ⁴⁶ Mrksich, M. *Cell. Mol. Life Sci.* **1998**, *54*, 653-662.
- ⁴⁷ Mrksich, M. *Chem. Soc. Rev.* **2000**, *29*, 267-273.
- ⁴⁸ General review on glycoproteins: Davis, B. G. *Chem. Rev.* **2002**, *102*, 579-601.
- ⁴⁹ a) Kingery-Wood, J. E.; Williams, K. W.; Sigal, G. G.; Whitesides, G. M. *J. Am. Chem. Soc.* **1992**, *114*, 7303-7305. b) Spevak, W.; Nagy, J. O.; Charych, D. H.; Schaefer, M. E.; Gilbert, J. H.; Bednarski, M. D. *J. Am. Chem. Soc.* **1993**, *115*, 1146-1147. c) Guo, C. T.; Sun, X. L.; Kanie, O. *Glycobiology* **2002**, *12*, 183-190.
- ⁵⁰ Bruehl, R. E.; Dasgupta, F.; Katsumoto, T. R.; Tan, J. H.; Bertozzi, C. R.; Spevak, W.; Ahn, D. J.; Rosen, S. D.; Nagy, J. O. *Biochemistry* **2001**, *40*, 5964-5974.
- ⁵¹ a) Pan, J. J.; Charych, D. *Langmuir* **1997**, *13*, 1365-1367. b) Spevak, W.; Foxall, C.; Charych, D. H.; Dasgupta, F.; Nagy, J. O. *J. Med. Chem.* **1996**, *39*, 1018-1020.

- ⁵² Particularly well-characterized aggregating systems can be found in: a) Olsen, L. R.; Dessen, A.; Gupta, D.; Sabesan, S.; Sacchettini, J. C. *Biochemistry* **1997**, *36*, 15073-15080. b) Dimick, S. A.; Powell, S. C.; McMahon, S. A.; Moothoo, D. N.; Naismith, J. H.; Toone, E. J. *J. Am. Chem. Soc.* **1999**, *121*, 10286-10296.
- ⁵³ Lundquist, J. J.; Toone, E. J. *Chem. Rev.* **2002**, *102*, 555-578.
- ⁵⁴ Dam, T. K.; Roy, R.; Sanjoy, K. D.; Oscarson, S.; Brewer, C. F. *J. Biol. Chem.* **2000**, *275*, 14223-14230.
- ⁵⁵ a) Lundquist, J. J.; Debenham, S. D.; Toone, E. J. *J. Org. Chem.* **2000**, *65*, 8245-8250. b) Corbell, J. B.; Lundquist, J. J.; Toone, E. J. *Tetrahedron Asymmetry* **2000**, *11*, 95-111.
- ⁵⁶ Gestwicki, J. E.; Cairo, C. W.; Strong, L. E.; Oeltjen, K. A.; Kiessling, L. L. *J. Am. Chem. Soc.* **2002**, *124*, 14922-14933.
- ⁵⁷ Page, D.; Roy, R. *Bioconjugate Chem.* **1997**, *8*, 714-723.
- ⁵⁸ a) Woller, E. K.; Cloninger, M. J. *Org. Lett.* **2002**, *4*, 7-10. b) Woller, E. K.; Walter, E. D.; Morgan, J. R.; Singel, D. J.; Cloninger, M. J. *J. Am. Chem. Soc.* **2003**, *125*, 8820-8826.
- ⁵⁹ Gestwicki, J. E.; Strong, L. E.; Cairo, C. W.; Boehm, F. J.; Kiessling, L. L. *Chem. Biol.* **2002**, *9*, 163-169.
- ⁶⁰ Burke, S. D.; Zhao, Q.; Schuster, M. C.; Kiessling, L. L. *J. Am. Chem. Soc.* **2000**, *122*, 4518-4519.
- ⁶¹ Ling, H.; Boodhoo, A.; Hazes, B.; Cummings, M. D.; Armstrong, G. D.; Brunton, J. L.; Read, R. J. *Biochemistry* **1998**, *37*, 1777-1788.
- ⁶² a) Yamaguchi, N.; Gibson, H. W. *Chem. Commun.* **1999**, 789-790. b) Yamaguchi, N.; Gibson, H. W. *Angew. Chem. Int. Ed.* **1999**, *38*, 143-147. c) Gibson, H. W.; Yamaguchi, N.; Jones, J. W. *J. Am. Chem. Soc.* **2003**, *125*, 3522-3533.
- ⁶³ a) Sijbesma, R. P.; Beijer, F. H.; Brunsveld, L.; Folmer, B. J. B.; Hirschberg, J. H. K. K.; Lange, R. F. M.; Lowe, J. K. L.; Meijer, E. W. *Science* **1997**, *278*, 1601-1604. b) Söntjens, S.; Sijbesma, R. P.; Van Genderen, M. H. P.; Meijer, E. W.; *Macromolecules* **2001**, *34*, 3815-3818.
- ⁶⁴ Glick, G. D.; Knowles, J. R. *J. Am. Chem. Soc.* **1991**, *113*, 4701-4703.
- ⁶⁵ Glick, G. D.; Toogood, P. L.; Wiley, D. C.; Skehel, J. J.; Knowles, J. R. *J. Biol. Chem.* **1991**, *266*, 23660-23669.
- ⁶⁶ Mandolini, L. *Adv. Phys. Org. Chem.* **1986**, *22*, 1-111.

- ⁶⁷ Kirby, J. A. *Adv. Phys. Org. Chem.* **1980**, *17*, 183-278.
- ⁶⁸ Galli, C.; Mandolini, L. *Eur. J. Org. Chem.* **2000**, 3117-3125.
- ⁶⁹ a) Ercolani, G. *J. Phys. Chem. B* **2003**, *107*, 5052-5057. b) Ercolani, G.; Ioele, M.; Monti, D. *New. J. Chem.* **2001**, *25*, 783-789. c) Ercolani, G. *J. Phys. Chem. B* **1998**, *102*, 5699-5703. d) Ercolani, G. *J. Am. Chem. Soc.* **1993**, *115*, 3901-3908.
- ⁷⁰ Bielejewska, A. G.; Marjo, C. E.; Prins, L. J.; Timmerman, P.; De Jong, F.; Reinhoudt, D. N. *J. Am. Chem. Soc.* **2001**, *123*, 7518-7533.
- ⁷¹ Fellunga, F.; Tecilla, P.; Hillier, L.; Hunter, C. A.; Licini, G.; Scrimin, P. *Chem. Commun.* **2000**, 1087-1088.
- ⁷² Rao, J.; Lahiri, J.; Weis, R. M.; Whitesides, G. M. *J. Am. Chem. Soc.* **2000**, *122*, 2698-2710.
- ⁷³ Kuhn, W. *Kolloid Z.* **1934**, *68*, 2-15.
- ⁷⁴ Winnik, M. A. *Chem. Rev.* **1981**, *81*, 491-524.
- ⁷⁵ Kitov, P. I.; Shimizu, H.; Homans, S. W.; Bundle, D. R. *J. Am. Chem. Soc.* **2003**, *125*, 3284-3294.
- ⁷⁶ Kramer, R. H.; Karpen, J. W. *Nature* **1998**, *395*, 710-713.
- ⁷⁷ The channels are situated at a protein surface and therefore the probing volume of the uncomplexed guest site is constituted of half a sphere ($2\pi r^3/3$).
- ⁷⁸ Mammen, M.; Shakhonovic, E. I.; Whitesides, G. M. *J. Org. Chem.* **1998**, *63*, 3168-3175.
- ⁷⁹ Ercolani, G. *J. Org. Chem.* **1999**, *64*, 3350-3353.
- ⁸⁰ The traditional idea is that multivalency is governed by entropy (refs. 1,21,53). In these approaches the binding enthalpy is typically assumed to be proportional to the number of interactions and the mode of binding is dependent on the entropy of binding. Intramolecular multivalent binding would be entropically favorable as the multivalent complex is assumed to involve the same rotational and translational entropy loss as its corresponding monovalent interaction, i.e. compared to n monovalent interaction a n -valent interaction is entropically more favorable by $n-1$ times the rotational and translational entropy loss (ref. 1). It is reasoned that the mode of binding is determined by the loss of conformational entropy upon intramolecular binding. If the overall entropy balance is positive, the multivalent entities will bind intramolecularly, and if the conformational entropy penalty paid exceeds the gained translation and rotation entropy the multivalent interaction will be intermolecular.

This philosophy implies that multivalent binding is associated with a favorable entropy term compared to the corresponding number of multiple monovalent interactions, an idealized phenomenon, which is in sharp contrast with the large negative entropy terms that are typically found for multivalent interactions.

- ⁸¹ Eblinger, F.; Schneider, H.-J. *Angew. Chem. Int. Ed.* **1998**, *37*, 826-829.
- ⁸² Leffler, J. E. *J. Org. Chem.* **1955**, *20*, 1202-1231.
- ⁸³ Bisson, A. P.; Hunter, C. A. *Chem. Commun.* **1996**, 1723-1724.
- ⁸⁴ Rao, J.; Colton, I. J.; Whitesides, G. M. *J. Am. Chem. Soc.* **1997**, *119*, 9336-9340.
- ⁸⁵ Rao, J.; Whitesides, G. M. *J. Am. Chem. Soc.* **1997**, *119*, 10286-10290.
- ⁸⁶ Rao, J.; Yan, L.; Xu, B.; Whitesides, G. M. *J. Am. Chem. Soc.* **1999**, *121*, 2629-2630.
- ⁸⁷ Rao, J.; Yan, L.; Lahiri, J.; Whitesides, G. M.; Weis, R. M.; Warren, H. S. *Chem. Biol.* **1999**, *6*, 353-359.
- ⁸⁸ Rao, J.; Lahiri, J.; Isaacs, L.; Weis, R. M.; Whitesides, G. M. *Science* **1998**, *280*, 708-711.
- ⁸⁹ Ercolani, G. *J. Am. Chem. Soc.* **2003**, *125*, 16097-16103.
- ⁹⁰ Perlmutter-Hayman, B. *Acc. Chem. Res.* **1986**, *19*, 90-96.
- ⁹¹ Perutz, M. F.; Fermi, G.; Luisi, B.; Shaanan, B.; Liddington, R. C. *Acc. Chem. Res.* **1987**, *20*, 309-321.
- ⁹² Schoen, A.; Freire, E. *Biochemistry* **1989**, *28*, 5019-5024.
- ⁹³ Philip, D.; Stoddart, J. F. *Angew. Chem. Int. Ed.* **1996**, *35*, 1154-1196.
- ⁹⁴ a) Mammen, M.; Gomez, F. A.; Whitesides, G. M. *Anal. Chem.* **1995**, *67*, 3526-3535. b) Nieba, L.; Krebber, A.; Pluckthun, A. *Anal. Biochem.* **1996**, *234*, 155-165. c) Sapsford, K. E.; Liron, Z.; Shubin, Y. S.; Ligler, F. S. *Anal. Biochem.* **2001**, *73*, 5518-5524. d) Thompson, N. L.; Poglitsch, C. L.; Thimbs, M. M.; Pisarchick, M. L. *Acc. Chem. Res.* **1993**, *26*, 567-573. e) Kalb, E.; Engel, J.; Tamm, L. K. *Biochemistry* **1990**, *29*, 1607-1613. f) Uzigris, E. E.; Kornberg, R. D. *Nature* **1983**, *301*, 125.
- ⁹⁵ Yang, T.; Baryshikova, O. K.; Mao, H.; Holden, M. A.; Cremer, P. S. *J. Am. Chem. Soc.* **2003**, *125*, 4779-4784.
- ⁹⁶ This article illustrates how comparison of two binding constants with different dimensions leads to incorrect conclusions concerning the extent of cooperativity. Cooperativity can only be assessed for binding constants having identical dimensions, see ref. 89.

- ⁹⁷ Doyle, E. L.; Hunter, C. A.; Philips, H. C.; Webb, S. J.; Williams, N. H. *J. Am. Chem. Soc.* **2003**, *125*, 4593-4599.
- ⁹⁸ Metallo, S. J.; Kane, R. S.; Holmin, R. E.; Whitesides, G. M. *J. Am. Chem. Soc.* **2003**, *125*, 4534-4540.
- ⁹⁹ Horan, N.; Yan, L.; Isono, H.; Whitesides, G. M.; Kahne, D. *Proc. Natl. Acad. Sci. USA* **1999**, *96*, 11782-11786.
- ¹⁰⁰ For comprehensive reviews on guest complexation by cyclodextrins see: a) Rekharsky, M.; Inoue, Y. *Chem. Rev.* **1998**, *98*, 1875-1917. b) Connors, K. A. in *Comprehensive Supramolecular Chemistry*, Vol. 3, Pergamon: Oxford, UK, **1996**.
- ¹⁰¹ a) Khan, A. R.; Forgo, P.; Stine, K. J.; D'Souza, V. T. *Chem. Rev.* **1998**, *98*, 1977-1996. b) Easton, C. J.; Lincoln, S. F. *Modified Cyclodextrins*, 1st ed., Imperial College Press: London, **1999**. c) Yuan, D.-Q.; Tahara, T.; Chen, W.-H.; Okabe, Y.; Yang, C.; Yagi, Y.; Nogami, Y.; Fukudome, M.; Fujita, K. *J. Org. Chem.* **2003**, *68*, 9456-9466.
- ¹⁰² Szejtli, J. *Chem. Rev.* **1998**, *98*, 1743-1754.
- ¹⁰³ Hedges, A. R. *Chem. Rev.* **1998**, *98*, 2035-2044.
- ¹⁰⁴ Larsen, K. L. *J. Inclusion Phenom. Macrocyclic Chem.* **2002**, *43*, 1-13.
- ¹⁰⁵ Szejtli, J. in *Comprehensive Supramolecular Chemistry*, Vol. 3, Pergamon: Oxford, UK, **1996**.
- ¹⁰⁶ Connors, K. A. in *Comprehensive Supramolecular Chemistry*, Vol. 3, Pergamon: Oxford, UK, **1996**.
- ¹⁰⁷ a) Easton, C. J.; van Eyk, S. J.; Lincoln, S. F.; May, B. L.; Papageorgiou, J.; Williams, M. L. *Aust. J. Chem.* **1997**, *50*, 9-12. b) Cieslinski, M. M.; Clements, P.; May, B. L.; Easton, C. J.; Lincoln, S. F. *J. Chem. Soc., Perkin Trans. 2* **2002**, 947-952.
- ¹⁰⁸ Yan, J.; Breslow, R. *Tetrahedron Lett.* **2000**, *41*, 2059-2062.
- ¹⁰⁹ Venema, F.; Nelissen, H. F. M.; Berthault, P.; Birlirakis, N.; Rowan, A. E.; Feiters, M. C.; Nolte, R. J. M. *Chem. Eur. J.* **1998**, *4*, 2237-2250.
- ¹¹⁰ Wang, Y.; Ueno, A.; Toda, F. *Chem. Lett.* **1994**, 167-170.
- ¹¹¹ Leung, D. K.; Atkins, J. H.; Breslow, R. *Tetrahedron Lett.* **2001**, *42*, 6255-6258.
- ¹¹² a) Breslow, R.; Yang, J.; Yan, J. *Tetrahedron Lett.* **2002**, *58*, 653-659. b) Yang, J.; Gabriele, B.; Belvedere, S.; Huang, Y.; Breslow, R. *J. Org. Chem.* **2002**, *67*, 5057-5067.
- ¹¹³ Tabushi, I.; Kuroda, Y.; Shimokawa, K. *J. Am. Chem. Soc.* **1979**, *101*, 1614-1615.

- ¹¹⁴ Luo, M.-M.; Chen, W.-H.; Yuan, D.-Q.; Xie, R.-G. *Synth. Commun.* **1998**, *28*, 3845-3848.
- ¹¹⁵ Yang, J.; Breslow, R. *Angew. Chem. Int. Ed.* **2000**, *39*, 2692-2694.
- ¹¹⁶ Michels, J. J.; Fiammengo, R.; Timmerman, P.; Huskens, J.; Reinhoudt, D. N. *J. Inclusion Phenom. Macrocyclic Chem.* **2001**, *41*, 163-172.
- ¹¹⁷ Jiang, T.; Li, M.; Lawrence, D. S. *J. Org. Chem.* **1995**, *60*, 7293-7297.
- ¹¹⁸ a) Nelissen, H. F. M.; Schut, A. F. J.; Venema, F.; Feiters, M. C.; Nolte, R. J. M. *Chem. Commun.* **2000**, 577-578. b) Nelissen, H. F. M.; Krecher, M.; De Cola, L.; Feiters, M. C.; Nolte, R. J. M. *Chem. Eur. J.* **2002**, *8*, 5407-5414.
- ¹¹⁹ a) Liu, J. Q.; Gao, S. J.; Luo, G. M.; Yan, G. L.; Shen, J. C. *Biochem. Biophys. Res. Commun.* **1998**, *247*, 397-400.
- ¹²⁰ Ren, X.; Liu, J.; Luo, Guimin, Zhang, Y.; Luo, Y.; Yan, G.; Shen, J. *Bioconjugate Chem.* **2000**, *11*, 682-687.
- ¹²¹ Akike, T.; Nagano, Y.; Yamamoto, Y.; Nakamura, A.; Ikeda, H.; Ueno, A.; Toda, F. *Chem. Lett.* **1994**, 1089-1092.
- ¹²² Wilson, D.; Perlson, L.; Breslow, R. *Bioorg. Med. Chem.* **2003**, *11*, 2649-2653.
- ¹²³ Easton, C. J.; Harper, J. B.; Lincoln, S. F. *New. J. Chem.* **1998**, 1163-1165.
- ¹²⁴ Van Bommel, K. J. C.; De Jong, M. R.; Metselaar, G. A.; Verboom, W.; Huskens, J.; Hulst, R.; Kooijman, H.; Spek, A. L.; Reinhoudt, D. N. *Chem. Eur. J.* **2001**, *7*, 3603-3615.
- ¹²⁵ De Jong, M. R.; Engbersen, J. F. J.; Huskens, J.; Reinhoudt, D. N. *Chem. Eur. J.* **2000**, *6*, 4043-4040.
- ¹²⁶ Nakamura, M.; Ikeda, T.; Nakamura, A.; Ikeda, H.; Ueno, A.; Toda, F. *Chem. Lett.* **1995**, 343-344.
- ¹²⁷ a) Alvarez-Parrilla, E.; Cabrer, P. R.; Al-Soufi, W.; Mejjide, F.; Núñez, E. R.; Tato, J. V. *Angew. Chem. Int. Ed.* **2000**, *39*, 2856-2858. b) Carber, P. R.; Alvarez-Parilla, E.; Mejjide, F.; Seijas, J. A.; Núñez, E. R.; Tato, J. V. *Langmuir* **1999**, *15*, 5489-5495.
- ¹²⁸ Liu, Y.; Li, L.; Fan, Z.; Zhang, H.-Y.; Wu, X.; Guan, X.-D.; Liu, S.-X. *Nano Lett.* **2002**, *2*, 257-261.
- ¹²⁹ Suzuki, I.; Egawa, Y.; Mizukawa, Y.; Hoshi, T.; Anzai, J.-I. *Chem. Commun.* **2002**, 164-165.
- ¹³⁰ Zhang, B.; Breslow, R. *J. Am. Chem. Soc.* **1993**, *115*, 9353-9354.

- ¹³¹ Breslow, R.; Zhang, B. *J. Am. Chem. Soc.* **1996**, *118*, 8495-8496.
- ¹³² Zhang, B.; Breslow, R. *J. Am. Chem. Soc.* **1997**, *119*, 1676-1681.
- ¹³³ Haskard, C. A.; Easton, C. J.; May, B. L.; Lincoln, S. F. *J. Phys. Chem. B* **1996**, *100*, 14457-14461.
- ¹³⁴ Harada, A.; Furue, M.; Nozakura, S.-I. *Polymer J.* **1980**, *12*, 29-33.
- ¹³⁵ Jiang, T.; Sukumaran, D. K.; Soni, S.-D.; Lawrence, D. S. *J. Org. Chem.* **1994**, *59*, 5149-5155.
- ¹³⁶ Edwards, W. B.; Reichert, D. E.; d'Avignon, D. A.; Welch, M. J. *Chem. Commun.* **2001**, 1312-1313.
- ¹³⁷ French, R. R.; Holzer, P.; Leuenberger, M. G.; Woggon, W.-D. *Angew. Chem. Int. Ed.* **2000**, *39*, 1267-1269.
- ¹³⁸ Yamamura, H.; Yamada, S.; Kohno, K.; Okuda, N.; Araki, S.; Kobayashi, K.; Katakai, R.; Kano, K.; Kawai, M. *J. Chem. Soc., Perkin Trans. I* **1999**, 2943-2948.
- ¹³⁹ a) Liu, Y.; Li, B.; You, C.-C.; Wada, T.; Inoue, Y. *J. Org. Chem.* **2001**, *66*, 225-232. b) Liu, Y.; Chen, Y.; Li, B.; Wada, T.; Inoue, Y. *Chem. Eur. J.* **2001**, *7*, 2528-2535. c) Liu, Y.; Li, L.; Zhang, H.-Y.; Song, Y. *J. Org. Chem.* **2003**, *68*, 527-536.
- ¹⁴⁰ West, L. C.; Wyness, O.; May, B. L.; Clements, P.; Lincoln, S. F.; Easton, C. J. *Org. Biomol. Chem.* **2003**, *1*, 887-894.
- ¹⁴¹ Jiang, T.; Lawrence, D. S. *J. Am. Chem. Soc.* **1995**, *117*, 1857-1858.
- ¹⁴² Breslow, R.; Halfon, S.; Zhang, B. *Tetrahedron* **1995**, *51*, 377-388.
- ¹⁴³ a) Pearce, A. J.; Sinaÿ, P. *Angew. Chem. Int. Ed.* **2000**, *39*, 3610-3612. b) Lecourt, T.; Mallet, J.-M.; Sinaÿ, P. *Tetrahedron Asymmetry* **2002**, *338*, 2417-2419.
- ¹⁴⁴ a) Wang, W.; Pearce, A. J.; Zhang, Y. M.; Sinaÿ, P. *Tetrahedron Asymmetry* **2001**, *12*, 517-523. b) du Roizel, B.; Baltaze, J. P.; Sinaÿ, P. *Tetrahedron Lett.* **2002**, *43*, 2371-2373.
- ¹⁴⁵ a) Lecourt, T.; Mallet, J.-M.; Sinaÿ, P. *Tetrahedron Lett.* **2002**, *43*, 5533-5536. b) Lecourt, T.; Mallet, J.-M.; Sinaÿ, P. *Eur. J. Org. Chem.* **2003**, 4553-4560.
- ¹⁴⁶ Birlirakis, N.; Henry, B.; Berthault, P.; Venema, F.; Nolte R. J. M. *Tetrahedron* **1998**, *54*, 3513-3522.
- ¹⁴⁷ Aoyagi, T.; Ueno, A.; Fukushima, M.; Osa, T. *Macromol. Rapid Commun.* **1998**, *19*, 103-105.
- ¹⁴⁸ Liu, Y.; Wu, C. T.; Xue, G. P.; Li, J. *J. Inclusion Phenom. Macrocyclic Chem.* **2000**, *36*, 95-100.

- ¹⁴⁹ a) Liu, Y.; You, C.-C.; Wada, T.; Inoue, Y. *Tetrahedron Lett.* **2000**, *41*, 6869-6873. b) Liu, Y.; Chen, Y.; Zhang, H. Y.; Liu, S.-X.; Guan, X.-D. *J. Org. Chem.* **2001**, *66*, 8518-8527. c) Liu, Y.; You, C.-C.; Li, B. *Chem. Eur. J.* **2001**, *7*, 1281-1288. d) Liu, Y.; Li, L.; Zhang, H.-Y.; Song, Y. *J. Org. Chem.* **2003**, *68*, 527-536.
- ¹⁵⁰ a) Ruebner, A.; Yang, Z.; Leung, D.; Breslow, R. *Proc. Natl. Acad. Sci. USA* **1999**, *96*, 14692-14693. b) Baugh, S. D. P.; Yang, Z.; Leung, D. K.; Wilson, D. M.; Breslow, R. *J. Am. Chem. Soc.* **2001**, *123*, 12488-12494.
- ¹⁵¹ a) Anasuma, H.; Kakazu, M.; Shibita, M.; Hishiya, T.; Komiyama, M. *Chem. Commun.* **1997**, 1971-1972. b) Hishiya, T.; Shibita, M.; Kakazu, M.; Anasuma, H.; Komiyama, M. *Macromolecules* **1999**, *32*, 2265-2269. c) Anasuma, H.; Hishiya, T.; Komiyama, M. *Adv. Mater.* **2000**, *12*, 1019-1030.
- ¹⁵² Harada, A.; Furue, M.; Nozakura, S.-I. *Macromolecules* **1976**, *9*, 705-710.
- ¹⁵³ Weickenmeier, M.; Wenz, G. *Macromol. Rapid Commun.* **1996**, *17*, 731-736.
- ¹⁵⁴ Davis, M. E.; Bellocq, N. C. *J. Inclusion Phenom. Macrocyclic Chem.* **2002**, *44*, 17-22.
- ¹⁵⁵ Harada, A.; Li, J.; Kamachi, M. *Nature* **1993**, *364*, 516-518.
- ¹⁵⁶ Sandier, A.; Brown, W.; Mays, H. *Langmuir* **2000**, *16*, 1634-1642.
- ¹⁵⁷ Weickenmeier, M.; Wenz, G.; Huff, J. *Macromol. Rapid Commun.* **1997**, *18*, 1117-1123.
- ¹⁵⁸ Ikeda, T.; Lee, W. K.; Ooya, T.; Yui, N. *J. Phys. Chem. B* **2003**, *107*, 14-19.
- ¹⁵⁹ a) Mazzaglia, A.; Donohue, R.; Ravoo, B. J.; Darcy, R. *Eur. J. Org. Chem.* **2001**, 1715-1721. b) Skiba, M.; Skiba-Lahiani, M.; Arnaud, P. *J. Inclusion Phenom. Macrocyclic Chem.* **2002**, *44*, 151-154. c) Auzély-Velty, R.; Péan, C.; Djedaïni-Pillard, F.; Zemb, T.; Perly, B. *Langmuir* **2001**, *17*, 504-510. d) Bügler, J.; Sommerdijk, N. A. J. M.; Visser, A. J. W. G.; Van Hoek, A.; Nolte, R. J. M.; Engbersen, J. F. J.; Reinhoudt, D. N. *J. Am. Chem. Soc.* **1999**, *121*, 28-33.
- ¹⁶⁰ Donohue, R.; Mazzaglia, A.; Ravoo, B. J.; Darcy, R. *Chem. Commun.* **2002**, 2864-2865.
- ¹⁶¹ Ravoo, B. J.; Darcy, R. *Angew. Chem. Int. Ed.* **2000**, *39*, 4324-4326.
- ¹⁶² Sukegawa, T.; Furuike, T.; Niikura, K.; Yamagashi, A.; Monde, K.; Nishiura, S.-I. *Chem. Commun.* **2003**, 430-431.
- ¹⁶³ Ravoo, B. J.; Jacquier, J.-C.; Wenz, G. *Angew. Chem. Int. Ed.* **2003**, *42*, 2066-2070.

- ¹⁶⁴ a) Mazzaglia, A.; Scolaro, L. M.; Darcy, R.; Donohue, R.; Ravoo, B. J. *J. Inclusion Phenom. Macrocyclic Chem.* **2002**, *44*, 127-132. b) Sortino, S.; Petralia, S.; Darcy, R.; Donohue, R.; Mazzaglia, A. *New J. Chem.* **2003**, *27*, 602-608.
- ¹⁶⁵ a) Ravoo, B. J. *J. Controlled Release* **2001**, *72*, 254-256. b) Nolan, D.; Darcy, R.; Ravoo, B. J. *Langmuir* **2003**, *19*, 4469-4472.
- ¹⁶⁶ Willner, I.; Eichen, Y. *J. Am. Chem. Soc.* **1987**, *109*, 6862-6863.
- ¹⁶⁷ Liu, Y. L.; Male, K. B.; Bouvrette, P.; Luong, J. H. T. *Chem. Mater.* **2003**, *15*, 4172-4180.
- ¹⁶⁸ a) Liu, J.; Ong, W.; Kaifer, A. E.; Peinador, C. *Langmuir* **2002**, *18*, 5981-5983. b) Liu, J.; Alvarez, J.; Ong, W.; Roman, E.; Kaifer, A. E. *J. Am. Chem. Soc.* **2001**, *123*, 11148-11154. c) Alvarez, J.; Liu, J.; Roman, E.; Kaifer, A. E. *Chem. Commun.* **2000**, 1151-1152. d) Liu, J.; Ong, W.; Roman, E.; Lynn, M. J.; Kaifer, A. E. *Langmuir* **2000**, *16*, 3000-3002.
- ¹⁶⁹ a) Liu, J.; Medoza, S.; Román, E.; Lynn, M. J.; Xu, R.; Kaifer, A. E. *J. Am. Chem. Soc.* **1999**, *121*, 4304-4305. b) Liu, J.; Alvarez, J.; Kaifer, A. E. *Adv. Mat.* **2000**, *12*, 1381-1383.
- ¹⁷⁰ a) Willner, I.; Mandler, D. *J. Am. Chem. Soc.* **1989**, *111*, 1330-1336. b) Willner, I.; Eichen, Y. *J. Am. Chem. Soc.* **1989**, *111*, 1884-1886.
- ¹⁷¹ a) Strimbu, L.; Liu, J.; Kaifer, A. E. *Langmuir* **2003**, *19*, 483-485. b) Liu, J.; Alvarez, J.; Kaifer, A. E. *Langmuir* **2001**, *17*, 6762-6764.
- ¹⁷² Liu, J.; Alvarez, J.; Ong, W.; Kaifer, A. E. *Nano Lett.* **2001**, *1*, 57-60.
- ¹⁷³ a) Velic, D.; Köhler, G. *Chem. Phys. Lett.* **2003**, *371*, 483-489. b) Michalke, A.; Janshoff, A.; Steinem, C.; Henke, C.; Sieber, M.; Galla, H.-J. *Anal. Chem.* **1999**, *71*, 2528-2533. d) Yamamoto, H.; Maeda, Y.; Kitano, H. *J. Phys. Chem. B* **1997**, *101*, 6855-6860. e) Maeda, Y.; Kitano, H. *J. Phys. Chem. B* **1995**, *99*, 487-488. f) Wang, Y.; Kaifer, A. *J. Phys. Chem. B* **1998**, *102*, 9922-9927. g) Weisser, M.; Nelles, G.; Wenz, G.; Mittler-Neher, S. *Sens. Actuators B* **1997**, *38-39*, 58-67.
- ¹⁷⁴ a) Henke, C.; Steinem, C.; Janshoff, A.; Steffan, G.; Luftmann, H.; Sieber, M.; Galla, H.-J. *Anal. Chem.* **1996**, *68*, 3158-3165. b) He, P.; Ye, J.; Fang, Y.; Suzuki, I.; Osa, T. *Anal. Chim. Acta* **1997**, *337*, 217-233. c) Lahav, M.; Ranjit, K. T.; Katz, E.; Willner, I. *Chem. Commun.* **1997**, 259-260.
- ¹⁷⁵ Qian, J.; Hentschke, R.; Knoll, W. *Langmuir* **1997**, *13*, 7092-7098.
- ¹⁷⁶ Almirall, E.; Fragoso, A.; Cao, R. *Electrochem. Commun.* **1999**, *1*, 10-13.

- ¹⁷⁷ Weisser, M.; Nelles, G.; Wohlfart, P.; Wenz, G.; Mittler-Neher, S. *J. Phys. Chem. B* **1996**, *100*, 17893-17900.
- ¹⁷⁸ a) Rojas, M. T.; Königer, R.; Stoddart, J. F.; Kaifer, A. E. *J. Am. Chem. Soc.* **1995**, *117*, 336-343. b) Kaifer, A. E. *Isr. J. Chem.* **1996**, *36*, 389-397. c) Kaifer, A. E. *Acc. Chem. Res.* **1999**, *32*, 62-71. d) Lee, J.-Y.; Park, S.-M. *J. Phys. Chem. B* **1998**, *102*, 9940-9945.
- ¹⁷⁹ Lee, J.-Y.; Park, S.-M. *J. Phys. Chem. B* **1998**, *102*, 9940-9945.
- ¹⁸⁰ Beulen, M. W. J.; Bügler, J.; De Jong, M. R.; Lammerink, B.; Huskens, J.; Schönherr, H.; Vancso, G. J.; Boukamp, B. A.; Wieder, H.; Offenhäuser, A.; Knoll, W.; Van Veggel, F. C. J. M.; Reinhoudt, D. N. *Chem. Eur. J.* **2000**, *6*, 1176-1183.
- ¹⁸¹ Beulen, M. W. J.; Bügler, J.; Lammerink, B.; Geurts, F. A. J.; Biemond, E. M. E. F.; Van Leerdam, K. G. C.; Van Veggel, F. C. J. M.; Engbersen, J. F. J.; Reinhoudt, D. N. *Langmuir* **1998**, *14*, 6424-6429.
- ¹⁸² Schönherr, H.; Beulen, M. W. J.; Bügler, J.; Huskens, J.; Van Veggel, F. C. J. M.; Reinhoudt, D. N.; Vancso, G. J. *J. Am. Chem. Soc.* **2000**, *122*, 4963-4967.
- ¹⁸³ De Jong, M. R.; Huskens, J.; Reinhoudt, D. N. *Chem. Eur. J.* **2001**, *7*, 4164-4170.
- ¹⁸⁴ a) Zapotoczny, S.; Auletta, T.; De Jong, M. R.; Schönherr, H.; Huskens, J.; Van Veggel, F. C. J. M.; Reinhoudt, D. N.; Vancso, G. J. *Langmuir* **2002**, *18*, 6988-6994. b) Auletta, T.; De Jong, M. R.; Mulder, A.; Zapotoczny, S.; Zou, S.; Schönherr, H.; Vancso, G. J.; Huskens, J.; Reinhoudt, D. N. *J. Am. Chem. Soc.* **2004**, *126*, 1577-1584.
- ¹⁸⁵ Fragoso, A.; Caballero, J.; Almirall, E.; Villalonga, R.; Cao, R. *Langmuir* **2002**, *18*, 5051-5054.
- ¹⁸⁶ Huskens, J.; Deij, M. A.; Reinhoudt, D. N. *Angew. Chem. Int. Ed.* **2002**, *41*, 4467-4471.
- ¹⁸⁷ Banerjee, I. A.; Yu, L.; Matsui, H. *J. Am. Chem. Soc.* **2003**, *125*, 9542-9543.

Photocontrolled release and uptake of a porphyrin guest by dithienylethene-tethered β -cyclodextrin host dimers*

3.1 Introduction

One of the ultimate challenges in chemistry is to obtain external control over molecular properties. This is especially true for the field of synthetic receptor molecules.¹ External control over the selectivity of receptors gives access to tunable host molecules and ideally enables the release and/or uptake of guest molecules at will. Illustrative examples can be found among the work on switchable cation receptors, which has led to tunable receptor molecules that enable the controlled release and transport of cations.²

Analogous to the work on cation receptors, Ueno et al. modified cyclodextrins with photoswitchable azobenzene moieties to obtain photocontrollable receptor molecules for small hydrophobic guests.³ Cyclodextrins are of special interest because of their ability to complex hydrophobic substrates in aqueous solutions, leading to their application in a wide variety of fields such as pharmaceuticals, artificial enzymes, and biomimetic materials.⁴ A variety of photoswitchable cyclodextrins have been synthesized, but only marginal differences in binding affinity have been observed for the different configurations of the photoswitchable unit,^{3b-e} except for an early study by Ueno.^{3a} More recently, there has been considerable interest in cyclodextrin dimers tethered via tunable linkers.⁵⁻⁸ Cyclodextrin dimers are able to

* Parts of this work have been published in: Mulder, A.; Juković, A.; Lucas, L. N.; Van Esch, J.; Feringa, B. L.; Huskens, J.; Reinhoudt, D. N. *Chem. Commun.* **2002**; 2734-2735; Mulder, A.; Juković, A.; Van Leeuwen, F. W. B.; Kooijman, H.; Spek, A. L.; Huskens, J.; Reinhoudt, D. N. *Chem. Eur. J.* **2004**, *10*, 1114-1123.

bind a large variety of guest molecules with relatively high binding constants compared to the parent cyclodextrin.

Ueno et al. were the first to report such a tunable cyclodextrin dimer.⁵ Tethering two β -cyclodextrin cavities with an azobenzene linker gave a photoswitchable β -cyclodextrin dimer. However, no guest species were found that displayed selectivity for one of the two configurations of the dimer.

The groups of Wu⁶ and Liu⁷ synthesized β -cyclodextrin dimers containing oligo(ethylenediamine) tethers. Upon coordination of metal ions the tether flexibility of these dimers is altered, which results in a change in binding affinity. For the guest molecules studied thus far, however, these dimers display only marginal differences in binding properties.

Breslow et al. presented a nice example of a cyclodextrin dimer able to release guest molecules, in which two β -cyclodextrin cavities were tethered via a photocleavable linker.⁸ Irradiation of a dimer-guest complex led to the cleavage of the linker and the precipitation of the guest molecule. However, these dimers were destroyed irreversibly upon photoirradiation.

The use of a photoswitchable tether between the two cyclodextrin cavities is likely the most elegant choice for a tunable cyclodextrin dimer: photons are used to switch between the two forms of the dimer, thereby avoiding the need of additives to initiate switching and the formation of side-products. With a proper choice of the photochromic unit, the switching process is fully reversible.

Among the various photochromic molecules suitable for implementation in a photoswitchable receptor, dithienylethenes are the most promising. Dithienylethenes are photoswitchable molecules that are able to undergo thermally irreversible, fatigue-resistant, photochromic cyclization reactions between two defined states: a relatively flexible open and a rigid closed form.^{9,10} Previously, dithienylethenes have been successfully exploited for the synthesis of photoswitchable saccharide¹¹ and alkali metal ion receptors.¹² In the open form, the two thiophene rings are capable of folding into a parallel conformation, enabling the (possibly cooperative) interaction between the two thiophene-appended moieties, whereas in the closed form these moieties are spaced apart from each other in a rigid fashion (Figure 3.1).¹¹⁻¹³ This work suggested that implementation of dithienylethene linkers in cyclodextrin dimers could enable photochemical tuning of the relative positions of two cyclodextrin cavities within a

cyclodextrin dimer, allowing the reversible switching between mono- and ditopic binding, thereby achieving substantial differences in binding affinity.

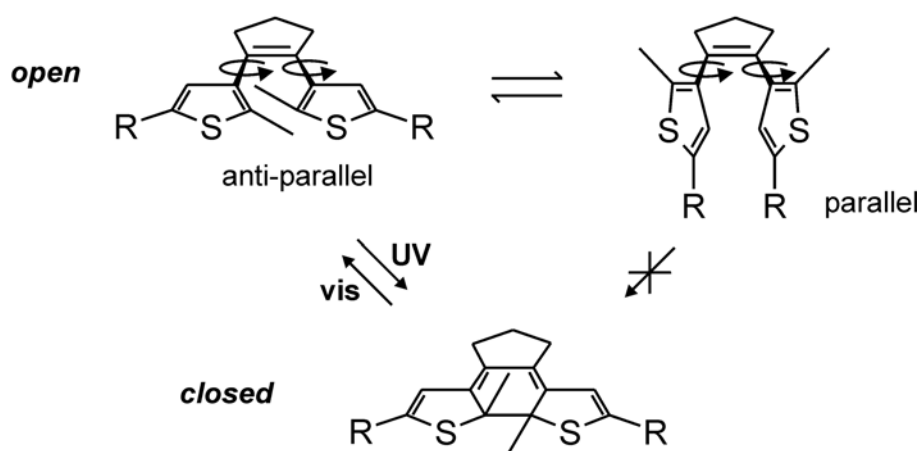
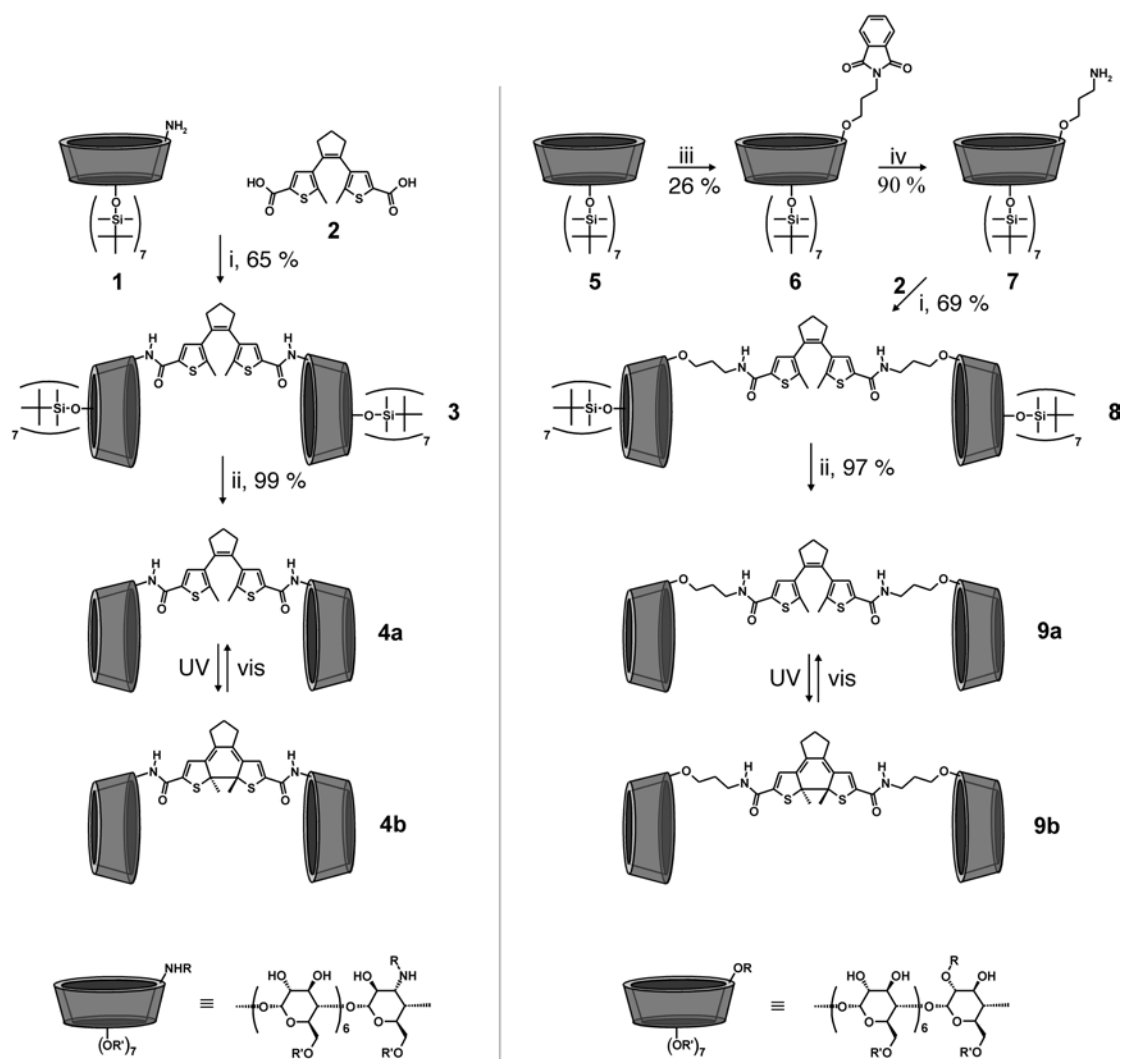


Figure 3.1 Possible conformations of dithienylethenes. In the open form the two thieryl rings can rotate freely with respect to the ethene tether, whereas in the closed form their positions are locked by the formation of an additional bond between the two rings.

This chapter deals with β -cyclodextrin (CD) dimers tethered by a dithienylethene linker. Two dithienylethene-tethered CD dimers have been synthesized (**4** and **9**) with a different connectivity between the CDs and the photochromic units (Scheme 3.1). In dimer **4**, the dithienylethene moiety is attached directly at the secondary sides of the CD cavities, giving a relatively rigid dimer, where most of the rotational freedom is present in the dithienylethene spacer. Therefore, any change in the flexibility of the photochromic spacer may lead to a change in conformational freedom of the dimer. Alternatively, the more flexible dimer **9** was synthesized in which the dithienylethene unit and the secondary sides of the CD cavities are separated by propyl spacers. The binding behavior of the dimers has been studied with isothermal titration microcalorimetry and UV-vis spectroscopy. Molecular modeling has been used as a supportive tool to explain the differences in binding affinities.



Scheme 3.1 Synthesis routes for dimers **4** and **9**. i, HBTU, DIPEA, THF, *r.t.*; ii, TFA, *r.t.*; iii, LiH, *N*-(3-bromopropyl)phthalimide, THF, reflux; iv, $H_2NNH_2 \cdot H_2O$, EtOH, reflux.

3.2 Results and discussion

3.2.1 Synthesis and characterization of the CD dimers

The synthesis of the CD dimers is outlined in Scheme 3.1. Dimer **4**, with the dithienylethene moiety connected directly at the secondary rim of the CD cavity, was synthesized starting from CD amine **1** and 5,5'-(dicarboxydithienyl)cyclopentene¹⁴ **2**. 3-Amino-3-deoxy-heptakis(6-*O*-*tert*-butyldimethylsilyl)- β -cyclodextrin¹⁵ **1** was used as a precursor for dimer **4** to assure a selective and rigid coupling of the dithienylethene unit directly onto the secondary side of the CD. It should be noted that

the modified sugar unit of the CD amine **1** is altrosidic, whereas the remaining sugar units are glucosidic, giving rise to a somewhat distorted CD cavity.¹⁶ An amide coupling of **1** and **2** using *O*-(benzotriazol-1-yl)-*N,N,N',N'*-tetramethyluronium hexafluoro-phosphate (HBTU) as a coupling agent gave the TBDMS-protected dimer **3** in 65 % yield. Subsequent deprotection of the primary hydroxyl groups, using trifluoroacetic acid, gave the water-soluble dimer **4** in near quantitative yield.

The ¹H NMR spectrum of dimer **4a** is depicted in Figure 3.2. The spectrum shows a total of five signals belonging to the dithienylethene tether. The non-equivalency observed for the two diastereotopic protons of the cyclopentene bridge is attributed to the close proximity of the chiral CD cavities.

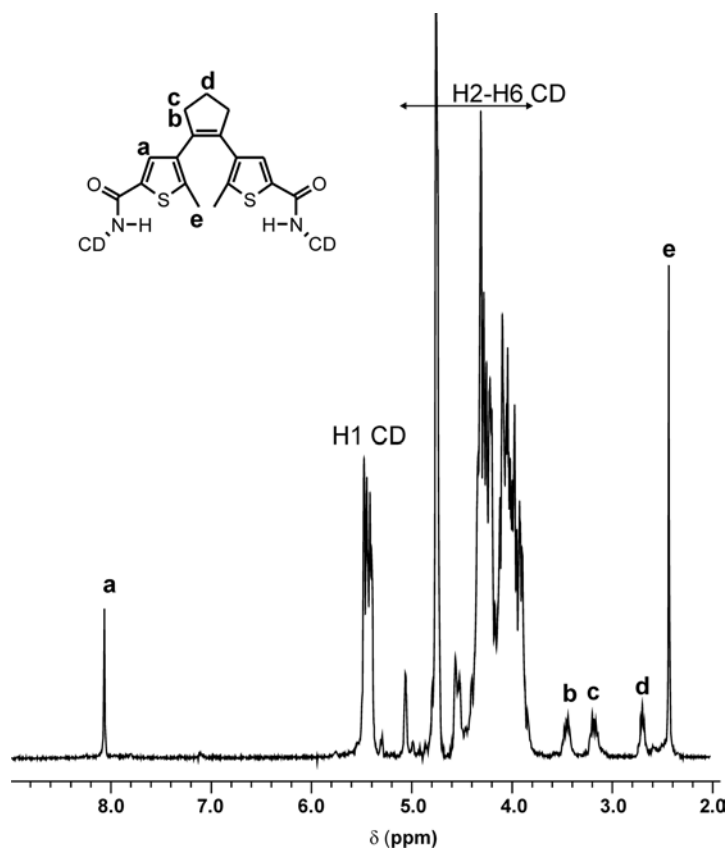


Figure 3.2 ¹H NMR (400 MHz) spectrum of **4a** in D₂O recorded at 353 K.

Partial assignment of the CD signals was achieved by systematic ¹H NMR studies at 800 MHz. The relatively small coupling constant ³J₁₂ found for the modified unit in dimer **4a** indicates that the altrose unit adopted a ⁴C₁ conformation in aqueous solution. This contrasts with coupling constants determined for the altrose unit of

mono(3-amino-3-deoxy)- β -cyclodextrin, ${}^3J_{12} = 7.3$ Hz,¹⁷ indicative of an axial-axial coupling implying that the altrose unit was in the more stable 1C_4 conformation. In aqueous solution, the conformational free energies of the 4C_1 and 1C_4 conformations of α -D-altrose are nearly identical.¹⁸ Apparently, hydrophobic interactions between the dithienylethene unit and the CD cavity forced the conformational equilibrium of the altrose unit to the 4C_1 conformation, in which the dithienylethene spacer was directed towards the cavity. Similar results have been reported by Nolte et al.¹⁹ for CD dimers having a flexible hydrophobic alkyl spacer as a linker. In aqueous solution these dimers formed self-inclusion complexes, where the hydrophobic alkyl tether is included in one of the CD cavities. However, no evidence exists for the formation of a self-inclusion complex for dimer **4a**. Most likely the dithienylethene spacer is positioned partly over the cavity rather than buried inside the cavity. The close proximity of the chiral CD cavities is probably also responsible for the non-equivalency observed for the two diastereotopic protons of the cyclopentene bridge of the dithienylethene linker.

Dimer **9** was synthesized analogously to dimer **4**, starting from **2** and mono-(2-*O*-(3-aminopropyl)-2-deoxy-heptakis(6-*O*-*tert*-butyldimethylsilyl)- β -cyclodextrin (**7**). The CD propylamine **7** was synthesized by selective deprotonation of the more acidic C2-OH of CD derivative **5**²⁰ using LiH and reaction with 1.1 equivalent of the commercially available 3-bromopropylphthalimide to give a statistical mixture of unreacted **5** and mono- and bis-functionalized CD species. Separation by column chromatography gave the mono-phthalimide **6** in 26 % yield. Alkylation of the OH groups of CD does not alter the stereochemistry of the glucose units and leaves the shape of the cavity unchanged. Removal of the phthalimide moiety by reaction with hydrazine gave the CD propylamine **7** after column chromatography in 90 % yield. Although CD derivative **7** has previously been synthesized by alkylation of the 2-*O* position with 3-azidopropyl tosylate and subsequent reduction of the azide functionality to an amine with H₂ and Pd/C,²¹ the alternative synthesis route depicted in Scheme 3.1 was preferred because of easier purification of the statistical mixture by column chromatography and the commercial availability of the propylamine precursor. Coupling of **2** and **7** gave in 69 % yield the TBDMS-protected dimer **8**, which was converted to the water-soluble dimer **9** in near quantitative yield.

The diastereotopic hydrogens of the cyclopentene bridge in dimer **9** appeared as a single signal in the ^1H NMR spectrum (not shown). Apparently, introduction of the propyl chains spaces the CD cavities and the dithienylethene unit apart thereby reducing the influence of the chiral CD cavities on the diastereotopic hydrogens.

3.2.2 Switching behavior of the dimers

The photochromic behavior of the dimers was studied by irradiation with a high-pressure mercury lamp with band-pass filters. Photochemical reactions were monitored by UV-vis and ^1H NMR spectroscopy. The absorption spectra of dimers **4** and **9** (Figure 3.3, left and right) show a high degree of similarity and are typical for the type of dithienylethene moiety used for the spacing of the dimers.¹⁴ Aqueous solutions of the open forms of both dimers showed strong absorption in the UV region with absorption maxima at 267 and 254 nm for dimers **4a** and **9a**, respectively. The colorless aqueous solutions turned red upon irradiation at 313 nm and an absorption band appeared around 344 nm together with a broad absorption band in the visible region of the absorption spectra with a maximum at 524 nm for both dimers **4b** and **9b**.

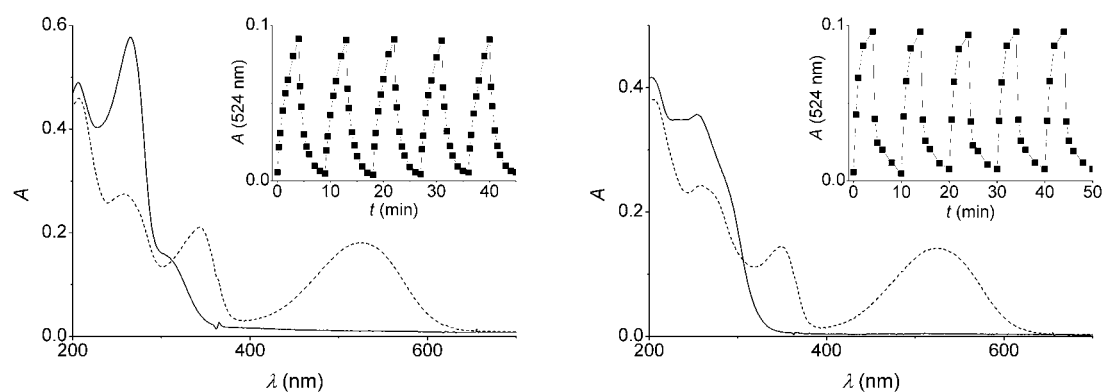


Figure 3.3 Absorption spectra of 20 μM **4** (left) and 19 μM **9** (right) in water before (open form, —) and after (photostationary state mixture, ---) photoirradiation with 313 nm light. The insets depict the absorbance at 524 nm during alternate irradiation with 313 and > 460 nm light.

UV-vis spectra recorded before reaching the photostationary state showed sharp isobestic points, indicative of only two interchanging species. ^1H NMR spectra of irradiated samples confirmed this, showing a clean conversion to a single new product with C_2 symmetry. Figure 3.4 gives the ^1H NMR spectrum of an irradiated sample of dimer **4** (left) and the conversion of the thienyl signals during irradiation (right). The thienyl hydrogens showed a very pronounced upfield chemical shift (1.0 ppm for dimer **4** and 0.7 ppm for dimer **9**) indicating the loss of aromatic character of the thienyl moiety. These spectral changes are characteristic for the formation of the closed form. Smaller upfield shifts are observed for the signals belonging to the protons of the cyclopentene bridge and methyl groups.

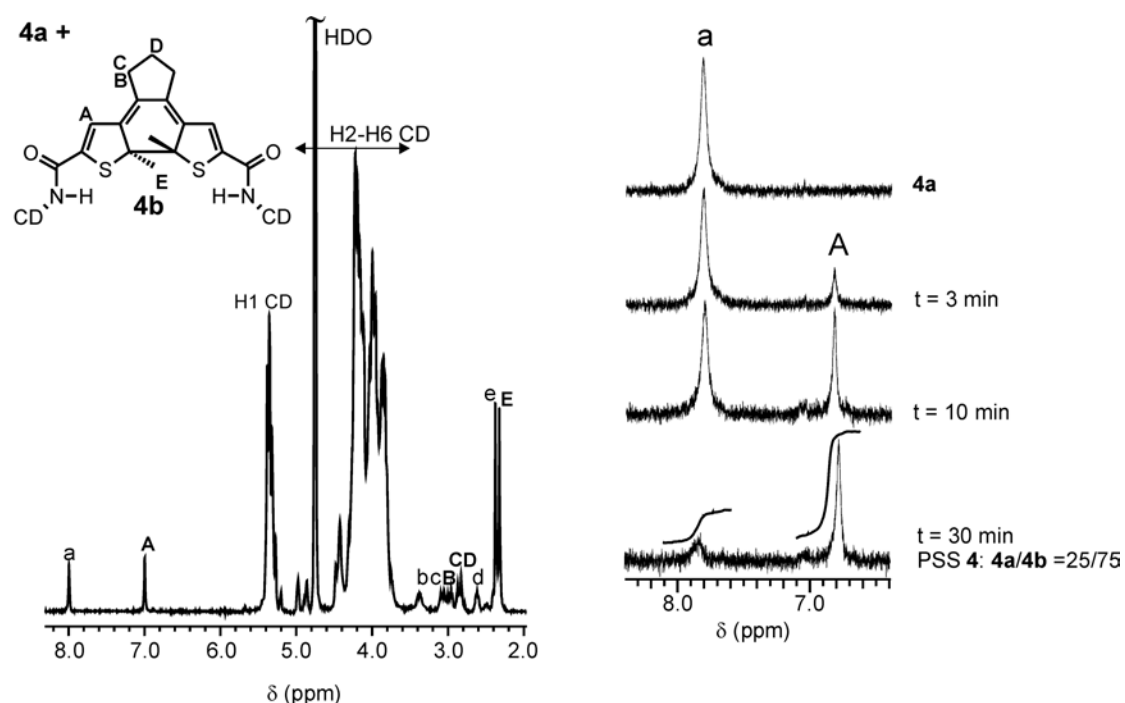


Figure 3.4 ^1H NMR (400 MHz, 353 K) spectrum of a sample of dimer **4** irradiated at 313 nm (left) and spectra (300 MHz, 298 K) of the thienyl signal of dimer **4** at various irradiation times (right).

Due to non-zero absorption of the closed forms in the UV region, both ring-closure and ring-opening take place during photoexcitation in the UV region, leading to a photostationary state (PSS) mixture. The absorption spectra of the PSS of **4a/4b** and **9a/9b** are given in Figure 3.3. The composition of the PSS mixture can be

obtained by ^1H NMR (Figure 3.4, right) or by modeling of the UV-vis spectra (see below). For both dimers the PSS at $\lambda = 313$ nm consisted of 25 % of the open and 75 % of the closed form. The PSS mixtures are stable at room temperature in the dark. Irradiation of the PSS mixtures with visible light ($\lambda > 460$ nm) led to the disappearance of the absorption bands in the visible region and completely restored the absorption spectra of the open forms, indicating that the photochemical ring-opening/ring-closure process is fully reversible.

The insets in Figure 3.3 show the absorption at 524 nm during alternate irradiation at $\lambda = 313$ nm and $\lambda > 460$ nm. Such alternate switching did not lead to any noticeable decomposition of the photochromic unit after five cycles, demonstrating the excellent fatigue-resistance⁹ of compounds **4** and **9**. Results obtained with dimers **4** and **9** are comparable to results obtained with similar dithienylethene switches and indicate that the coupling and close proximity of the CD cavities does not interfere with the switching process and that the characteristics of the dithienylethene tether are maintained.¹⁴

3.2.3 UV-vis modeling

Modeling of the UV-vis spectra, in order to directly determine the composition of a mixture of the open and closed forms of a dimer, offers an easy and practical alternative compared to the generally used integration of the characteristic thiophene proton signals in the ^1H NMR spectra. Modeling of the UV-vis spectra was performed by fitting a set of Gaussians to the absorption bands of the spectra of the open forms of the dimers. It was assumed that the decreasing bands between 250-310 nm stem only from the open forms. Therefore, spectra of irradiated samples were fitted with this set of Gaussians for the open form and a second set of Gaussians at < 250 nm and at around 350 and 520 nm representing the closed form of the dimer. Fitting ten or more UV-vis spectra of a dimer recorded at different irradiation times (313 nm) allowed the calculation of the extinction coefficients and the full absorption spectra of the closed form of the dimers (see Table 3.1).

Table 3.1 Parameters for the sets of Gaussians used for the fitting of the absorption spectra of **4** and **9**.^a

4a			4b		
λ_{\max}	FWHM	ϵ_{\max}	λ_{\max}	FWHM	ϵ_{\max}
195.5	57.2	23.7	171.3	105.6	12.6
266.3	14.0	17.6	208.6	10.0	10.6
315.2	11.5	4.3	343.2	15.3	10.0
			521.2	47.4	11.5
9a			9b		
λ_{\max}	FWHM	ϵ_{\max}	λ_{\max}	FWHM	ϵ_{\max}
197.2	26.5	25.2	207.5	15.9	17.2
251.8	19.1	15.2	264.5	34.8	11.5
286.9	19.4	11.2	346.1	19.7	11.4
			520.3	48.2	11.7

^a λ_{\max} (nm), FWHM (nm), ϵ_{\max} ($10^3 \text{ cm}^{-1} \text{ M}^{-1}$).

The top part of Figure 3.5 shows the recorded and modeled absorption spectra of the open form and PSS mixture of dimer **4** and the calculated absorption spectrum of the closed form **4b**. The sets of Gaussians that constitute the calculated absorption spectrum of the open and closed forms of **4** are shown at the left and right lower half of Figure 3.5, respectively. Equally good fits were obtained for dimer **9** (data shown in Table 3.1).

Knowing the extinction coefficients of both the open and closed forms of the dimer allowed the determination of the ratio of the open and closed forms of a dimer from a single UV-vis spectrum. Control experiments showed a good correlation between ratios determined by integration of the thiophene peaks using ^1H NMR spectroscopy and modeling of the UV-vis spectra.²²

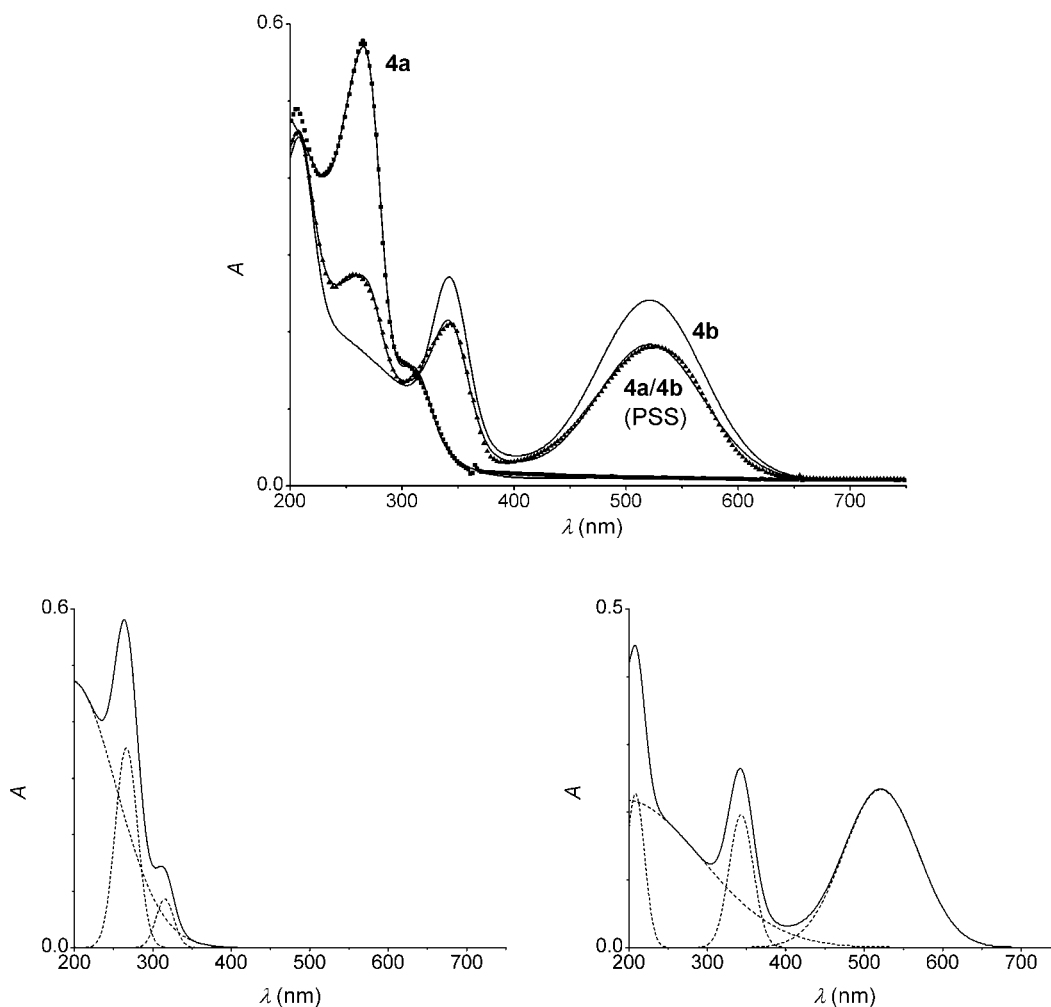


Figure 3.5 Measured (markers) and modeled (lines) absorption curves of $19 \mu\text{M}$ **4** in water (top; **4a** (■), PSS mixture of **4a/4b** (▲), and **4b**). Set of Gaussians (---) that constitute the calculated absorption spectra (—) of **4a** (bottom left) and **4b** (bottom right).

3.2.4 Complexation studies

As a guest molecule for the binding studies meso-tetrakis(4-sulfonatophenyl)porphyrin (TSPP) was used. The binding of TSPP by CD²³ and CD dimers¹⁹⁻²⁴ has been well studied. TSPP is especially interesting because of its symmetry, imposing a well-defined symmetrical binding mode. TSPP has four sulfonatophenyl moieties attached to the porphyrin ring, which functions as a flat and rigid platform. The four sulfonatophenyl moieties offer a total of four available binding sites for CD complexation. Previous studies have shown, however, that native CD binds TSPP in a 2:1 fashion, complexing two opposite 4-sulfonatophenyl

moieties.^{23a} Complexation of two adjacent binding sites is sterically less favorable and gives rise to weaker complexation.²⁵

Binding of TSPP by the open and closed forms of the dimers **4** and **9** was studied using isothermal titration microcalorimetry. Binding curves of the open forms of the dimers were fitted with a 1:1 binding model using the association constant, K , and the binding enthalpy, ΔH° , as independent fitting parameters. In order to determine the thermodynamic binding parameters for the binding of TSPP in the closed forms of the dimers, **4b** and **9b**, calorimetric studies were performed with mixtures of the open and closed forms of a dimer. Compositions of the mixtures were determined beforehand by UV-vis spectroscopy using the UV-vis modeling described above. Binding curves obtained for these mixtures were fitted by calculating the net heat effects for the binding of TSPP to the open form of the dimer using the composition of the mixture and the binding parameters as obtained for the titration of TSPP to the open form of the dimer, while optimizing the binding constant and enthalpy of the closed forms. For comparison, microcalorimetry experiments were performed for the complexation of TSPP by native CD. The obtained thermodynamic parameters are summarized in Table 3.2.

Table 3.2 Thermodynamic parameters of the complexation of TSPP to the open and closed forms of **4** and **9**, as determined by isothermal titration microcalorimetry at 298 K.

host	K (M^{-1})	ΔG° (kcal mol ⁻¹)	ΔH° (kcal mol ⁻¹)	$T\Delta S^\circ$ (kcal mol ⁻¹)
CD	$(3.1 \pm 0.4) \times 10^4$	-6.1 ± 0.1	-4.3 ± 0.2	1.8 ± 0.3
4a	$(3.3 \pm 0.4) \times 10^6$	-8.9 ± 0.1	-12.8 ± 0.4	-3.9 ± 0.5
4b	$(9.7 \pm 1.3) \times 10^4$	-6.8 ± 0.1	-5.3 ± 1.1	1.5 ± 1.2
9a	$(3.3 \pm 0.2) \times 10^6$	-8.9 ± 0.1	-11.1 ± 0.8	-2.2 ± 0.9
9b	$(1.2 \pm 0.2) \times 10^6$	-8.3 ± 0.1	-11.2 ± 1.0	-2.9 ± 1.1

In Figure 3.6 the net heat evolved per injection is plotted against the molar ratio of guest to host for the titrations of TSPP to dimer **4**. The titration of TSPP to the open form of the dimer, **4a**, gave a binding curve typical of a 1:1 complex formation (Figure 3.6, left). The obtained thermodynamic parameters (K and ΔH°) are indicative of a strong 1:1 complex with both CD cavities participating in binding; the measured

K value is substantially larger than the binding constant of CD to TSPP and the binding enthalpy is close to twice the binding enthalpy of a single CD cavity. The negative entropy value accompanying the binding of TSPP by **4a** is attributed to enthalpy-entropy compensation²⁶ and restriction of the mobility of the spacer of the dimer upon binding the guest molecule.

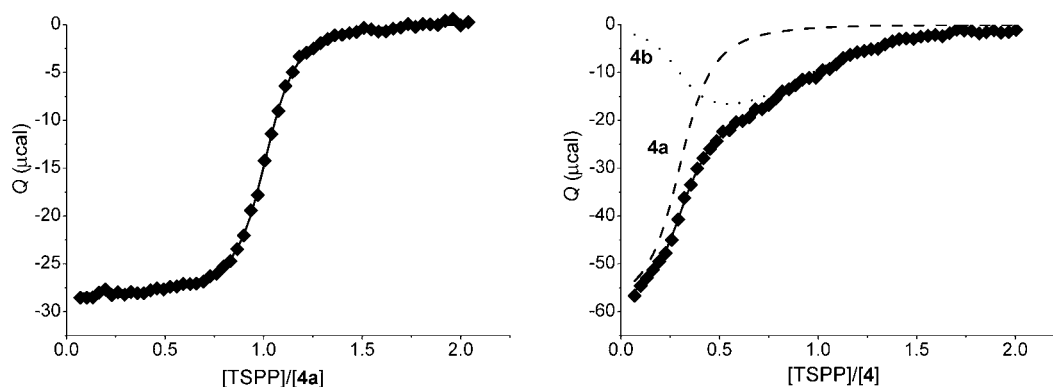


Figure 3.6 Heat evolved per injection plotted against the $[TSPP]/[4]$ ratio (markers) and fit (solid line) for the calorimetric titrations of TSPP to **4a** (left) and to the PSS mixture of **4** (right) in water at 298 K. For the PSS mixture, the calculated contributions for the binding of TSPP by **4a** (--) and **4b** (···) to the heat profile are given.

Figure 3.6, right, shows the titration curve for the titration of TSPP to the PSS mixture of the open and closed forms of dimer **4**. The obtained titration curve shows the presence of two superimposed binding curves, as witnessed by an inflection point around 0.3 and a faint one around 1. The former nicely corresponds to the fraction of the open form **4a** in the PSS mixture. Therefore, the initial strong binding displayed in the binding curve is attributed to binding of TSPP in the open form. Fitting of the titration curve as described above, taking into account the previously determined parameters for the binding of the open form **4a**, gave the thermodynamic parameters for the binding of TSPP in the closed form **4b**. As can be seen from Table 3.2 and is evident from the titration curves, there is a marked difference between the binding of TSPP in the open and closed forms of dimer **4**. There is a factor of 35 difference in binding constant between the binding of TSPP in the open form, **4a**, and the closed form, **4b**. In fact, all thermodynamic parameters of the binding of TSPP by the closed dimer **4b** are indicative for a monovalent CD-TSPP interaction and are in the same

range as the thermodynamic values obtained for the complexation of TSPP by native CD. Apparently, the closed form does not sterically allow a 1:1 binding with TSPP where both cavities are strongly binding a sulfonatophenyl ring of TSPP in a cooperative fashion.

With the introduction of the propyl spacer between the CD cavities and the dithienylethene moiety, the difference in binding affinity between the open and closed forms of dimer **9** is lost. As can be seen from the thermodynamic parameters obtained for the binding of TSPP in **9a** and **9b** (Table 3.2), very similar binding enthalpy and entropy values were obtained for both the open and closed forms of dimer **9**. The measured binding enthalpies indicate that both dimers bind TSPP using two CD cavities. It seems that the flexible propyl spacers provide enough rotational freedom for the dimers to overcome the imposed rigidity upon closure of the dithienylethene moiety. As observed for **4a**, also dimers **9a** and **9b** show negative binding entropies. Apparently the strong binding employing both cavities restricts the mobility of host and guest in the complex.

Nolte et al. have found both 1:1 and 2:2 binding modes for the binding of TSPP by CD dimers.^{24b} Flexible alkyl chain-tethered CD dimers display mostly 1:1 binding, whereas the sigmoidal shape of the fluorescence titration curve for the binding of TSPP by a relatively rigid 2,2'-bipyridine-tethered CD dimer was explained by a 2:2 binding mode. The inflection points in the calorimetric titration curves obtained for the titrations of the dimers **4** and **9** with TSPP does not exclude the possibility of 2:2 binding. A 2:2 binding mode, however, should be expressed in a higher concentration dependence compared to a 1:1 binding mode. In order to reveal the binding mode of the open and closed forms of dimers **4** and **9**, all titrations were performed at three different concentrations. For all four dimers the obtained titration curves were best fitted with a 1:1 binding model. Additionally, fluorescence titrations were performed with the relatively rigid dimer **4a**. Figure 3.7 shows the obtained titration curve for the binding of TSPP by the open form **4a**. The binding of TSPP by the cavities of dimer **4a** resulted in an exponential decrease in fluorescence intensity, giving a titration curve that corresponds to the formation of a 1:1 complex. Clearly, no sigmoidal behavior is observed that would imply a 2:2 binding mode. Fitting of the titration curve with a 1:1 model gave a binding constant of $1 \times 10^7 \text{ M}^{-1}$, which is in good agreement with the binding constant found using microcalorimetry. The shape of the titration curve for the binding of TSPP by **4b** could not be determined. Fluorescence

titrations performed with a PSS mixture of **4** were dominated by the stronger binding **4a**.

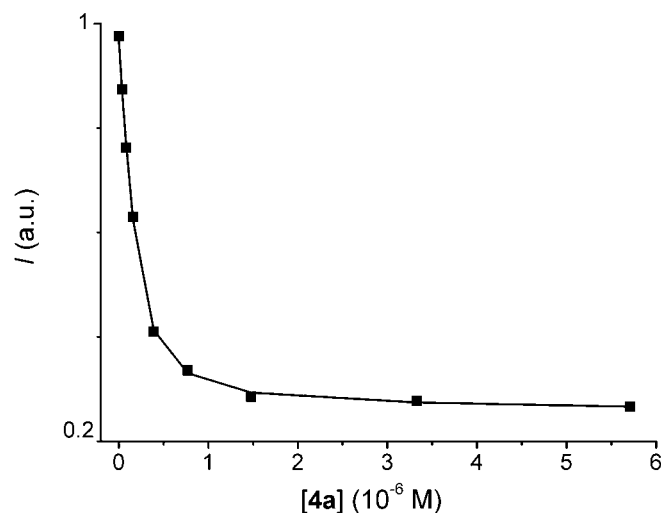


Figure 3.7 Fluorescence titration curve (markers) and 1:1 fit (solid line) for the complexation of TSPP ($0.2 \mu\text{M}$) by **4a**.

Another point that needs consideration with CD dimer-TSPP complexes is the binding geometry of the guest. Both syn and anti 1:1 binding geometries have been observed for the complexes of CD dimers with TSPP, depending on the tether length and flexibility.^{24b} The peak splitting of the porphyrin ring protons in ^1H NMR spectra can be used to elucidate the binding fashion of TSPP with CD dimers. However, for the complexes of TSPP with dimers **4a** and **9a**, very complex ^1H NMR spectra were obtained, in which signals of both TSPP and the dithienylethene moieties of the dimers show extensive splitting and broadening. Even at -10 °C, using a mixture of MeOD and D_2O , the spectra were too complicated and the signals too broad to be exploited for assignment of the binding fashion. CPK models suggest that dimers **4** and **9** are able to bind TSPP in the sterically less demanding anti fashion, both in their open and closed forms. It is therefore likely that both dimers bind TSPP in the anti fashion and that the relatively slow exchange process and possibly asymmetric positioning of the dithienylethene units over the porphyrin face cause the complicated ^1H NMR spectra.

3.2.5 Molecular Modeling

Molecular modeling was used to further validate the interpretation of the observed complexation differences between the dimers. The CD dimers were built using the data available for CD obtained from the Cambridge Crystallographic Database and the X-ray crystal structure of 5,5'-(dialdehydodithienyl)cyclopentene, which is a precursor for the synthesis of **2** (Figure 3.8).

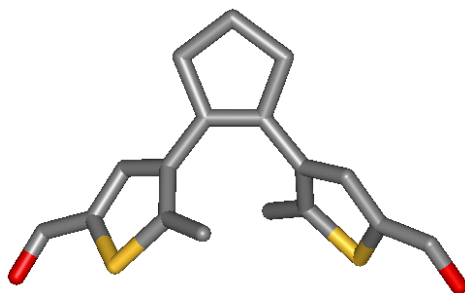


Figure 3.8 X-ray crystal structure of 5,5'-(dialdehydodithienyl)cyclopentene. Hydrogens are omitted for clarity.

Figure 3.9 shows the energy-minimized structures of the complexes of TSPP with the open and closed forms of dimers **4** and **9**. The structure obtained for the complex of the open form **4a** and TSPP (Figure 3.9, top left) suggests that the dimer is able to form a strong complex with TSPP employing both cavities. The rotational freedom in the open form of the dithienylethene moiety allows the dimer to fold over the porphyrin guest and allows both CD cavities to participate in the binding of TSPP. Most importantly, both cavities are shifted far over the sulfonatophenyl moieties and even over part of the porphyrin base, shielding the most hydrophobic parts of TSPP from the bulk water. The hydrophilic sulfonate groups are sticking out from the primary sides of the CD cavities.

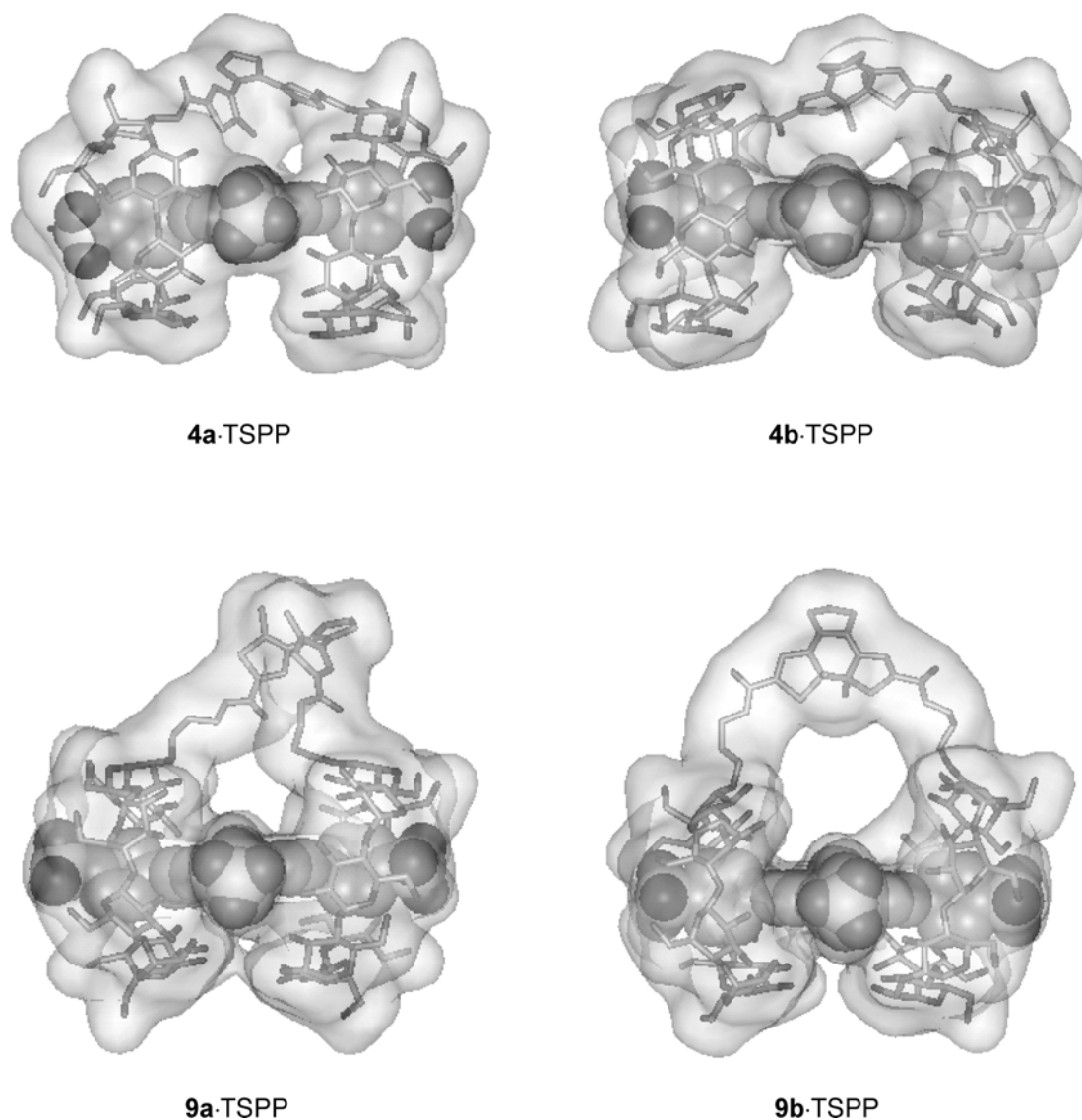


Figure 3.9 CHARMm-minimized structures of the complexes with TSPP of dimers **4** and **9**.

The structure obtained for the closed form **4b** and TSPP (Figure 3.9, top right) indicates that the CD cavities are spaced too far apart by the rigid closed form of the dithienylethene tether to allow both cavities to contribute to the binding of TSPP to the same extent as in **4a**. The dithienylethene moiety is situated diagonally over the porphyrin base in the minimized structure thus minimizing the distance between the two CD cavities. Nevertheless, even in this conformation it is not possible for both cavities to completely shift over the sulfonatophenyl rings to interact with and fully shield the porphyrin base. This corroborates the conclusions from the calorimetric data for TSPP and **4b** that the binding of TSPP is mainly due to a monovalent CD-

sulphonatophenyl interaction with possibly a slight contribution from the second CD cavity. Likely, the guest moves back and forth between the two cavities in the complex with **4b**.

Dimers **9a** and **9b** are both able to tightly bind TSPP (Figure 3.9, bottom). In both complexes, both CD cavities are shifted partly over the porphyrin-base, assuring a strong interaction with and shielding of the hydrophobic parts of the guest molecule. The flexible propyl spacers between the dithienylethene moiety and the CD cavities are able to compensate for the rigidity imposed by the closed dithienylethene switch and allow the CD cavities to come in close proximity to each other, enabling the tight binding of TSPP. The similar binding modes found for the binding of TSPP by the open and closed forms of dimer **9** are reflected in the similar thermodynamic parameters found for the complex formation of these dimers.

3.2.6 Photo-triggered release and uptake

UV-vis spectroscopy allows the real-time determination of the ratio of uncomplexed and complexed TSPP upon irradiation of dimer-TSPP complexes. The absorption maximum of TSPP shifts to the red and the absorbance decreases upon complexation by CD.^{23b} Figure 3.10 shows part of the absorption spectra of complexes of TSPP and dimers **4a** and **9a** upon irradiation at 313 nm. The absorption maximum of TSPP in aqueous solution at 413 nm showed a red shift to 418 and 420 nm upon addition of the dimers **4a** and **9a**, respectively, indicative of the complex formation between TSPP and the dimers. The absorption of TSPP decreased upon irradiation of its complex with dimer **4a** at 313 nm, and simultaneously the absorption of uncomplexed TSPP increased, with an isosbestic point at 416 nm (Figure 3.10, left). Apparently, upon closing the dithienylethene moiety, TSPP is released from the CD dimer. This is in agreement with the data obtained by microcalorimetry: TSPP will be strongly bound by **4a** at the concentrations used for the UV-vis measurement, whereas the closed form **4b** will not significantly bind TSPP.

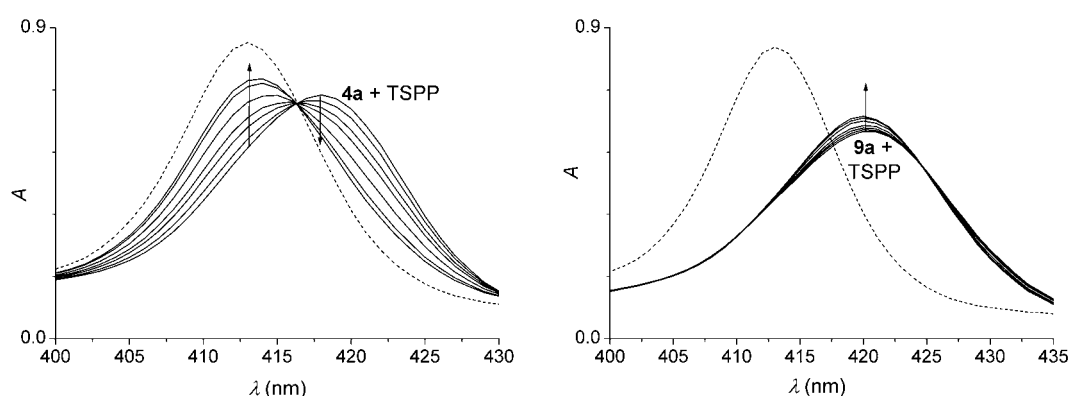


Figure 3.10 Absorption spectra (0 to 25 min) of 2 μM of the complexes of TSPP with **4a** (left) and **9a** (right) in water upon irradiation at $\lambda = 313$ nm. Also shown is the spectrum of 2 μM TSPP in water (···).

Irradiation of the complex of dimer **9a** and TSPP at 313 nm did not lead to any noteworthy release of TSPP (Figure 3.10, right). A slight increase of absorbance at 420 nm was observed, which might indicate that the molecular environment around the complexed TSPP molecule is changing upon closing the dithienylethene tether, but the absorbance of uncomplexed TSPP at 413 nm remained constant during the experiment. From these results it can be concluded that both the open and closed forms of dimer **9** are binding TSPP strongly at these concentrations, which is in good agreement with the microcalorimetric data.

Figure 3.11 depicts the absorbance of dimer **4a** and uncomplexed TSPP at their absorption maxima (267 and 413 nm, respectively) upon alternate irradiation at 313 nm and > 460 nm of a 1:1 solution of dimer **4** and TSPP (both 2.0 μM). Irradiation at 313 nm led to the conversion of **4a** to **4b** resulting in a decrease of the absorbance of **4a** and at the same time TSPP was released from the CD cavities leading to an increase of the absorbance of free TSPP. Irradiation of the solution with visible light regenerated the open form of the dimer and simultaneously led to the uptake of uncomplexed TSPP from solution until the initial equilibrium between TSPP and **4a** was completely restored. Control experiments showed no significant reduction of the absorbance of TSPP during irradiation at 313 or > 460 nm. As is evident from Figure 3.11, the release and uptake cycle can be repeated several times without significant degradation, and within the limits of this system any ratio of free and uncomplexed

TSPP can be achieved, simply by tuning the relative amount of **4a** and **4b**, which can be regulated by photoirradiation.

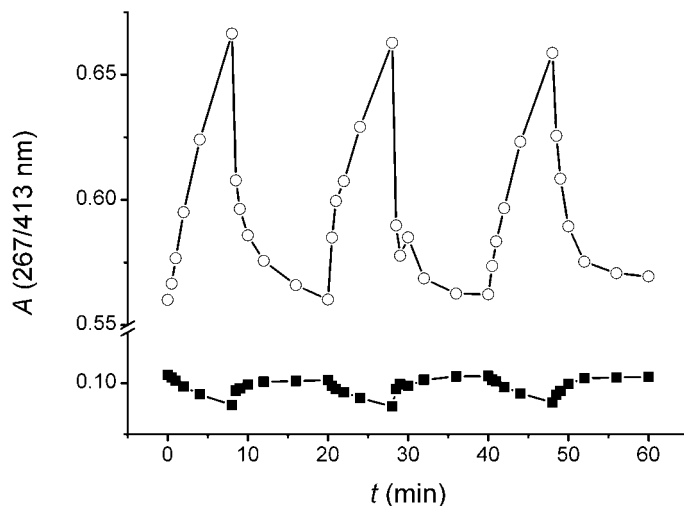


Figure 3.11 Absorbance at 267 (■, absorption maximum of **4a**) and 413 nm (○, absorption maximum of uncomplexed TSPP) of 2 μM of the complex of **4a** and TSPP upon alternate irradiation at 313 and > 460 nm.

3.3 Conclusions

The tethering of two CD cavities using a dithienylethene moiety gives access to photoswitchable CD dimers. These dimers can be switched between a relatively flexible (open) and a more rigid (closed) form by irradiation with light. The switching properties of the dithienylethene unit are unaffected by the covalent linkage of the CD cavities and the switching process is completely reversible and fatigue resistant. Depending on the molecular architecture, the switching of the dithienylethene unit can lead to a change of the binding affinity of the dimer for specific guest molecules. In this respect the rigidity between the dithienylethene tether and the CD cavities plays an important role. A certain amount of rigidity is required in order to obtain a substantial transfer of the switching effect taking place in the dithienylethene unit to the CD dimer as a whole. Effective transfer of the switching process can be achieved by direct coupling of the photochromic unit to the rim of the CD cavity, resulting in different binding affinities between the open and closed forms. This in turn enables

the photocontrolled release and uptake of guest molecules to and from solution and gives full control over the ratio of complexed and free guest molecules in solution. Photoswitchable CD dimers such as **4** are interesting candidates for use as photocontrollable (drug) delivery systems and might for example find application in photodynamic cancer therapy.^{8,27}

3.4 Experimental section

Materials and methods. All chemicals were used as received, unless stated otherwise. Solvents were purified according to standard laboratory methods.²⁸ Thin-layer chromatography was performed on aluminum sheets precoated with silica gel 60 F254 (Merck). The CD spots were visualized by dipping the sheets in 5% sulfuric acid in ethanol and subsequent heating. Chromatographic separations were performed on silica gel 60 (Merck, 0.040-0.063 mm, 230-240 mesh). 3-Amino-3-deoxyheptakis(6-*O*-*tert*-butyldimethylsilyl)- β -cyclodextrin (**1**),¹⁵ 5,5'-dicarboxydithienylethene (**2**),¹⁴ and heptakis(6-*O*-*tert*-butyldimethylsilyl)- β -cyclodextrin (**5**)¹⁶ were prepared according to literature procedures. FAB mass spectra were recorded with a Finnigan MAT90 spectrometer with *m*-nitrobenzylalcohol as a matrix. MALDI-TOF mass spectra were recorded using a PerSpective Biosystems Voyager-DE-RP MALDI-TOF mass spectrometer. NMR spectra were recorded at 25 °C using a Varian Inova 300 spectrometer. ¹H NMR chemical shifts (300 MHz) are given relative to residual CHCl₃ (7.25 ppm) or HDO (4.65 ppm). ¹³C NMR chemical shifts (75 MHz) are given relative to CDCl₃ (77.0 ppm) or to CH₃OD (49.3 ppm, used as an external standard for samples measured in D₂O).

All synthesized compounds containing the dithienylethene moiety are light-sensitive and were therefore exclusively handled in the dark using brown-stained glassware.

TBDMS-protected dithienylethene-tethered CD dimer 3. To a cooled solution of **2** (67 mg, 0.19 mmol) in dry THF (50 mL) were added HBTU (218 mg, 0.58 mmol) and DIPEA (0.17 mL, 0.96 mmol). The solution was stirred for 30 min and then allowed to warm to room temperature. **1** (929 mg, 0.48 mmol) was added and the solution was stirred for 2 days at room temperature. The solvent was removed in

vacuo, and chloroform was added. The solution was washed twice with 1 M HCl and brine. After removal of the solvent, the crude product was purified by gradient column chromatography (ethyl acetate/ethanol/water 100:2:1 to 100:8:4) to give **3** (open form) as a white powder in 65 % yield. ^1H NMR (CDCl_3): δ 8.15 (d, $J = 6.6$ Hz, 2 H), 6.96 (s, 2 H), 5.06 - 4.73 (m, 14 H), 4.53 (d, $J = 7.3$ Hz, 2 H), 4.21 - 3.41 (m, 66 H), 3.28 (t, $J = 9.2$ Hz, 2 H), 2.99 (qnt, $J = 7.3$ Hz, 2 H), 2.48 (qnt, $J = 7.3$ Hz, 2 H), 1.96 (t, $J = 7.3$ Hz, 2H), 1.84 (s, 6 H), 0.93 - 0.81 (m, 124 H), 0.05 - 0.00 (m, 84 H); ^{13}C NMR (CDCl_3): δ 166.2, 143.9, 136.1, 134.9, 133.1, 132.1, 104.3, 102.0 - 100.2, 82.6 - 79.2, 73.9 - 71.6, 62.5 - 60.4, 53.6, 37.3, 29.3, 26.0 - 25.8, 18.3, 14.5, -4.8 - -5.5; MS (MALDI-TOF): m/z calcd for $[\text{M}+\text{Na}]^+$ 4199.0; found 4199.8.

Dithienylethene-tethered CD dimer 4a. TBDMS-protected dimer **3** (210 mg, 0.05 mmol) was dissolved in trifluoroacetic acid (25 mL). The solution was stirred at room temperature for 10 min. The solvent was removed in vacuo. Methanol was added and evaporated in vacuo for azeotropic removal of any residual trifluoroacetic acid. The residue was dissolved in water and washed three times with diethylether. After freeze-drying dimer **4a** was obtained as a white solid in 99 % yield. ^1H NMR (D_2O): δ 7.79 (s, 2H), 5.11 - 5.02 (m, 14 H), 4.72 (bs, 2 H), 4.22 - 4.15 (m, 4 H), 3.93 - 3.51 (m, 64 H), 3.14 (qn, $J = 7.1$ Hz, 2 H), 2.77 (qnt, $J = 7.1$ Hz, 2 H), 2.37 (t, $J = 7.3$ Hz, 2 H), 1.98 (s, 6H); ^{13}C NMR (D_2O , ref. CH_3OD): δ 166.8, 143.2, 140.3, 137.9, 136.4, 134.8, 106.5, 105.2 - 104.8, 85.0 - 84.3, 78.1, 76.6 - 74.6, 70.9, 63.5 - 63.3, 54.0, 41.8, 25.8, 17.3; MS (MALDI-TOF): m/z calcd for $[\text{M}+\text{Na}]^+$ 2601.8; found 2602.1.

Mono-(2-O-(3-propylphthalimide))-heptakis-(6-O-tert-butyl dimethylsilyl)- β -cyclodextrin 6. A solution of silylated CD **5** (8.6 g, 4.4 mmol, dried for 5 h at 0.05 mmHg, 80 °C) and LiH (31 mg, 4.0 mmol) in THF (250 mL) was stirred at room temperature for 18 h followed by 1 h at reflux. A solution of *N*-(3-bromopropyl)phthalimide (1.1 g, 4.0 mmol) in THF (50 mL) was added dropwise to the reaction mixture, which was kept at reflux for 2 h. The solvent was evaporated in vacuo and the residue was dissolved in CHCl_3 and washed twice with water and once with brine. The organic phase was dried over MgSO_4 and filtered. The solvent was evaporated in vacuo and the residue was purified by gradient column chromatography (ethyl acetate/ethanol/water 100:2:1 to 50:7:4) to give **6** as a white powder in 26 %

yield. ^1H NMR (CD_3OD): δ 7.78 (dd, $J = 5.5$ and $J = 3.3$ Hz, 2 H), 7.70 (dd, $J = 5.5$ Hz and $J = 3.3$ Hz, 2 H), 5.03 (d, $J = 3.3$ Hz, 1 H), 4.86 (d, $J = 3.3$ Hz, 6 H), 3.96 - 3.46 (m, 34 H), 3.36 (dd, $J = 9.7$ Hz and $J = 3.3$ Hz, 6 H), 3.25 (t, $J = 1.8$ Hz, 1 H), 3.17 (dd, $J = 9.7$ Hz and $J = 3.3$ Hz, 1 H), 1.94 (qnt, $J = 6.3$ Hz, 2 H), 0.87 - 0.84 (m, 63 H), 0.03 - 0.00 (m, 42 H); ^{13}C NMR (CD_3OD): δ 169.7, 135.1, 133.0, 123.0, 103.5, 101.8, 82.7, 82.1, 74.3 - 73.3, 71.0, 62.9, 58.1, 35.6, 30.4, 29.6 26.5, 18.3, -4.6, -4.7; MS (MALDI-TOF): m/z calcd for $[M+\text{Na}]^+$ 2145.0; found 2144.8.

Mono-(2-*O*-(3-aminopropyl))-heptakis-(6-*O*-*tert*-butyldimethylsilyl)- β -

cyclodextrin 7. To a solution of **6** (1.2 g, 0.6 mmol, dried for 5 h at 0.05 mmHg, 80 °C) in EtOH (50 mL) was added hydrazine monohydrate (0.3 mL, 5.7 mmol). The solution was stirred at reflux for 8 h. The solvent was evaporated in vacuo and CHCl_3 was added. The organic phase was washed with 1 M aqueous HCl, 1 M aqueous NaOH and brine. The solvent was evaporated in vacuo and the residue was purified using gradient column chromatography (ethyl acetate/ethanol/water 100:2:1 to 50:15:8) to give **7** as a white powder in 90 % yield. ^1H NMR (CDCl_3): δ 5.06 (d, $J = 2.6$ Hz, 1 H), 4.92 - 4.85 (m, 6 H), 4.18 - 3.35 (m, 38 H), 3.22 (dd, $J = 10.3$ Hz and $J = 2.6$ Hz, 1 H), 2.29 (bs, 2 H), 0.86 - 0.84 (m, 63 H), 0.05 - 0.00 (m, 42 H); ^{13}C NMR (CDCl_3): δ 102.0 - 100.2, 97.7, 82.6 - 79.2, 73.9 - 71.6, 62.5 - 60.4, 40.0, 27.4, 26.0 - 25.8, 18.3, 14.2, -5.1 - -5.5; MS (MALDI-TOF): m/z calcd for $[M+\text{H}]^+$ 1991.0; found 1990.8.

TBDMS-protected dithienylethene-tethered CD dimer 8. To a cooled solution of **2** (30 mg, 0.09 mmol) in dry DMF (50 mL) were added HBTU (95 mg, 0.25 mmol) and DIPEA (0.07 mL, 0.46 mmol). The solution was stirred for 30 min and then allowed to warm to room temperature. **7** (420 mg, 0.21 mmol) was added and the solution was stirred for 3 days at room temperature. The solvent was removed in vacuo, and chloroform was added. The solution was washed twice with 1 M HCl and brine. After removal of the solvent, the crude product was purified by gradient column chromatography (ethyl acetate/ethanol/water 100:2:1 to 100:8:4) to give **8** (open form) as a white powder in 69 % yield. ^1H NMR (CDCl_3): δ 7.47 (s, 2 H), 4.90 - 4.89 (m, 14 H), 3.94 - 3.32 (m, 76 H), 3.12 (d, $J = 8.8$ Hz, 2 H), 2.96 (qnt, $J = 7.3$ Hz, 2 H), 2.75 (qnt, $J = 7.3$ Hz, 2 H), 2.14 (t, $J = 7.3$ Hz, 2H), 1.96 (s, 6 H), 1.86 (bs, 2 H),

1.75 (bs, 2 H), 0.84 – 0.81 (m, 124 H), 0.04 – 0.00 (m, 84 H); ^{13}C NMR (CDCl_3): δ 163.4, 140.6, 136.8, 135.2, 134.3, 130.1, 102.4 - 101.9, 100.1, 81.8 – 80.7, 73.8 – 71.8, 61.6 – 60.6, 38.3, 37.6, 31.9, 29.6, 25.8 – 25.6, 18.3, 14.6, 14.0, -5.2 - -5.3; MS (MALDI-TOF): m/z calcd for $[M+\text{Na}]^+$ 4319.3; found 4320.0.

Dithienylethene-tethered CD dimer 9a. TBDMS-protected dimer **8** (155 mg, 0.04 mmol) was dissolved in trifluoroacetic acid (25 mL). The solution was stirred at room temperature for 10 min. The solvent was removed in vacuo. Methanol was added and evaporated in vacuo for azeotropic removal of any residual trifluoroacetic acid. The residue was dissolved in water and washed three times with diethylether. After freeze-drying, dimer **9a** was obtained as a white solid in 97 % yield. ^1H NMR (D_2O): δ 7.30 (s, 2 H), 5.24 (d, $J = 3.3$ Hz, 2 H), 5.10 – 5.07 (m, 12 H), 4.10 – 3.53 (m, H), 3.46 (d, $J = 7.7$ Hz, 2 H), 2.83 (qnt, $J = 7.1$ Hz, 4 H), 2.36 (s, 6 H), 2.14 (t, $J = 7.1$ Hz, 2 H), 1.93 (bs, 4 H); ^{13}C NMR (D_2O , ref. CH_3OD): δ 164.2, 140.6, 136.0, 135.2, 133.7, 129.0, 101.6-100.2, 81.8-80.4, 73.0-71.2, 59.9-59.6, 38.3, 28.7, 22.6, 13.5; MS (MALDI-TOF): m/z calcd for $[M+\text{Na}]^+$ 2717.9; found 2717.9.

UV-vis spectroscopy. UV-vis spectra were recorded on a Hewlett Packard HP 8452 UV-vis spectrophotometer. Irradiation experiments were performed in situ by irradiation of the samples in a 1 cm quartz cuvette in the UV-vis setup, using a 200W mercury lamp with a 313 nm band-pass or a 460 nm high pass filter.

Preparation of PSS mixtures. Solutions of the open form of the dimer in Millipore water (1 to 10 mM) in a 1 cm quartz cuvette were irradiated with a high intensity mercury lamp for 10 to 15 min. UV-vis spectra of diluted samples were used to follow the photochromic reaction. Once the PSS was reached, samples were freeze dried to give the PSS mixture as a purple solid.

Calorimetry. Calorimetric titrations were performed at 25 °C using a Microcal VP-ITC titration microcalorimeter. Sample solutions were prepared in Millipore water. Titrations were performed by adding aliquots of a guest solution to the host solution. The titrant typically contained 0.1 to 1 mM of guest, while the cell solutions contained 10 to 100 μM of host. All calorimetric titrations were corrected for dilution heats by

subtraction of the calorimetric dilution experiments from the calorimetric titration experiments. The titrations were analyzed with a least-squares curve fitting procedure. The thermodynamic data reported in Table 3.2 are based on at least three independent titrations performed at three different concentrations.

Fluorescence spectroscopy. In the fluorescence titration experiments the emission of TSPP was monitored at various ratios of TSPP and CD-dimer, while keeping the concentration TSPP constant. Emission spectra were recorded on an Edinburgh FS900 fluorospectrophotometer in which a 450 W xenon arc lamp was used as excitation source. M300 gratings with 1800 1/mm were used on both excitation and emission arms. Signals were detected by a Peltier element cooled, red sensitive, Hamamatsu R928 photomultiplier system. Quartz sample cells of 1 cm were used.

Crystal structure determination. Crystals of 5,5'-(dialdehydodithienyl)cyclopentene, prepared by Fijis van Leeuwen, were obtained by slow diffusion of methanol into a solution of 5,5'-(dialdehydodithienyl)cyclopentene in dichloromethane.

Crystal data: $C_{17}H_{16}O_2S_2$, $M_r=316.44$, brown crystal of dimensions $0.15 \times 0.15 \times 0.30$ mm, orthorhombic, space group *Pbcn* (no. 60) with $a = 10.9081(10)$, $b = 8.2278(10)$, $c = 17.231(2)$ Å, $V = 1546.5(3)$ Å³, $Z = 4$, $\rho_{\text{calc}} = 1.359$ g cm⁻³, $F(000) = 664$, $\mu_{\text{MoK}\alpha} = 0.345$ mm⁻¹. 42400 reflections were measured on a Nonius KappaCCD diffractometer on rotating anode ($\lambda_{\text{MoK}\alpha} = 0.71073$ Å, $T = 150$ K, $\theta_{\text{max}} = 27.5$ deg), 1776 of which were unique ($R_{\text{int}} = 0.0361$). The structure was solved with SHELXS-86.²⁹ 120 parameters were refined with SHELXL-97,³⁰ including all hydrogen atom coordinates and anisotropic displacement parameters for all non-H atoms. The displacement parameters of the hydrogen atoms were coupled to the equivalent displacement parameters of their carrier atoms. The refinement converged at $wR2 = 0.0790$, $w^{-1} = \sigma^2(F_o^2) + (0.0400P)^2 + 0.61P$ (where $P = (\text{Max}(F_o^2, 0) + 2F_c^2)/3$), $R1 = 0.0288$ (for 1628 $F_o > 4\sigma(F_o)$), $S = 1.067$, $-0.24 < \Delta\rho < 0.29e$ Å⁻³.

CCDC 220072 contains the supplementary crystallographic data for this structure. These data can be obtained free of charge via www.ccdc.cam.ac.uk/conts/retrieving.html (or form the Cambridge Crystallographic Data Centre, 12 Union Road, Cambridge CB2 1EZ, UK; fax: (+44)1223-336-033; or e-mail: deposit@ccdc.cam.ac.uk).

Molecular mechanics calculations. Initial structures, created by manual modification of X-ray crystal structures of CD and 5,5'-dialdehyde-dithienylethene as well as visualizations were carried out with Quanta 97.³¹ Parameters were taken from Quanta 97 and point charges were assigned with the charge-template option. Residual charge was smoothed on carbon and non-polar hydrogen atoms rendering overall neutral residues. A distance-dependent relative permittivity was applied with $\epsilon = 1$. No cut-offs on the non-bonded interactions were used. Energy minimizations of the structures were performed in a solvent box of water molecules using the steepest descent and adopted basis-set Newton-Raphson methods until the root-mean-square of the energy gradient was $< 0.001 \text{ kcal mol}^{-1} \text{ \AA}^{-1}$.

3.5 References and notes

¹ Hartley, J. H.; James, T. D.; Ward, C. J. *J. Chem. Soc., Perkin Trans. 1* **2000**, 3155-3184.

² Shinkai, S.; Manabe, O. *Top. Curr. Chem.* **1984**, *121*, 67. For a more recent review see: Alfimov, M. V.; Fedorova, O. A.; Gromov, S. P. *J. Photochem. Photobiol. A* **2003**, *158*, 183-198.

³ a) Ueno, A.; Yoshimaru, H.; Saka, R.; Osa, T. *J. Am. Chem. Soc.* **1979**, *101*, 2779-2780. b) Ueno, A.; Tomita, Y.; Osa, T. *Tetrahedron Lett.* **1983**, *24*, 5245-5284. c) Ueno, A.; Fukushima, M.; Osa, T. *J. Chem. Soc., Perkin Trans. 2* **1990**, 1067-1072. d) Fukushima, M.; Osa, T.; Ueno, A. *Chem. Lett.* **1991**, 709-712. e) Hamada, F.; Fukushima, M.; Osa, T.; Ikeda, H.; Toda, F.; Ueno, A. *Macromol. Rapid Commun.* **1993**, *14*, 287-291.

⁴ Szejtli, J. *Chem. Rev.* **1998**, *98*, 1743-1754.

⁵ Aoyagi, T.; Ueno, A.; Fukushima, M.; Osa, T. *Macromol. Rapid. Commun.* **1998**, *19*, 103-105.

⁶ Liu, Y.; Wu, C. T.; Xue, G. P.; Li, J. *J. Inclusion Phenom. Macrocyclic Chem.* **2000**, *36*, 95-100.

⁷ a) Liu, Y.; You, C.-C.; Wada, T.; Inoue, Y. *Tetrahedron Lett.* **2000**, *41*, 6869-6873. b) Liu, Y.; Chen, Y.; Zhang, H.Y.; Liu, S.-X.; Guan, X.-D. *J. Org. Chem.* **2001**, *66*, 8518-8527. c) Liu, Y.; You, C.-C.; Li, B. *Chem. Eur. J.* **2001**, *7*, 1281-1288. d) Liu, Y.; Li, L.; Zhang, H.-Y.; Song, Y. *J. Org. Chem.* **2003**, *68*, 527-536.

- ⁸ a) Ruebner, A.; Yang, Z.; Leung, D.; Breslow, R. *Proc. Natl. Acad. Sci. U. S. A.* **1999**, *96*, 14692-14693. b) Baugh, S. D. P.; Yang, Z.; Leung, D. K.; Wilson, D. M.; Breslow, R. *J. Am. Chem. Soc.* **2001**, *123*, 12488-12494.
- ⁹ Irie, M. *Chem. Rev.* **2000**, *100*, 1685-1716.
- ¹⁰ Feringa, B. L. *Molecular Switches*, Wiley-VCH, Weinheim, **2001**.
- ¹¹ Takeshita, M.; Uchida, K.; Irie, M. *Chem. Commun.* **1996**, 1807-1808.
- ¹² a) Takeshita, M.; Irie, M. *Tetrahedron Lett.* **1998**, *39*, 613-616. b) Takeshita, M.; Irie, M. *J. Org. Chem.* **1998**, *63*, 6643-6649. c) Takeshita, M.; Soong, C. F.; Irie, M. *Tetrahedron Lett.* **1998**, *39*, 7717-7720. d) Kawai, S. H. *Tetrahedron Lett.* **1998**, *39*, 4445-4448.
- ¹³ Irie, M.; Miyataka, O.; Uchida, K.; Eruguchi, T. *J. Am. Chem. Soc.* **1994**, *116*, 9894-9900.
- ¹⁴ Lucas, L. N.; de Jong, J. J. D.; Van Esch, J. H.; Kellogg, R. M.; Feringa, B. L. *Eur. J. Org. Chem.* **2003**, 155-166.
- ¹⁵ Van Dienst, E.; Snellink, B. H. M.; Von Piekartz, I.; Grote Gansey, M. H. B.; Venema, F.; Feiters, M. C.; Nolte, R. J. M.; Engbersen, J. F. J.; Reinhoudt, D. N. *J. Org. Chem.* **1995**, *60*, 6537-6545.
- ¹⁶ Yuan, D.-Q.; Ohta, K.; Fujita, K. *Chem. Commun.* **1996**, 821-822.
- ¹⁷ Ikeda, H.; Nagano, Y.; Du, Y.-Q.; Ikeda, T.; Toda, F. *Tetrahedron Lett.* **1990**, *31*, 5045-5048.
- ¹⁸ Stoddart, J. F. *Stereochemistry of Carbohydrates*, Wiley Interscience, London, **1971**, pp. 87-89.
- ¹⁹ Venema, F.; Nelissen, H. F. M.; Berthault, P.; Birlirakis, N.; Rowan, A. E.; Feiters, M. C. N.; Nolte, R. J. M. *Chem. Eur. J.* **1998**, *4*, 2237-2250.
- ²⁰ Pregel, M. J.; Buncel, E. *Can. J. Chem.* **1991**, *69*, 130-137.
- ²¹ Nelissen, H. F. M.; Feiters, M. C.; Nolte, R. J. M. *J. Org. Chem.* **2002**, *67*, 5901-5906.
- ²² Typical data obtained with a 5 mM aqueous solution of dimer **4** in an NMR tube, irradiated at 313 nm for 2.5 h: ¹H NMR spectroscopy: 34 % open form and 66 % closed form; UV-vis spectroscopy and modeling: 33 % open form, 67 % closed form.
- ²³ a) Kano, K.; Nishiyabu, R.; Asada, T.; Kuroda, Y. *J. Am. Chem. Soc.* **2002**, *124*, 9937-9944. b) Wang, X.-P.; Pan, J.-H.; Shuang, S.-M. *Spectrochimica Acta A* **2001**,

57, 2755-2762. c) Ribo, J. M.; Farrera, J.-A.; Valero, M. L.; Virgili, A. *Tetrahedron* **1995**, *51*, 3705-3712.

²⁴ a) Michels, J. J.; Fiammengo, R.; Timmerman, P.; Huskens, J.; Reinhoudt, D. N. *J. Inclusion Phenom. Macrocyclic Chem.* **2001**, *41*, 163-172. b) Venema, F.; Rowan, A. E.; Nolte, R. J. M. *J. Am. Chem. Soc.* **1996**, *118*, 257-258.

²⁵ a) Manka, J. S.; Lawrence, D. S. *J. Am. Chem. Soc.* **1990**, *112*, 2440-2442. b) Dick, D. L.; Rao, T. V. S.; Sukumaran, D.; Lawrence, D. S. *J. Am. Chem. Soc.* **1992**, *114*, 2664-2669.

²⁶ Rekharsky, M. V.; Inoue, Y. *Chem. Rev.* **1998**, *98*, 1875-1918.

²⁷ a) Sternberg, E. D.; Dolphin, D.; Bruckner, C. *Tetrahedron* **1998**, *54*, 4151-4202. b) Stilts, C. E.; Nelen, M. I.; Hilmey, D. G.; Davies, S. R.; Gollnick, S. O.; Oseroff, A. R.; Gibson, S. L.; Hilf, R.; Detty, M. R. *J. Med. Chem.* **2000**, *43*, 2403-2410. c) Edwards, W. B.; Reichert, D. E.; d'Avignon, D. A.; Welch, M. J. *Chem. Commun.* **2001**, 1312-1313. d) Moser, J. G.; Rose, I.; Wagner, B.; Wieneke, T.; Vervoorts, A. *J. Inclusion Phenom. Macrocyclic Chem.* **2001**, *39*, 13-18.

²⁸ Perrin, D. D.; Armarego, W. F. L. *Purification of Laboratory Chemicals*, 3rd ed., Pergamon, Oxford, **1989**.

²⁹ Sheldrick, G. M. SHELX-86 Program for crystal structure determination, University of Göttingen, Germany, **1986**.

³⁰ Sheldrick, G. M. SHELX-97 Program for crystal structure refinement, University of Göttingen, Germany, **1997**.

³¹ Quanta 97, Molecular Simulations, Waltham, USA.

Bis(phenylthienyl)ethene-tethered β -cyclodextrin dimers as photoswitchable hosts*

4.1 Introduction

As was shown in the previous chapter, tethering of two β -cyclodextrin (CD) cavities by a photoswitchable dithienylethene moiety gave access to photoswitchable CD dimers. The dimers were able to undergo thermally irreversible, fatigue-resistant, photochromic cyclization reactions between two defined states: a relatively flexible open form and a rigid closed form, characteristic for the dithienylethene moieties.^{1,2} This subtle difference in flexibility between the two forms of dithienylethenes was used to achieve a surprisingly large difference in binding affinity, up to a factor of 35, between the open and closed states of the photoswitchable CD dimer for binding of a porphyrin guest molecule. Therewith, this dimer displayed one of the most pronounced differences in binding properties of the various tunable receptor molecules reported in the literature,³⁻⁸ and it is one of the few tunable receptor molecules for which the photocontrolled release and uptake of guest species has been demonstrated.^{3b,c,6d}

The work in this chapter describes the synthesis and photochromic properties of two CD dimers tethered by a bis(phenylthienyl)ethene, in an attempt to obtain even larger differences in binding affinity. Compared to the dithienylethenes used in the CD dimers described in Chapter 3, the bis(phenylthienyl)ethenes have an additional phenyl ring attached to the photoswitchable core (see Figure 4.1). As a consequence,

* Part of this work will be published in: Mulder, A; Juković, A; Huskens, J.; Reinhoudt, D. N. *Org. Biomol. Chem.* **2004**, *2*, in press.

the difference in spacing of the photoswitch-appended moieties between the open and closed forms of the photoswitch is larger for the latter type of molecules. Therefore, bis(phenylthienyl)ethene tethers potentially enable larger differences in binding affinity compared to dithienylethene tethers. An additional advantage of the bis(phenylthienyl)ethenes over the dithienylethenes is that they can be switched almost completely to the closed form. The fraction of the closed form in the photostationary state often exceeds 90 %, which is substantially higher than that obtained for dithienylethenes.⁹

The switching behavior and binding properties of the bis(phenylthienyl)ethene-tethered CD dimers reported in this chapter are compared to the dithienylethene-tethered CD dimers described in Chapter 3. Binding studies with meso-tetrakis(4-sulfonatophenyl)porphyrin (TSPP) have been performed to assess the potential use of the bis(phenylthienyl)ethene-tethered CD dimers as tunable receptors.

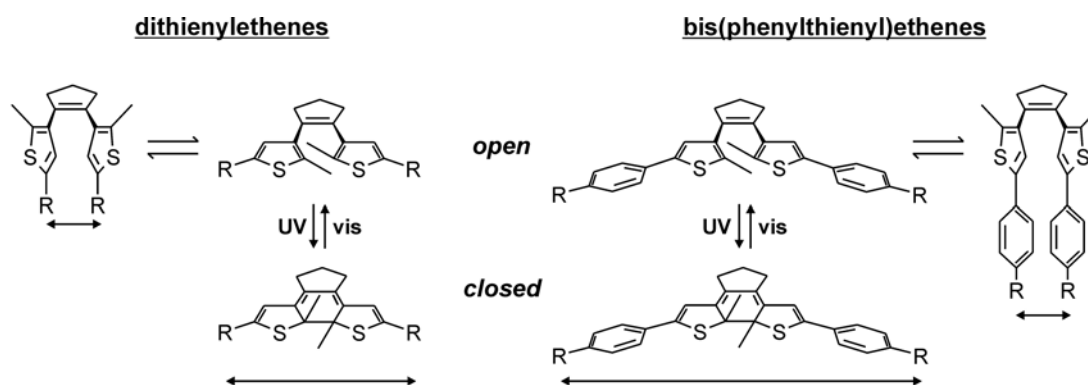


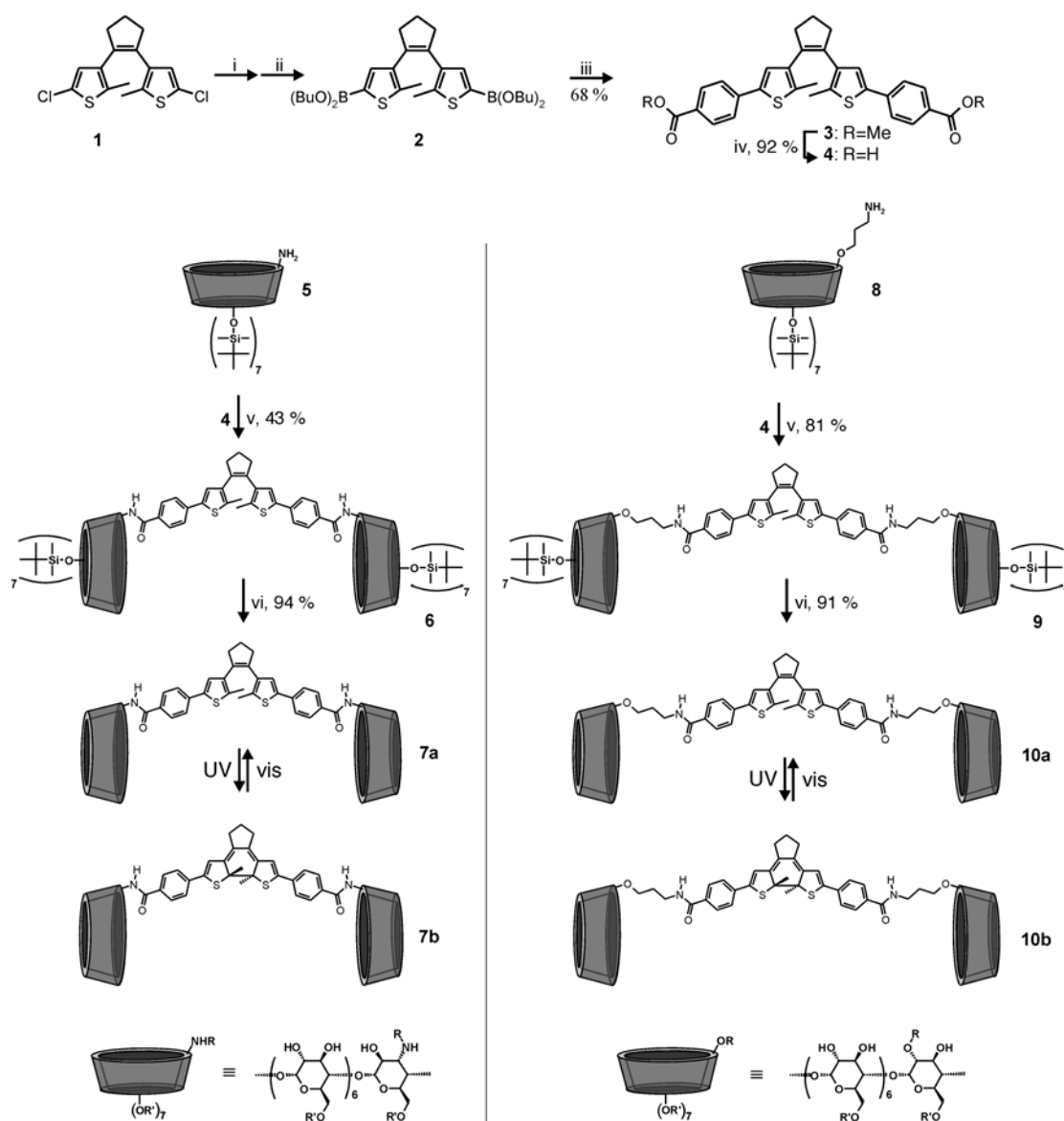
Figure 4.1 Possible spacing of appended groups (*R*) for the different forms (open and closed) of dithienylethenes (left) and bis(phenylthienyl)ethenes (right).

4.2 Results and discussion

4.2.1 Synthesis and characterization of the CD dimers

The synthesis of the CD dimers is outlined in Scheme 4.1. The two bis(phenylthienyl)ethene-tethered CD dimers (**7** and **10**) have a different connectivity between the CDs and the photochromic units. In dimer **7**, the bis(phenylthienyl)ethene moiety is attached directly at the secondary sides of the CD cavities, giving a relatively rigid dimer, where most of the rotational freedom is present in the bis(phenylthienyl)ethene tether. Alternatively, the more flexible dimer **10** was

synthesized in which the bis(phenylthienyl)ethene unit and the secondary sides of the CD cavities are spaced by propyl spacers.



Scheme 4.1 Synthesis routes for dimers **7** and **10**. i, *n*-BuLi, THF, r.t.; ii, (*n*-BuO)₃B; iii, Me-4-bromobenzoate, Pd(PPh₃)₄, 2 M Na₂CO₃, ethylene glycol, THF, reflux; iv, 4 M NaOH, dioxane, reflux; v, HBTU, DIPEA, THF, r.t.; vi, TFA, r.t.

The top part of Scheme 4.1 details the synthesis of the photoswitchable tether, bis(carboxyphenylthienyl)ethene **4**, used for coupling of the CD cavities. The synthesis of **4** was achieved by extension of the photoswitchable unit 2,2'-dichlorodithienylethene¹⁰ **1** via a Suzuki coupling with methyl-4-bromobenzoate,

analogous to a procedure recently reported by Feringa et al.⁹ The resulting bis(methylester) **3** was purified by column chromatography and subsequently hydrolyzed to give **4**. Direct coupling of tether **4** to the secondary rim of the CD cavities was realized by an amide coupling of **4** with 3-amino-3-deoxy-heptakis(6-*O*-tertbutyldimethylsilyl)- β -cyclodextrin¹¹ **5** using *O*-benzotriazol-1-yl-*N,N,N,N*-tetramethyluronium hexafluorophosphate (HBTU) as a coupling agent analogous to the procedure described in Chapter 3. The resulting protected dimer **6** was purified by gradient column chromatography. Deprotection of the primary hydroxyl groups, using trifluoroacetic acid, gave dimer **7** in the open form (**7a**). Similarly, dimer **10a** was synthesized from bis(carboxyphenylthienyl)ethene **4** and mono-(2-*O*-(3-aminopropyl))-2-deoxy-heptakis(6-*O*-tertbutyldimethylsilyl)- β -cyclodextrin (**8**).¹²

Both dimers **7** and **10** were poorly water-soluble, which is probably inherent to their large hydrophobic tether. ¹H NMR spectroscopy indicated that the dimers strongly aggregated in aqueous solution. Figure 4.2 (top) shows the ¹H NMR spectrum of dimer **7a** in D₂O, which is a typical example of the spectra obtained for the dimers **7** and **10** in aqueous solution. The spectrum is dominated by a set of broad peaks around 3-4 and 5 ppm, characteristic for the CD protons. The only indication for the presence of the bis(phenylthienyl)ethene tether is an extremely broad and barely visible hump in the aromatic region (~8 ppm). The spectra in aqueous solution sharpened only slightly at elevated temperatures. Spectra recorded with the dimers in DMSO-*d*₆ or mixtures of D₂O and MeOD (1:1, v/v) showed relatively sharp peaks for both the CD protons and the bis(phenylthienyl)ethene tether with integral ratios in agreement with the molecular structure of the dimer (Figure 4.2, center and bottom). Both ¹H NMR spectra of dimers **7** and **10** in DMSO-*d*₆ show three signals for the phenylthienyl moiety in accordance with the C₂ symmetry of the dimer, and the cyclopentene bridge protons occur at 2.1 and 2.8 ppm, characteristic for these switching units.⁹ Additionally, the spectrum of dimer **10** (Figure 4.2, bottom) shows a multiplet around 1.8 ppm, which originates from the C2 methylene group of the propyl spacers. Only moderate sharpening of the spectra recorded for the D₂O solutions of the dimers is obtained when the dimer concentration is systematically decreased from 5 to 0.1 mM (spectra not shown), suggesting that intramolecular aggregation is responsible for the poor resolution observed in these ¹H NMR spectra.

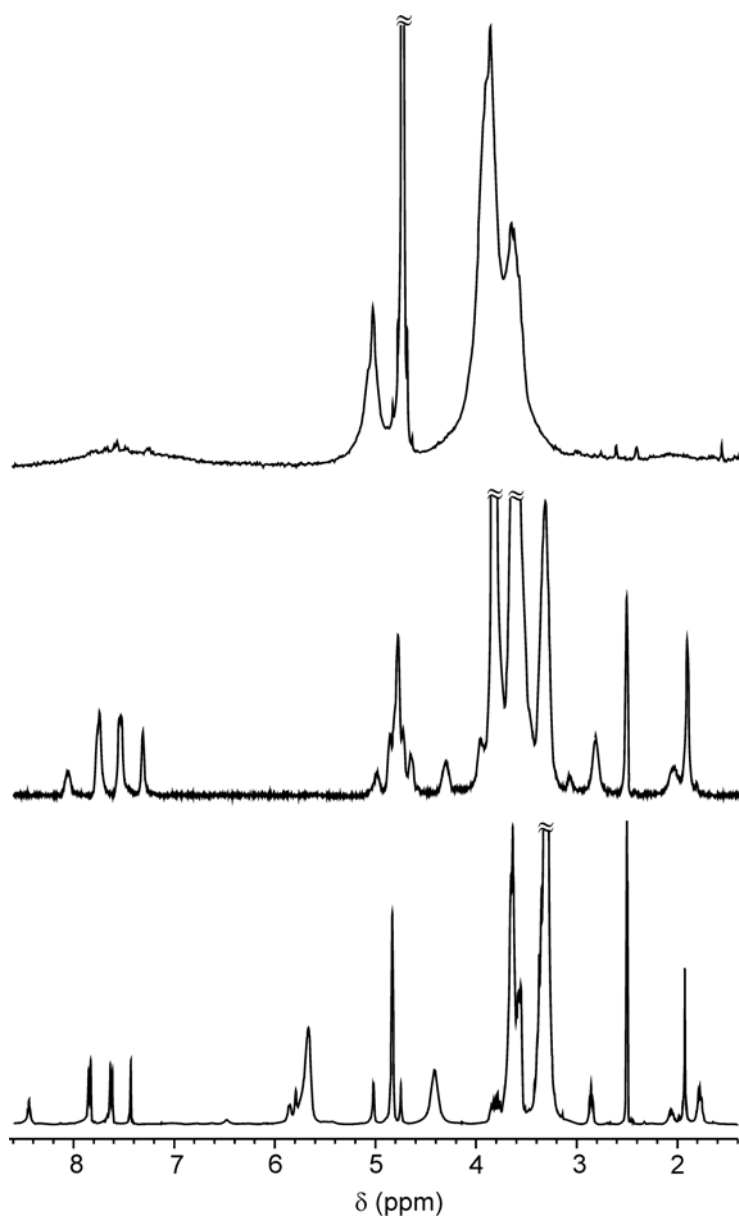


Figure 4.2 ^1H NMR (400 MHz, 298 K) spectra of **7a** in D_2O (top) and in DMSO-d_6 (center), and of **10a** in DMSO-d_6 (bottom).

4.2.2 Switching behavior of the CD dimers

The photochromic behavior of the dimers was studied by irradiation with a high-pressure mercury lamp with band-pass filters. The photochemical reactions were monitored by UV-vis spectroscopy. The absorption spectra of dimers **7** and **10** are shown in Figure 4.3 (left and right, respectively). The open forms of both dimers showed strong absorption in the UV region with absorption maxima at 331 nm for dimer **7a** and at 298 and 334 nm for dimer **10a**, respectively (Figure 4.3, solid lines).

The colorless aqueous solutions turned purple upon irradiation at 313 nm and strong absorption bands appeared in the visible region of the absorption spectra with maxima at 564 nm for dimer **7b** and 553 nm for dimer **10b**.

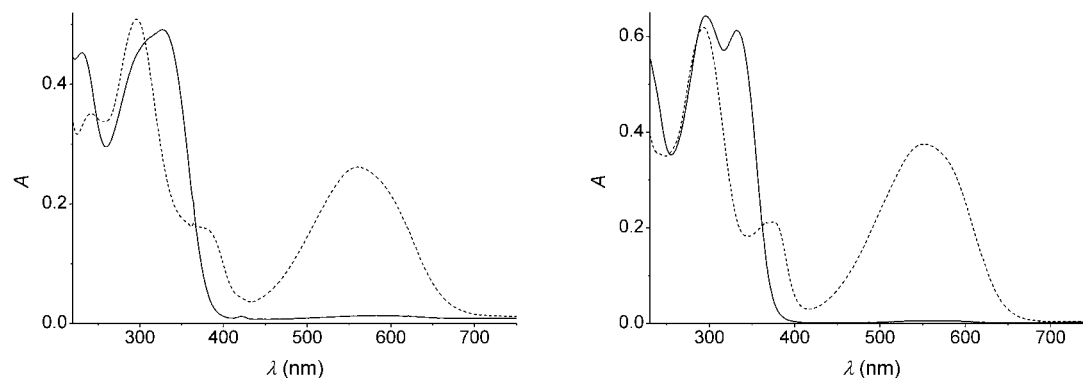


Figure 4.3 Absorption spectra of 16 μM **7** (left) and 20 μM **10** (right) in water before (open form, —) and after (PSS mixture, ---) photoirradiation with 313 nm light.

Photostationary states (PSS) of both dimers were readily obtained, suggesting that aggregation, if present at these concentrations, has little effect on the switching behavior of the dimers. UV-vis spectra recorded before reaching the PSS showed sharp isosbestic points, indicative of only two interchanging species. The absorption spectra of the PSS mixtures of **7a/7b** and **10a/10b** are given by the dotted lines in Figure 4.3. The PSS mixtures were stable at room temperature in the dark. Irradiation of the PSS mixtures with visible light ($\lambda > 460$ nm) led to the disappearance of the absorption bands in the visible region and to restoration of the absorption spectra of the open forms, demonstrating the reversibility of the photochemical ring-opening/ring-closure process. The compositions of the PSS mixtures were determined by modeling of the UV-vis spectra, as reported in Chapter 3. A minimum of ten UV-vis spectra, obtained during irradiation of the dimers, was fitted with a set of Gaussians representing the open form (directly obtained from the UV-vis spectra of the open forms, see solid lines Figure 4.3) and a set of Gaussians representing the absorption spectra of the closed form (optimized in the fitting procedure). Typical fits are given in Figure 4.4, which shows the recorded and modeled absorption spectra of the open form and the PSS mixture of dimer **7** and the calculated absorption spectrum of the closed form **7b**. Equally good fits were obtained for dimer **10**. Table 4.1 lists

the parameters for the sets of Gaussians used for the fitting procedure. For both dimers, the photostationary state was composed of 8 % of the open and 92 % of the closed form. These photostationary states are in accordance with results obtained for similar bis(phenylthienyl)ethene switches,⁹ and indicate that the coupling with and close proximity of the CD cavities do not interfere with the switching process.

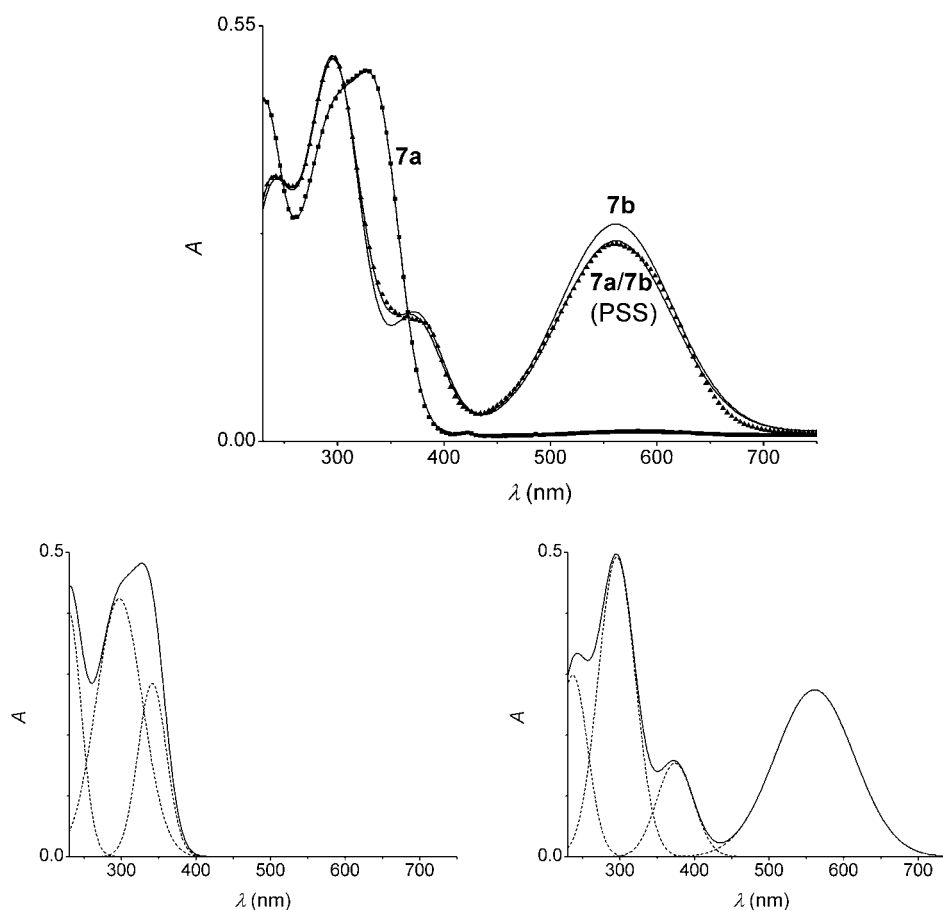


Figure 4.4 Measured (markers) and modeled (lines) absorption curves of 16 μM **7** in water (top; **7a** (■), PSS mixture of **7a/7b** (▲), and **7b**). Set of Gaussians (---) that constitute the calculated absorption spectrum (—) of **7a** (bottom left) and **7b** (bottom right).

The nearly complete conversion between the open and closed forms of dimers **7** and **10** is ideal for their use as photoswitchable receptor molecules. In this respect, the bis(phenylthienyl)ethene-tethered CD dimers reported here are superior to the dithienylethene CD dimers reported in Chapter 3, which showed a PSS composition of only 75 % of the closed form. Consequently, strong differences in binding affinity

between the open and closed states of the bis(phenylthienyl)ethene-tethered CD dimers might lead to a more pronounced release of guest molecules.

Table 4.1 Parameters for the sets of Gaussians used for the fitting of the absorption spectra of **7** and **10**.^a

7a			7b		
λ_{\max}	FWHM	ϵ_{\max}	λ_{\max}	FWHM	ϵ_{\max}
229.0	17.2	25.2	237.0	20.0	18.6
297.2	31.0	26.5	295.9	24.7	30.8
341.4	19.2	17.8	347.0	24.6	9.6
			561.2	53.0	17.1
10a			10b		
λ_{\max}	FWHM	ϵ_{\max}	λ_{\max}	FWHM	ϵ_{\max}
219.9	24.0	29.7	230.0	25.0	16.8
294.7	23.4	31.1	293.8	23.1	30.1
339.8	16.1	24.4	371.0	18.8	11.3
			549.5	50.3	20.8

^a λ_{\max} (nm), FWHM (nm), ϵ_{\max} ($10^3 \text{ cm}^{-1} \text{ M}^{-1}$).

4.2.3 Complexation studies

Complexation studies were performed with meso-tetrakis(4-sulfonatophenyl)porphyrin (TSPP). The binding of TSPP by the open and closed forms of the dimers **7** and **10** was studied with isothermal titration microcalorimetry. Despite the aggregation behavior of dimers **7** and **10**, titrations were performed in aqueous solutions in order to enable comparison with the previously obtained calorimetric data for the shorter dithienylethene-tethered dimers. Aqueous solutions of dimer **10** showed limited stability at the concentrations required for calorimetric experiments. Shortly after solubilization in water, precipitation was observed. Therefore, titrations with dimer **7** were performed in water, whereas for dimer **10** mixtures of DMSO and water (1:9 v/v) were used to prevent precipitation of the dimer from solution.

Figure 4.5 depicts two typical titration curves obtained for the titration of TSPP to **7a** (left) and a PSS mixture of **7** (right). The initial, less exothermic heat effects observed for the titration of TSPP to dimer **7a** (Figure 4.5, left) were attributed to

deaggregation of the dimer upon complexation of TSPP. Similar heat effects were seen for titrations with dimer **10** in the DMSO-water mixtures. The deaggregation only affects the heat effects for the first additions, and the remainder of the curves could be fitted well with a 1:1 interaction. The aggregation behavior of dimers **7a** and **10** was not further quantified.

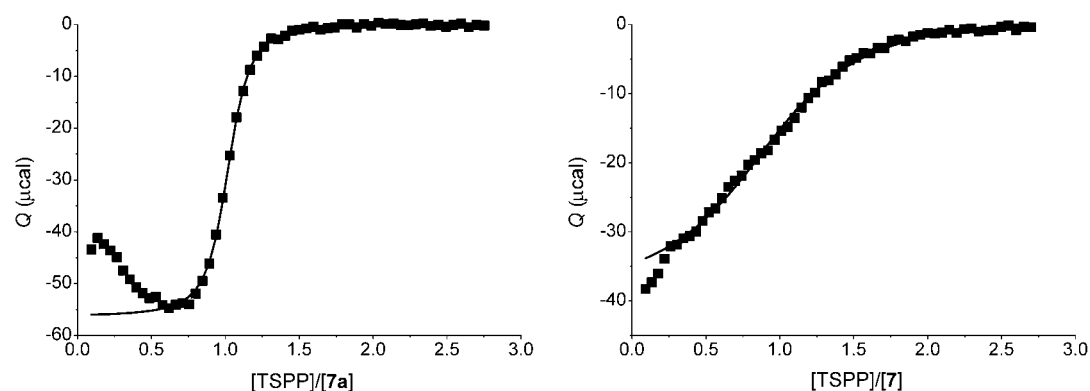


Figure 4.5 Heat evolved per injection plotted against the $[TSPP]/[7]$ ratio (markers) and fit (solid line) for the calorimetric titrations of TSPP to **7a** (left) and to the PSS mixture of **7** (right) in water at 298 K.

Interestingly, no pronounced heat effects due to deaggregation were observed for the titrations of TSPP to solutions of the PSS mixture of **7** (Figure 4.5, right). The PSS of **7** mainly consists of **7b** (see above), and the titration curves performed with the PSS mixtures of **7** showed no pronounced effects for the binding of TSPP by **7a**. The titration curves could be fitted well using a 1:1 model and a single host site **7b** (Figure 4.5, right). Similarly good fits were obtained when fitting titration curves obtained with the PSS mixture of dimer **10** taking into account only the closed dimer **10b**. Therefore, binding curves obtained with the PSS were considered to be the result of binding of TSPP by the closed form of the dimer, and both binding curves of the open and PSS mixtures of the dimers were fitted with a 1:1 binding model using one single association constant, K , and binding enthalpy, ΔH° , as independent fitting parameters. The thermodynamic parameters obtained for the complexation of TSPP by the open and closed forms of dimers **7** and **10** are summarized in Table 4.2, together with those determined for the binding of TSPP by native CD.

Table 4.2 Thermodynamic parameters of the complexation of TSPP to the open and closed forms of **7** and **10**, as determined by isothermal titration microcalorimetry at 298 K.

	K	ΔG°	ΔH°	$T\Delta S^\circ$	solvent
host	(M^{-1})	(kcal mol $^{-1}$)	(kcal mol $^{-1}$)	(kcal mol $^{-1}$)	
CD ^[a]	$(3.1 \pm 0.4) \times 10^4$	-6.1 ± 0.1	-4.3 ± 0.2	1.8 ± 0.3	H ₂ O
7a	$(2.8 \pm 1.3) \times 10^6$	-8.7 ± 0.3	-12.8 ± 0.6	-4.1 ± 0.9	H ₂ O
7b	$(3.4 \pm 2.0) \times 10^5$	-7.4 ± 0.5	-9.6 ± 0.3	-2.1 ± 0.8	H ₂ O
10a	$(6.3 \pm 1.8) \times 10^5$	-7.9 ± 0.2	-10.7 ± 0.4	-2.8 ± 0.6	H ₂ O/DMSO 9/1
10b	$(6.6 \pm 2.4) \times 10^5$	-7.9 ± 0.2	-12.6 ± 0.4	-4.7 ± 0.6	H ₂ O/DMSO 9/1

^[a] Taken from Chapter 3.

The thermodynamic parameters (K and ΔH°) for the complexation of TSPP by dimer **7a** are indicative of strong 1:1 binding. The enthalpy of binding, -12.8 kcal mol $^{-1}$, is more than double that found for the complexation of TSPP by native CD, and the association constant for complexation of TSPP with **7a**, 2.8×10^6 M $^{-1}$, is two orders of magnitude higher. It is noteworthy that the thermodynamic parameters obtained for the complexation of TSPP by dimer **7a** are, within experimental error, identical to the parameters determined for the corresponding binding of TSPP by the analogous dithienylethene dimer discussed in Chapter 3. This similarity implies that both dimers bind TSPP in a similar fashion. Apparently the energetic costs for bringing the two CD cavities together for complexation of TSPP is the same for both the short dithienylethene dimer and the longer bis(phenylthienyl)ethene dimer **7a**. Given the similarity of both dimers, i.e. connectivity and degrees of freedom present in the dimers, this seems sensible. The correspondence of these results verifies the assumption that the deaggregation observed in the titration curves only affects the initial part of the curve.

Dimer **7b** bound TSPP less effectively than dimer **7a**. The association constant obtained for the complexation of TSPP by dimer **7b**, 3.4×10^5 M $^{-1}$, was a factor of 8 lower than that found for dimer **7a**. The strongly reduced enthalpy of binding, -9.6

kcal mol⁻¹, suggests that the weaker binding is likely due to less cooperative binding of TSPP by the two CD cavities, which are spaced far apart by the rigid bis(phenylthienyl)ethene tether. The less favorable enthalpy of binding is partly compensated by a relatively more favorable entropy of binding. This so-called enthalpy-entropy compensation¹³ is a well-known phenomenon for complexation studies with CDs and CD dimers,^{14,15} and the more favorable entropy associated with less strong enthalpic binding is typically explained in terms of reduced fixation of the host-guest complex. It is noted that the enthalpy of binding found for the complexation of **7b** is considerably more favorable than that found with native CD. Given the length and rigidity of the closed bis(phenylthienyl)ethene tether it is not likely that the second CD cavity has any contribution to the binding of TSPP by the first CD cavity in case of dimer **7b**.¹⁶ A possible explanation for the relatively large enthalpy value found for **7b**, compared to native CD, might be that the tether itself contributes to the binding of TSPP, e.g. by π - π interactions between tether and TSPP.

The open and closed dimers of **10** did not show any difference in binding affinity for TSPP. Both states bound TSPP with an association constant of 6×10^5 M⁻¹. These somewhat lower association constants, compared to those found with dimer **7a**, are probably caused by the presence of DMSO in solution. Although the association constants are similar, there are some striking differences between the binding enthalpies and entropies found for the complexation of the open and closed forms of dimer **10**. Dimer **10a** is the most flexible dimer of the dimers discussed in this chapter and consequently it is expected to effectively bind TSPP with both CD cavities. The thermodynamic parameters found for the complexation of TSPP by **10a**, a strongly negative enthalpy value accompanied by a negative entropy value, support this idea. Interestingly, the enthalpy of binding found for the closed dimer **10b** was 1.9 kcal mol⁻¹ more favorable compared to the open dimer **10a**. This is remarkable because CPK modeling suggests that the rigidity imposed on the dimer by the closed bis(phenylthienyl)ethene tether, and the therewith associated spacing of the CD cavities, cannot be completely overcome by the flexible propyl spacers between the CD cavities and the tether. Therefore, **10b** is probably not able to bind TSPP using both CD cavities to the full extent. Nevertheless, a more favorable binding enthalpy is found for complexation of TSPP by the closed dimer **10b**, compared to **10a**, which is able to use both its CD cavities for the complexation of TSPP. For comparison, the

complexation studies performed with the corresponding dithienylethene tethered dimer with propyl spacers and TSPP also gave similar association constants for the open and closed forms of the dimer, but showed no pronounced differences in binding enthalpy (see Chapter 3). These results indicate that additional interactions between the closed bis(phenylthienyl)ethene tether and TSPP substantially contribute to the binding of TSPP by the dimers. These findings might also explain the moderate difference in binding affinity found for the open and closed form of dimer **7**. The more favorable binding enthalpy found for **10b** is counteracted by a less favorable, i.e. more negative entropy term, to give a binding energy that is similar to that found for the complexation of TSPP by **10a**, rendering dimer **10** unsuitable for phototriggered release of TSPP.

4.2.4 Photo-triggered release and uptake

To test whether the binding difference between the open and closed state of dimer **7** would be sufficient to allow phototriggered release of TSPP, the absorption of the dimer-TSPP complex was followed during irradiation at 313 nm. UV-vis spectroscopy allows the real-time determination of the ratio of uncomplexed and complexed TSPP upon irradiation of dimer-TSPP complexes. It is known that the absorption maximum of TSPP shifts to the red and the absorbance decreases upon complexation by CD.¹⁷ Figure 4.6 shows part of the absorption spectra of the complexes of TSPP and dimers **7** upon irradiation at 313 nm. The absorption maximum of TSPP in aqueous solution at 413 nm showed a red shift to 424 nm upon addition of dimer **7a**, indicative of complex formation between TSPP and the dimer (upper right absorbance band). The shoulder around 413 nm indicated the presence of excess TSPP. Irradiation of the solution at 313 nm led to a decrease of absorption of complexed TSPP (424 nm), and simultaneously an increase of the absorbance at lower wavelengths. Comparison of the separate absorption curves suggests that the increase of absorbance at lower wavelengths is due to an increase in absorbance of uncomplexed TSPP and an additional, less well visible increase in absorbance around 420 nm. The latter can be explained by assuming that the absorbance for the complex of TSPP with the closed dimer **7b** is different from that with open dimer **7a** and that its absorbance maximum lies at lower wavelength. The appearance of two new TSPP-species upon irradiation of the complex of TSPP and dimer **7a** corroborates the data

obtained by calorimetry. At the concentrations used for the experiment, **7b** should still be able to give considerable complexation of TSPP, and consequently only a moderate amount of TSPP is released from the dimer upon closure of the bis(phenylthienyl)ethene tether. In this respect dimer **7** is inferior to the corresponding dithienylethene-tethered CD dimer reported in Chapter 3, which displayed a more substantial release of TSPP upon irradiation at 313 nm.

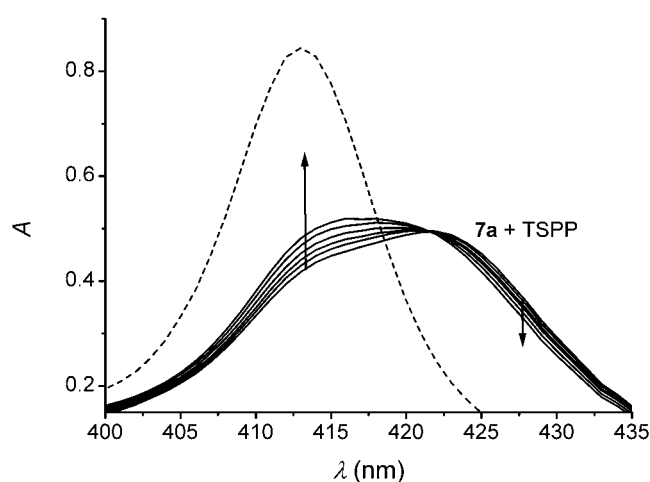


Figure 4.6 Absorption spectra (0 to 10 min) of a 2 μM complex of TSPP with **7a** in water upon irradiation at $\lambda = 313$ nm. Also shown is the spectrum of 2 μM TSPP in water (···).

4.3 Conclusions

The implementation of a bis(phenylthienyl)ethene tether in CD dimers gives photoswitchable receptor molecules that can be reversibly switched between a flexible open and a more rigid closed form. Compared to CD dimers tethered by the shorter dithienylethene tethers, these dimers have a number of advantages and disadvantages. The advantages of the bis(phenylthienyl)ethene tethers are the near complete conversion between the two forms of the CD dimer that can be achieved and the more pronounced separation of the CD cavities of the dimers obtained upon ring-closure of the bis(phenylthienyl)ethene tether. Disadvantages are the low water solubility of the CD dimers, inherent to the large hydrophobicity of the tethers, and the substantial participation of the closed bis(phenylthienyl)ethene tether in the binding of guest molecules as observed for TSPP. The latter leads to a partial compensation for the

possible diminished cooperativity of the CD cavities achieved by the rigid and distant spacing by the closed tether. Consequently, less pronounced binding differences between the open and closed forms of the dimers were observed compared to the corresponding dithienylethene dimers, and only moderate release of complexed TSPP upon irradiation of the complexes could be achieved. This does not imply that dimers **7** and **10** are only moderately tunable receptor molecules. This is the case for TSPP, but strong differences in binding between the two forms of the bis(phenylthienyl)ethene dimers might be achieved with small ditopic guest molecules that have weaker interactions with the closed form of the tether, i.e. guest moieties tethered by relatively hydrophilic non-aromatic linkers.

Taken together, the results given in this chapter illustrate that full addressability of both forms of the tunable receptor and the minimization of possible cooperativity between two host sites for one of the forms of the receptor are not the only criteria in the design of tunable ditopic receptors. Also the relative contributions of the tethers to the binding process should be considered, as these can severely diminish potentially large differences in binding. On the other hand, the tether contributions to binding might be dependent on the form and state of the tether, and this could possibly be used to achieve tunable binding.

4.4 Experimental section

Materials and methods. All chemicals were used as received, unless stated otherwise. Solvents were purified according to standard laboratory methods.¹⁸ Thin-layer chromatography was performed on aluminum sheets precoated with silica gel 60 F254 (Merck). The CD spots were visualized by dipping the sheets in 5% sulfuric acid in ethanol and subsequent heating. Chromatographic separations were performed on silica gel 60 (Merck, 0.040-0.063 mm, 230-240 mesh). 2,2'-(Dichlorodithienylethene)-cyclopentene (**1**)¹⁰ and 3-amino-3-deoxy-heptakis(6-*O*-*tert*-butyldimethylsilyl)- β -cyclodextrin (**5**)¹¹ were prepared according to literature procedures. The synthesis of mono-(2-*O*-(3-aminopropyl))-heptakis-(6-*O*-*tert*-butyldimethylsilyl)- β -cyclodextrin (**8**) is reported in Chapter 3.

FAB mass spectra were recorded with a Finnigan MAT90 spectrometer with *m*-nitrobenzylalcohol as a matrix. MALDI-TOF mass spectra were recorded using a PerSpective Biosystems Voyager-DE-RP MALDI-TOF mass spectrometer. NMR

spectra were recorded at 25 °C using a Varian Inova 300 spectrometer. ¹H NMR chemical shifts (300 MHz) are given relative to residual CHCl₃ (7.25 ppm) or DMSO-d₆ (2.50 ppm). ¹³C NMR chemical shifts (75 MHz) are given relative to CDCl₃ (77 ppm) or to DMSO-d₆ (39.5 ppm).

All synthesized compounds containing the bis(phenylthienyl)ethene moiety are light-sensitive and were therefore exclusively handled in the dark using brown-stained glassware.

1,2-Bis[5'-(4''-carboxymethylphenyl)-2'-methylthien-3'-yl]cyclopentene 3. 2,2'-(Dichlorodithienylethene)-cyclopentene **1** (0.8 g, 2.4 mmol) was converted to 1,2-bis(5'-dibutoxyboryl-2'-methylthien-3'-yl)cyclopentene **2** by reaction with *n*-BuLi (2 mL, 5.1 mmol), and subsequently (*n*-BuO)₃B (2 mL, 7.3 mmol) in freshly distilled anhydrous THF (10 mL) as previously reported by Feringa et al.⁹ The boronic ester **2** was not isolated because it tends to hydrolyze during work-up. In the meantime methyl-4-bromobenzoate (1.56 g, 7.26 mmol) was dissolved in freshly distilled anhydrous THF (15 mL), and Pd(PPh₃)₄ (0.3 g, 0.23 mmol) was added to the stirred solution. The suspension was stirred at room temperature for 15 min, after which 2 M Na₂CO₃ (15 mL) and 10 drops of triethylene glycol were added. The solution of the boronic ester **2** (see above) was slowly added to this suspension. After the addition was complete the suspension was heated to reflux for 2 h, and allowed to cool to room temperature. Diethyl ether (40 mL) and water (40 mL) were added, and the organic layer was isolated and dried over Na₂SO₄. After evaporation of the solvent the product was purified by column chromatography (hexane/CH₂Cl₂ 1/9) to give **3** as a white solid in 68 % overall yield. ¹H NMR (CDCl₃): δ 8.01 (d, *J* = 6.6 Hz, 4H), 7.55 (d, *J* = 6.6 Hz, 4H), 7.17 (s, 2H), 3.9 (s, 6H), 2.87 (t, *J* = 7.5 Hz, 4H), 2.18-2.07 (m, 2H), 2.05 (s, 6H). ¹³C NMR (CDCl₃): δ 166.8, 138.6, 138.5, 137.0, 136.3, 134.7, 130.2, 128.2, 125.4, 124.8, 52.0, 38.5, 23.0, 14.5. FAB-MS: *m/z* calcd for [*M*+H] 528.1, found 528.1.

1,2 Bis[5'-(4''-carboxyphenyl)-2'-methylthien-3'-yl]cyclopentene 4. Compound **3** (0.4 g, 0.76 mmol) was dissolved in dioxane (10 mL) and 4 M NaOH (10 mL) was added to the solution. The stirred suspension was heated to reflux for 10 h, and allowed to cool to room temperature. The aqueous layer was isolated and carefully

acidified by dropwise addition of 12 M HCl. The resulting precipitate was isolated by filtration and extensively washed with water. The residue was dried over CaCl₂ in a vacuum oven at 60 °C to give **4** as a white solid in 92 % yield. ¹H NMR (THF-d₈): δ 7.95 (d, *J* = 8.4 Hz, 4H), 7.52 (d, *J* = 8.4 Hz, 4H), 7.20 (s, 2H), 2.89 (t, *J* = 7.5 Hz, 4H), 2.19-2.11 (m, 2H), 2.01 (s, 6H). ¹³C NMR (THF-d₈): δ 166.9, 139.5, 138.9, 137.8, 136.4, 135.4, 130.8, 129.9, 126.1, 125.6, 125.1, 39.0, 23.5, 14.3. FAB-MS: *m/z* calcd for [*M*] 500.1, found 500.0.

TBDMS-protected bis(phenylthienyl)ethene-tethered CD dimer 6. To a cooled solution of **4** (98 mg, 0.2 mmol) in dry DMF (50 mL) were added HBTU (223 mg, 0.6 mmol) and DIPEA (0.17 mL, 0.98 mmol). The solution was stirred for 30 min and then allowed to warm to room temperature. **5** (950 mg, 0.5 mmol) was added and the solution was stirred for 3 days at room temperature. The solvent was removed in vacuo, and chloroform was added. The solution was washed twice with 1 M HCl and brine. After removal of the solvent, the crude product was purified by gradient column chromatography (ethyl acetate/ethanol/water 100:2:1 to 100:8:4) to give **6** (open form) as a white powder in 43 % yield. ¹H NMR (CDCl₃): δ 8.23 (d, *J* = 7.6 Hz, 2H), 7.86 (d, *J* = 8.4 Hz, 4H, H-Ar), 7.45 (d, *J* = 8.4 Hz, 4H), 7.05 (s, 2H), 4.94-4.86 (m, 12H), 4.69 (d, *J* = 7.3 Hz, 2H), 4.13-3.38 (m, 84H), 2.84 (t, *J* = 7.5 Hz, 4H), 2.14 (m, 2H), 2.00 (s, 6H), 1.1-0.7 (m, 126H), 0.05-0.00 (m, 84H). ¹³C NMR (CDCl₃): δ 170.3, 138.6, 137.8, 136.1, 135.1, 134.2, 131.5, 127.9, 126.3, 124.7, 105.9, 104.8, 101.9-100.2, 82.7-79.4, 73.4-71.6, 62.6-60.3, 51.9, 38.0, 26.0-25.8, 23.4, 15.4, -4.8 - -5.1. MALDI-TOF: *m/z* calcd for [*M*+Na]⁺ 4351.1, found 4353.5.

Bis(phenylthienyl)ethene-tethered CD dimer 7. TBDMS-protected dimer **6** (245 mg, 0.09 mmol) was dissolved in trifluoroacetic acid (25 mL). The solution was stirred at room temperature for 10 min. The solvent was removed in vacuo. Methanol was added and evaporated in vacuo for azeotropic removal of any residual trifluoroacetic acid. The residue was dissolved in water and washed three times with diethyl ether. After freeze-drying dimer **7a** was obtained as a white solid in 94 % yield. ¹H NMR (DMSO-d₆): δ 8.12 (br, 2H), 7.82 (d, *J* = 8.4 Hz, 4H), 7.60 (d, *J* = 8.4 Hz, 4H), 7.39 (s, 2H), 4.89-4.76 (m 12H), 4.67 (d, *J* = 6.6 Hz), 4.35 (br, 2H), 3.97 (br, 2H), 3.78-3.29 (m, 82H), 2.85 (br, 4H), 2.10 (m, 2H), 2.00 (s, 6H). ¹³C NMR

(DMSO- d_6): δ 170.4, 139.8, 139.0, 138.5, 137.3, 136.4, 133.3, 129.6, 126.7, 126.0, 105.8, 103.9-102.8, 82.9-80.4, 74.9-73.0, 61.8-61.3, 53.3, 38.1, 23.2, 14.7. MALDI-TOF: m/z calcd for $[M+Na]^+$ 2753.9, found 2755.4.

TBDMS-protected bis(phenylthienyl)ethene-tethered CD dimer 9. The same procedure as described for dimer **6** was used starting from **4** (28 mg, 0.06 mmol), HBTU (64 mg, 0.16 mmol) and DIPEA (48 μ L, 0.28 mmol), and followed by addition of **8** (275 mg, 0.14 mmol). The crude product was purified by gradient column chromatography (ethyl acetate/ethanol/water 100:2:1 to 100:8:4) to give **9** (open form) as a white powder in 81 % yield. 1H NMR ($CDCl_3$): δ 8.05 (br, 2H), 7.81 (d, $J = 8.4$ Hz, 4H), 7.58 (d, $J = 6.6$ Hz, 4H, H-Ar), 7.06 (s, 2H), 5.04-4.99 (m, 14H), 3.98-3.44 (m, 84H), 3.18 (d, $J = 9.9$ Hz, 2H), 2.80 (t, $J = 7.5$ Hz, 4H), 2.09-1.98 (m, 8H), 1.86 (m, 4H), 0.9-0.7 (m, 126H), 0.05-0.00 (m, 84H). ^{13}C NMR ($CDCl_3$): δ 173.2, 143.6, 138.7, 136.9, 136.1, 135.3, 132.6, 127.9, 125.5, 125.1, 103.2-102.2, 82.0-80.1, 74.0-72.7, 71.8, 61.9-60.2, 37.8, 32.1, 26.1-24.5, 22.8, 14.8, -4.8 - -5.2. MALDI-TOF: m/z calcd for $[M+Na]^+$ 4467.1, found 4468.4.

Bis(phenylthienyl)ethene-tethered CD dimer 10. Analogous to the procedure outlined for the deprotection of dimer **7**, dimer **9** (201 mg, 0.05 mmol) was deprotected using trifluoroacetic acid (25 mL) to give dimer **10** after freeze-drying as a white solid in 91 % yield. 1H NMR (DMSO- d_6): δ 8.43 (br, 2H), 7.83 (d, $J = 8.4$ Hz, 4H), 7.64 (d, $J = 8.4$ Hz, 4H), 7.42 (s, 2H), 5.84-5.66 (m, 14H), 4.82-3.07 (m, 84H), 2.85 (t, $J = 7.5$ Hz, 4H), 2.06 (m, 2H), 1.92 (s, 6H), 1.77 (m, 4H). ^{13}C NMR (DMSO- d_6): δ 166.1, 138.5, 137.4, 136.5, 135.2, 134.7, 133.3, 128.5, 125.9, 124.9, 102.6-101.9, 100.8, 82.7, 82.3-81.7, 81.3, 73.8-71.8, 70.3, 60.7-60.1, 36.5, 30.0, 23.9, 14.6. MALDI-TOF: m/z calcd for $[M+Na]^+$ 2871.8, found 2872.4.

UV-vis spectroscopy. UV-vis spectra were recorded on a Hewlett Packard HP 8452 UV-vis spectrophotometer. Irradiation experiments were performed in situ by irradiation of the samples in a 1 cm quartz cuvette in the UV-vis setup, using a 200W mercury lamp with a 313 nm band-pass or a 460 nm high pass filter.

Preparation of the PSS mixtures. Solutions of the open form of the dimer in Millipore water (1 to 10 mM) in a quartz cuvette were irradiated with a high intensity mercury lamp for 10 to 15 min. UV-vis spectra of diluted samples were used to follow the photochromic reaction. Once the PSS was reached, samples were freeze-dried to give the PSS mixture as a purple solid.

Calorimetry. Calorimetric titrations were performed at 25 °C using a Microcal VP-ITC titration microcalorimeter. Sample solutions were prepared in Millipore water for dimer **7**, and in mixtures of DMSO and Millipore water (1:9, v:v) for dimer **10**. Titrations were performed by adding aliquots of a TSPP solution to the host solution. The titrant typically contained 0.1 to 1 mM of guest, while the cell solutions contained 10 to 100 µM of host. All calorimetric titrations were corrected for dilution heats by subtraction of the calorimetric dilution experiments from the calorimetric titration experiments. The titrations were analyzed with a least-squares curve fitting procedure. The thermodynamic data reported in Table 4.2 are based on at least three independent titrations performed at three different concentrations.

4.5 References and notes

¹ Irie, M. *Chem. Rev.* **2000**, *100*, 1685-1716.

² Feringa, B. L. *Molecular Switches*, Wiley-VCH, Weinheim, **2001**.

³ For photoswitchable CD dimers see: a) Aoyagi, T.; Ueno, A.; Fukushima, M.; Osa, T. *Macromol. Rapid Commun.* **1998**, *19*, 103-105. b) Ruebner, A.; Yang, Z. W.; Leung, D.; Breslow, R. *Proc. Natl. Acad. Sci. U. S. A.* **1999**, *96*, 14692-14693. c) Baugh, S. D. P.; Yang, Z. W.; Leung, D. K.; Wilson, D. M.; Breslow, R. *J. Am. Chem. Soc.* **2001**, *123*, 12488-12494.

⁴ For metal-switchable CD dimers see: a) Liu, Y.; Wu, C. T.; Xue, G. P.; Li, J. J. *Inclusion Phenom. Macrocyclic Chem.* **2000**, *36*, 95-100. b) Liu, Y.; You, C.-C.; Wada, T.; Inoue, Y. *Tetrahedron Lett.* **2000**, *41*, 6869-6873. c) Liu, Y.; Chen, Y.; Zhang, H.-Y.; Liu, S.-X. Guan, X.-D. *J. Org. Chem.* **2001**, *66*, 8518-8527. d) Liu, Y.; You, C.-C.; Li, B. *Chem. Eur. J.* **2001**, *7*, 1281-1288. e) Liu, Y.; Li, L.; Zhang, H.-Y.; Song, Y. *J. Org. Chem.* **2003**, *68*, 527-536.

⁵ For CDs capped with photoswitchable moieties see: a) Ueno, A.; Yoshimaru, H.; Saka, R.; Osa, T. *J. Am. Chem. Soc.* **1979**, *101*, 2779-2780. b) Ueno, A.; Tomita, Y.; Osa, T. *Tetrahedron Lett.* **1983**, *24*, 5245-5284. c) Ueno, A.; Fukushima, M.; Osa, T. *J. Chem. Soc. Perkin Trans. 2* **1990**, 1067-1072. d) Fukushima, M.; Osa, T.; Ueno, A. *Chem. Lett.* **1991**, 709-712. e) Hamada, F.; Fukushima, M.; Osa, T.; Ikeda, H.; Toda, F.; Ueno, A. *Macromol. Rapid Commun.* **1993**, *14*, 287-291.

⁶ For photoswitchable crown ethers see: a) Alfimov, M. V.; Fedorova, O. A.; Gromov, S. P. *J. Photochem. Photobiol. A* **2003**, *158*, 183-198. b) Shinkai, S.; Ogawa, T.; Nakaji, T.; Kusano, Y.; Manabe, O. *Tetrahedron Lett.* **1979**, 4569-4572. c) Shinkai, S.; Nakaji, T.; Nishida, Y.; Ogawa, T.; Manabe, O. *J. Am. Chem. Soc.* **1980**, *102*, 5860-5865. d) Shinkai, S.; Manabe, O. *Top. Curr. Chem.* **1984**, *121*, 67-104.

⁷ For recent examples of photoswitchable receptors based on other host molecules see: a) Hunter, C. A.; Togrul, M.; Tomas, S. *Chem. Commun.* **2004**, 108-109. b) Winkler, T.; Dix, I.; Jones, P. G.; Herges, R. *Angew. Chem. Int. Ed.* **2003**, *42*, 3541-3544. c) Srinivas, O.; Mitra, N.; Surolia, A.; Jayaraman, N. *J. Am. Chem. Soc.* **2002**, *124*, 2124-2125. d) Goswami, S.; Ghosh, K.; Halder, M. *Tetrahedron Lett.* **1999**, *40*, 1735-1738. e) Bencini, A.; Bernardo, M. A.; Bianchi, A.; Ciampolini, M.; Fusi, V.; Nardi, N.; Parola, A. J.; Pina, F.; Valtancoli, B. *J. Chem. Soc., Perkin Trans. 2* **1998**, 413-418. f) Starck, F.; Jones, P. G.; Herges, R. *Eur. J. Org. Chem.* **1998**, 2533-2539. g) Kimura, K.; Utsumi, T.; Teranishi, T.; Yokoyama, M.; Sakamoto, H.; Okamoto, M.; Arakawa, R.; Moriguchi, H.; Miyaji, Y. *Angew. Chem. Int. Ed. Engl.* **1997**, *36*, 2452-2455. h) Takeshita, M.; Uchida, K.; Irie, M. *Chem. Commun.* **1996**, 1807-1808. i) Würthner, F.; Rebek, J. Jr. *J. Chem. Soc., Perkin Trans. 2* **1995**, 1727-1734. j) Würthner, F.; Rebek, J. Jr. *Angew. Chem. Int. Ed. Engl.* **1995**, *34*, 446-448.

⁸ For recent examples of metal-switchable receptors based on other host molecules see: a) Lützen, A.; Haß, O.; Bruhn, T. *Tetrahedron Lett.* **2002**, *43*, 1807-1811. b) Haino, T.; Yamanaka, Y.; Araki, H.; Fukazawa, Y. *Chem. Commun.* **2002**, 402-403. c) Monti, D.; La Monica, L.; Scipioni, A.; Mancini, G. *New J. Chem.* **2001**, *25*, 780-782. d) Monti, D.; Venanzi, M.; Mancini, G.; Marotti, F.; La Monica, L.; Boschi, T. *Eur. J. Org. Chem.* **1999**, *8*, 1901-1906.

⁹ De Jong, J. J. D.; Lucas, L. N.; Hania, R.; Pugzlys, A.; Kellogg, R. M.; Feringa, B. L.; Duppen, K.; Van Esch, J. H. *Eur. J. Org. Chem.* **2003**, 1887-1893.

¹⁰ Lucas, L. N.; De Jong, J. J. D.; Van Esch, J. H.; Kellogg, R. M.; Feringa B. L. *Eur. J. Org. Chem.* **2003**, 155-166.

¹¹ Van Dienst, E.; Snellink, B. H. M.; Von Piekartz, I.; Grote Gansey, M. H. B.; Venema, F.; Feiters, M. C.; Nolte, R. J. M.; Engbersen, J. F. J.; Reinhoudt, D. N. *J. Org. Chem.* **1995**, *60*, 6537-6545.

¹² The synthesis of this compound is described in Chapter 3.

¹³ Leffler, J. E. *J. Org. Chem.* **1955**, *20*, 1202-1231.

¹⁴ Rekharsky, M. V.; Inoue, Y. *Chem. Rev.* **1998**, *98*, 1875-1917.

¹⁵ a) Zhang, B.; Breslow, R. *J. Am. Chem. Soc.* **1993**, *115*, 9353-9354. b) Liu, Y.; Chen, Y.; Li, B.; Wada, T.; Inoue, Y. *Chem. Eur. J.* **2001**, *7*, 2528-2535.

¹⁶ For comparison, the closed form of the dithienylethene-tethered dimer was found to bind TSPP with an enthalpy of binding only slightly higher (1 kcal mol⁻¹) than the binding enthalpy for the complexation of TSPP by native CD (see Chapter 3).

¹⁷ Carofiglio, T.; Fornasier, R.; Lucchini, V.; Rosso, C.; Tonelatto, U. *Tetrahedron Lett.* **1996**, *37*, 8019-8022.

¹⁸ Perrin, D. D.; Armarego, W. F. L. *Purification of Laboratory Chemicals*, 3rd ed., Pergamon, Oxford, **1989**.

Complexation of charged porphyrins by charged and metal-chelated EDTA-tethered β -cyclodextrin dimers: a thermodynamic study on the influence of tether charge and flexibility on binding affinity

5.1 Introduction

Since the first publication of a cyclodextrin dimer by Tabushi in 1979,¹ a large number of cyclodextrin dimers have been synthesized.² Among these, cyclodextrin dimers tethered by a metal chelating linker are of particular interest as these tethers offer an additional functionality. For instance, metallo-cyclodextrin dimers are interesting for catalysis, as they possess two hydrophobic pockets, which can rigidly organize substrate molecules in close proximity to a catalytically active metal center. Such metallo-cyclodextrin dimers have shown impressive reaction rate accelerations and high specificities.^{3,4} Metal chelation has also been employed to organize multiple β -cyclodextrin (CD) dimers around a metal ion.^{5,6} Additionally, metal chelating tethers have been utilized to tune binding affinity and selectivity.⁷⁻⁹

There are several ways in which metal ligation by the tether can alter the binding affinities of the cyclodextrin dimer. The most impressive results have been obtained when the ligated metal serves as an additional binding site for the guest molecule complexed by the cyclodextrin dimer. An illustrative example in this respect is the binding of bis(1-adamantylethyl)phosphate by a bipyridine-tethered CD dimer, reported by Breslow and Zhang (entry 6, Table 2.1).^{3d} The dimer bound the phosphodiester a factor of 55 more strongly in the presence of zinc(II), which was attributed to the coordination of the phosphate anion to the metal cation.

Alternatively, metal ligation can be used to impose a charge on the cyclodextrin dimer and thereby influence its binding affinity for charged guest species by means of attractive or repulsive electrostatic interactions. Lincoln, Easton and co-workers demonstrated that coordination of sodium(I) by diazocoronand-tethered CD dimers led to a five-fold increase in binding affinity of the dimers for the Brilliant Yellow tetraanion.⁷

Furthermore, ligation of the tether to metal ions can strongly influence the flexibility of the tether and the relative orientation of the two cyclodextrin cavities, thus altering the binding properties of the dimer. This has been demonstrated by the groups of Wu⁸ and Liu⁹ who synthesized CD dimers with oligo(ethylenamine) tethers. Chelation of metal ions by the tethers of these dimers resulted in enhanced binding affinities for small organic dye molecules, with maximum binding enhancements of a factor of 5.^{9a,b}

This chapter presents ethylenediamine-*N,N,N',N'*-tetraacetate- (EDTA-) tethered CD dimers as a new class of tunable receptors. By partial protonation and/or metal complexation of the EDTA moiety both the tether charge and flexibility can be controlled. Therefore, in principle both the possible contribution of electrostatic interactions in complexation and the extent of possible cooperation of the two CD cavities can be controlled. These two handles can be used independently or simultaneously to control the binding properties of the CD dimers. The potential of these dimers as tunable receptors has been assessed in complexation studies with charged porphyrins. Isothermal titration calorimetry was used to elucidate the fundamental complexation behavior and the role and relative contributions of the hydrophobic and electrostatic interactions.

5.2 Results and discussion

Chart 5.1 depicts the two EDTA-tethered CD dimers and porphyrin guests used for the complexation studies. The dimers differ in the connectivity between the two CD cavities and the EDTA moieties. In dimer **1**, the CD cavities are connected to the EDTA moiety through flexible propyl spacers, whereas in dimer **2** the EDTA moiety is coupled directly to the secondary rim of the CD cavities.

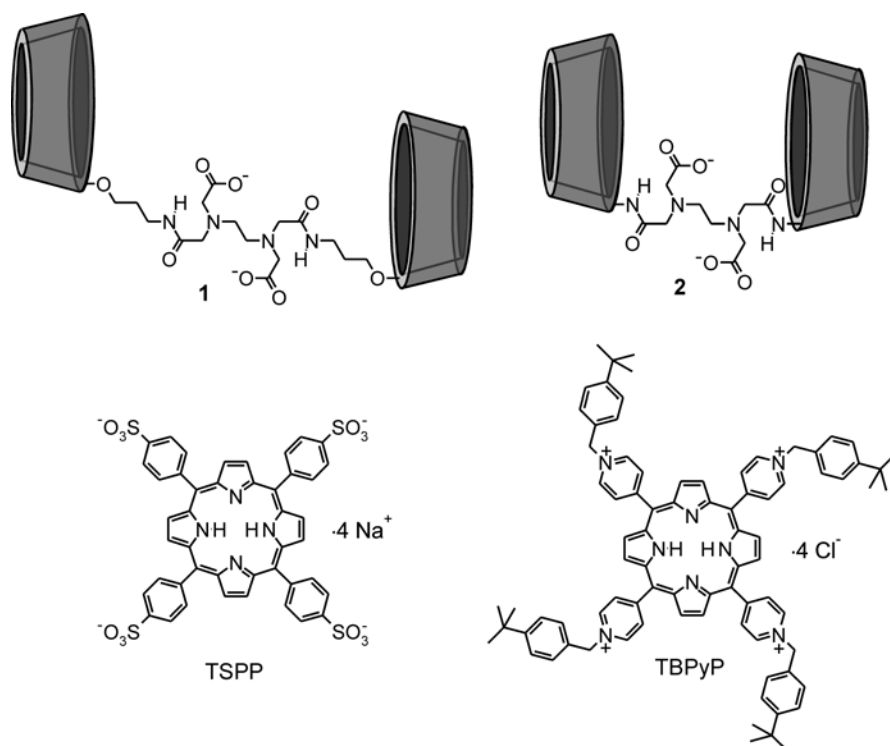


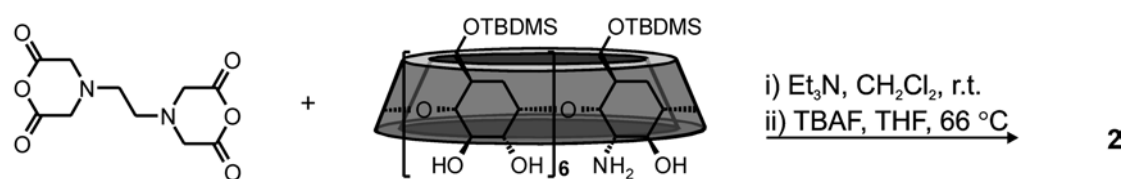
Chart 5.1 EDTA-tethered CD dimers and porphyrin guest molecules used in this study.

Porphyrins were chosen as guest molecules for complexation by the CD dimers because they offer multiple equivalent binding sites for CD, which are symmetrically positioned at a single molecular platform, giving rise to well-defined symmetrical binding modes.¹⁰ For the complexation studies meso-tetrakis(4-sulfonatophenyl)porphyrin (TSPP) and *p*-*tert*-butylbenzyl-functionalized *p*-pyridylporphyrin (TBPYP) were used. These molecules are structurally similar but are differently sized and oppositely charged enabling a detailed assessment of the influence of changes in both tether flexibility and charge on the binding properties of the dimers. The smaller tetraanionic TSPP is commercially available and the larger tetracationic TBPYP was synthesized from the corresponding tetrapyridylporphyrin as reported previously.¹¹ Both TSPP and TBPYP have been used previously for complexation studies with CD and CD dimers.¹⁰⁻¹⁴

5.2.1 Synthesis and characterization of the CD dimers

The synthesis of EDTA-tethered CD dimer **1** has been reported previously.¹⁵ For the synthesis of CD dimer **2** an analogous procedure, outlined in Scheme 5.1, was followed. Reaction of the commercially available EDTA-bis(anhydride) with

TBDMS-protected mono-3-amino-3-deoxy- β -cyclodextrin¹⁶ gave the TBDMS-protected precursor of dimer **2**, which was purified by silica column chromatography. Subsequent deprotection using tetrabutylammonium fluoride yielded the water-soluble dimer **2**. The spectroscopic data obtained for dimer **2** were in accordance with the data found by the group of Fujita, who synthesized this same dimer from EDTA-bis(anhydride) and unprotected 3-amino-3-deoxy- β -cyclodextrin in DMF.¹⁷



Scheme 5.1 Synthesis of the EDTA-tethered dimer **2**.

It should be noted that the CD moieties of dimer **1** and **2** are different in the sense that the modified sugar units of the CDs of dimer **2** are altrosidic (see Scheme 5.1). This is inherent to the synthetic pathway towards the TBDMS-protected 3-amino-3-deoxy- β -cyclodextrin,¹⁶ which involves the ring opening of manno-mono-2,3-epoxy- β -cyclodextrin with ammonia, leading to an inversion at the C3 carbon.¹⁸ The presence of the altrose units gives rise to a certain extent of mobility of the CD ring, and as a consequence the CD cavities of dimer **2** are relatively flexible compared to those of dimer **1**. Dimer **1** was synthesized from TBDMS-protected mono(2-*O*-aminopropyl)- β -cyclodextrin,¹⁵ which is obtained by alkylation of TBDMS-protected β -cyclodextrin, leaving the original structure of the CD cavity intact. The complexation studies with photoswitchable CD dimers reported in Chapter 3 showed that both types of cavities gave comparable results for the complexation of TSPP, indicating that the degree of flexibility of the CD cavities has little effect on the binding affinity of the CD dimers for this type of guest.

5.2.2 Charged and metal-chelated CD dimers

The EDTA tether is a particularly versatile moiety. EDTA is zwitterionic and capable of complexing a variety of metal ions. These characteristic features of EDTA were used to access four different forms of dimers **1** and **2** (see Chart 5.2), which

differ in tether charge ($z = -2, -1, 0,$ and $+1$) and tether flexibility (free ligand and protonated forms versus metal complexes).

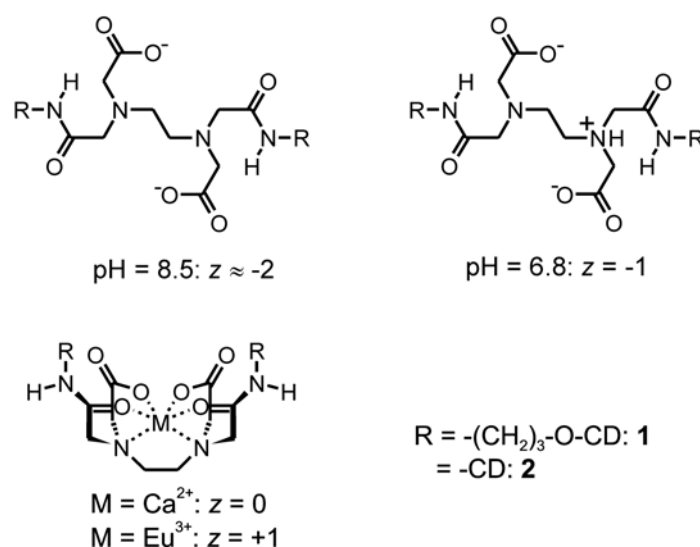


Chart 5.2 Charged free ligand, protonated and metal-chelated forms of the EDTA-tethered CD dimers assessed in the complexation studies.

The ligand protonation constants for dimers **1** and **2** were assumed to be comparable to those determined for EDTA-bis(propyl amide) by Peters and co-workers ($\text{p}K_{a1} = 7.2, \text{p}K_{a2} = 3.6, \text{p}K_{a3} = 2.0$).¹⁹ From these values it can be concluded that especially the free ligand ($\text{pH} > 8, z = -2$) and the mono-protonated species ($4.5 < \text{pH} < 7, z = -1$) are well accessible. Accordingly, complexation studies were performed at $\text{pH} 8.5$ to assess the binding properties of the free ligands, $\mathbf{1}^{2-}$ and $\mathbf{2}^{2-}$, and at physiological $\text{pH} (6.8)$, where the protonated dimers $[\text{H}\cdot\mathbf{1}]^{1-}$ and $[\text{H}\cdot\mathbf{2}]^{1-}$ are assumed to be predominant.

Metal chelation was used to obtain neutral and positively charged dimers. Addition of CaCl_2 to aqueous solutions of dimers **1** and **2** gave the neutral complexes $[\text{Ca}\cdot\mathbf{1}]^0$ and $[\text{Ca}\cdot\mathbf{2}]^0$, respectively. Similarly, EuCl_3 was used to obtain the positively charged complexes $[\text{Eu}\cdot\mathbf{1}]^{1+}$ and $[\text{Eu}\cdot\mathbf{2}]^{1+}$. Metal chelation is associated with the organization of the EDTA tether around the metal ion, and consequently the metal-chelated dimers have restricted tether flexibility compared to the uncomplexed dimers. This is especially true for dimer **2**, in which the CD cavities are directly linked to the EDTA moiety. Restrictions for dimer **1** are expected to be less dramatic

as the propylamine linkers are able to overcome the rigidity imposed on the EDTA moiety to some extent.

5.2.3 Complexation studies

The complexation of the EDTA-tethered dimers with the porphyrin guest molecules TSPP and TBPYP was studied with isothermal titration calorimetry (ITC). ITC measurements allow the direct determination of the association constant, K , and the binding enthalpy, ΔH° , and thus provide a complete thermodynamic picture of the interactions under investigation.

Figure 5.1 depicts a typical series of exothermic heat profiles obtained for the titration of TSPP to the different ligand and metal complex forms of dimer **1**. All four titration curves depicted in Figure 5.1 were recorded for the same concentrations of TSPP and **1**. The inflection points in the titration curves indicate the formation of a complex with 1:1 binding stoichiometry, typical for TSPP and CD dimers.^{11,12,14} Due to its small size TSPP can only accommodate two CD cavities, i.e. one CD dimer. Typically two opposite phenyl rings are complexed in a so-called anti-geometry and complexation of the remaining phenyl rings is sterically not feasible.²⁰ The titration curves could be fitted well with a 1:1 binding model (solid lines, Figure 5.1) using the association constant, K , and the binding enthalpy, ΔH° , as independent fitting parameters.

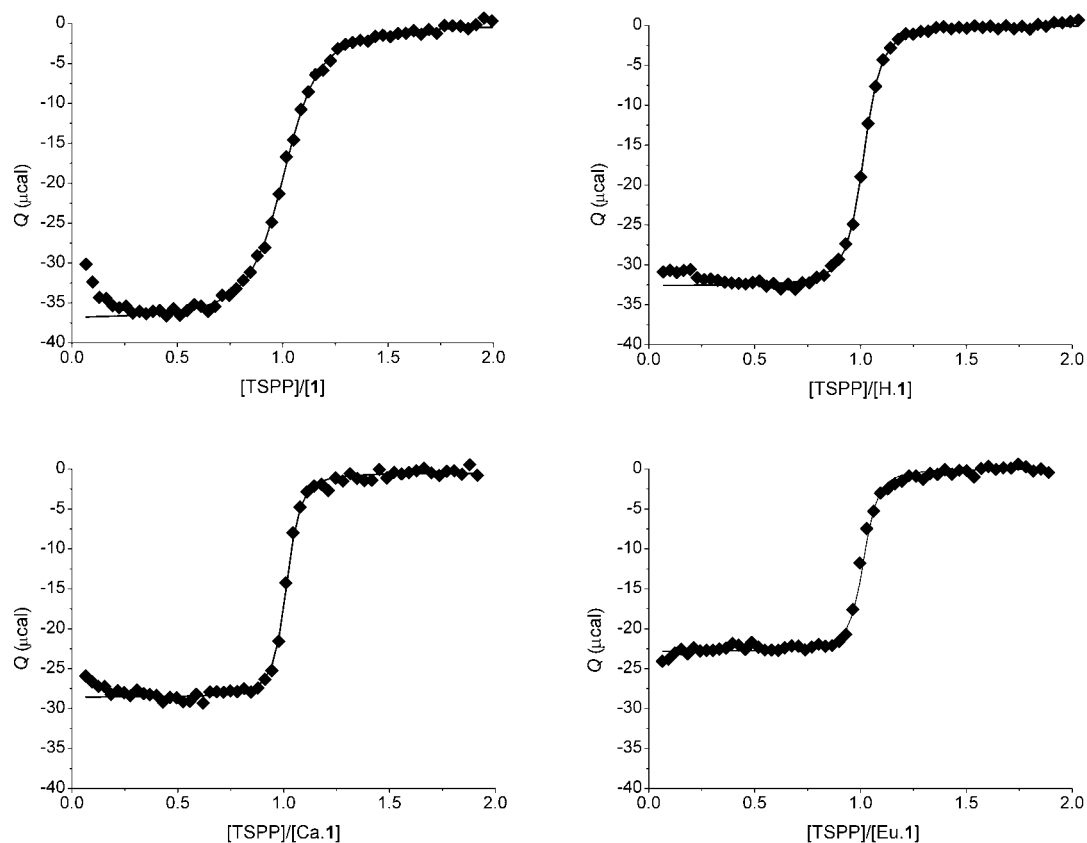


Figure 5.1 Heat evolved per injection plotted against the molar ratio $[TSPP]/[I]$ (markers) and fits (solid lines) for the calorimetric titrations of 0.5 mM TSPP to 50 μM of I^{2-} (top left), $[H\cdot I]^{1-}$ (top right), $[Ca\cdot I]^0$ (bottom left), or $[Eu\cdot I]^{1+}$ (bottom right) in water at 298 K.

Table 5.1 gives the thermodynamic parameters for the complexation of TSPP by native CD and the different forms of dimer **1**. For all four systems, the thermodynamic parameters were indicative of a strong 1:1 complex with both CD cavities participating in binding. The association constants were orders of magnitude higher than that found for the binding of TSPP by native CD, and the enthalpies of binding were more than double the enthalpy of the CD-TSPP complex.

Table 5.1 Thermodynamic parameters of the complexation of TSPP by the different ligand and metal complex forms of **1** and β -cyclodextrin (CD), as determined by ITC at 298 K.

Host	K (M^{-1})	ΔG° ($kcal\ mol^{-1}$)	ΔH° ($kcal\ mol^{-1}$)	$T\Delta S^\circ$ ($kcal\ mol^{-1}$)
CD ^[a]	$(3.1 \pm 0.4) \times 10^4$	-6.1 ± 0.1	-4.3 ± 0.2	1.8 ± 0.3
1 ²⁻	$(6.4 \pm 3.8) \times 10^6$	-9.2 ± 0.4	-16.6 ± 0.4	-7.4 ± 0.8
[H· 1] ¹⁻	$(2.0 \pm 1.1) \times 10^7$	-9.9 ± 0.4	-15.3 ± 0.4	-5.4 ± 0.8
[Ca· 1] ⁰	$(2.0 \pm 1.3) \times 10^7$	-9.9 ± 0.4	-13.7 ± 0.2	-3.8 ± 0.6
[Eu· 1] ¹⁺	$(3.4 \pm 1.9) \times 10^7$	-10.2 ± 0.3	-11.8 ± 0.6	-1.6 ± 0.9

^[a] Taken from Chapter 3.

Comparison of the thermodynamic parameters obtained for the different forms of **1** showed some interesting trends. Upon going from **1**²⁻ to [Eu·**1**]¹⁺ the association constant for TSPP steadily increased to give a factor of 5 maximum difference. The highest association constant was found for the complex involving two oppositely charged species, whereas the complexes formed by two similarly charged species gave relatively low association constants. The increase in association constant was the result of large, apparently systematic, and partly counteracting changes in the enthalpies and entropies of binding. Upon going from **1**²⁻ to [Eu·**1**]¹⁺ the enthalpy of binding became less favorable as it increased with 1.3 to 1.9 kcal per added charge unit. These systematic increases in enthalpy were well visible in the calorimetric titration curves, which showed stronger exothermic heat plateaus for the more negatively charged dimers (see Figure 5.1). The less favorable enthalpies of binding were overridden by systematically increasing entropies. Per added charge unit the entropy contributions ($T\Delta S$) became 1.6 to 2.2 $kcal\ mol^{-1}$ more favorable.

These apparently charge-related systematic changes in enthalpy and entropy and the absence of additional, possibly tether flexibility-related effects between **1**²⁻ and [H·**1**]¹⁻ on the one hand and [Ca·**1**]⁰ and [Eu·**1**]¹⁺ on the other, imply that electrostatic interactions affect the binding of TSPP by dimer **1** significantly, while the difference in tether flexibility has no strong influence. Considering the small size of TSPP and the flexible propyl spacers of dimer **1** this is not surprising. The studies with the photoswitchable dithienylethene-tethered CD dimer coupled via propyl

linkers, reported in Chapter 3, also gave only minor differences in binding affinity for TSPP with varying tether flexibility. Influences of electrostatic interactions on the binding properties as seen for dimer **1** and TSPP are not uncommon. Similarly, electrostatic interactions have been shown to influence the binding properties of diazocoronand-tethered CD dimers,⁷ and cationic mono- and diamino-CDs are known to exhibit higher/lower affinities towards negatively/positively charged guests compared to native CDs.^{21,22,23}

The thermodynamic parameters listed in Table 5.1 enabled the elucidation of the role of electrostatic interactions in the binding of TSPP by dimer **1**. The thermodynamic parameters obtained for the interaction between $[\text{Ca}\cdot\mathbf{1}]^0$ and TSPP are most readily interpreted. $[\text{Ca}\cdot\mathbf{1}]^0$ did not bear a charge that could possibly interact with TSPP, and therefore the complexation was solely attributed to the hydrophobic interactions between TSPP and the two CD cavities. The thermodynamic parameters obtained for the binding of TSPP by $[\text{Ca}\cdot\mathbf{1}]^0$ were comparable to those obtained for the binding of TSPP by the dithienylethene-tethered dimers reported in Chapter 3. Comparison of the thermodynamic parameters obtained for $[\text{Ca}\cdot\mathbf{1}]^0$ and $[\text{Eu}\cdot\mathbf{1}]^{1+}$ showed that the latter complex formation with TSPP was accompanied by an additional endothermic, entropy-driven process. The enthalpy of binding for complexation of TSPP by $[\text{Eu}\cdot\mathbf{1}]^{1+}$ was $1.9 \text{ kcal mol}^{-1}$ less favorable compared to $[\text{Ca}\cdot\mathbf{1}]^0$, while the $T\Delta S^\circ$ contribution was $2.2 \text{ kcal mol}^{-1}$ more favorable. Overall this resulted in a favorable contribution to the free energy of binding of $0.3 \text{ kcal mol}^{-1}$.

It is well known that attractive electrostatic interactions between two oppositely charged species are governed by positive entropy values.^{24,25} These arise from partial desolvation of the ion groups (ion-pairing). Associated endothermic enthalpies of binding have been ascribed to the energetic cost required to desolvate the charged groups.²⁶ The differences in thermodynamic parameters for the binding of TSPP by $[\text{Ca}\cdot\mathbf{1}]^0$ and $[\text{Eu}\cdot\mathbf{1}]^{1+}$ suggest that such attractive electrostatic interactions might also be involved in the interaction of the positively charged dimer $[\text{Eu}\cdot\mathbf{1}]^{1+}$ and the negatively charged sulfonate groups of TSPP.

Similarly, increases in solvation might explain the observed decreases in entropy and the corresponding decreases in enthalpy associated with the complexation of TSPP by the negatively charged dimers, $\mathbf{1}^{2-}$ and $[\text{H}\cdot\mathbf{1}]^{1-}$. The close proximity of two oppositely charged molecules requires relatively large amounts of structured water for

stabilization. As a result the complexation of TSPP by $\mathbf{1}^{2-}$ compared to the corresponding binding by $[\text{H}\cdot\mathbf{1}]^{1-}$ is $0.7 \text{ kcal mol}^{-1}$ less favorable. Taken together, the trends in thermodynamic parameters found for the interaction of TSPP with the different forms of dimer **1** indicate that the interaction strengths of the complexes is governed by electrostatic interactions.

The thermodynamic parameters for the complexation of TSPP by the different forms of dimer **2** are listed in Table 5.2. Dimer $[\text{H}\cdot\mathbf{2}]^{1-}$ was not investigated due to the limited quantity of dimer **2** that was available for the complexation studies. Similar to the complexation studies performed with dimer **1**, all titration curves indicated the formation of complexes with a 1:1 stoichiometry, and the titration curves could be well fitted using a 1:1 binding model.

Table 5.2 Thermodynamic parameters of the complexation of TSPP by the different ligand and metal complex forms of **2**, as determined by ITC at 298 K.

Host	K (M^{-1})	ΔG° (kcal mol^{-1})	ΔH° (kcal mol^{-1})	$T\Delta S^\circ$ (kcal mol^{-1})
$\mathbf{2}^{2-}$	$(2.7 \pm 1.0) \times 10^5$	-7.4 ± 0.2	-11.7 ± 0.3	-4.2 ± 0.5
$[\text{Ca}\cdot\mathbf{2}]^0$	$(3.1 \pm 0.9) \times 10^5$	-7.4 ± 0.2	-11.4 ± 0.2	-4.0 ± 0.4
$[\text{Eu}\cdot\mathbf{2}]^{1+}$	$(2.7 \pm 1.0) \times 10^5$	-7.4 ± 0.3	-10.2 ± 0.6	-2.8 ± 0.9

For dimer **2**, the electrostatic interactions between the EDTA tether and TSPP do not seem to have a strong effect on the association constants. The three assessed forms of dimer **2** all bind TSPP with an association constant of $3 \times 10^5 \text{ M}^{-1}$. These association constants are two orders of magnitude lower than those found for the binding of TSPP by dimer **1**. Comparison of the thermodynamic parameters for the complexation of TSPP by the different forms of dimers **1** and **2** showed that the lower association constants observed for the latter dimer were mainly due to a less exothermic enthalpy of binding, which indicated a less effective cooperation of the CD cavities in binding the porphyrin guest. For the metal-chelated dimers this is explainable. Metal chelation strongly limits the rotational freedom present in dimer **2**, therewith hampering the ideal intramolecular orientation of the two CD cavities required to strongly bind TSPP. This effect of imposed rigidity has no pronounced

influence on the binding properties of the more flexible dimer **1** (see above and Table 5.1).

The thermodynamic parameters and relatively low association constant obtained for the binding of TSPP by dimer **2**²⁻ are more difficult to explain. Given the flexibility of this dimer it would be expected to bind TSPP with an association constant similar to that found for dimer **1**. Furthermore, the thermodynamic parameters for the formation of complex [2·TSPP]²⁻ were not in line with the typical trend in enthalpy and entropy of binding upon going to more negatively charged dimers, as observed for the binding of TSPP by dimer **1**. This effect was only seen for the binding of TSPP by [Eu·2]¹⁺, which was associated with a less exothermic enthalpy of binding and a less negative entropy value compared to the binding of TSPP by [Ca·2]⁰, indicating that favorable electrostatic interactions might be involved in the binding of TSPP by [Eu·2]¹⁺. The absolute effects, however, were smaller than observed for **1**. Given the small differences in thermodynamic parameters it is difficult to attribute the effect of tether flexibility and charge on the binding affinity of dimer **2** for TSPP.

Figure 5.2 depicts two typical binding curves obtained for the titration of the larger tetracationic porphyrin TBPYP to dimer **1**. Both titrations were performed with identical concentrations of dimer **1** and TBPYP. As is evident from the different slopes in the binding curves of TBPYP to [H·1]¹⁻ (Figure 5.2, left) and TBPYP to [Eu·1]¹⁺ (right), the binding of TBPYP by dimer **1** is strongly dependent on the state of the EDTA tether. The inflection points in the binding curves imply a 2:1 (dimer:TBPYP) binding mode, in accordance with previously obtained results.¹¹ Due to the increased space per binding site compared to TSPP (the CD cavities bind to the *tert*-butylbenzyl moieties of TBPYP), TBPYP is able to accommodate a total of four CDs or two CD dimers.¹¹ The binding curves could be well fitted using a 2:1 binding model, assuming independent binding of the two dimers to the porphyrin. For the fitting procedure only the intrinsic stability constants K_i and ΔH_i° were used as independent fitting parameters.²⁷

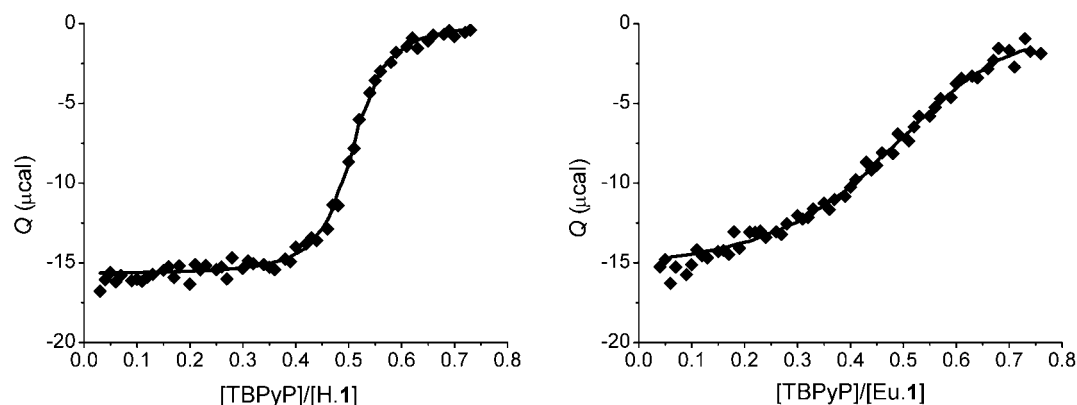


Figure 5.2 Heat evolved per injection plotted against the molar ratio $[TBPyP]/[2]$ (markers) and fits (solid lines) for the calorimetric titrations of 0.16 mM TBPyP to 50 μM $[\text{H}\cdot\mathbf{1}]^{-}$ (left) or $[\text{Eu}\cdot\mathbf{1}]^{1+}$ (right) in water at 298 K.

Table 5.3 lists the thermodynamic parameters obtained for the complexation of TBPyP by the different forms of dimer **1**. Comparison of the enthalpy and entropy values obtained for the complexation of TBPyP by the metal-chelated dimers $[\text{Ca}\cdot\mathbf{1}]^0$ and $[\text{Eu}\cdot\mathbf{1}]^{1+}$ indicated that electrostatic interactions also influence the binding properties of this system. Whereas the binding of TSPP by the europium complexes of dimers **1** and **2** gave more endothermic enthalpy values compared to the binding of TSPP by the neutral calcium-chelated dimers (Table 5.1 and Table 5.2), the binding of TBPyP by $[\text{Eu}\cdot\mathbf{1}]^{1+}$ is associated with a more exothermic enthalpy of binding compared to the binding of TBPyP by $[\text{Ca}\cdot\mathbf{1}]^0$. The 1.7 kcal mol⁻¹ more favorable enthalpy of binding is overridden by a strong decrease in the entropy of binding of -3.3 kcal mol⁻¹. These values are in line with the trends in enthalpy and entropy values observed for the binding of TSPP by the negatively charged dimers of **1** compared to the binding of TSPP by $[\text{Ca}\cdot\mathbf{1}]^0$ (see Table 5.1), and are likely due to the relative large amount of structured water involved in the complexation of TSPP by $[\text{Eu}\cdot\mathbf{1}]^{1+}$ compared to the corresponding complexation by $[\text{Ca}\cdot\mathbf{1}]^0$.

Table 5.3 Thermodynamic parameters of the 2:1 complexation TBPYP by the different ligand and metal complex forms of **1**, as determined by ITC at 298 K.

Host	$K_i^{[a]}$ (M^{-1})	ΔG° (kcal mol $^{-1}$)	ΔH° (kcal mol $^{-1}$)	$T\Delta S^\circ$ (kcal mol $^{-1}$)
1 $^{2-}$	$(4.4 \pm 1.4) \times 10^6$	-9.0 ± 0.2	-11.5 ± 0.2	-2.5 ± 0.4
[H· 1] $^{1-}$	$(9.1 \pm 3.8) \times 10^6$	-9.5 ± 0.3	-9.6 ± 0.2	-0.1 ± 0.5
[Ca· 1] 0	$(6.3 \pm 1.7) \times 10^6$	-9.2 ± 0.2	-8.7 ± 0.2	0.5 ± 0.4
[Eu· 1] $^{1+}$	$(4.1 \pm 1.1) \times 10^5$	-7.6 ± 0.2	-10.4 ± 0.5	-2.8 ± 0.7

^[a] Intrinsic binding constants obtained in a 2:1 binding model assuming independent binding sites (see text and ref. 27).

Comparison of the thermodynamic parameters obtained for the complexation of TBPYP by [Ca·**1**] 0 with those obtained for the negatively charged dimers, [H·**1**] $^{1-}$ and **1** $^{2-}$, indicated that restriction of tether length and flexibility by metal complexation hampers the binding abilities of the metal-chelated dimers. Given the attractive electrostatic interactions that are potentially involved in the binding of TBPYP by [H·**1**] $^{1-}$, a less negative enthalpy and a more positive entropy of binding would be expected. However, more exothermic enthalpy values were found, which are accompanied by relatively large negative values for the entropy of binding, resulting in overall larger association constants. These thermodynamic parameters, and in particular the stronger negative enthalpy values, imply that TBPYP is more effectively bound by [H·**1**] $^{1-}$ compared to the metal-chelated dimers [Eu·**1**] $^{1+}$ and [Ca·**1**] 0 . The negative entropy values can be explained in terms of enthalpy-entropy compensation,²⁸ which is often observed for CDs and CD dimers.^{21,29} Apparently, the increased tether flexibility allows a better cooperation of the CD cavities in complexation of TBPYP. The factor of 22 higher association constant observed for the complexation of TBPYP with [H·**1**] $^{1-}$ compared to [Eu·**1**] $^{1+}$ can therefore probably be assigned to both a more favorable electrostatic interaction and a more effective binding by the CD cavities.

The differences in the thermodynamic parameters found for complexation of TBPYP with [H·**1**] $^{1-}$ and **1** $^{2-}$ are not readily interpretable. It is not likely that [H·**1**] $^{1-}$ and **1** $^{2-}$ have different tether flexibilities. Furthermore, considering the trends in

enthalpy and entropy observed for the complexation of TSPP by dimers **1** and **2**, and also for the binding of TBPYP by dimers $[\text{Eu}\cdot\mathbf{1}]^{1+}$ and $[\text{Ca}\cdot\mathbf{1}]^0$, a less exothermic enthalpy of binding would be expected, which is overridden by a more favorable entropy of binding. This is in sharp contrast with the thermodynamic values found for the complex of $\mathbf{1}^{2-}$ with TBPYP, which indicated that this formation is more exothermic and entropically less favorable compared to the complexation of TBPYP by $[\text{H}\cdot\mathbf{1}]^{1-}$. It might be that strong attractive electrostatic interactions (ion-pairing) are involved in the complexation TBPYP by the negatively charged dimers $[\text{H}\cdot\mathbf{1}]^{1-}$ and $\mathbf{1}^{2-}$. The pyridinium ions of TBPYP are situated close to the binding site of the CD cavities, and are well accessible. Therefore interactions between the carboxylates of the EDTA tether and the positively charged pyridinium moieties of TBPYP are not unlikely. Strong ion-pairing is typically associated with exothermic heat effects, and in this respect the more exothermic enthalpy found for the binding of TBPYP by $\mathbf{1}^{2-}$ could be attributed to the possible formation of an additional ion-pair. Such strong electrostatic interactions do not necessarily have to result in an overall much stronger energy of binding as ion-pairing can interfere with ideal complexation of the *tert*-butylbenzyl moieties by the CD cavities. This has been observed for the binding of anionic guests by mono-6-amino-6-deoxy- β -cyclodextrin.^{21a} However, it is not reasonable to assume that such interference would lead to an overall less favorable energy of binding. Furthermore, the formation of ion-pairs contradicts with the relatively large negative entropy values found for the complexation of TBPYP by the negatively charged dimers. The fact that these complexations probably involve an interplay between hydrophobic and electrostatic interactions makes it difficult to draw conclusion on the extent of the relative contributions of the two interactions and on the outcome of the combination of the two.

CPK modeling suggested that the tether of dimer **2** is of insufficient length to bind TBPYP in a ditopic fashion. The relatively weak association constants ($K < 2 \times 10^4 \text{ M}^{-1}$) obtained for initial ITC experiments with TBPYP and dimer $\mathbf{2}^{2-}$ confirmed this. Therefore, the interaction between the different forms of dimer **2** with TBPYP was not further investigated.

5.3 Conclusions

Tethering of two CDs by an EDTA moiety gives access to tunable CD dimers of which the binding properties can be altered by metal chelation and protonation. The binding affinity of these dimers towards charged guest molecules is strongly dependent on the charge and rigidity imposed on the EDTA tether. Electrostatic interactions between charged guest molecules and charged dimers give rise to systematic changes in the thermodynamic parameters of complexation. ITC experiments revealed that the association of charged porphyrins and oppositely charged dimers is entropically more favorable compared to the corresponding binding of the porphyrins by the neutral forms of the dimer. This is attributed to improved desolvation of the formed complex, which is associated with an unfavorable enthalpy contribution that is overridden by a more favorable entropy of binding. In contrast, the interaction between charged porphyrins and similarly charged dimers is less strong because of less favorable entropies of binding, which is ascribed to an increase in structured water upon complex formation. Association constants determined for the differently charged dimers were found to differ up to a factor of 5 in case of the complexation of TSPP by dimer **1**, which was solely attributed to changes in tether charge, not in tether flexibility.

Restriction of tether flexibility by metal chelation can have a more pronounced influence on the binding properties of the dimer. Suitable design of the CD dimer with respect to size-fit compatibility with the guest molecule may lead to significant differences in binding. This was shown by the complexation of the relatively large guest porphyrin TBPYP by dimer **1**. Metal chelation of the tether resulted in a restricted tether flexibility and consequently led to less favorable enthalpies of binding, which was ascribed to less efficient cooperation of the two CD cavities. For the interaction of TBPYP with dimer **1**, metal chelation of the EDTA tether led to a binding affinity that was reduced by a factor of 22. Such significant differences in binding can be sufficient to achieve substantial release of guest molecules from the CD dimer upon metal chelation.¹²

Calorimetry was shown to be a powerful tool for the elucidation of the complexation thermodynamics, as it allows the interpretation of the influence of metal chelation and charges upon the binding properties of the EDTA-tethered dimers. Relative attribution of the separate contributions of electrostatic and hydrophobic

interactions is readily achieved for interactions in which one of the two is systematically changed. Comparison of interactions for which both contributions are altered are more difficult to analyze and require further, preferably structural, investigation.

5.4 Acknowledgements

I am grateful to Dr. Jasper J. Michels and Dr. Roberto Fiammengo for the synthesis of EDTA-tethered CD dimer **1** and TBPYP, respectively.

5.5 Experimental section

Materials and methods. All chemicals were used as received, unless stated otherwise. Solvents were purified according to standard laboratory methods.³⁰ 3-Amino-3-deoxy-heptakis(6-*O*-*tert*-butyldimethylsilyl)- β -cyclodextrin¹⁶ was prepared according to literature procedures. Chromatographic separations were performed on silica gel 60 (Merck, 0.040-0.063 mm, 230-240 mesh). MALDI-TOF mass spectra were recorded using a PerSpective Biosystems Voyager-DE-RP MALDI-TOF mass spectrometer using dihydroxybenzoic acid as a matrix. NMR spectra were recorded at 25 °C using a Varian Inova 300 spectrometer. ¹H NMR chemical shifts (300 MHz) are given relative to residual HDO (4.65 ppm). ¹³C NMR chemical shifts (75 MHz) are given relative to CH₃OD (49.3 ppm, used as an external standard for samples measured in D₂O).

EDTA-tethered CD dimer 2. A solution of EDTA-bisanhydride (12 mg, 0.05 mmol) in CH₂Cl₂ was added dropwise to a solution of TBDMS-protected 3-amino-3-deoxy- β -cyclodextrin **4** (200 mg, 0.10 mmol) and Et₃N (20 μ L, 0.15 mmol) in CH₂Cl₂ at room temperature. The reaction mixture was stirred overnight, after which the solution was diluted with CH₂Cl₂ and washed with 0.1 M HCl and brine. The organic layer was dried over Na₂SO₄. The product was purified over silica gel using ETOAc/EtOH/H₂O = 12/2/1 as the eluent, and used as such in the deprotection step. The TBDMS-protected precursor of **2** (125 mg, 0.03 mmol) was dissolved in THF at room temperature, and 1 mL (1.0 mmol) of a 1 M solution of tetrabutylammonium fluoride (TBAF) in THF was added. The reaction mixture was refluxed overnight.

The solvent was evaporated in vacuo, and the residue was diluted with water and washed twice with diethyl ether. The aqueous layer was freeze-dried to give 76 mg of dimer **2** as a white solid in overall 64 % yield. ^1H NMR (D_2O): δ 5.01-4.92 (m, 12 H), 4.88 (d, $J = 5.5$ Hz, 2H), 4.25 (br, 2H), 4.07 (br, 2H), 4.00 (br, 2H), 3.91-3.43 (m, 78H), 3.29 (br, 4H), 3.20 (br, 4H). ^{13}C NMR (D_2O , ref. CH_3OD): δ 167.6, 167.1, 104.0 - 101.2, 81.8 - 81.0, 73.8 - 72.2, 60.5 - 59.7, 56.6, 54.0, 51.2. MALDI-TOF-MS: m/z calcd for $[M+\text{Na}]^+$ 2545.8; found 2546.1.

Preparation of the protonated ligand and metal complex forms of **1 and **2**.** The metal complexes of the EDTA-tethered dimers **1** and **2** were prepared by adding aliquots of a concentrated solution of CaCl_2 or EuCl_3 in doubly distilled water (Millipore) to solutions of **1** and **2**. The addition of the metal salts to solutions of the EDTA-tethered dimers was followed by monitoring the pH. Strong decreases in pH indicated the formation of the metal complexes. A slight excess of dimers **1** and **2** relative to the metal salts was maintained (1:0.95) to prevent the formation of metal hydroxides. After addition of the metal salts the solutions were adjusted to pH 7 using NaOH. The free ligands of **1** and **2** were prepared by adjusting the pH of solutions of **1** and **2** to pH 8.5, using NaOH.

Calorimetric titrations. Calorimetric titrations were performed at 25 °C using a Microcal VP-ITC titration microcalorimeter. Sample solutions were prepared as described above. For the titrations performed with dimer solution of pH 8.5, the pH of the guest solutions were adjusted to the pH of the host solution using NaOH. Titrations were performed by adding 5 or 10 μL aliquots of a guest solution to a host solution. For the titrations of TSPP to dimer **1**, the titrant contained 0.01 to 0.1 mM of TSPP, while the cell solutions contained 10 to 100 μM of dimer **1**. Titrations of TSPP to dimer **2** were performed with 0.1 to 1 mM of TSPP as the titrant and 0.01 to 0.1 mM solutions of dimer **2** in the cell. For the titrations of TBPYP to dimer **1**, the titrant contained 0.05 to 0.5 mM of TBPYP, while the cell solutions contained 10 to 100 μM of dimer **1**. All calorimetric titrations were corrected for dilution heats by subtraction of the calorimetric dilution experiments from the calorimetric titration experiments. The titrations were analyzed with a least-squares curve fitting procedure. The sets of

thermodynamic parameters given in Tables 5.1 to 5.3 are based on at least three independent titrations performed at three different concentrations.

5.6 References and notes

- ¹ Tabushi, I.; Kuroda, Y.; Shimokawa, K. *J. Am. Chem. Soc.* **1979**, *101*, 1614-1619.
- ² Lecourt, T.; Mallet, J.-M.; Sinay, P. *Eur. J. Org. Chem.* **2003**, 4553-4560, and references cited therein.
- ³ a) Luo, M.-M.; Xie, R.-G.; Xia, P.-F.; Tao, L.; Yuan, D.-Q.; Zhao, H.-M. *J. Phys. Org. Chem.* **2001**, *14*, 515-520. b) Yan, J.; Breslow, R. *Tetrahedron Lett.* **2000**, *41*, 2059-2062. c) Ren, X.; Liu, J.; Luo, G.; Zhang, Y.; Luo, Y.; Yan, G.; Shen, J. *Bioconjugate Chem.* **2000**, *11*, 682-687. d) Zhang, B.; Breslow, R. *J. Am. Chem. Soc.* **1997**, *119*, 1676-1681.
- ⁴ a) Yang, J.; Gabriele, B.; Belvedere, S.; Huang, Y.; Breslow, R. *J. Org. Chem.* **2002**, *67*, 5057-5067. b) Breslow, R.; Yang, J.; Yan, J. *Tetrahedron* **2002**, *58*, 653-659. c) Yang, J.; Breslow, R. *Angew. Chem. Int. Ed.* **2000**, *39*, 2692-2695.
- ⁵ a) Nelissen, H. F. M.; Schut, A. F. J.; Venema, F.; Feiters, M. C.; Nolte, R. J. M. *Chem. Commun.* **2000**, 577-578. b) Nelissen, H. F. M.; Kercher, M.; De Cola, L.; Feiters, M. C.; Nolte, R. J. M. *Chem. Eur. J.* **2002**, *8*, 5407-5414.
- ⁶ Liu, Y.; Chen, Y.; Li, L.; Zhang, H.-Y.; Liu, S.-X.; Guan, X.-D. *J. Org. Chem.* **2001**, *66*, 8518-8527.
- ⁷ West, L. C.; Wyness, O.; May, B. L.; Clements, P.; Lincoln, S. F.; Easton, C. J. *Org. Biomol. Chem.* **2003**, *1*, 887-894.
- ⁸ Liu, Y.; Wu, C.-T.; Xue, G. P.; Li, J. *J. Inclusion Phenom. Macrocyclic Chem.* **2000**, *36*, 95-100.
- ⁹ a) Liu, Y.; You, C. C.; Wada, T.; Inoue, Y. *Tetrahedron* **2000**, *41*, 6869-6873. b) Liu, Y.; You, C.-C.; Li, B. *Chem. Eur. J.* **2001**, *7*, 1281-1288. c) Liu, Y.; Li, L.; Zhang, H.-Y.; Song, Y. *J. Org. Chem.* **2003**, *68*, 527-536.
- ¹⁰ Kano, K.; Nishiyabu, R.; Asada, T.; Kuroda, Y. *J. Am. Chem. Soc.* **2002**, *124*, 9937-9944.
- ¹¹ Michels, J. J.; Fiammengo, R.; Timmerman, P.; Huskens, J.; Reinhoudt, D. N. *J. Inclusion Phenom. Macrocyclic Chem.* **2001**, *41*, 163-172.

- ¹² a) Mulder, A.; Juković, A.; Lucas, L. N.; Van Esch, J.; Feringa, B. L.; Huskens, J.; Reinhoudt, D. N. *Chem. Commun.* **2002**, 2734-2735. b) Mulder, A.; Juković, A.; Van Leeuwen, F. W. B.; Kooijman, H.; Spek, A. E.; Huskens, J.; Reinhoudt, D. N. *Chem. Eur. J.* **2004**, *10*, 1114-1123.
- ¹³ a) Wang, X.-P.; Pan, J.-H.; Shuang, S.-M. *Spectrochimica Acta A*, **2001**, *57*, 2755-2762. b) Carofiglio, T.; Fornasier, R.; Lucchini, V.; Rosso, C.; Tonelatto, U. *Tetrahedron Lett.* **1996**, *37*, 8019-8022. c) Ribo, J. M.; Farrera, J. A.; Valero, M. L.; Virgili, A. *Tetrahedron* **1995**, *51*, 3705-3712.
- ¹⁴ a) Venema, F.; Rowan, A. E.; Nolte, R. J. M. *J. Am. Chem. Soc.* **1996**, *118*, 257-258. b) Venema, F.; Nelissen, H. F. M.; Berthault, P.; Birlirakis, N.; Rowan, A. E.; Feiters, M. C. N.; Nolte, R. J. M. *Chem. Eur. J.* **1998**, *4*, 2237-2250.
- ¹⁵ Michels, J. J.; Huskens, J.; Reinhoudt, D. N. *J. Am. Chem. Soc.* **2002**, *124*, 2056-2064.
- ¹⁶ Van Dienst, E.; Snellink, B. H. M.; Von Piekartz, I.; Grote Gansey, M. H. B.; Venema, F.; Feiters, M. C.; Nolte, R. J. M.; Engbersen, J. F. J.; Reinhoudt, D. N. *J. Org. Chem.* **1995**, *60*, 6537-6545.
- ¹⁷ Yan, J.-M.; Atsumi, M.; Yuan, D.-Q.; Fujita, K. *Helv. Chim. Acta* **2002**, *85*, 1496-1504.
- ¹⁸ a) Breslow, R.; Czarnik, A. W.; Lauer, M.; Leppkes, R.; Winkler, J.; Zimmerman, S. *J. Am. Chem. Soc.* **1986**, *108*, 1969-1979. b) Yuan, D.-Q.; Ohta, K.; Fujita, K. *Chem. Commun.* **1996**, 821-822.
- ¹⁹ Platas-Iglesias, C.; Corsi, D. M.; Vander Elst, L.; Muller, R. N.; Imbert, D.; Bünzli, J.-C. G.; Tóth, É.; Maschmeyer, T.; Peters, J. A. *J. Chem. Soc., Dalton Trans.* **2003**, 727-737.
- ²⁰ a) Manka, J. S.; Lawrence, D. S. *J. Am. Chem. Soc.* **1990**, *112*, 2440-2442. b) Dick, D. L.; Rao, T. V. S.; Sukumaran, D.; Lawrence, D. S. *J. Am. Chem. Soc.* **1992**, *114*, 2664-2669.
- ²¹ a) Rekharsky, M. V.; Inoue, Y. *J. Am. Chem. Soc.* **2002**, *124*, 813-826. b) Rekharsky, M. V.; Inoue, Y. *Chem. Rev.* **1998**, *98*, 1875-1917.
- ²² Brown, S. E.; Coates, J. H.; Duckworth, P. A.; Lincoln, S. F.; Easton, C. J.; May, B. L. *J. Chem. Soc., Faraday Trans.* **1993**, *89*, 1035-1040.

- ²³ a) Kitae, T.; Takashima, H.; Kano, K. *J. Inclusion Phenom. Macrocyclic Chem.* **1999**, *33*, 345-359. b) Kitae, T.; Nakayama, T.; Kano, J. *J. Chem. Soc., Perkin Trans. 2* **1998**, 207-212. c) Kano, K. *J. Phys. Org. Chem.* **1997**, *10*, 286-291.
- ²⁴ a) Foguel, D.; Silva, J. L. *Proc. Natl. Acad. Sci. U.S.A.* **1994**, *91*, 8244-8247. b) Mahtab, R.; Harden, H. H.; Murphy, C. J. *J. Am. Chem. Soc.* **2000**, *122*, 14-17. c) Lynch, T. W.; Sligar, S. G. *J. Biol. Chem.* **2000**, *275*, 30561-30565.
- ²⁵ a) Stodeman, M.; Dhar, N. *J. Chem. Soc., Faraday Trans.* **1998**, *94*, 899-903. b) Prohens, R.; Rotger, M. C.; Pina, M. N.; Deya, P. M.; Morey, J.; Ballester, P.; Costa, A. *Tetrahedron Lett.* **2001**, *42*, 4933-4936. c) Meissner, R.; Garcias, X.; Mecozzi, S.; Rebek Jr., J. *J. Am. Chem. Soc.* **1997**, *119*, 77-85. d) Cram, D. J.; Choi, H. J.; Bryant, J. A.; Knobler, C. B. *J. Am. Chem. Soc.* **1992**, *114*, 7748-7765.
- ²⁶ a) Tobey, S.; Anslyn, E. V. *J. Am. Chem. Soc.* **2003**, *125*, 14807-14815. b) Corbellini, F.; Fiammengo, R.; Timmerman, P.; Crego-Calama, M.; Versluis, K.; Heck, A. J. R.; Luyten, I.; Reinhoudt, D. N. *J. Am. Chem. Soc.* **2002**, *124*, 6569-6575. c) Sebo, L.; Schweizer, B.; Diederich, F. *Helv. Chim. Acta* **2000**, *83*, 80-92.
- ²⁷ CPK modeling of the complexes of TBPYP and the different forms of dimer **1** indicated that in all cases the tether length is insufficient to bind two opposite tert-butylphenyl moieties. All dimers are capable of binding two adjacent tert-butylphenyl moieties. These implications make that $K_1 = 4K_i = 8K_2$.
- ²⁸ Leffler, J. E. *J. Org. Chem.* **1955**, *20*, 1202-1231.
- ²⁹ a) Zhang, B.; Breslow, R. *J. Am. Chem. Soc.* **1993**, *115*, 9353-9354. b) Liu, Y.; Chen, Y.; Li, B.; Wada, T.; Inoue, Y. *Chem. Eur. J.* **2001**, *7*, 2528-2535.
- ³⁰ Perrin, D. D.; Armarego, W. F. L. *Purification of Laboratory Chemicals*, 3rd ed., Pergamon, Oxford, **1989**.

Divalent binding of a bis(adamantyl)-functionalized calix[4]arene to β -cyclodextrin-based hosts: an experimental and theoretical study on multivalent binding in solution and at self-assembled monolayers*

6.1 Introduction

The use of supramolecular interactions for the positioning and/or immobilization of (bio)molecules at self-assembled monolayers (SAMs) is of high current interest.¹⁻⁶ SAMs of 2-aminoethanethiol hydrochloride have been used for the anchoring of crown ether-appended fullerenes¹ and cyclic peptides.² As these interactions are based on only one crown ether-cation interaction, the stability of these complexes is limited. This can be overcome by using the concept of multivalency. Tampé and co-workers used this approach for the immobilization of enzymes at SAMs by metal chelation.³ More recently, adamantyl groups have been used to immobilize cytochrome C,⁴ nanotubes,⁵ and dendrimers⁶ at β -cyclodextrin (CD) SAMs by means of multiple hydrophobic interactions.

In principle such supramolecular positioning allows controllable adsorption and desorption rates simply by tuning the number and type of interactions and therefore constitutes a new paradigm for reversible and versatile nanofabrication schemes. In

* Parts of this work have been published in: Auletta, T.; Dordi, B.; Mulder, A.; Sartori, A.; Onclin, S.; Bruinink, C. M.; Péter, M.; Nijhuis, C. A.; Beijleveld, H.; Schönherr, H.; Vancso, G. J.; Casnati, A.; Ungaro, R.; Ravoo, B. J.; Huskens, J.; Reinhoudt, D. N. *Angew. Chem. Int. Ed.* **2004**, *43*, 369-373; Mulder, A.; Auletta, T.; Sartori, A.; Del Ciotto, S.; Casnati, A.; Ungaro, R.; Huskens, J.; Reinhoudt, D. N. *J. Am. Chem. Soc.* **2004**, *126*, in press.

this respect, supramolecular positioning can be superior to the more commonly used bio-affinity-based immobilization techniques that use antigen-antibody interactions or the biotin-avidin recognition motif, since the latter is very often quasi-irreversible, which means that control over the adsorption and especially the desorption rates is limited.^{7,8}

For the successful design and application of multivalent ligands in nanofabrication at SAMs, a fundamental understanding of the multivalent interactions involved is crucial. Recently, Lees and co-workers published a general model for multivalent binding.⁹ Although this model was shown to give excellent correlations for a variety of multivalent model systems, its application is restricted to well-defined multivalent receptors with binding sites spaced at specific distances and not readily applicable to multivalent binding at SAMs. Multivalent binding at SAMs can be very different from multivalent binding in solution. Previously, our group qualitatively addressed the thermodynamic and kinetic issues related to the use of multiple interactions for stable surface attachment of adamantyl-functionalized dendrimers at CD SAMs.⁶ In this chapter a quantitative study on the use of multiple hydrophobic interactions for the positioning of molecules on surfaces is presented. It discusses the simplest case of multivalency, i.e. a divalent interaction. The divalent binding of a bis-adamantyl-derivatized guest molecule with CD or a CD dimer in solution is compared to its binding at CD SAMs in order to resolve the current lack of understanding on multivalent interactions at surfaces.

6.2 Results and discussion

6.2.1 Design of the model system

As a model system to study multivalent interactions at SAMs the interaction between an adamantyl-functionalized calix[4]arene **1** and a CD SAM of **3**¹⁰ on gold was chosen (Chart 6.1). The synthesis of **1** was performed by Andrea Sartori.¹¹

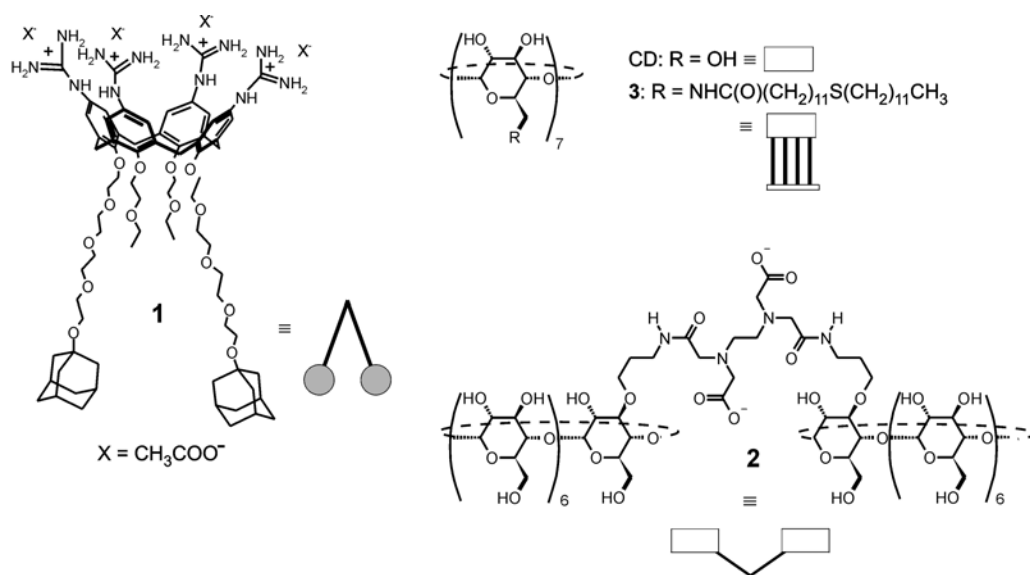


Chart 6.1 Guest and host compounds used in this study.

Molecule **1** has been developed specifically for the interaction with CD SAMs. The calix[4]arene is used as a synthetic platform and bears four guanidinium functionalities at the upper rim to increase water solubility. The lower rim is A-C bis-functionalized with adamantyl groups for the interaction with CD. Poly(ethylene glycol) chains are used to space the two adamantyl groups in order to allow a divalent interaction with CD SAMs, while retaining water-solubility and preventing non-specific interactions.

As the adsorbate for the formation of the CD SAMs, hepta(thioether)-modified CD **3** was used.^{10,12} These CD SAMs are particularly ideal for this type of study for a number of reasons: (i) The adsorbate forms densely and hexagonally packed, well-ordered SAMs^{10,12} with a defined lattice constant;¹³ (ii) Binding affinities at these SAMs can be studied with a variety of techniques such as electrochemical impedance,¹⁰ surface plasmon resonance (SPR) spectroscopy,^{10,14} and atomic force microscopy;^{13,15} (iii) Simple, monovalent organic guests, such as adamantyl derivatives, show similar selectivities and binding strengths to such SAMs as to native CD in solution.¹⁴ These allow the direct correlation between binding events in solution and at CD SAMs, which is advantageous for a fundamental understanding of multivalent binding on surfaces (see below). In order to correlate the multivalent nature of the binding of **1** at CD SAMs to binding in solution, the interactions of **1** with native CD and the divalent EDTA-based CD dimer **2**¹⁶ (see Chart 6.1) were studied as well.

6.2.2 Binding to CD substrates in solution

Binding studies with **1** in aqueous solution were performed using isothermal titration calorimetry (ITC). Calorimetric titrations were performed with CD and the EDTA-based CD dimer **2**¹⁶ in order to gain insight into the mono- and divalent binding behavior of **1** in solution. Figure 6.1 depicts the (exothermic) heat profiles obtained from the calorimetric titration of **1** with CD (left) and the titration of **2** with **1** (right).

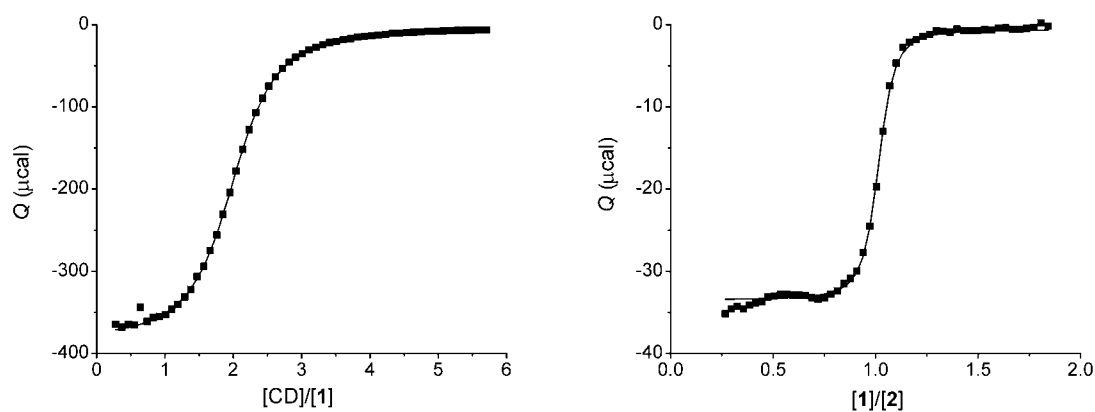


Figure 6.1 Heat evolved per injection plotted against the molar ratio (markers) and fits (solid lines) for the calorimetric titrations (25 °C) of CD (10 mM) to **1** (0.4 mM) (left) and of **1** (0.4 mM) to **2** (0.05 mM) (right) in water at 298 K.

The inflection point in the titration curve obtained for the binding of **1** with CD indicates a 2:1 (host:guest) stoichiometry implying that **1** is bound by two CD cavities, one for each adamantane group. The curve was fitted to a 2:1 binding model (solid line, Figure 6.1, left), considering the two adamantyl groups as two identical independent binding sites and using the intrinsic association constant, K_i , and the enthalpy of binding, ΔH_i° , as independent fitting parameters.¹⁷ The obtained thermodynamic parameters are listed in Table 6.1. The intrinsic binding constant K_i of ($4.6 \times 10^4 \text{ M}^{-1}$) and the enthalpy of binding ($-7.0 \text{ kcal mol}^{-1}$) are typical of a CD-adamantane interaction.¹⁸ The observed 2:1 stoichiometry and the quality of the fit using independent binding sites (Figure 6.1, left) indicate that both adamantyl groups bind a CD cavity in a similar fashion, without interference between the two binding processes.

Table 6.1 Thermodynamic parameters of the complexation of **1** to CD and **2**, as determined by ITC at 298 K.

host	stoichiometry (host:guest)	K (M ⁻¹)	ΔG° kcal mol ⁻¹	ΔH° kcal mol ⁻¹	$T\Delta S^\circ$ kcal mol ⁻¹
CD	2:1	$(4.6 \pm 0.3) \times 10^4$ ^[a]	-6.4 ± 0.1	-7.0 ± 0.5	-0.6 ± 0.6
2	1:1	$(1.2 \pm 0.1) \times 10^7$	-9.6 ± 0.1	-14.8 ± 0.5	-5.1 ± 0.6

^[a] Intrinsic binding constant, K_i (see text and ref 17).

The titration curve for the titration of **2** with **1** (Figure 6.1, right) shows an inflection point at a molar ratio of 1, suggesting a 1:1 binding mode. Fitting of the titration curve with a 1:1 model and using the association constant and the binding enthalpy as independent fitting parameters gave thermodynamic parameters typical of a divalent interaction. The binding constant of $1.2 \times 10^7 \text{ M}^{-1}$ is orders of magnitude higher than the intrinsic binding constant for a single CD-adamantane interaction and the binding enthalpy, $-14.8 \text{ kcal mol}^{-1}$, is twice the value found for the intrinsic binding enthalpy of **1** with CD (see Table 6.1). The strongly negative entropy of binding is attributed to restriction of mobility for both **1** and **2** caused by the divalent interaction. Dimer **2** did not show any evidence for the self-inclusion of the rather hydrophilic EDTA tether into one of the CD cavities. Furthermore, the thermodynamic parameters obtained for the divalent binding of **1** to **2** imply that the interaction between **1** and **2** only involves the two hydrophobic CD-adamantane interactions. Therefore, the overall divalent binding can be directly related to the intrinsic binding of **1** with native CD as determined with ITC (see Table 6.1) and can be well analyzed in terms of multivalency.¹⁹

Several approaches for the analysis of multivalent binding have been reported in the literature. Whitesides et al. proposed that multivalent binding should be analyzed in terms of entropy, assuming that the overall enthalpy of binding is the sum of the binding enthalpies of the individual ligands.^{19,20} Alternatively, multivalent binding has been explained in terms of intrinsic binding constants and effective concentrations.^{9,21,22} A general model for multivalent binding to rigid, multivalent receptors in solution based on the latter concept was recently published by Lees et al.⁹ For ideal multivalent interactions, comprised of multiple, independent and equal

monotopic interactions, these two binding models are basically similar. In principle, both approaches seem equally well applicable to the interaction between **1** and **2**; as stated above, the enthalpy of binding found for the interaction between **1** and **2** is the sum of the enthalpy of the binding of two CD-adamantane interactions (see Table 6.1) and the divalent binding is directly related to an intrinsic monovalent binding. However, the correct interpretation of the entropy term for multivalent interactions is far from trivial.²⁰ Moreover, when studying binding of guests at CD SAMs, only stability constants are readily accessible. Therefore, for our study, the latter approach, which is based on intrinsic binding constants, is more easily applicable.

As illustrated for the binding of **1** by **2** in Figure 6.2, the divalent binding can be considered to consist of two independent, sequential binding events, and the overall binding process can be described in terms of two host-guest (CD-adamantane) interactions. As stated above, these sequential interactions are directly related to the intrinsic binding constant of the individual host-guest interaction, i.e. as determined for **1**·(CD)₂. The first, intermolecular, interaction can be directly related to the intrinsic binding constant ($K_I=4K_i$). The second, *intramolecular*, interaction is the product K_i and an effective concentration term (C_{eff}), which accounts for the uncomplexed host (CD) concentration experienced by the uncomplexed guest site (adamantyl group) ($K_2=\frac{1}{2}C_{eff}K_i$). The term effective concentration is used to differentiate between inter- and intramolecular reactivity, and accounts for the close proximity of two reactive or complementary species in an intramolecular reaction or binding event.²³ The effective concentration represents a probability of interaction between the two reactive or complementary species. The effective concentration symbolizes a “physically real” concentration of one of the reacting or interacting species as experienced by its complementary counterpart.²¹⁻²⁴ C_{eff} is conceptually similar to the more generally used term effective molarity (EM),^{24,25} which represents the ratio of rate or association constants for intra- and intermolecular processes.²⁴

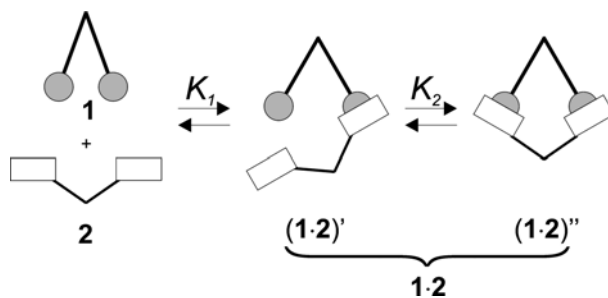


Figure 6.2 Equilibria for the sequential binding of **1** to **2**.

The overall binding constant for a divalent interaction in solution consisting of two identical, independent binding processes can thus be expressed in terms of the effective concentration and the intrinsic binding constant using equation 1.

$$K = K_1 \cdot K_2 = 2C_{eff} (K_i)^2 \quad (1)$$

Based on the intrinsic binding constant determined for $\mathbf{1} \cdot (\text{CD})_2$, $K_i = 4.6 \times 10^4 \text{ M}^{-1}$, and the binding constant of $\mathbf{1} \cdot \mathbf{2}$, $1.2 \times 10^7 \text{ M}^{-1}$, an experimental C_{eff} of $2.8 \pm 0.6 \text{ mM}$ is calculated.²⁶

A theoretical estimate for C_{eff} can be obtained using the well-known formula for cyclization probability, Equation 2.^{23,27,28}

$$C_{eff} = \frac{1}{N_{AV}} \left(\frac{3}{(2\pi\bar{r}_0^2)} \right)^{3/2} \quad (2)$$

Here, N_{AV} is Avogadro's number, and \bar{r}_0 is the root-mean-square distance between the two ends of the chain. Equation 2 is based on Gaussian probability functions and random walk statistics,^{27,28} and gives the probability for the presence of two interlinked chain ends within an infinitely small volume. It shows that C_{eff} has an inverse cubic relation to \bar{r}_0 .

A crude approximation of C_{eff} , which is also applicable to CD SAMs (see below), can be made by considering the number of available receptor sites within the probing volume of the uncomplexed guest (Figure 6.3, top).^{21,24} The radius of the

probing volume is defined by the average end-to-end distance between the uncomplexed ligand (adamantane) and the free receptor sites (CD cavities). Here it is assumed that the probability of an interaction between the two species is uniformly distributed within this volume.

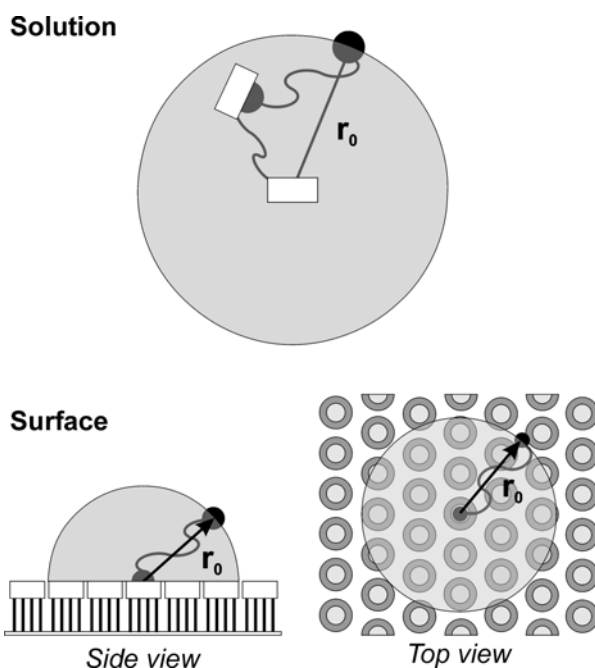


Figure 6.3 Schematical representation of the concept of C_{eff} for the interaction between **1** and **2** (top) and of **1** to CD SAMs (bottom).

For a divalent binding in solution C_{eff} is therefore given by Equation 3.^{21,24,29}

$$C_{eff} = \frac{3}{4\pi\bar{r}_0^3 N_{AV}} \quad (3)$$

Comparison of Equations 2 and 3 shows that the approximation of C_{eff} as given by Equation 3 differs by a prefactor $\left(\frac{\pi}{6}\right)^{1/2}$ ($= 0.72$) from Equation 2. This factor is within experimental error of accessible C_{eff} values (see above) and within the range of possible C_{eff} values based on \bar{r}_0 (see below). Furthermore, in the case of the modeling

of binding to CD SAMs, which is our prime objective, it will be shown that K_i values obtained using this model are fairly insensitive to the value of C_{eff} (see below).

An estimate for the average root-mean-square end-to-end distance, \bar{r}_0 , is obtained using 3-dimensional random walk statistics.³⁰

$$\bar{r}_0 = a\sqrt{n} \quad (4)$$

Equation 4 is a rudimentary formula commonly used in polymer chemistry, where n is the number of segments that make up the chain, and a is related to the length between two segments, a_0 . The ratio a/a_0 is a quantitative measure of the stiffness of the chain incorporating effects such as rotational barriers, bond angles, and restricted volume. Values for a/a_0 typically range from 1.5 to 5.5, depending on the stiffness of the chain, where flexible chains are characterized by relatively low values for a/a_0 .³⁰

Equation 4 allows the estimation of \bar{r}_0 for unisegmental polymers. Guest molecule **1** and complex (**1·2**)', however, are made up of segments with different degrees of rotational freedom and its flexibilities are thus less well defined. Therefore **1** and the complex (**1·2**)' were modeled using a chain made up of carbon-carbon bonds and the ratio a/a_0 was applied to describe the average stiffness of the complex.

For the complex (**1·2**)' molecular modeling calculations gave a maximum distance of 6.2 nm between the ether linkage of the uncomplexed adamantane moiety and the center of the uncomplexed CD cavity in the fully extended complex (**1·2**)'. A chain made up of 50 sequentially linked carbon atoms is representative for this length.³¹ Equation 4 together with the possible values for the ratio a/a_0 (see above) gave an average end-to-end distance, \bar{r}_0 , ranging from 1.6 to 5.9 nm, depending on the stiffness of the chain. Substitution of this range of \bar{r}_0 into Equation 4 gave values for C_{eff} ranging from 1.8 to 92.0 mM. The experimentally determined C_{eff} of 2.8 mM is within this range of calculated theoretical C_{eff} values. The low value for the experimentally determined C_{eff} may imply that the rotational mobility within complex (**1·2**)' is rather limited.

This result suggests that the concept, where the divalent binding of **1** and **2** is considered to consist of two sequential binding steps, is viable and that C_{eff} ,

approximated by considering the physically real concentration of available host sites within the probing volume of the uncomplexed guest, can be used to account for the difference between the intra- and intermolecular complexation steps.

6.2.3 Binding at CD SAMs

The binding of **1** to CD SAMs was studied by surface plasmon resonance spectroscopy (SPR). Figure 6.4 shows five SPR titration curves performed at different CD buffer concentrations. The SPR curves were obtained by the addition of increasing amounts of a 1 μM solution of **1** to a CD solution on top of a CD SAM. Additions of **1** resulted in an increase of the SPR angle, indicative of adsorption. The adsorption was followed for 200 s after which the surface was regenerated by repeatedly rinsing the cell with 10 mM CD to obtain complete restoration of the SPR signal, indicating the desorption of **1** from the surface.

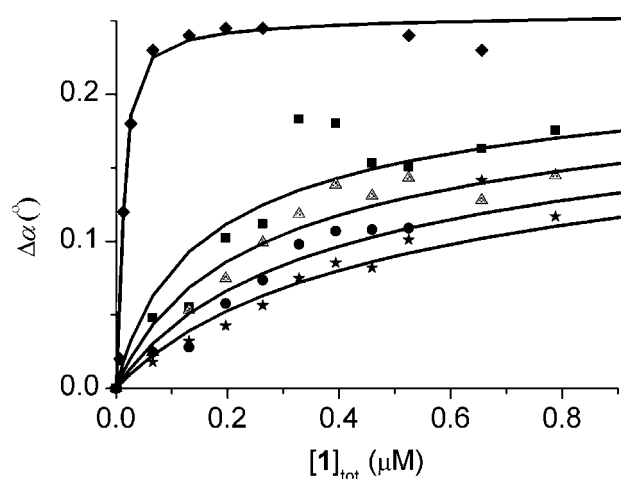


Figure 6.4 SPR titrations (data points) and corresponding fits for the sequential binding model (solid lines) for different titrations of **1** to CD SAMs at five different CD concentrations in solution (◆ = 0.1 mM; ■ = 0.5 mM; ▲ = 1.0 mM; ● = 2.5 mM; ★ = 5.0 mM).

The interaction of **1** with CD SAMs was studied at different concentrations of CD in solution in order to test the influence of competition between CDs in solution and the CDs of the SAM. CD concentrations in solution higher than 0.1 mM were required in order to obtain reliable binding constants. As can be seen in Figure 6.4,

titration of **1** at 0.1 mM gave nearly quantitative adsorption, and led to the depletion of **1** from solution for the first few data points. Therefore, titrations at higher CD concentrations were needed. The decreasing slopes of the binding curves at increasing CD concentration indicate that the CD in solution competed with the CD sites at the surface.

Titrations performed with **1** on 11-mercapto-1-undecanol reference SAMs only gave a small concentration effect on the SPR signal, which could be easily restored by washing the SAMs with water. No binding curves could be recorded, indicating the absence of specific interactions between **1** and the reference SAMs. SPR titrations at CD SAMs performed in the presence of 0.1 M KCl gave binding curves similar to those obtained without a background electrolyte, indicating that possible electrostatic repulsion at the monolayer can be neglected.

The titration curves could be fitted well to Langmuir isotherms using a model representing a single binding event in which it was assumed that both adamantyl moieties of **1** simultaneously interact with a CD cavity at the surface.³² Using the binding constants for the interaction of **1** with the competing CD in solution as determined by ITC (see above), each binding curve of Figure 6.4 was satisfactorily fitted giving complexation constants K_{LM} ranging from 2.8×10^9 to $7.9 \times 10^{10} \text{ M}^{-1}$ (see Table 6.2). Using this “traditional” interpretation a range of binding constants is obtained that differ by up to a factor of 30. The obtained binding constants for the divalent binding of **1** at CD SAMs are two to three orders of magnitude higher compared to the binding constant found for the divalent binding of **1** to **2** in solution ($1.2 \times 10^7 \text{ M}^{-1}$, see above). Such large differences between divalent binding in solution and at SAMs are not uncommon and have been observed before.^{33,34} These differences in binding affinity found for the divalent interaction in solution and at surfaces can be rationalized when interpreted as two sequential binding events, using the effective concentration concept, as will be discussed below.

Figure 6.5 depicts the possible routes for the sequential divalent binding of **1** to CD SAMs and the equilibria involved. The equilibria contain solution (top row) and surface species (lower two rows) and they describe the interaction of **1** with CDs in solution (CD_i ; from left to right) and with CDs at the surface (CD_s ; from top to bottom). As for the sequential binding in solution, the sequential binding events at the surface are considered equal and independent. Consequently, all binding constants can

be expressed in terms of intrinsic binding constants, here taken separately for binding to a solution host ($K_{i,l}$) and a surface host ($K_{i,s}$), similarly as described above for the binding of **1** to **2** in solution. For $K_{i,l}$ the value as determined above using ITC for the binding of **1** and CD in solution is used ($4.6 \times 10^4 \text{ M}^{-1}$). It is assumed to hold for the binding of a surface-confined guest as well (Figure 6.5, equilibrium in second row). Consequently, the equilibria expressed in rows can be expressed in terms of $K_{i,l}$.

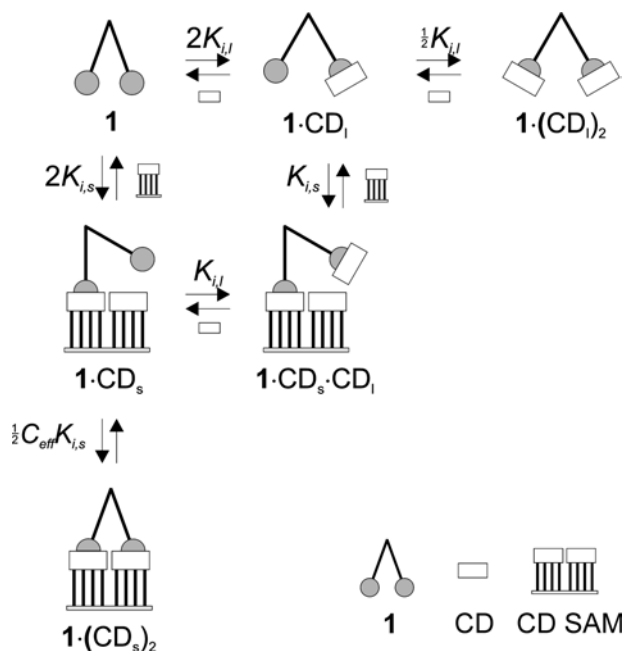


Figure 6.5 Equilibria for the sequential binding of **1** to CD SAMs.

The first binding constant of **1** with the CD SAM is given by Equation 5.³⁵

$$\frac{[\mathbf{1} \cdot \text{CD}_s]}{[\mathbf{1}][\text{CD}_s]} = 2K_{i,s} \quad (5)$$

The equilibrium is expressed in terms of the free, surface-confined host concentration in the total sample volume, $[\text{CD}_s]$, (in M). In principle it is also possible to express the equilibrium in terms of absolute or relative surface coverages, however, the use of $[\text{CD}_s]$ simplifies the solving of the mass balances as shown below.

The second, intramolecular binding event at the surface, the formation of $\mathbf{1} \cdot (\text{CD}_s)_2$, is accompanied by an effective concentration term, C_{eff} , similar to the

second binding event for the sequential divalent binding of **1** in solution. C_{eff} represents the effective concentration of *free* host sites at the surface and is thus surface coverage-dependent. This is accounted for by multiplying the maximum effective concentration, $C_{eff,max}$, which is the number of accessible host sites in the probing volume (see Figure 6.3, bottom, and see below), with the fraction of free host sites at the surface ($= [CD_s]/[CD_s]_{tot}$) giving Equation 6.

$$\frac{[\mathbf{1} \cdot (CD_s)_2]}{[\mathbf{1} \cdot (CD_s)]} = \frac{1}{2} C_{eff,max} \frac{[CD_s]}{[CD_s]_{tot}} K_{i,s} \quad (6)$$

In our model, $K_{i,s}$ is optimized as a fitting parameter independently of the fixed value of $K_{i,l}$. The optimized value of $K_{i,s}$ is then compared to previously obtained intrinsic binding constants for the complexation of monovalent adamantyl derivatives at SAMs of **3** in the evaluation of the data.

Combination of the equilibrium constant definitions with the mass balances for $[\mathbf{1}]$, $[CD_l]_{tot}$ and $[CD_s]_{tot}$ gives the numerically solvable Equations 7 – 9 in which the only two unknown parameters are $K_{i,s}$ and $C_{eff,max}$.

$$\begin{aligned} [\mathbf{1}]_{tot} &= [\mathbf{1}] + [\mathbf{1} \cdot CD_l] + [\mathbf{1} \cdot (CD_l)_2] + [\mathbf{1} \cdot CD_s] + [\mathbf{1} \cdot CD_l \cdot CD_s] + [\mathbf{1} \cdot (CD_s)_2] = \\ &[\mathbf{1}] + 2K_{i,l}[\mathbf{1}][CD_l] + K_{i,l}^2[\mathbf{1}][CD_l]^2 + 2K_{i,s}[\mathbf{1}][CD_s] + 2K_{i,l}K_{i,s}[\mathbf{1}][CD_l][CD_s] \\ &+ K_{i,s}^2[\mathbf{1}][CD_s]^2 \frac{C_{eff,max}}{[CD_s]_{tot}} \end{aligned} \quad (7)$$

$$\begin{aligned} [CD_l]_{tot} &= [CD_l] + [\mathbf{1} \cdot CD_l] + 2[\mathbf{1} \cdot (CD_l)_2] + [\mathbf{1} \cdot CD_l \cdot CD_s] = \\ &[CD_l] + 2K_{i,l}[\mathbf{1}][CD_l] + 2K_{i,l}^2[\mathbf{1}][CD_l]^2 + 2K_{i,l}K_{i,s}[\mathbf{1}][CD_l][CD_s] \end{aligned} \quad (8)$$

$$\begin{aligned} [CD_s]_{tot} &= [CD_s] + [\mathbf{1} \cdot CD_s] + [\mathbf{1} \cdot CD_l \cdot CD_s] + 2[\mathbf{1} \cdot (CD_s)_2] = \\ &[CD_s] + 2K_{i,s}[\mathbf{1}][CD_s] + 2K_{i,l}K_{i,s}[\mathbf{1}][CD_l][CD_s] + 2K_{i,s}^2[CD_s]^2 \frac{C_{eff,max}}{[CD_s]_{tot}}[\mathbf{1}] \end{aligned} \quad (9)$$

Analogous to the binding in solution, $C_{eff,max}$ can be estimated by considering the number of accessible host sites in the probing volume of the uncomplexed adamantyl moiety of **1**-CDs, which in this case is constituted of a hemisphere with \bar{r}_0 (see Figure 6.3, bottom). Based on the common formula for cyclization probability (Equation 2), Lees et al. developed an expression for the calculation of a maximally attainable C_{eff} for rigid multivalent hosts, in which the host sites are spaced by a *specific* distance, in combination with ideal multivalent guests, having an *optimal* spacing between the individual ligand sites.²³ The CD SAMs used in this study consist of an infinite number of bindings sites and, depending on the spacer length between the two adamantyls, there are multiple possible binding sites spaced at multiple possible distances that enable a divalent binding. Therefore, the calculation of C_{eff} as proposed by Lees et al. is not readily applicable to the interaction of **1** at the CD SAMs. Instead, the method used for the approximation of C_{eff} in solution offers a viable alternative for the approximation of $C_{eff,max}$ at surfaces as well.

The methodology used for the approximation of $C_{eff,max}$ at the surface is similar to that used for the approximation of C_{eff} in solution, with the exception that the number of available CD sites at the surface exceeds 1 and is dependent on the root-mean-square end-to-end distance, \bar{r}_0 . The maximum number of available CDs, N_{CD} , within a probing volume defined by \bar{r}_0 is given by Equation 10, in which A_{CD} is the surface area occupied by a single CD cavity.

$$N_{CD} = \frac{\pi\bar{r}_0^2}{A_{CD}} - 1 \quad (10)$$

Consequently the maximally attainable concentration of available surface-confined CD sites, $C_{eff,max}$, is given by Equation 11.

$$C_{eff,max} = \frac{3N_{CD}}{2N_{AV}\pi\bar{r}_0^3} = \frac{3(\pi\bar{r}_0^2 - A_{CD})}{2A_{CD}N_{AV}\pi\bar{r}_0^3} \quad (11)$$

The surface area occupied by a single CD cavity, A_{CD} , can be easily calculated. In a densely packed CD SAM, as for **3**, the spacing of the CD cavities is determined by the packing of the underlying thioether chains. Optimal packing of the seven thioether

chains gives an A_{CD} of 2.8 nm^2 .¹⁰ For a hexagonally packed monolayer, this A_{CD} corresponds to a lattice constant of 1.8 nm , which is in reasonable agreement with the lattice constant of 2.1 nm that was found for similar CD SAMs with the use of atomic force microscopy.¹³ Given this value for A_{CD} , Equation 11 can be approximated by Equation 12 for $\bar{r}_0 > 1.5 \text{ nm}$.³⁶

$$C_{eff,max} = \frac{3}{2A_{CD}N_{AV}\bar{r}_0} \quad (12)$$

$C_{eff,max}$ scales with \bar{r}_0^{-1} and therefore the effective concentration at the surface is much less dependent on \bar{r}_0 than in solution ($C_{eff} \sim \bar{r}_0^{-3}$). Consequently, the approximation of $C_{eff,max}$, based on a range of \bar{r}_0 , gives a relatively narrow range of $C_{eff,max}$ values (0.20 to 0.50 M).³⁷ Analogous to the solution case (see above), the lower limit of $C_{eff,max}$ (0.20 M) was used for the fitting of the SPR titration curves.

SPR curves were fitted to the sequential binding model outlined above in a least squares optimization routine using $K_{i,s}$ as a variable and fixed values for $K_{i,l}$ ($4.6 \times 10^4 \text{ M}^{-1}$) and $C_{eff,max}$ (0.20 M). The SPR angle change, $\Delta\alpha$, was considered linearly dependent on the surface coverage and was calculated using Equation 13.³²

$$\Delta\alpha_{calc} = \frac{[\mathbf{1} \cdot \text{CD}_s] + [\mathbf{1} \cdot (\text{CD}_s)_2] + [\mathbf{1} \cdot \text{CD}_s \cdot \text{CD}_1]}{[\text{CD}_s]_{tot}} \Delta\alpha_{max} \quad (13)$$

Results obtained by fitting the SPR curves using the sequential binding model are given in Table 6.2. The values for $K_{i,s}$ obtained for different concentrations of CD in solution are within the same order of magnitude and in good agreement with the previously obtained binding constant for the interaction of acetamidoadamantane with SAMs of **3**.¹⁴ These results confirm that the concept of sequential binding interpreted in terms of C_{eff} and $K_{i,s}$ is also applicable to the interaction of **1** with CD SAMs. Comparison of the values for $K_{i,s}$ and K_{LM} indicate that fitting of the SPR curves using the sequential binding model gave a more understandable result for the interaction of **1** with the CD SAMs than the Langmuir fittings. By using the sequential binding model, the difference found in the binding constants for the divalent binding of **1** in solution and at CD SAMs can be explained in terms of effective concentrations; the

effective concentration as experienced by monovalently bound **1** at CD SAMs is two orders of magnitude higher compared to the corresponding complex in solution with dimer **2**.

Table 6.2 Binding constants for the interaction of **1** with CD SAMs.

[CD] _{sol} (mM)	$K_{LM}^{[a]}$ (M ⁻¹)	$K_{i,s}^{[b]}$ (M ⁻¹)
0.1	1.7×10^{10}	3.3×10^5
0.5	2.8×10^9	1.1×10^5
1.0	6.4×10^9	1.6×10^5
2.5	2.8×10^{10}	3.1×10^5
5	7.9×10^{10}	5.1×10^5

^[a] Langmuir fit to a 1:1 model; ^[b] Fit to the multivalency model, using $C_{eff,max} = 0.2$ M.

Calculation of the complete speciation showed that the total concentration of surface-confined species at any point of the titration curves consisted of over 99% of **1**·(CD_s)₂, indicating that the intramolecular binding to the surface is dominant over the intermolecular binding. This can be explained by the fact that in all cases $C_{eff} \gg [CD]_{tot}$. Consequently, the observed binding constant for the interaction of **1** to CD SAMs is related to the intrinsic binding constants at the surface, $K_{i,s}$, and the maximum effective concentration at the surface, $C_{eff,max}$, as stated in Equation 14.

$$K_{LM} = C_{eff,max} (K_{i,s})^2 \quad (14)$$

Apart from the statistical factor Equation 14 is similar to Equation 1, the formula for the calculation of K for a divalent interaction in solution. Both divalent binding in solution and at surfaces can therefore be interpreted in terms of an effective concentration and intrinsic binding constants, and the relation between di- and monovalent binding is given by the simple Equations 1 and 14.

6.2.4 Patterning of surfaces

The SPR measurements indicated that **1** had a high affinity for the CD SAMs and that the complexes formed at the surface were probably thermodynamically stable in pure water, as almost no desorption was observed upon rinsing with water. These results implied that **1** could be used in surface patterning schemes. Microcontact printing (μ CP) constitutes a technique for the preparation of patterns of molecules on surfaces by transfer of molecules from a soft polymeric stamp to a substrate.³⁸ Transfer of the molecules is limited to the areas where stamp and substrate are in contact. In dip-pen nanolithography (DPN) this same concept is applied for the transfer of molecules from an AFM tip to surfaces.³⁹ Thus far, the application of these techniques has been mainly focused on the transfer of molecules to bare substrates by means of physisorption or coordinative interactions, i.e. the transfer of thiols to gold.^{38,39} Here these techniques have been employed for the transfer of **1** to CD SAMs at which the stability of the patterns is governed by specific supramolecular interactions.

Figure 6.6 shows patterns of **1** obtained by μ CP and DPN.⁴⁰ The patterns were obtained by contacting SAMs with oxidized PDMS stamps or silicon nitride (Si_3N_4) AFM tips inked with **1**. For the μ CP experiments PDMS stamps were hydrophilized by mild oxidation with oxygen plasma in order to assure a good adhesion of aqueous **1** at the stamps.⁴⁰ The hydrophilized stamps were soaked in an aqueous solution of **1** and blown dry prior to use. The inked stamps were applied by hand onto the SAM for 60 s. The μ CP substrates were imaged by contact mode AFM friction imaging using a bare Si_3N_4 AFM tip. Transfer of **1** to the CD as well as 11-mercapto-1-undecanol (OH) SAMs was achieved (bright areas in the μ CP images). The presence of **1** in the contacted areas was confirmed by secondary ion mass spectroscopy (SIMS) imaging.^{40c} Rinsing experiments using Millipore water and 10 mM aqueous CD solutions illustrated the need of specific interactions for sustained pattern stability. The ink transferred to the OH SAMs was instantly removed upon washing with water, implying that **1** is merely physisorbed at these SAMs. Patterns created at CD SAMs remained clearly visible after rinsing with water and 50 mM aqueous NaCl. Substantial removal of **1** from the CD SAMs could be achieved only by prolonged washing of the patterned substrates with a competing 10 mM aqueous CD solution.

These results indicate that the stability of these patterns can be attributed to the presence of multiple host-guest interactions.

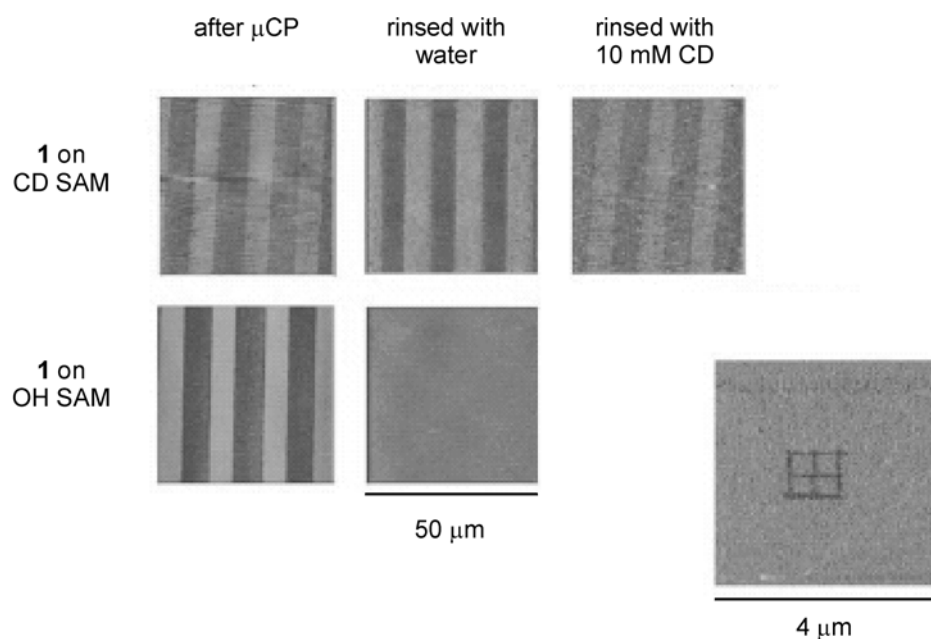


Figure 6.6 Contact mode AFM friction force images (acquired in air) of patterns obtained by μ CP of **1** on CD (top) and 11-mercapto-1-undecanol (OH) SAMs (bottom, left two images): before rinsing, after rinsing with Millipore water, and after rinsing with 10 mM aqueous CD, respectively (image size: $50 \times 50 \mu\text{m}^2$; friction forces (a.u.) increase from dark to bright contrast). Bottom right: Contact mode AFM friction force image in air (friction forces (a.u.) increase from dark to bright) of an array of lines with mean widths (\pm standard deviation) of $60 \pm 20 \text{ nm}$ produced by DPN on a CD SAM using **1** as the ink.

DPN allowed the creation of local patterns of **1** at CD SAMs with sub-100 nm dimensions. This is exemplified in the AFM image of an array of 60 nm wide lines written by DPN (Figure 6.6, bottom right). For the DPN experiments, silicon nitride AFM tips were inked using a procedure analogous to that used for the inking of the PDMS stamps as described above. The inked AFM tips were mounted at the AFM head and subsequently scanned across a CD SAM. DPN patterns were imaged directly after patterning, using the same inked AFM tip. The friction inversion observed for the DPN images with respect to the μ CP images is attributed to the remaining ink at the AFM tip.^{40a,b} Similar to the μ CP experiments, only patterns written at CD SAMs were found to be stable towards rinsing with water and 50 mM aqueous NaCl.⁴⁰

6.3 Conclusions

A significant difference in binding affinity of three orders of magnitude was observed for the divalent interaction of the bis(adamantyl)-modified guest molecule **1** with CD dimer **2** in solution compared to the corresponding divalent interaction at CD SAMs. This difference in binding affinity was rationalized by considering the divalent binding to consist of two sequential binding steps that can be expressed in terms of intrinsic binding constants and an effective concentration. Modeling indicated that this methodology is viable for the studied divalent binding interactions both in solution and at the CD SAMs. By approximation of the effective concentration, intrinsic binding constants were obtained that gave a good correlation with experimentally determined values. The difference in binding affinity for the divalent interaction in solution with dimer **2** compared to the divalent interaction at CD SAMs was shown to mainly originate from a difference in effective concentration, which is two orders of magnitude higher at the CD SAMs. These differences in effective concentration in solution and at SAMs should be taken into account when analyzing multivalent binding at surfaces, as it can give rise to significant differences in binding compared to solution studies.

The methodology presented in this chapter can easily be expanded to higher order multivalent binding and in principle allows the interpretation of any multivalent binding, whether in solution or at a surface, once the intrinsic binding constant for the corresponding monovalent interaction and the effective concentration are known.⁴¹ The former is often readily available from literature and otherwise easily determined. The latter can be roughly estimated using the approaches presented above.

The current understanding of multivalent interactions as presented in this chapter, combined with the more qualitative studies reported previously,⁶ will offer a solid basis for the rational use of multivalency in nanoconstruction. The study presented here indicates that the effective concentration at SAMs is much less sensitive to changes in the spacer length compared to the effective concentration in solution. For this reason high affinity interactions at SAMs can be achieved with molecules containing limited directionality with respect to their guest moieties, and this can be taken advantage of in the design of multivalent guest molecules for the interaction with SAMs. The interaction between **1** and CD SAMs is well suitable for this purpose. With the use of soft and probe lithographic techniques patterns of **1** at

CD SAMs could be created that were stable in aqueous solution, but on the other hand could be almost completely erased by exposure to high molarity CD concentrations. Therefore, these CD SAMs can be used as molecular printboards at which patterns of multivalent complexes can be created. The thermodynamic and kinetic stability of these complexes can be tuned by controlling the number and strength of the interactions between the guest molecules and the CD SAMs.⁴¹

6.4 Experimental section

Adsorbate synthesis and substrates preparation. Adsorbate **3** was synthesized according literature procedures.¹⁰ Round glass-supported substrates for SPR (2.54 cm diameter; 47.5 nm gold thickness) were obtained from Ssens B.V. (Hengelo, The Netherlands) as well as the gold substrates for μ CP and DPN (20 nm of gold on a 3" silicon wafer with a 2 nm titanium adhesion layer). Directly before use, the substrates were cut to the desired shape and size. Substrates were cleaned by oxygen plasma treatment for 5 min and the resulting oxide layer was removed in EtOH. The substrates were subsequently immersed in a solution of **3** (0.1-1 mM) for ca. 16 hrs at 60 °C. The samples were removed from the solution and rinsed thoroughly with CHCl₃, EtOH, and Millipore water.

Calorimetric titrations. Calorimetric measurements were carried out using a Microcal VP-ITC instrument with a cell volume of 1.4115 mL. Solutions for titration were prepared in Millipore water. For studying the complexation of **1** to native β -cyclodextrin (CD), 5 μ L aliquots of 5-10 mM solution of CD were added to a 0.2-0.4 mM solution of **1** in the calorimetric cell, monitoring the heat change after each addition. For studying the complexation of **1** to the EDTA-dimer **2**, 5 μ L aliquots of a 0.4 mM solution of **1** were added to a 0.05 mM solution of **2**. Dilution experiments showed that at the experimental concentrations employed here none of the species showed any detectable aggregation in water. All thermodynamic parameters given above are based on three independent calorimetric titrations.

Surface plasmon resonance titrations. SPR measurements were performed in a two-channel vibrating mirror angle scan setup based on the Kretschmann configuration, described by Kooyman and co-workers.⁴² Light from a 2 mW HeNe laser is directed onto a prism surface by means of a vibrating mirror. The intensity of the light is measured by means of a large-area photodiode. This setup allows the determination of changes in plasmon angle with an accuracy of 0.002°. The gold substrate with the monolayer was optically matched to the prism using an index matching oil. A cell placed on the monolayer was filled with 800 µL of an aqueous CD solution (0.1, 0.5, 1.0, 2.5 or 5.0 mM). After stabilization of the SPR signal, titrations were performed by removing a known amount of CD solution and adding the same amount of a solution of **1** (1.05 µM) in the corresponding CD buffer. Between additions, the cell was cleaned by repeated washings (five times with a 10 mM CD solution), after which the solution was replaced with the initial CD solution. SPR measurements were repeated three times at each CD concentration. All solutions used for the SPR measurements were made using Millipore water and filtered through micropore filters prior to use.

µCP and DPN experiments. For details on the µCP and DPN experiments, the reader is referred to the work of Tommaso Auletta and Barbara Dordi.⁴⁰

6.5 References and notes

¹ Arias, F.; Godinez, L. A.; Wilson, S. R.; Kaifer, A. E.; Echegoyen, L. *J. Am. Chem. Soc.* **1996**, *118*, 6086-6087.

² Miura, Y.; Kimura, S. *Langmuir* **1998**, *14*, 2761-2767.

³ a) Dietrich, C.; Schmitt, L.; Tampé, R. *Proc. Natl. Acad. Sci. U. S. A.* **1995**, *92*, 9014-9018. b) Thess, A.; Hutschenreiter, S.; Hofmann, M.; Tampé, R.; Baumeister, W.; Guckenberger, R. *J. Biol. Chem.* **2002**, *277*, 36231-36328.

⁴ Fragoso, A.; Caballero, J.; Almirall, E.; Villalonga, R.; Cao, R. *Langmuir* **2002**, *18*, 5051-5054.

⁵ Banerjee, I. A.; Yu, L.; Matsui, H. *J. Am. Chem. Soc.* **2003**, *125*, 9542-9543.

⁶ Huskens, J.; Deij, M. A.; Reinhoudt, D. N. *Angew. Chem. Int. Ed.* **2002**, *41*, 4467-4471.

⁷ For streptavidin and biotin: $K_a \approx 10^{15} \text{ M}^{-1}$; $-21 \text{ kcal mol}^{-1}$ (Green, N. M. *Methods Enzymol.* **1990**, *184*, 14-45). For the antibody-antigen interaction: $K_a = \text{up to } 10^{14}$; $-19 \text{ kcal mol}^{-1}$ (Portmann, A. J.; Levison, S. A.; Dandliker, W. B. *Immunochemistry* **1975**, *12*, 461-466).

⁸ For an extensive review on binding affinities and the comparison of cyclodextrin-guest interactions with biomolecular interactions see: Houk, K. N.; Leach, A. G.; Kim, S. P.; Zhang, X. *Angew. Chem. Int. Ed.* **2003**, *42*, 4872-4897.

⁹ Gargano, J. M.; Ngo, T.; Kim, Y.; Acheson, D. W. K.; Lees, W. J. *J. Am. Chem. Soc.* **2001**, *123*, 12909-12910.

¹⁰ Beulen, M. W. J.; Bügler, J.; De Jong, M. R.; Lammerink, B.; Huskens, J.; Schönherr, H.; Vancso, G. J.; Boukamp, B. A.; Wieder, H.; Offenhäuser, A.; Knoll, W.; Van Veggel, F. C. J. M.; Reinhoudt, D. N. *Chem. Eur. J.* **2000**, *6*, 1176-1183.

¹¹ For experimental details see: Mulder, A.; Auletta, T.; Sartori, A.; Casnati, A.; Ungaro, R.; Huskens, J.; Reinhoudt, D. N. *J. Am. Chem. Soc.* **2004**, *126*, in press.

¹² Beulen, M. W. J.; Bügler, J.; Lammerink, B.; Geurts, F. A. J.; Biemond, E. M. E. F.; van Leerdam, K. G. C.; Van Veggel, F. C. J. M.; Engbersen, J. F. J.; Reinhoudt, D. N. *Langmuir*, **1998**, *14*, 6424-6429.

¹³ Schönherr, H.; Beulen, M. W. J.; Bügler, J.; Huskens, J.; Van Veggel, F. C. J. M.; Reinhoudt, D. N.; Vancso, G. J. *J. Am. Chem. Soc.* **2000**, *122*, 4963-4967.

¹⁴ De Jong, M. R.; Huskens, J.; Reinhoudt, D. N. *Chem. Eur. J.* **2001**, *7*, 4164-4170.

¹⁵ Zapotoczny, S.; Auletta, T.; De Jong, M. R.; Schönherr, H.; Huskens, J.; Van Veggel, F. C. J. M.; Reinhoudt, D. N.; Vancso, G. J. *Langmuir* **2002**, *18*, 6988-6994.

¹⁶ Michels, J. J.; Huskens, J.; Reinhoudt, D. N. *J. Am. Chem. Soc.* **2002**, *124*, 2056-2064.

¹⁷ For two independent, sequential binding events this implies: $K_1 = 2K_i$, $K_2 = \frac{1}{2}K_i$, and $\Delta H_1^\circ = \Delta H_2^\circ = \Delta H_i^\circ$.

¹⁸ Rekharsky, M.; Inoue, Y. *Chem. Rev.* **1998**, *98*, 1875-1917.

¹⁹ Mammen, M.; Choi, S.-K.; Whitesides, G. M. *Angew. Chem. Int. Ed.* **1998**, *37*, 2754-2794.

²⁰ Rao, J.; Lahiri, J.; Weis, R. M.; Whitesides, G. M. *J. Am. Chem. Soc.* **2000**, *122*, 2698-2710.

²¹ Kramer, R. H.; Karpen, J. W. *Nature* **1998**, *395*, 710-713.

- ²² Kitov, P. I.; Shimizu, H.; Homans, S. W.; Bundle, D. R. *J. Am. Chem. Soc.* **2003**, *125*, 3284-3294.
- ²³ Winnink, M. A. *Chem. Rev.* **1981**, *81*, 491-524.
- ²⁴ Mandolini, L. *Adv. Phys. Org. Chem.* **1986**, *22*, 1-111.
- ²⁵ For the concept of *EM* applied to reaction kinetics see for example: a) Kirby, J. A. *Adv. Phys. Org. Chem.* **1980**, *17*, 183-278. b) Galli, C.; Mandolini, L. *Eur. J. Org. Chem.* **2000**, 3117-3125. For the concept of *EM* applied to self-assembly in solution see for example: Ercolani, G. *J. Phys. Chem. B* **2003**, *107*, 5052-5057.
- ²⁶ In case of intrinsic binding, *EM* equals C_{eff} (see Chapter 2 for further information).
- ²⁷ Kuhn, W. *Kolloid Z.* **1934**, *68*, 2-15.
- ²⁸ Jacobson H.; Stockmayer, W. H. *J. Phys. Chem.* **1950**, *18*, 1600-1606.
- ²⁹ This concept has also been applied successfully to the pentavalent binding to toxins. a) Fan, E.; Zhang, Z.; Minke, W. E.; Hou, Z.; Verlinde, C. L. M. J.; Hol, W. G. J. *J. Am. Chem. Soc.* **2000**, *122*, 2663-2664. b) Merrit, E. A.; Zhang, Z.; Pickens, J. C.; Ahn, M.; Hol, W. G. J.; Fan, E. *J. Am. Chem. Soc.* **2002**, *124*, 8818-8824.
- ³⁰ Flory, P. J. *Principles of Polymer Chemistry*, Cornell Univ. Press, Ithaca, New York, **1953**.
- ³¹ Length of a carbon-carbon bond: 0.154 nm; bond angle: 109.5°.
- ³² All titration curves were fitted with the maximum SPR response ($\Delta\alpha_{max}$) as obtained for the titration at 0.1 mM CD in solution.
- ³³ Major, R. C.; Zhu, X. Y. *J. Am. Chem. Soc.* **2003**, *123*, 8454-8455.
- ³⁴ a) Rao, J.; Yan, L.; Xu, B.; Whitesides, G. M. *J. Am. Chem. Soc.* **1999**, *121*, 2629-2630. b) Rao, J.; Yan, L.; Lahiri, J.; Whitesides, G. M.; Weis, R. M.; Warren, H. S. *Chem. Biol.* **1999**, *6*, 353-359.
- ³⁵ The statistical factor for the first interaction at the surface is 2 as it accounts for the interaction of a divalent guest molecule with a single host site at the surface.
- ³⁶ This is reasonable as the minimum distance between two CD cavities at the surface is 1.8 nm.
- ³⁷ Molecular modeling of **1** gave a maximum spacing of 4.2 nm between the two adamantyl moieties in the extended conformation of **1**. Application of Equation 4 and the methodology associated with this formula gave values for the \bar{r}_0 of **1** ranging from 1.4 to 4.9 nm. However, the minimum value of \bar{r}_0 enabling a divalent interaction

with the CD SAMs is governed by the minimum spacing between two adjacent CDs at the surface (= 1.8 nm).

³⁸ Xia, Y.; Whitesides, G. M. *Angew. Chem. Int. Ed.* **1998**, *37*, 568-594.

³⁹ Krämer, S.; Fuierer, R. R.; Gorman, C. B. *Chem. Rev.* **2003**, *103*, 4367-4418.

⁴⁰ The μ CP, DPN, and AFM experiments were performed by Tommaso Auletta and Barbara Dordi. For experimental details see: a) Auletta, T. *Ph. D. Thesis*, University of Twente Press: University of Twente, Enschede, **2003**. b) Dordi, D. *Ph. D. Thesis*, University of Twente Press: University of Twente, Enschede, **2003**. c) Auletta, T.; Dordi, B.; Mulder, A.; Sartori, A.; Onclin, S.; Bruinink, C. M.; Péter, M.; Nijhuis, C. A.; Beijleveld, H.; Schönherr, H.; Vancso, G. J.; Casnati, A.; Ungaro, R.; Ravoo, B. J.; Huskens, J.; Reinhoudt, D. N. *Angew. Chem. Int. Ed.* **2004**, *43*, 369-373.

⁴¹ A general model for multivalent binding on surfaces will be presented: Huskens, J.; Mulder, A.; Auletta, T.; Nijhuis, C. A.; Ludden, M. J. W.; Reinhoudt, D. N. *J. Am. Chem. Soc.* **2004**, *126*, in press.

⁴² Lenferink, A. T. M.; Kooyman, R. P. H.; Greve, J. *Sens. Actuators, B* **1991**, *3*, 261-265.

Multivalent host-guest interactions at β -cyclodextrin monolayers on silicon oxide*

7.1 Introduction

As was demonstrated in the previous chapter, self-assembled monolayers (SAMs) of β -cyclodextrin (CD) on gold can be used for the complexation of suitably modified molecules via multiple specific, hydrophobic interactions. With the use of lithographic techniques, such as microcontact printing and dip-pen nanolithography, patterns of guest molecules were created on CD SAMs, which were imaged by atomic force spectroscopy (AFM). Fluorescence imaging techniques, such as laser scanning confocal microscopy (LSCM), form another class of powerful and sensitive microscopic techniques that allow the study of interactions of molecules at monolayers. Like AFM, LSCM allows the imaging of (sub-)micrometer patterns, as well as single molecule studies.^{1,2} Additionally, LSCM enables online monitoring of processes occurring at the surface and possible quantification of the (relative) amounts of molecules present at the surface, and in this respect it is superior to AFM.

Unfortunately, fluorescence techniques like LSCM are not compatible with gold substrates such as those used in Chapter 6. The reason for this is that the excited state of fluorescent molecules situated at or near the gold couples with the surface plasmons of the gold, resulting in energy transfer from the fluorescent dye to the surface without emission of light. This quenching process is a well-known phenomenon for fluorescent molecules near metallic interfaces,^{3,4} and for this reason

* Parts of this work have been published: Auletta, T.; Dordi, B.; Mulder, A.; Sartori, A.; Onclin, S.; Bruinink, C. M.; Péter, M.; Nijhuis, C. A.; Beijleveld, H.; Schönherr, H.; Vancso, G. J.; Casnati, A.; Ungaro, R.; Ravoo, B. J.; Huskens, J.; Reinhoudt, D. N. *Angew. Chem. Int. Ed.* **2004**, *44*, 369-373; Onclin, S.; Mulder, A.; Huskens, J.; Ravoo, B. J.; Reinhoudt, D. N. *Langmuir*, submitted.

fluorescence imaging is typically limited to oxide, e.g. silicon oxide (SiO_2), surfaces. Therefore, in order to study multivalent hydrophobic interactions at CD monolayers by means of fluorescence techniques, CD monolayers on SiO_2 are required.

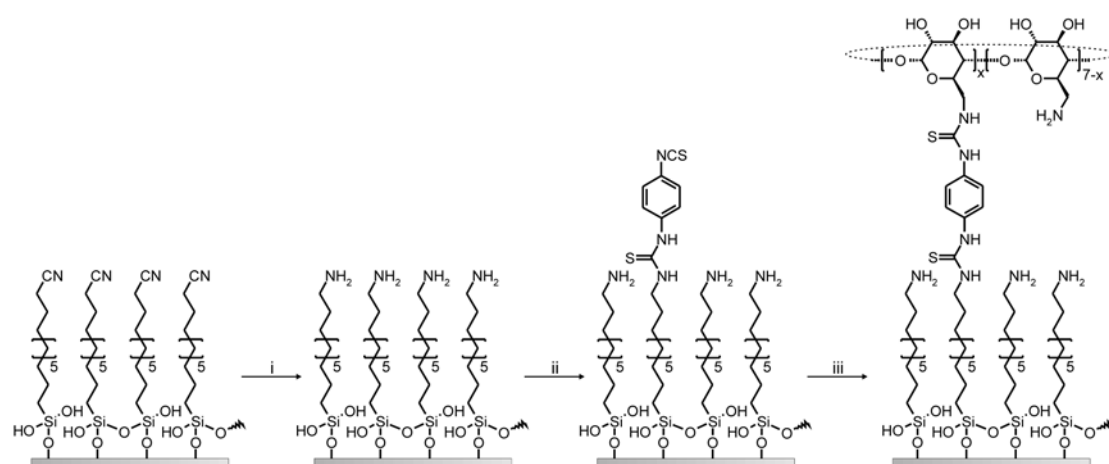
Since their discovery in the early 1980s,⁵ monolayers of trichloro- and trialkoxysilanes on hydroxyl-terminated surfaces (e.g. glass, oxidized silicon wafers) have been investigated extensively.⁶ However, the high reactivity of the trichloro- and trialkoxysilanes limits the number of functional groups and molecules that can readily be used in monolayer formation.⁷ This is especially true for CDs, as these molecules are rich in hydroxyl groups. Not surprisingly, direct modification of CD with trialkoxysilanes leads to the formation of multilayer thin films.⁸ Selective and dense immobilization of a monolayer of CDs at SiO_2 surfaces requires the formation of a well-packed coupling monolayer, which is selectively reactive towards (modified) CD. Li and co-workers have reported the covalent binding of CDs to SiO_2 surfaces using bis(trichlorosilyl)hexane as a coupling layer.⁹ Disadvantages of this approach are the partial backfolding of bis(trichlorosilyl)hexane to the SiO_2 surface, giving rise to disordered monolayers, and the need of protective groups for the secondary hydroxyl groups, which likely have a strong influence on the binding properties of the CDs.¹⁰ Wenz and Mittler employed an epoxy-terminated monolayer to immobilize heptakis-(6-deoxy-6-amino)- β -cyclodextrin (per-6-amino-CD).¹¹ Although these CD monolayers gave reasonable interactions with volatile organic compounds, they are likely to show only limited stability in aqueous solution. The short epoxy-terminated monolayers only have a limited thickness and order, and are thus susceptible to hydrolysis. This chapter presents an alternative, conceptually similar, strategy to obtain very stable, densely packed CD monolayers at SiO_2 substrates, which were used to study the interaction of adamantyl-functionalized fluorescent molecules with CD monolayers by LSCM.

7.2 Results and discussion

7.2.1 Monolayer preparation

The synthesis route for the preparation of the CD monolayers on silicon oxide (SiO_2) is outlined in Scheme 7.1. Monolayers were prepared and characterized by Steffen Onclin, and experimental data and details are described elsewhere.^{12,13}

Monolayers were prepared on microscope glass slides and oxidized silicon wafers. The former substrates were used for fluorescence experiments (sections 7.2.3 to 7.2.5) and the latter for the AFM studies (sections 7.2.4 and 7.2.5). Both substrates were cleaned and activated prior to monolayer formation by immersion in boiling piranha, followed by rinsing with copious amounts of Milli-Q water. The first step in the CD monolayer preparation was the formation of a cyano-terminated monolayer from 1-cyano-11-trichlorosilylundecane.¹⁴ After reduction using Red Al,¹⁵ the substrates were sonicated in a 1 M HCl solution for 5 min to remove the aluminum salts and subsequently in 0.5 M NaOH for another min.¹⁶ This method to obtain amine-terminated monolayers was preferred over direct functionalization of SiO₂ with *N*-2-(aminoethyl)-3-aminopropyl-triethoxysilane or 3-aminopropyl-triethoxysilane as these compounds give disordered monolayers that display limited stabilities in aqueous solutions.¹⁷ In contrast, the densely packed 1-amino-11-trichlorosilylundecane monolayers were stable in water and could even stand the acidic and basic rinsing procedures outlined above. Monolayers that are stable in water are a prerequisite as all binding studies at the CD monolayers are to be performed in aqueous media. By reaction of the amines with 1,4-phenylene diisothiocyanate (DITC), a reactive isothiocyanate-terminated layer was obtained,¹⁸ which was reacted with per-6-amino-CD¹⁹ in aqueous solutions to give the CD-terminated monolayers.



Scheme 7.1 Synthesis scheme for the preparation of CD monolayers on SiO₂: i, Red Al, toluene, 40 °C; ii, DITC, toluene, 50 °C; iii, per-6-amino-CD, H₂O, 50 °C.

All steps in the synthesis of the CD monolayers were characterized extensively by contact angle measurements, ellipsometry, Brewster angle FT-IR, X-ray photoelectron spectroscopy (XPS), and TOF-SIMS.^{12,13} Changes in the wettability of the monolayers as determined by contact angle measurements were in accordance with the relative hydrophobicities of the different end group functionalities. XPS measurements gave atomic compositions for the cyano and amino-terminated monolayers that were in line with calculated data. Introduction of the DITC moiety and per-6-amino-CD led to increases in ellipsometric thickness of 0.4 and 0.8 nm, respectively, which is in good agreement with the dimensions of these molecules. TOF-SIMS experiments revealed predominant and characteristic peaks for the end group functionalities of each monolayer, i.e. nitrile-based peaks for the cyano-terminated layer, a prominent NCS peak for the isothiocyanate-terminated layer, and peaks belonging to oxygen-containing hydrocarbons in the case of the CD-terminated monolayers. From the changes in the carbon/nitrogen ratios determined by XPS, it was estimated that one out of three amine adsorbates reacted with DITC, and that one CD molecule reacted on average with three NCS functionalities. Therefore, it was concluded that using this methodology densely-packed CD-terminated monolayers were obtained, with roughly one CD per nine alkyl chains. These CDs are rigidly anchored to the monolayer as a consequence of three attachment points, rendering the secondary sides of the CD cavities exposed to the solution and accessible for complexation of guest molecules. This suggests that both the packing and orientation of the CD cavities at the SiO₂ surface are comparable to those of the CD SAMs on gold, and that the CD-terminated SiO₂ substrates are potentially equally well capable of binding hydrophobic molecules via specific host-guest interactions.

7.2.2 Synthesis of the fluorescent guest molecules

Three different fluorescent adamantyl-functionalized molecules, **1-3**, were synthesized for interaction with the CD-terminated monolayers on SiO₂ (see Chart 7.1). Molecule **1** is based on a second-generation poly(propylene imine)- (PPI-) dendritic wedge and has four adamantyl groups at its periphery and a fluorescent lissamine moiety in the focal point. Considering molecular structure, **1** is similar to adamantyl-functionalized PPI dendrimers, which have been shown to interact via specific adamantyl-CD interactions with CD SAMs on gold.²⁰ From these studies it

was derived that a second generation PPI wedge was required in order to allow a divalent interaction with the CD SAMs on gold. The spacing of the CD cavities on gold does not allow two adamantyl moieties of a single branch to simultaneously bind to the SAM. As the packing of the CDs on SiO₂ is expected to be similar as on gold, a second-generation wedge was synthesized for the interaction with the CD-terminated SiO₂ surfaces.

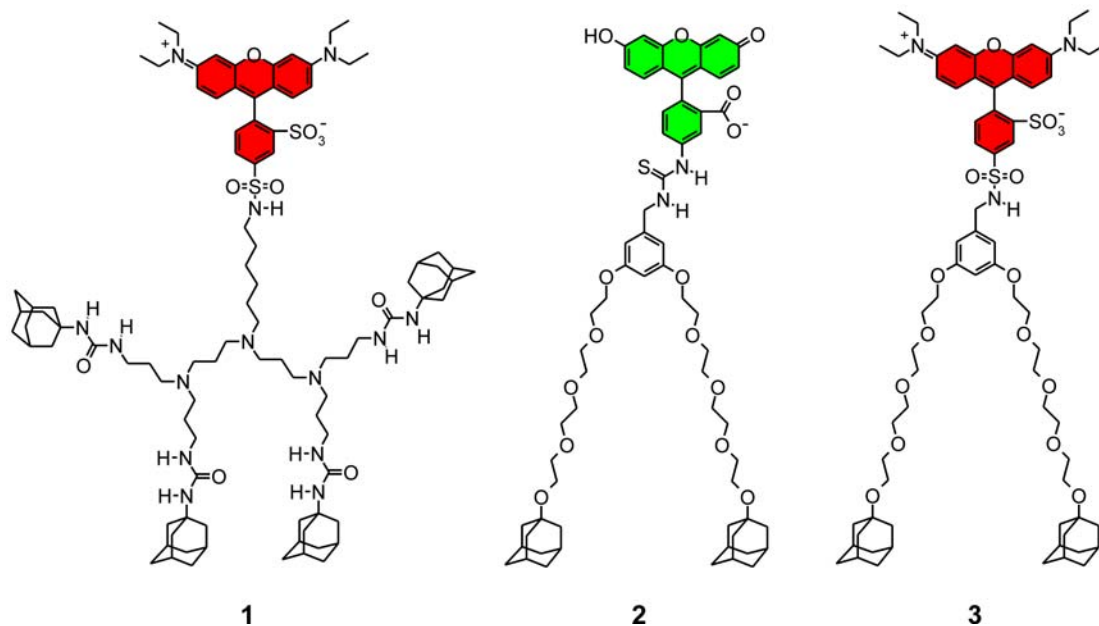
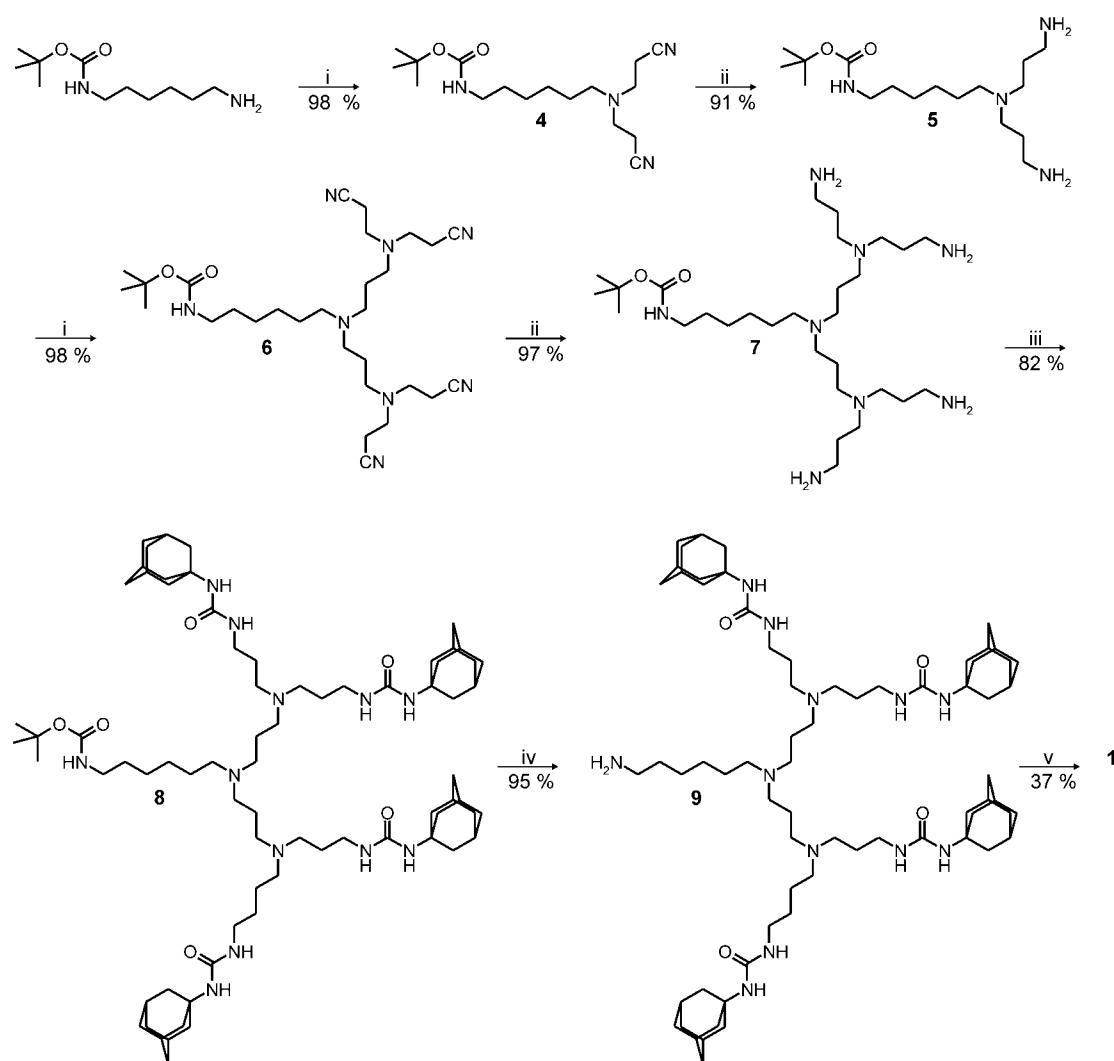


Chart 7.1 Fluorescent adamantyl-terminated dendritic wedges used for interaction with the CD monolayers on SiO₂.

For molecules **2** and **3**, long flexible tetraethylene glycol spacers were employed to assure a divalent interaction with the CDs at SiO₂, and in this respect these molecules are similar to the bis(adamantyl)-calix[4]arene discussed in Chapter 6. Here, a phenyl unit was used to couple a fluorescent dye to two adamantyl moieties. Molecule **2** bears the green fluorescent fluorescein dye, whereas the red fluorescent lissamine dye is used in molecule **3**. The syntheses of molecules **1-3** are outlined below.

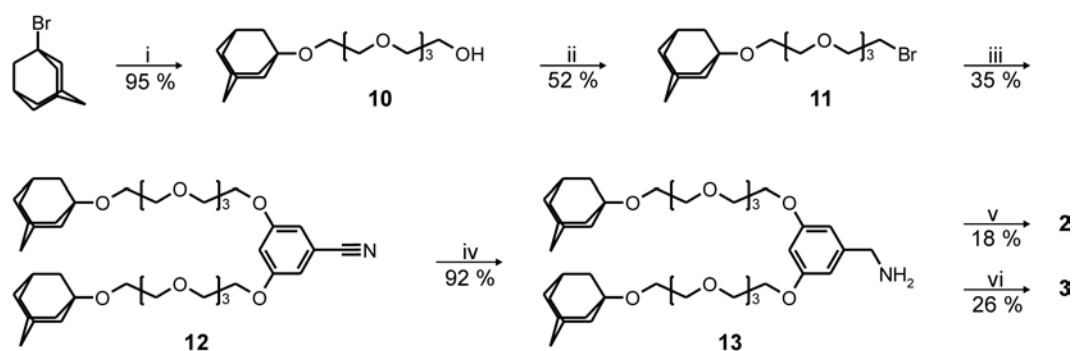
The synthesis route for the fluorescent adamantyl-terminated PPI wedge **1** is outlined in Scheme 7.2. The synthesis starts from *N*-Boc-1,6-diamino-hexane and the build-up of the dendritic wedge is analogous to the synthesis of PPI dendrimers.²¹ *N*-Boc-1,6-diamino-hexane was dispersed in water and treated with acrylonitrile to form dinitrile **4** via a Michael addition. Reduction of the nitrile groups of **4** with Raney-

cobalt and hydrogen in methanol/ammonia/water at 8 bar and room temperature gave diamine **5**. This diamine was cyanoethylated, according to the procedure outlined above, to form the second-generation tetranitrile wedge **6**, which was subsequently reduced to tetraamine **7**. The free amino groups of **7** were reacted with 1-adamantyl isocyanate to give the tetraadamantyl-functionalized Boc-protected amine wedge **8**. The Boc group was removed using TFA, and the resulting free amine **9** was reacted with lissamine sulfonyl chloride to give **1**.



Scheme 7.2 Synthesis route towards fluorescent PPI wedge **1**: i, acrylonitrile, H_2O , $100\text{ }^\circ\text{C}$, overnight; ii, Raney-Co, 8 bar H_2 , NH_3 (aq), r.t., 5 h; iii, 1-adamantyl isocyanate, $CHCl_3$, r.t., overnight; iv, TFA, CH_2Cl_2 , $0\text{ }^\circ\text{C}$, 30 min; v, lissamine sulfonyl chloride (mixture of isomers), DIPEA, CH_2Cl_2 , r. t., overnight.

The synthesis route towards **2** and **3** is depicted in Scheme 7.3. Nucleophilic substitution on 1-bromo-adamantane with tetraethylene glycol in the presence of triethylamine gave the mono-adamantyl-functionalized tetraethylene glycol **10**.²² Subsequent conversion of the remaining hydroxyl functionality to a bromide, using PBr_3 in toluene, gave bromide **11**. Reaction of **11** with 3,5-dihydroxybenzonitrile under conditions as used by Hawker and Fréchet,²³ i.e. acetone, K_2CO_3 , and 18-crown-6, gave the divalent guest unit **12**. The nitrile functionality of **12** was converted to an amine by hydrogenation with 5 bar H_2 to yield **13**, which was used as a precursor for the fluorescent wedges **2** and **3**. Fluorescein-functionalized wedge **2** was obtained by reaction of **13** with fluorescein isothiocyanate. Lissamine-functionalized wedge **3** was formed by reaction of **13** with lissamine sulfonyl chloride.



Scheme 7.3 Synthesis route towards the fluorescent adamantyl-functionalized guests **2** and **3**: i, Et_3N , tetraethylene glycol, 180°C , overnight; ii, PBr_3 , toluene, r.t., overnight; iii, 3,5-dihydroxybenzonitrile, K_2CO_3 , 18-crown-6, acetone, reflux, 72 h; iv, Raney-Co, 6 M NH_3 in ethanol, 5 bar H_2 , r.t., overnight; v, fluorescein isothiocyanate, DIPEA, MeOH, CH_2Cl_2 , r.t., overnight; vi, lissamine sulfonyl chloride (mixture of isomers), DIPEA, acetonitrile, r.t., overnight.

Wedges bearing more adamantyl moieties are readily accessible by using 3,5-dihydroxybenzylalcohol instead of 3,5-dihydroxybenzonitrile. Analogous to the synthesis used for Fréchet dendrimers,²³ bromination of the resulting bis(adamantyl)benzylalcohol and subsequent nucleophilic substitution of the bromide with 3,5-dihydroxybenzylalcohol would give a molecule with four adamantyl moieties.²⁴ This procedure can be repeated to obtain wedges bearing up to 32 adamantyl groups.²⁴ However, these larger molecules have poor water-solubility, even

in the presence of CD.²⁴ For this reason the synthesis was limited to the bis(adamantyl)-functionalized fluorescent molecules **2** and **3**.

Molecules **1-3** had moderate to poor water-solubility. The fluorescein-functionalized molecule **2** had the highest water-solubility, up to 0.1 mM at high pH. To achieve similar concentrations of the lissamine-functionalized molecules **1** and **3** in water, the adamantyl moieties of these molecules needed to be complexed with CD. The free ligands displayed only limited water solubility, up to $\sim 1 \mu\text{M}$.

Figure 7.1 depicts the combined and normalized excitation and emission spectra of molecules **2** (left) and **3** (right). Both emission and excitation spectra are typical of the fluorescent dyes incorporated in the molecules. Fluorescein-functionalized **2** showed an excitation maximum in aqueous solution at 493 nm and an emission maximum in the green at 521 nm. Lissamine-functionalized **3** showed an excitation maximum in aqueous solution at 569 nm with an emission maximum in the red at 589 nm. The spectra recorded for **1** were similar to those of **3**.

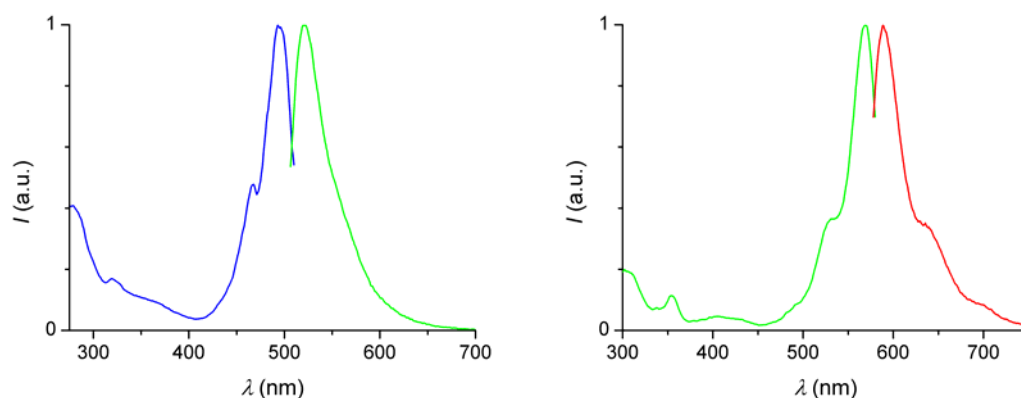


Figure 7.1 Emission and excitation spectra ($1 \mu\text{M}$ in water) of fluorescein-functionalized wedge **2** (left) and lissamine-functionalized wedge **3** (right).

7.2.3 Binding of the fluorescent wedges at the CD monolayers

There are only a limited number of techniques to study the binding of guests at SiO_2 substrates. SiO_2 is a strong insulator and therefore it is not possible to use techniques such as surface plasmon resonance or electrochemical impedance spectroscopy, which are typically applied in our group to study the interaction of guest molecules at CD SAMs on gold.^{20,22,25}

Instead, the interaction strength of the fluorescent wedges with the CD monolayers on SiO₂ was studied by desorption experiments, which were monitored by fluorescence spectroscopy. In a typical experiment a CD substrate was immersed in a 10⁻⁵ M aqueous solution of the fluorescent adamantyl-functionalized wedge in order to saturate the CD monolayers with guest molecules. The substrates were subsequently rinsed with 10 mM phosphate buffer and water to remove any physisorbed material. Thereafter, defined areas of the substrate were exposed to various concentrations of a CD solution by placing a container on top of the substrate, which was then filled with 100 μL of a CD solution (0.5 to 10 mM). After 5 min 60 μL of the CD solution was withdrawn, diluted to 600 μL, after which the emission spectrum was recorded in a fluorescence spectrophotometer.²⁶

Figure 7.2 shows a typical desorption curve obtained with the procedure outlined above and depicts the fluorescence intensity at variable CD concentrations for the desorption of **2** from a CD substrate. The desorption curve could be well fitted with the model given in Chapter 6, i.e. considering a surface coverage-dependent effective concentration, C_{eff} , with a $C_{eff,max}$ of 0.2 M, and an intrinsic binding constant for the interaction of CD with the adamantyl moieties in solution, $K_{i,l}$, of $5 \times 10^4 \text{ M}^{-1}$. It was assumed that prior to the desorption experiment the CD-terminated substrates were saturated with a monolayer of **2**. The initial concentration of surface-confined **2** was calculated from the concentration of CD cavities at the surface,²⁷ expressed as a solution concentration, which was divided by the number of host-guest interactions between **2** and the CD monolayer (used as a fitting parameter). The concentrations of **2** in solution after desorption were calculated from the emission intensity of these solutions. Fitting of the desorption curves indicated that **2** bound to the CD monolayers on SiO₂ via two adamantyl-CD interactions, with an intrinsic binding constant, $K_{i,s}$, of $\sim 3 \times 10^5 \text{ M}^{-1}$, which implied a divalent binding constant, K_2 , of $\sim 10^{10} \text{ M}^{-1}$.²⁸ These values are similar to those found for the interaction of the bis(adamantyl)-calix[4]arene with the CD SAMs on gold (see Chapter 6), and indicate that the binding properties of the CD cavities immobilized at the SiO₂ substrates are retained and are comparable to those of CD SAMs on gold.

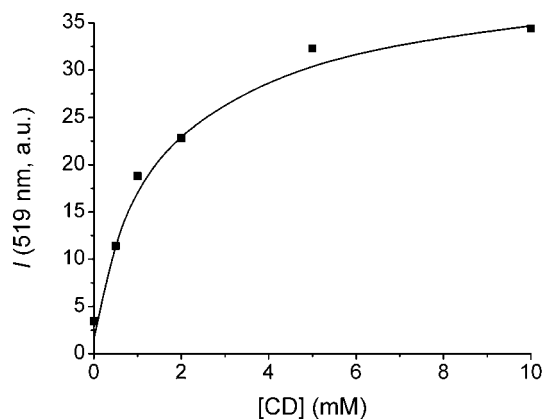


Figure 7.2 Desorption curve for the CD concentration-dependent desorption of fluorescein-functionalized wedge **2** from a saturated CD monolayer (markers) and fit to the binding model for multivalent interactions at surfaces as described in Chapter 6 (solid line).

Similar desorption experiments with **1** gave desorption curves that were less readily interpretable. Exposure of CD-terminated substrates saturated with **1** to concentrated CD solutions did not result in a near complete desorption of **1**, and therefore it was not possible to achieve a proper desorption curve that would allow the determination of the interaction strength of **1** with the CD surfaces. It is unlikely that **1** has more than two interactions with the CD substrates. The spacing between two adamantyl moieties on a single branch of the wedge is insufficient to allow both of them to simultaneously interact with a CD cavity, even when the closest packing of CD cavities at the surface is considered. Therefore, the low desorption of **1** from the CD substrates is probably inherent to the poor water-solubility of this molecule. Because **3** was also hardly soluble in water, it was not assessed in a desorption experiment.

7.2.4 Patterning of surfaces

Microcontact printing (μ CP) and dip-pen nanolithography (DPN) were applied to achieve patterns of assemblies on the CD-terminated SiO_2 substrates. μ CP of bis(adamantyl)-calix[4]arene (see Chapter 6) on the CD-terminated SiO_2 , as studied by AFM, gave results similar to those obtained with the CD SAMs on gold, both regarding ink transfer and pattern stability. For the printing experiments, CD-terminated silicon wafers were used. The silicon wafers are relatively flat compared to the microscope glass slides and therefore more suitable for imaging with AFM.

For fluorescence imaging, μ CP of **1** on CD-terminated glass slides was performed. As a reference experiment, **1** was also printed on a poly(ethylene glycol)-(PEG-) terminated layer.²⁹ Printing of **1** was done from aqueous solution of the per-CD complex of **1**, using oxidized PDMS stamps. The per-CD complex of **1** was used to achieve sufficiently concentrated solutions for printing. The PDMS stamps (10 μ m features spaced by 5 μ m) were mildly oxidized using UV-ozone in order to ensure a good adhesion of the ink solution to the stamp. Figure 7.3 (page 158) depicts the images obtained by LSCM. As is evident from Figure 7.3, ink transfer is achieved both on the CD- and PEG-terminated monolayers, giving an exact reproduction of the stamp features. When the printed substrates were rinsed with copious amounts of 10 mM phosphate buffer, the patterns were completely removed from the PEG-terminated substrates, whereas this rinsing procedure hardly affected the patterns printed on the CD substrates. Only rinsing with 10 mM CD led to significant reduction of the fluorescence intensity on the latter.

These results indicate that multivalent, specific interactions between **1** and the CD-terminated substrate are responsible for the observed stability of the patterns. Furthermore, they illustrate that per-CD complexed molecules can also be used in printing experiments. Apparently, the concentration of CD cavities at the surface is sufficiently high to compete with the CD molecules that are transferred together with **1** upon printing. These findings are in line with the theoretical model outlined in Chapter 6, and corroborate the assumption that the CD cavities are closely packed at the SiO₂ substrates, giving rise to a considerable effective surface CD concentration experienced by the guest molecules.

Printing experiments with **2** and **3** gave similar results. Figure 7.4 (page 158) shows the LSCM images of CD-terminated SiO₂ substrates patterned with **2**. Because of its reasonable water solubility **2** could be printed as the free guest. As for **1**, printed patterns were stable towards thorough rinsing with phosphate buffer, and substantial reduction of fluorescence intensity was only achieved by rinsing with 10 mM CD.

LSCM allows an easy discrimination between different dye molecules present at the surface. Figure 7.5 depicts the LSCM images, acquired at different emission wavelengths, for a substrate that was patterned with **1** by μ CP and subsequently immersed in a 10⁻⁶ M aqueous solution of **2**. The LSCM emission image recorded above 600 nm is dominated by the emission of the printed lines of **1** (Figure 7.5, left).

The lissamine dye of **1** has a strong emission above 600 nm, whereas the emission of the fluorescein-functionalized **2** is very limited at these wavelengths (see Figure 7.1). As is evident from the LSCM emission image recorded between 500 and 530 nm, the range of wavelengths at which fluorescein strongly emits (Figure 7.5, center), **2** was specifically adsorbed at the vacant CD cavities that had not been in contact with the PDMS stamp. The sharp contrast in the patterns suggests that there is only limited replacement of **1** by **2**.

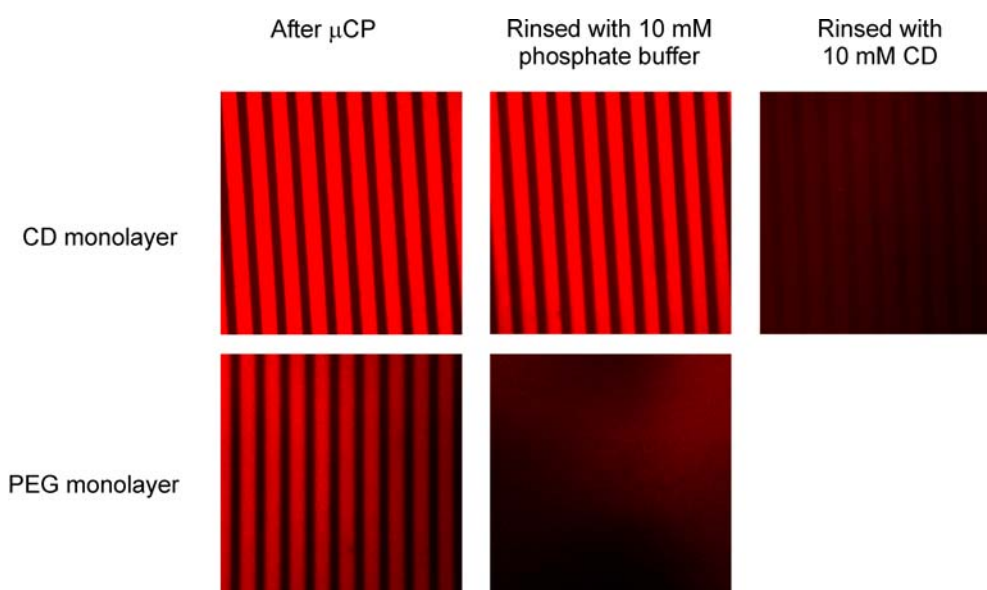


Figure 7.3 Confocal microscopy images ($150 \times 150 \mu\text{m}$) after μ CP of the per-CD complex of **1** on CD- (top) and PEG- (bottom) terminated monolayers on SiO_2 . Images shown after printing from left to right: without rinsing; after rinsing with 200 mL of 10 mM phosphate buffer; after rinsing with 200 mL of a 10 mM aqueous CD solution.

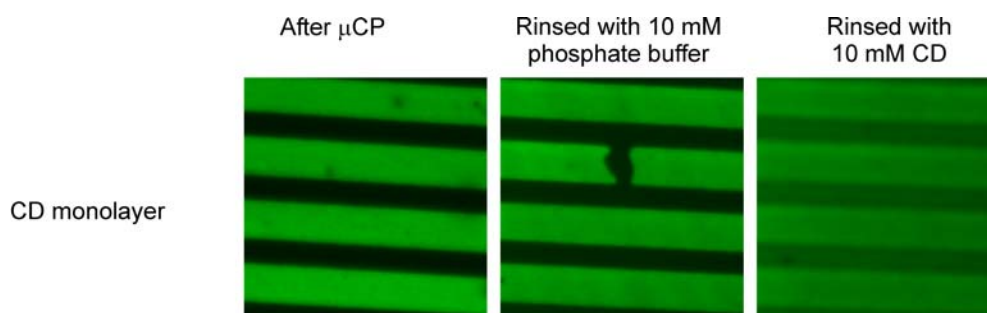


Figure 7.4 Confocal microscopy images ($60 \times 60 \mu\text{m}$) after μ CP of **2** on CD-terminated monolayers on a glass slide. Images obtained after printing from left to right: without rinsing; after rinsing with 200 mL of 10 mM phosphate buffer; after rinsing with 200 mL of a 10 mM aqueous CD solution.

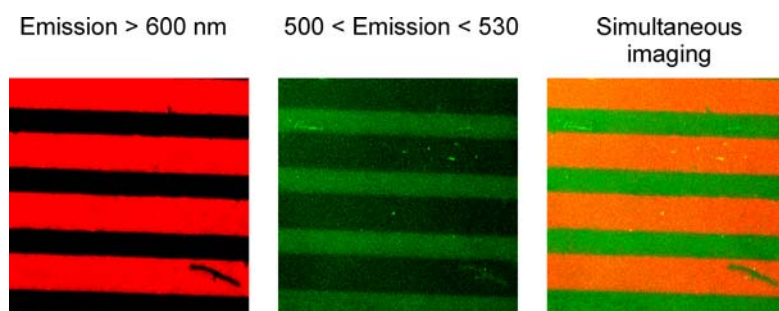


Figure 7.5 Confocal microscopy images ($60 \times 60 \mu\text{m}$) taken at different emission wavelengths of a CD-terminated monolayer on a glass slide patterned with **1** by μCP and subsequently immersed in an aqueous solution of **2**. The substrate was simultaneously excited at 488 and 543 nm and images were recorded by measuring the emission above 600 nm (left) and between 500 and 530 nm (center). The picture at the right shows the combined image.

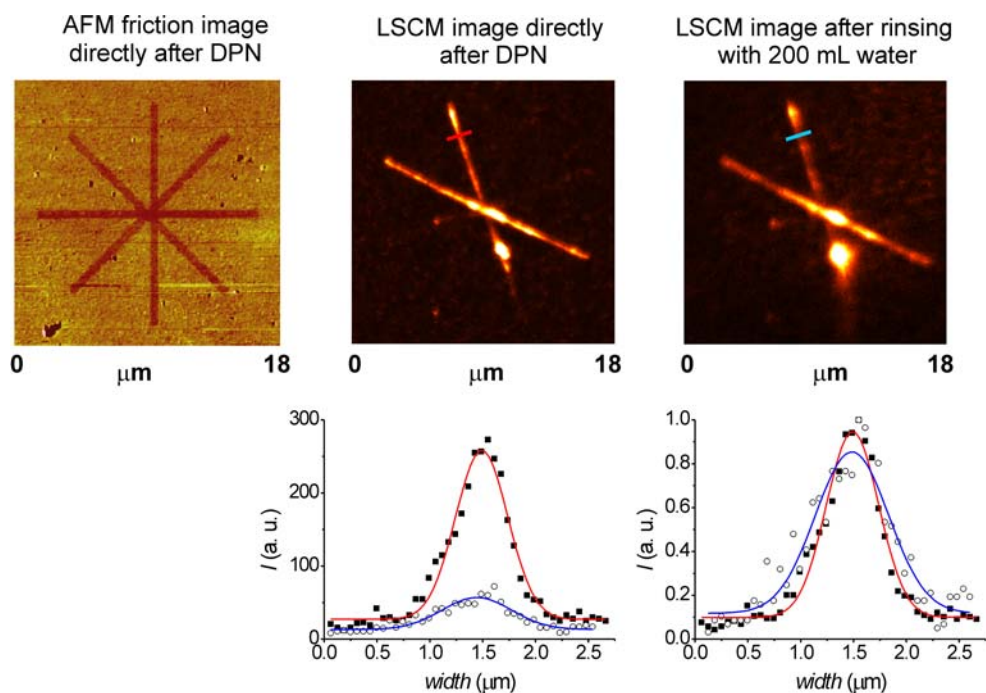


Figure 7.6 Top: AFM friction force image (friction forces (a.u) increase from dark to bright contrast) of $15 \mu\text{m}$ long and 470 nm wide lines of **1** produced by DPN on a CD-terminated monolayer on a silicon wafer (left, image acquired in air), and confocal microscopy images of a similar pattern produced by DPN on a CD-terminated glass slide; directly after writing (center) and the same pattern after rinsing with 200 mL water (right). The bottom graphs show the relative (left) and normalized (right) emission intensity line scans (markers) and Gaussian fits (solid lines) for the cross-sections of the fluorescent lines before (■) and after (○) rinsing. The positions of the line scans are marked in the top LSCM graphs by the colored bars.

DPN was used to produce local fluorescent patterns on CD-terminated SiO₂ substrates. The top left two images of Figure 7.6 show patterns of **1** directly imaged after writing a pattern by DPN on a silicon wafer (left) and on a glass slide (center). In both cases it was attempted to draw a star made up of four 15 μm long lines with a width of 470 nm. The pattern written on the silicon wafer was measured by contact-mode AFM, whereas the pattern written on the glass slide was imaged by LSCM.

The DPN experiments performed at the CD-terminated silicon wafers resulted in well-defined high-quality patterns. In contrast, the quality of the pattern produced by DPN on the glass slide was poor, which is probably due to the inherently larger roughness of this surface. AFM imaging of CD-terminated microscope glass slides showed the presence of small, undefined clusters at the surface. These features make it difficult to ensure continuous and good contact between the AFM tip and the surface during the DPN experiments. Contact between the tip and small clusters at the surface may be the reason for the inhomogeneity of the lines in the LSCM image.

One of the potential advantages of the combination of CD monolayers on SiO₂ and a LSCM-setup is that it enables a more quantitative visualization of the amount of material that is transferred to the surface during a DPN experiment and of the effect that rinsing procedures have on the created patterns. The top right image of Figure 7.6 shows the LSCM image of the pattern after rinsing with water. In this experiment, the sample was removed from the holder, thoroughly rinsed with copious amounts of water, and remounted on the LSCM setup for relocation of the pattern. The graphs in Figure 7.6 depict the relative (bottom left graph) and normalized emission intensity line scans (bottom right graph) of the patterns before and after the rinsing procedure. The pattern is still well visible after rinsing, indicating that it is governed by specific multivalent hydrophobic interactions. The line scans of the fluorescent pattern (relative emission intensities, bottom left graph) indicate that the fluorescence intensity of the rinsed pattern was substantially diminished. However, this might be due to photobleaching of the lissamine dye, and therefore care should be taken with the relative quantification of the dye molecules present at the surface. The bottom right graph in Figure 7.6, showing the normalized emission intensities for the same line scans, indicated that the width of the fluorescent lines increased by about 30 % after rinsing with water. This broadening might be caused by migration of **1** over the surface, which is promoted by a strong effective concentration- (C_{eff}) gradient present

at the surface, i.e. the C_{eff} in the substrate areas where most of the CD cavities are complexed by **1** is substantially lower than the C_{eff} in the substrate areas where all CDs are free for complexation. Additionally, it could be that more than a monolayer of **1** was transferred during the DPN experiment, and that part of the excess of **1** was able to interact with the CD surface upon rinsing of the pattern.³⁰ Further, more quantitative experiments are required for more conclusive explanations.

7.3 Conclusions

Very stable, densely packed CD-terminated monolayers on SiO₂ can be synthesized through a four-step synthesis route starting from 1-cyano-11-trichlorosilylundecane. Binding studies with suitably modified guest molecules indicated that the binding properties of the immobilized CD cavities are retained, and that these monolayers are well suited for the strong complexation of molecules by means of multivalent hydrophobic interactions. μ CP and DPN experiments demonstrated that it was possible to create reversible patterns at CD-terminated SiO₂ surfaces, which thereby act as molecular printboards on glass and form an addition to the molecular printboards on gold as presented in Chapter 6.

In many respects, the CD monolayers on SiO₂ are comparable to the CD SAMs on gold. Both characterization of the CD monolayers on SiO₂ and the desorption experiments performed on these monolayers with fluorescent guests indicated that the packing of the CDs at the SiO₂ surface is similar to that for the CD SAMs on gold. The interaction of a bis(adamantyl)-functionalized guest molecule with the CD monolayers at SiO₂ gave a binding constant of $\sim 10^{10} \text{ M}^{-1}$, which is similar to that found for the interaction of the bis(adamantyl)-calix[4]arene with CD SAMs on gold, indicating that multivalent guest molecules interact with both CD monolayers in a similar fashion. Furthermore, both surfaces are well suited for patterning with multivalent guest molecules using techniques such as μ CP or DPN.

The advantage of the CD monolayers on silicon oxide is that they enable the use of fluorescence techniques, such as LSCM, which can be used to achieve a more quantitative visualization of the created patterns compared to AFM. Additionally, these techniques allow the straightforward discrimination between different species present at the CD monolayers. In contrast, to make differentiation by AFM feasible, the probed molecules should display substantially different wetting properties in order

to achieve contrast by AFM.³¹ The work described in this chapter mainly concerns the fundamental aspects of the combination of LSCM and CD monolayers on SiO₂. In principle, LSCM enables the online monitoring of processes occurring at the CD surfaces. The use of flow cells would allow the straightforward determination of binding constants, either directly in case of fluorescent guests or indirectly for non-fluorescent guests using competition experiments.^{32,33} Not only is this approach more practical than the static desorption experiments performed in this chapter, it might also give an insight into the kinetics of host-guest interactions at the CD-terminated surfaces.

7.4 Acknowledgement

The major part of the work presented in this chapter was performed in collaboration with Steffen Onclin, who has been responsible for the preparation and characterization of the CD-terminated silicon oxide surfaces.

7.5 Experimental section

Materials and methods. All chemicals were used as received, unless stated otherwise. Heptakis-(6-deoxy-6-amino)- β -cyclodextrin (per-6-amino-CD) was synthesized according to literature procedures.¹⁹ Solvents were purified according to standard laboratory methods.³⁴ Thin-layer chromatography was performed on aluminum sheets precoated with silica gel 60 F254 (Merck). The Boc-protected PPI-wedge spots were visualized by dipping in iodine and bromocresolgreen. Chromatographic separations were performed on silica gel 60 (Merck, 0.040-0.063 mm, 230-240 mesh). FAB mass spectra were recorded with a Finnigan MAT90 spectrometer with *m*-nitrobenzylalcohol as a matrix. MALDI-TOF mass spectra were recorded using a PerSpective Biosystems Voyager-DE-RP MALDI-TOF mass spectrometer using dihydroxybenzoic acid as a matrix. NMR spectra were recorded at 25 °C using a Varian Inova 300 spectrometer. ¹H NMR chemical shifts (300 MHz) are given relative to residual CHCl₃ (7.25 ppm) or CHD₂OD (3.35 ppm). ¹³C NMR chemical shifts (75 MHz) are given relative to CDCl₃ (77.0 ppm) or to CD₃OD (49.3 ppm).

Dinitrile Boc-protected amine wedge 4. *N*-Boc-1,6-diamino-hexane hydrochloride (1.87 g, 8.65 mmol) was washed with 1 M NaOH and dispersed in water (18 mL). To the dispersion was added acrylonitrile (1.45 mL, 21.6 mmol). The mixture was stirred for 30 min at room temperature, followed by refluxing overnight. The excess acrylonitrile was azeotropically removed with water under reduced pressure. Dichloromethane was added, and the organic layer was washed with water, dried over MgSO₄, and the dichloromethane was removed under reduced pressure to give **4** as a colorless oil (2.72 g, 8.42 mmol; 98 %). ¹H NMR (CDCl₃): δ 4.52 (s, 1H, NH), 3.07 (q, *J* = 6.6 Hz, 2H, NHCH₂), 2.82 (t, *J* = 6.8 Hz, 4H, CH₂CN), 2.49 (t, *J* = 7.0 Hz, 2H, NCH₂), 2.43 (t, *J* = 6.8 Hz, 4H, NCH₂), 1.47-1.27 (m, 8H, CH₂CH₂CH₂CH₂), 1.41 (s, 9H, CH₃); ¹³C NMR (CDCl₃): δ 155.5, 118.1, 78.5, 52.9, 49.2, 39.9, 29.5, 27.9, 26.8, 26.2, 26.1, 16.5; MS (FAB): *m/z* calcd for [M+H]⁺ 323.2; found 323.2.

Diamine Boc-protected amine wedge 5. To a nitrogen-flushed solution of dinitrile wedge **4** (0.30 g, 0.93 mmol) in methanol was added an excess of ammonia in water. Cr-promoted Raney-cobalt (Grace 2724) was added and the mixture was flushed with hydrogen and subsequently hydrogenated at 8 bar H₂ in an autoclave for 5 h at room temperature. Hydrogen was removed by purging with nitrogen and the Raney-cobalt was removed over a hyflofilter. The solvent was removed under reduced pressure to give **5** as a colorless oil (0.28 g, 0.85 mmol; 91 %). ¹H NMR (CD₃OD): δ 3.06 (t, *J* = 7.0 Hz, 2H, NHCH₂), 2.70 (t, *J* = 7.0 Hz, 4H, CH₂NH₂), 2.70 (m, 6H, NCH₂), 1.67 (m, *J* = 7.2 Hz, 4H, NCH₂CH₂CH₂N), 1.53-1.35 (m, 8H, CH₂CH₂CH₂CH₂), 1.47 (s, 9H, CH₃); ¹³C NMR (CD₃OD): δ 121.3, 80.1, 55.3, 53.2, 41.6, 41.4, 31.3, 30.7, 29.1, 28.7, 28.1, 27.8; MS (FAB): *m/z* calcd for [M+H]⁺ 331.3; found 331.3.

Tetranitrile Boc-protected amine wedge 6. The same procedure as for wedge **4** was used, starting from diamine wedge **5** (0.28 g, 0.85 mmol) and acrylonitrile (0.28 mL, 4.24 mmol) in water (5 mL), to give **6** as a yellow oil (0.45 g, 0.84 mmol; 98 %). ¹H NMR (CDCl₃): δ 4.52 (s, 1H, NH), 3.08 (q, *J* = 6.7 Hz, 2H, NHCH₂), 2.83 (t, *J* = 6.6 Hz, 8H, CH₂CN), 2.55 (t, *J* = 7.1 Hz, 4H, NCH₂CH₂CH₂N), 2.46 (m, 12H, NCH₂), 2.36 (t, *J* = 7.1 Hz, 2H, NCH₂), 1.57 (m, *J* = 7.0 Hz, 4H, NCH₂CH₂CH₂N), 1.48-1.22 (m, 8H, CH₂CH₂CH₂CH₂), 1.42 (s, 9H, CH₃); ¹³C NMR (CDCl₃): δ 155.6, 118.3,

78.5, 53.5, 51.2, 51.0, 49.2, 40.1, 29.6, 28.0, 26.8, 26.5, 26.3, 24.7, 16.5; MS (MALDI-TOF): m/z calcd for $[M+H]^+$ 543.4; found 543.5.

Tetraamine Boc-protected amine wedge 7. The same procedure as for wedge **5** was used, starting from tetranitrile wedge **6** (0.45 g, 0.84 mmol), to give **7** as a yellow oil (0.46 g, 0.82 mmol; 97 %). ^1H NMR (CD_3OD): δ 3.07 (t, $J = 7.0$ Hz, 2H, NHCH_2), 2.72 (t, $J = 7.1$ Hz, 8H, CH_2NH_2), 2.67-2.48 (m, 18H, NCH_2), 1.68 (m, $J = 7.2$ Hz, 12H, $\text{NCH}_2\text{CH}_2\text{CH}_2\text{N}$), 1.51-1.36 (m, 8H, $\text{CH}_2\text{CH}_2\text{CH}_2\text{CH}_2$), 1.47 (s, 9H, CH_3); ^{13}C NMR (CD_3OD): δ 158.4, 80.1, 55.3, 53.5, 53.1, 41.6, 41.4, 31.3, 30.7, 29.1, 28.7, 28.2, 27.8, 25.0, 24.8; MS (MALDI-TOF): m/z calcd for $[M+H]^+ = 559.5$, found 559.9.

Tetraadamantylurea-functionalized Boc-protected amine wedge 8. To a solution of tetraamine wedge **7** (0.46 g, 0.82 mmol) in chloroform (10 mL) was added 1-adamantyl isocyanate (0.64 g, 3.62 mmol). The mixture was stirred overnight at room temperature under argon. The solvent was removed under reduced pressure. Diethyl ether was added, and the formed precipitate was isolated and dried under reduced pressure to give **8** as a white solid (0.85 g, 0.67 mmol; 82 %). ^1H NMR (CDCl_3): δ 5.72 (s, 4H, CH_2NHCONH), 5.06 (s, 4H, NHCONHAd), 4.66 (s, 1H, NHCO), 3.09 (m, 10H, NHCH_2), 2.38 (m, 18H, NCH_2), 2.03 (s, 12H, CH), 1.96 (s, 24H, NHCCCH_2), 1.64 (s, 24H, CHCH_2CH), 1.58 (m, 12H, $\text{NCH}_2\text{CH}_2\text{CH}_2\text{N}$), 1.43 (s, 9H, CH_3), 1.46-1.24 (m, 8H, $\text{NCH}_2\text{CH}_2\text{CH}_2\text{CH}_2\text{CH}_2\text{CH}_2$); ^{13}C NMR (CDCl_3): δ 158.4, 156.2, 52.1, 51.7, 51.6, 50.6, 42.6, 38.3, 36.5, 30.9, 30.1, 29.6, 28.4, 27.9, 26.8, 26.6; MS (MALDI-TOF): m/z calcd for $[M+H]^+$ 1268.0, found 1268.6.

Amino-tetraadamantylurea wedge 9. To a cooled solution of Boc-tetraadamantylurea **8** (201 mg, 0.16 mmol) in CH_2Cl_2 (10 mL) was added trifluoroacetic acid (0.5 mL). The solution was stirred for 30 min, after which the solvent was evaporated. The excess trifluoroacetic acid was removed azeotropically with toluene. The residue was triturated with diethyl ether to give **9** as a white solid (177 mg, 0.15 mmol; 95 %). ^1H NMR (CDCl_3): δ 3.24-2.83 (m, 30H, $\text{NHCH}_2 + \text{NCH}_2 + \text{CH}_2\text{NH}_2$), 1.97 (s, 12H, CH), 1.86 (s, 24H, NHCCCH_2), 1.78 (m, 12H, $\text{NCH}_2\text{CH}_2\text{CH}_2\text{N}$), 1.58 (s, 24H, CHCH_2CH), 1.40-1.21 (m, 8H,

$\text{NCH}_2\text{CH}_2\text{CH}_2\text{CH}_2\text{CH}_2\text{CH}_2$); ^{13}C NMR (CDCl_3): δ 158.7, 52.6, 50.4, 49.3, 42.6, 41.7, 39.6, 35.9, 30.7, 30.0, 29.1, 28.9, 27.9, 25.6, 25.5, 24.2; MS (MALDI-TOF): m/z calcd for $[\text{M}+\text{Na}]^+$ 1189.9; found 1190.2.

Lissamine tetraadamantylurea wedge 1. To a solution of adamantyl-terminated dendritic wedge **8** (93 mg, 0.080 mmol) and DIPEA (40 μl , 0.24 mmol) in CH_2Cl_2 (20 mL) was added lissamine sulfonyl chloride (mixed isomers, 46 mg, 0.24 mmol). The solution was stirred overnight at room temperature. The solvent was evaporated under reduced pressure, and the residue was purified by gradient column chromatography ($\text{CH}_2\text{Cl}_2/\text{MeOH}/\text{Et}_3\text{N} = 97.5/2/0.5$ to $89.5/10/0.5$) to give the desired product as a purple solid (53 mg, 0.031 mmol; 37 % yield). ^1H NMR (CDCl_3): δ 8.67 (s, 1H, ArH), 8.02 (d, $J = 7.7$ Hz, 1H, ArH), 7.17-7.13 (m, 3H, ArH), 6.79 (d, $J = 9.3$ Hz, 2H, ArH), 6.64 (s, 2H, ArH), 6.26 (s, 1H, ArH), 6.01-5.75 (m, 5H, $\text{NHSO}_2 + \text{CH}_2\text{NHCO}$), 5.38-5.08 (bs, 4H, AdNHCO), 3.56 (qtr, $J = 7.3$ Hz, 8H, $\text{ArNCH}_2\text{CH}_3$), 3.27 (qtr, $J = 7.3$ Hz, 2H, CH_2NHSO_2), 3.01 (bs, 8H, CH_2NHCONH), 2.58-2.19 (m, 18H, CH_2NCH_2), 1.91 (bs, 12H, AdH), 1.84 (bs, 24H, AdH), 1.61-1.40 (m, 36H, AdH + $\text{NCH}_2\text{CH}_2\text{CH}_2\text{N} + \text{NCH}_2\text{CH}_2\text{CH}_2\text{NHCO}$), 1.35-1.02 (m, 20H, $\text{CH}_3\text{CH}_2 + \text{NCH}_2\text{CH}_2\text{CH}_2\text{CH}_2\text{CH}_2\text{CH}_2\text{NSO}_2$); ^{13}C NMR (CDCl_3): δ 159.5, 158.6, 157.9, 155.6, 146.8, 143.1, 139.3, 133.5, 133.3, 129.1, 127.9, 127.3, 95.8, 52.4, 51.6, 51.4, 50.7, 46.0, 44.4, 42.5, 37.8, 36.6, 31.4, 29.6, 29.4 - 26.4, 22.7, 12.6; MS (MALDI-TOF): m/z calcd for $[\text{M}+\text{Na}]^+$ 1731.1; found 1731.2.

Tetraethylene glycol mono-adamantyl ether 10. A solution of 1-bromoadamantane (15.0 g, 69.8 mmol) and triethylamine (30 mL, 216 mmol) in tetraethylene glycol (250 mL) was stirred overnight at 180 $^\circ\text{C}$. After cooling to room temperature, dichloromethane (250 mL) was added. The solution was washed with 2 M hydrochloric acid (4 x 100 mL) and once with brine (100 mL). The organic layer was dried over MgSO_4 and the solvent was evaporated under reduced pressure to give **10** as a yellow-brown oil (21.8 g, 66.4 mmol; 95 %). ^1H NMR (CDCl_3): δ 3.73 (t, $J = 4.6$ Hz, 2H, $\text{AdOCH}_2\text{CH}_2$), 3.69-3.66 (m, 8H, TEG CH_2), 3.64-3.58 (m, 6H, $\text{AdOCH}_2\text{CH}_2 + \text{CH}_2\text{CH}_2\text{OH}$), 2.89 (s, 1H, CH_2OH), 2.15 (m, 3H, $\text{CH}_2\text{CHCH}_2[\text{Ad}]$), 1.75-1.76 (m, 6H, $\text{CHCH}_2\text{C}[\text{Ad}]$), 1.67-1.57 (m, 6H, $\text{CHCH}_2\text{CH}[\text{Ad}]$); ^{13}C NMR (CDCl_3): δ 72.0,

71.8, 70.8, 70.1, 70.0, 69.8, 61.2, 58.7, 40.9, 35.9, 30.0; MS (FAB): m/z calcd for $[M+H]^+$ 329.3; found 329.3.

Triethylene glycol bromoethyl adamantyl ether 11. To a cooled (0 °C) solution of **10** (4.03 g, 12.2 mmol) in toluene (100 mL) was added dropwise a solution of phosphorus tribromide (1.30 g, 4.80 mmol) in toluene (50 mL). The mixture was stirred overnight at room temperature. The solvent was removed under reduced pressure and the residue was partitioned between dichloromethane (100 mL) and water (100 mL). The organic layer was washed with water (3 x 50 mL) and brine (1 x 50 mL) and dried over $MgSO_4$. The solvent was removed under reduced pressure and the residue was purified by column chromatography ($CH_2Cl_2/MeOH = 99/1$) to give **11** as a colorless oil (2.48 g, 6.4 mmol; 52 %). 1H NMR ($CDCl_3$): δ 3.83 (t, $J = 6.2$ Hz, 2H, $AdOCH_2CH_2$), 3.70-3.67 (m, 8H, TEG CH_2), 3.62-3.60 (m, 4H, $AdOCH_2CH_2 + CH_2CH_2Br$), 3.49 (t, $J = 6.4$ Hz, 2H, CH_2CH_2Br), 2.15 (m, 3H, $CH_2CHCH_2[Ad]$), 1.76-1.75 (m, 6H, $CHCH_2C[Ad]$), 1.64-1.62 (m, 6H, $CHCH_2CH[Ad]$); ^{13}C NMR ($CDCl_3$): δ 72.2, 71.3, 71.2, 70.7-70.5, 59.2, 41.4, 36.4, 30.4; MS (FAB): m/z calcd for $[M+H]^+$ 391.1; found 391.2.

3,5-Bis(tetraethylene glycol adamantyl ether)benzonitrile 12. A suspension of **11** (1.68 g, 4.29 mmol), 3,5-dihydroxybenzonitrile (0.28 g, 2.04 mmol), dried potassium carbonate (0.71 g, 5.14 mmol), and 18-crown-6 (0.11 g, 0.42 mmol) in acetone (50 mL) was refluxed for 72 h. The solvent was evaporated and the residue was partitioned between water (50 mL) and diethyl ether (50 mL). The aqueous layer was extracted with diethyl ether (3 x 25 mL) and the combined extracts were dried over $MgSO_4$. The solvent was evaporated and the residue was purified by column chromatography ($CH_2Cl_2:MeOH = 98:2$) to give **12** as a colorless oil (0.54 g, 0.72 mmol; 35 %). 1H NMR ($CDCl_3$): δ 6.80 (d, $J = 2.2$ Hz, 2H, ArH), 6.73 (t, $J = 2.2$ Hz, 1H, ArH), 4.13 (t, $J = 4.8$ Hz, 4H, $ArOCH_2$), 3.87 (t, $J = 4.8$ Hz, 4H, $AdOCH_2$), 3.76-3.67 (m, 16H, TEG CH_2), 3.63-3.58 (m, 8H, $AdOCH_2CH_2 + CH_2CH_2OAr$), 2.15 (m, 3H, $CH_2CHCH_2[Ad]$), 1.75-1.76 (m, 6H, $CHCH_2C[Ad]$), 1.68-1.58 (m, 6H, $CHCH_2CH[Ad]$); ^{13}C NMR ($CDCl_3$): δ 160.1, 118.7, 113.3, 110.7, 106.7, 72.3, 71.3, 70.9, 70.6-70.5, 69.4, 67.9, 59.2, 41.4, 36.4, 30.5; MS (FAB): m/z calcd for $[M+H]^+$ 756.5; found 756.3.

(3,5-Bis(tetraethylene glycol adamantyl ether)phenyl)methylamine 13. Compound **12** (0.54 g, 0.71 mmol) was dissolved in 6 M ammonia in ethanol (50 mL) and some Raney-cobalt was added. The mixture was placed in an autoclave and stirred overnight under 5 bar hydrogen at room temperature. The suspension was filtered over Celite and washed with methanol (1 L). The solvent was evaporated under reduced pressure and the residue was dissolved in chloroform (50 mL). The solution was washed with a 0.1 M NaOH solution, the organic layer was separated, and the aqueous layer was extracted with chloroform (3 x 200 mL). The solvent of the combined organic fractions was evaporated under reduced pressure to give **13** as a colorless oil (0.50 g, 0.66 mmol; 92 %). ^1H NMR (CDCl_3): δ 6.55 (s, 2H, ArH), 6.39 (s, 1H, ArH), 4.13 (t, $J = 4.8$ Hz, 4 H, ArOCH_2), 3.86 (m, 6H, $\text{AdOCH}_2 + \text{CH}_2\text{NH}_2$), 3.76-3.65 (m, 18H, TEG $\text{CH}_2 + \text{CCH}_2\text{NH}_2$), 3.60 (m, 8H, $\text{AdOCH}_2\text{CH}_2 + \text{CH}_2\text{CH}_2\text{OAr}$), 2.16 (m, 6H, $\text{CH}_2\text{CHCH}_2[\text{Ad}]$), 1.75-1.76 (m, 12H, $\text{CHCH}_2\text{C}[\text{Ad}]$), 1.68-1.58 (m, 12H, $\text{CHCH}_2\text{CH}[\text{Ad}]$); ^{13}C NMR (CDCl_3): δ 160.0, 106.3, 100.3, 72.4, 71.2, 70.7-70.5, 69.8, 67.4, 65.0, 59.2, 41.4, 36.4, 30.5; MS (FAB): m/z calcd for $[\text{M}+\text{H}]^+$ 760.5; found 760.3.

1-Fluorescein-3-(3,5-di(tetraethylene glycol adamantyl ether))benzyl thiourea 2. A solution of **13** (290 mg, 0.38 mmol), fluorescein isothiocyanate (297 mg, 0.76 mmol), *N,N*-diisopropylethylamine (0.5 mL, 2.87 mmol) in an 8:2 methanol/dichloromethane mixture (50 mL) was stirred overnight at room temperature. The solvent was evaporated under reduced pressure and the residue was purified by gradient column chromatography ($\text{CH}_2\text{Cl}_2/\text{MeOH} = 99/1$ to $96/4$) to give **2** as a yellow solid (80 mg, 0.070 mmol; 18 %). ^1H NMR (CDCl_3): δ 10.25 (b, 1H, ArCOOH), 9.83 (s, 1H, ArOH), 8.36 (s, 1H, ArH), 8.05 (b, ArNHCS), 7.95 (d, $J = 8.4$ Hz, 1H, ArH), 6.98 (d, $J = 8.4$ Hz, 1H, ArH), 6.77 (s, 2H, ArH), 6.62-6.52 (m, 6 H, ArH), 6.29 (s, 1H, ArH), 4.76 (s, 2H, ArCH_2NH), 4.01-3.95 (m, 5H, $\text{ArOCH}_2 + \text{CH}_2\text{NHCS}$), 3.75 (m, 4H, AdOCH_2), 3.66-3.56 (m, 24H, TEG $\text{CH}_2 + \text{AdOCH}_2\text{CH}_2 + \text{CH}_2\text{CH}_2\text{OAr}$), 2.10 (m, 6H, $\text{CH}_2\text{CHCH}_2[\text{Ad}]$), 1.71 (m, 12H, $\text{CHCH}_2\text{C}[\text{Ad}]$), 1.62-1.52 (m, 12H, $\text{CHCH}_2\text{CH}[\text{Ad}]$); ^{13}C NMR (CDCl_3): δ 181.2, 169.8, 159.8, 152.8, 141.4, 140.2, 130.5, 129.9, 129.1, 128.3, 127.5, 122.2, 118.1, 110.5, 108.0, 106.5, 103.1, 100.6, 72.7, 71.2, 70.5-70.4, 69.6, 67.3, 59.2, 54.0, 48.1, 42.2, 41.3, 36.3, 30.4; MS (FAB): m/z calcd for $[\text{M}+\text{H}]^+$ 1149.5; found 1149.6.

1-Lissamine-3,5-di(tetraethylene glycol adamantyl ether)benzyl sulfonamide 3. A solution of **13** (210 mg, 0.28 mmol), lissamine sulfonyl chloride (mixture of isomers, 319 mg, 0.55 mmol), *N,N*-diisopropylethylamine (0.5 mL, 2.87 mmol) in acetonitrile (50 mL) was stirred overnight at room temperature. The solvent was evaporated under reduced pressure and the residue was purified by gradient column chromatography (CH₂Cl₂/MeOH = 99/1 to 94/6) to give the single isomer **3** as a purple solid (92 mg, 0.071 mmol; 26%). ¹H NMR (CDCl₃): δ 8.85 (s, 1H, ArH), 7.90 (d, *J* = 9.5 Hz, 1H, ArH), 7.26 (d, *J* = 9.5 Hz, 2H, ArH), 7.13 (d, *J* = 8.1 Hz, 1H, ArH), 6.85 (d, *J* = 9.5 Hz, 2H, ArH), 6.67 (s, 2H, ArH), 6.52 (s, 2H, ArH), 6.34 (s, 1H, ArH), 6.16 (br, 1H, CH₂NHS), 4.18 (d, *J* = 5.9 Hz, 2H, CCH₂NH), 4.08 (t, *J* = 4.6 Hz, 4H, ArOCH₂), 3.80 (t, *J* = 4.8 Hz, 4H, AdOCH₂), 3.72-3.62 (m, 16H, TEG CH₂), 3.62-3.50 (m, 16H, AdOCH₂CH₂ + CH₂CH₂OAr + NCH₂CH₃), 2.13 (m, 6H, CH₂CHCH₂[Ad]), 1.74 (m, 12H, CHCH₂C[Ad]), 1.66-1.56 (m, 12H, CHCH₂CH[Ad]), 1.31 (t, *J* = 7.1 Hz, 12H, NCH₂CH₃); ¹³C NMR (CDCl₃): δ 159.8, 158.9, 157.8, 155.4, 147.8, 142.1, 139.2, 133.6, 133.4, 129.5, 127.3, 127.0, 114.3, 113.5, 106.4, 101.5, 95.5, 72.2, 71.1, 70.6-70.5, 69.6, 67.4, 59.2, 47.3, 45.8, 41.4, 36.4, 30.4, 12.6. MS (MALDI-TOF): *m/z* calcd for [M+H]⁺ 1300.6; found 1300.4.

Substrate preparation. Four-inch polished, 100-cut, p-doped silicon wafers, cut into 2 × 2 cm² samples, and microscope glass slides were used for monolayer preparation. For information on the preparation and characterization of the monolayers, the reader is referred to the work of Steffen Onclin.^{12,13}

Fluorescence spectroscopy. Emission and excitation spectra of the fluorescent wedges were recorded on an Edinburgh FS900 fluorospectrophotometer in which a 450 W xenon arc lamp was used as excitation source. M300 gratings with 1800 1/mm were used on both excitation and emission arms. Signals were detected by a Peltier element cooled, red sensitive, Hamamatsu R928 photomultiplier system. Quartz sample cells of 1 cm were used. The titration experiments with the fluorescent wedges **1** and **2** were performed as outlined in the main text of this chapter and for these experiments quartz cells of 1 mm were used.

Microcontact printing. The dendritic wedges were stamped from 0.1 mM aqueous solutions of the per-CD complex (**1**) or the free fluorescent molecules (**2** and **3**). PDMS stamps (10 μm wide lines spaced by 5 μm wide gaps) were mildly oxidized using UV-ozone for 15 min to render them hydrophilic. The oxidized stamps were soaked in the ink solution, blown dry in a stream of nitrogen, and brought into contact with the surface for 1 min without external pressure.

DPN. The substrates that were to be imaged by LSCM after the DPN experiments were hand-marked with a diamond-tip pen to give a V-shaped scratch. Prior to dip-pen nanolithography these substrates were extensively bleached, in order to reduce background fluorescence. For bleaching, the substrates were exposed to the 254 and the 435 and 546 nm lines of a mercury lamp, with a power of approximately 900 mW at 488 nm. The light was focused on the marker using an oil immersion lens (N.A. 1.4, 63 \times). The exposure time was at least 20 min for each line.

For the DPN experiments, silicon nitride tips coated with 50 nm gold were used (Ssens BV, The Netherlands). In order to promote the wetting of the tips by the aqueous ink solutions, the tips were coated with a monolayer of 1-mercapto-11-undecanol. Cleaned gold tips were immersed in a 0.1 mM solution of 1-mercapto-11-undecanol in ethanol for 6-12 h. After monolayer formation the tips were rinsed with ethanol and dried in a stream of nitrogen. For the writing experiments the tips were inked by soaking them in a 10 μM solution of per-CD complexed **1** in water for 5 min and blown dry. The tips were mounted in the AFM head, and the AFM cantilever was positioned within the V-shaped marker with the use of a CCD camera. Line patterns were created in the vicinity of the marker. The star-shaped patterns were produced by scanning over each line 10 times (contact force \sim 20 nN, scan speed 0.75 Hz, $T = 25$ $^{\circ}\text{C}$, relative humidity 35-40 %). For direct AFM imaging of the patterns produced by DPN, the scan size was increased to $30 \times 30 \mu\text{m}^2$, and the scan velocity was increased to 1.5 Hz.

Laser scanning confocal microscopy. Confocal images of the microcontact printed substrates were taken on a Carl Zeiss LSM 510 microscope. The light was focused on the substrate using an oil immersion lens (N.A. 1.4, 63 \times). The lissamine-functionalized wedges were excited at 543 nm, while the fluorescein-functionalized

wedge was excited at 488 nm. The emitted fluorescence was collected on a PMT Hamamatsu R6357 spectrophotometer. All confocal microscopy images were acquired in air.

Fluorescence imaging of the DPN patterns was carried out using an inverted confocal microscope (Zeiss Axiovert) with an oil-immersion lens (N.A. 1.4, 100x). An ArKr ion laser (Spectra Physics BeamLok 2060) operated at 514 nm was used to excite the fluorophores. The excitation light was filtered using a 514 nm bandpass filter (Omega 514.5/10). A dichromic mirror (Omega 540DRLP) and a long-pass filter (Omega 550APL) were used to separate the emitted light from the excitation light. The fluorescence signal was detected using an avalanche photodiode (EG&G Electro Optics SPCM-AQ-14). The sample was scanned over an area typically 30 x 30 μm with 512 x 512 pixels and a pixel dwell time of 1 ms. The excitation power was 3.5 kW/cm². All confocal microscopy images were acquired in air.

7.6 References and notes

¹ Weiss, S. *Science* **1999**, *283*, 1676-1683.

² Chan, V. C. H.; Codd, S. L.; Van der Helm, M.; Spatz, J. P.; Röcker, C.; Nienhaus, G. U.; Levi, S. A.; Van Veggel, F. C. J. M.; Reinhoudt, D. N.; Möller, M. *J. Mater. Res.* **2001**, *676*, Y4.4.

³ a) Chance, R.; Prock, A.; Silbey, R. *Adv. Chem. Phys.* **1978**, *37*, 1-65. b) Enderlein, J. *Chem. Phys.* **1999**, *247*, 1-9. c) Kümmerlen, J.; Leitner, A.; Brunner, H.; Aussenegg, F. R.; Wokaun, A. *Mol. Phys.* **1993**, *80*, 1031-1046. d) Reese, S.; Fox, M. A. *J. Phys. Chem. B* **1998**, *102*, 9820-9824.

⁴ Quenching especially hampers fluorescence spectroscopy at continuous metallic films, but is less predominant at metallic nanoparticles or islands, see for example ref. 2 and: a) Levi, S. A.; Mourran, A.; Spatz, J. P.; Van Veggel, F.C. J. M.; Reinhoudt, D. N.; Möller, M. *Chem. Eur. J.* **2002**, *8*, 3808-3814. b) Dulkeith, W.; Morteani, A. C.; Niedereichholz, T.; Klar, T. A.; Feldmann, J.; Levi, S. A.; Van Veggel, F. C. J. M.; Reinhoudt, D. N.; Möller, M.; Gittins, D. I. *Phys. Rev. Lett.* **2002**, *89*, 203002, 1-3. c) Chumanov, G.; Sokolov, K.; Gregory, B. W.; Cotton, T. M. *J. Phys. Chem.* **1995**, *99*, 9466-9471.

⁵ Sagiv, J. *J. Am. Chem. Soc.* **1980**, *102*, 92-98.

- ⁶ a) Ulman, A. *An Introduction to Ultrathin Organic Films*, Academic Press: Boston, **1991**. b) Ulman, A. *Chem. Rev.* **1996**, *96*, 1533-1554.
- ⁷ The number of functional groups that can be directly introduced onto SiO₂ substrates is very limited, see: Sullivan, T. P.; Huck, W. T. S. *Eur. J. Org. Chem.* **2003**, 17-29.
- ⁸ Yang, X.; Shi, J.; Johnson, S.; Swanson, B. *Sens. Actuators, B* **1997**, *45*, 79-84.
- ⁹ a) Moore, L. W.; Springer, K. N.; Shi, J.-X.; Yang, X. G.; Swanson, B. I.; Li, D. Q. *Adv. Mater.* **1995**, *7*, 729-731. b) Li, D. Q.; Ma, M. *Sens. Actuators, B* **2000**, *69*, 75-84.
- ¹⁰ Beulen, M. W. J.; Bügler, J.; Lammerink, B.; Geurts, F. A. J.; Biemond, E. M. E. F.; Van Leerdam, K. G. C.; Van Veggel, F. C. J. M.; Engbersen, J. F. J.; Reinhoudt, D. N. *Langmuir* **1998**, *14*, 6424-6429.
- ¹¹ Busse, S.; DePaoli, M.; Wenz, G.; Mittler, S. *Sens. Actuators, B* **2001**, *80*, 116-124.
- ¹² Onclin, S.; Mulder, A.; Huskens, J.; Ravoo, B. J.; Reinhoudt, D. N. *Langmuir*, **2004**, submitted.
- ¹³ Onclin S. *Ph.D. Thesis*, Enschede, **2004**, in preparation.
- ¹⁴ This reaction was performed at low temperature to assure the formation of well-ordered monolayers: a) Brzoska, J. B.; Shahidzadeh, N.; Rondelez, F. *Nature* **1992**, *360*, 719-721. b) Carraro, C.; Yauw, O. W.; Sung, M. M.; Maboudian, R. *J. Phys. Chem. B* **1998**, *102*, 4441-4445. c) Parikh, A. N.; Allara, D. L.; Ben Azouz, I.; Rondolez, F. *J. Phys. Chem.* **1994**, *98*, 7577-7590. d) Richter, A. G.; Durbin, M. K.; Yu, C.-J.; Dutta, P. *Langmuir* **1998**, *14*, 5980-5983.
- ¹⁵ Red Al is a trade name for solutions of sodium bis(2-methoxyethoxy)aluminum dihydride in toluene.
- ¹⁶ Lee, M. T.; Ferguson, G. S. *Langmuir* **2001**, *17*, 762-767.
- ¹⁷ Bierbaum, K.; Kinzler, M.; Wöll, Ch.; Grunze, M.; Hähner, G.; Heid, S.; Effenberger, F. *Langmuir*, **1995**, *11*, 512-518.
- ¹⁸ Similarly, other *p*-substituted phenylenes have been used previously as linking groups at SAMs: Persson, H. H. J.; Caseri, W. R.; Suter, U. W. *Langmuir* **2001**, *17*, 3643-3650.
- ¹⁹ Ashton, P. R.; Koniger, R.; Stoddart, J. F.; Alker, D.; Harding, V. D. *J. Org. Chem.* **1996**, *61*, 903-908.
- ²⁰ Huskens, J.; Deij, M. A.; Reinhoudt, D. N. *Angew. Chem. Int. Ed.* **2002**, *41*, 4467-4471.

- ²¹ a) Bell, J. A.; Kenworthy, C. *Commun. Synth.* **1971**, 650-652. b) De Brabander-Vanden Berg, E. M. M.; Meijer, E. W. *Angew. Chem. Int. Ed. Engl.* **1993**, *32*, 1308-1311. c) De Brabander, E. M. M.; Brackman, J.; Mure-Mak, M.; De Man, H.; Hogeweg, M.; Keulen, J.; Scherrenberg, R.; Coussens, B.; Mengerink, Y.; Van der Wal, S. *Macromol. Symp.* **1996**, *102*, 9-17. d) Baars, M. W. P. L. *Ph.D. Thesis*, University of Eindhoven, The Netherlands, **2000**, Chapter 2.
- ²² Mulder, A.; Auletta, T.; Sartori, A.; Del Ciotto, S.; Casnati, A.; Ungaro, R.; Huskens, J.; Reinhoudt, D. N. *J. Am. Chem. Soc.* **2004**, *126*, in press.
- ²³ Hawker, C. J.; Fréchet, J. M. J. *J. Am. Chem. Soc.* **1990**, *112*, 7638-7647.
- ²⁴ Van Bommel, K. J. C.; Metselaar, G. A.; Verboom, W.; Reinhoudt, D. N. *J. Org. Chem.* **2001**, *66*, 5405-5412.
- ²⁵ a) Beulen, M. W. J.; Bügler, J.; De Jong, M. R.; Lammerink, B.; Huskens, J.; Schönherr, H.; Vancso, G. J.; Boukamp, B. A.; Wieder, H.; Offenhäuser, A.; Knoll, W.; van Veggel, F. C. J. M.; Reinhoudt, D. N. *Chem. Eur. J.* **2000**, *6*, 1176-1183. b) De Jong, M. R.; Huskens, J.; Reinhoudt, D. N. *Chem. Eur. J.* **2001**, *7*, 4164-4170.
- ²⁶ Time-dependent experiments showed that 5 min were sufficient to achieve equilibration of the system.
- ²⁷ The concentration of surface-confined CDs was calculated from the number of CD cavities per surface area, which was approximated from the XPS data (see 7.2.1), and the substrate area that was exposed to the CD solutions in the container (38.5 mm²).
- ²⁸ Calculated using $K_2 = C_{eff,max}(K_{i,s})^2$. See Chapter 6 for deduction of this formula.
- ²⁹ The PEG-terminated SAMs were made by exposure of a cleaned and activated SiO₂ substrate to a commercially available mixture of 2-[methoxypoly(ethylenoxy)-propyl]trimethoxysilane (6 to 9 ethylene glycol units per molecule), according to a procedure given by: Papra, A.; Gadegaard, N.; Larsen, N. B. *Langmuir* **2001**, *17*, 1457-1460.
- ³⁰ It has been shown that typically more than a monolayer is transferred during μ CP: Auletta, T.; Dordi, B.; Mulder, A.; Sartori, A.; Onclin, S.; Bruinink, C. M.; Péter, M.; Nijhuis, C. A.; Beijleveld, H.; Schönherr, H.; Vancso, G. J.; Casnati, A.; Ungaro, R.; Ravoo, B. J.; Huskens, J.; Reinhoudt, D. N. *Angew. Chem. Int. Ed.* **2004**, *44*, 369-373.
- ³¹ a) Hong, S.; Mirkin, C. A. *Science* **2000**, *288*, 1808-1811. b) Hong, S.; Zhu, J.; Mirkin, C. A. *Science* **1999**, *286*, 523-525.

³² Yang, T.; Baryshikova, O. K.; Mao, H.; Holden, M. A.; Cremer, P. S. *J. Am. Chem. Soc.* **2003**, *125*, 4779-4784.

³³ Elbs, M.; Brock, R. *Anal. Chem.* **2003**, *75*, 4793-4800.

³⁴ Perrin, D. D.; Armarego, W. F. L. *Purification of Laboratory Chemicals*, 3rd ed., Pergamon, Oxford, **1989**.

Summary

This thesis deals with multivalent β -cyclodextrin (CD) host-guest interactions in solution and at interfaces. In solution, multivalency has been exploited to develop strongly binding CD dimers. Switchable tethers have been implemented to control the possible relative orientations of the two CD cavities of the CD dimers and therewith the extent of multivalency in the binding of guest molecules, giving access to tunable receptor molecules, the binding properties of which can be controlled by external stimuli. Different approaches towards tunable receptor molecules are described in Chapters 3 to 5. At interfaces, multivalent CD host-guest interactions have been applied for strong and selective complexation of multivalent guest molecules at CD monolayers. These CD monolayers have been used as molecular printboards at which patterns of supramolecular, multivalent assemblies were created with the use of lithographic techniques. Two different types of CD monolayers (on gold and on glass) are described in Chapters 6 and 7.

Multivalency has been defined in Chapter 2, and a general overview of the characteristic features of multivalent interactions has been given. A special section has been devoted to multivalent CD assemblies. It has been shown that the strength of multivalent interactions is governed by the strength and number of the participating individual interactions, and that the stability of an assembly based on multivalent interactions is strongly influenced by the presence of competing species in solution. Throughout this thesis, these aspects have been used as tools to achieve control over the stability of assemblies.

Chapter 3 describes two photoswitchable dithienylethene-tethered CD dimers as receptor molecules with phototunable binding properties. The two CD dimers differ in the connectivity of the tether and the CD cavities. A short CD dimer was obtained by direct coupling of the dithienylethene moiety to the secondary rims of the CD cavities. A longer CD dimer was synthesized by using flexible propyl spacers to couple the CD cavities with the dithienylethene moiety. By irradiation with UV light these CD dimers were switched from a relatively flexible open to a rigid closed form. For both CD dimers, the photostationary states consisted of 25 % of the open and 75 % of the closed forms. The CD dimers were completely switched back to the open forms by irradiation with visible light ($\lambda > 460$ nm). Repeated irradiation cycles

showed no sign of degradation, indicating that the switching process is fatigue resistant. Calorimetric studies with meso-tetrakis(4-sulfonatophenyl)porphyrin (TSPP) as a guest indicated that the binding properties of the CD dimers were dependent on the configuration of the dithienylethene tether. For the short CD dimer the open form bound TSPP 35 times more strongly than the closed form. The enthalpies of complexation indicated that the closed form of the short CD dimer was not capable of binding TSPP in an effective divalent fashion, i.e. using both CD cavities to the full extent. This was supported by molecular modeling, which showed that the rigid closed dithienylethene tether spaces the two CD cavities too far apart to allow cooperation in binding TSPP. The longer CD dimer gave no significant differences in binding affinity for TSPP. For both the open and closed forms, association constants similar to that found for the open short CD dimer were obtained. The enthalpies of binding for both the open and closed forms were twice that of native CD, indicating that both forms were able to strongly complex TSPP in a divalent fashion. Molecular modeling showed that the propyl spacers of the long CD dimer were able to overcome the rigidity imposed on the CD dimer by the closed tether. The difference in binding affinity between the open and closed forms of the short CD dimer enabled the photocontrolled release and uptake of TSPP, rendering the external control over the ratio of complexed and free TSPP in solution possible.

Chapter 4 describes two photoswitchable CD dimers tethered by a larger bis(phenylthienyl)ethene moiety. The bis(phenylthienyl)ethene tethers have been studied to achieve a more complete switching and stronger differences in binding properties between the two forms of the CD dimers, compared to the dithienylethene-tethered CD dimers discussed in Chapter 3. Apart from the photoswitchable moiety, the CD dimers were similar in structure to those described in Chapter 3, i.e. a short CD dimer with a directly coupled tether and a longer CD dimer in which propyl spacers were used. UV-vis spectroscopy showed that by irradiation of the CD dimers with UV light a nearly complete conversion from the open to the closed forms was achieved. For both CD dimers the photostationary states consisted of 8 % of the open and 92 % of the closed forms. Irradiation with visible light led to the complete conversion to the open forms. The binding properties of the two forms of the CD dimers have been investigated by calorimetric studies with TSPP. The most pronounced differences were observed for the short CD dimer, which gave a factor of 8 difference in binding affinity between the open and closed forms. This relatively

small difference, compared to the short dithienylethene-tethered CD dimer from Chapter 3, is due to a relatively strong complexation of TSPP by the closed form of the CD dimer. The enthalpy of binding TSPP by the closed form, which was considerably more exothermic than that of native CD, and CPK modeling, which showed that it was not possible for both cavities of the closed form to cooperate in binding TSPP, indicated that the large hydrophobic bis(phenylthienyl)ethene tether contributed to the binding process. This was corroborated by the thermodynamic parameters found for the longer CD dimer, which showed that the closed form had a stronger, more favorable enthalpy contribution in binding TSPP than the open form, despite the restricted tether flexibility. UV-vis spectroscopy experiments were used to demonstrate that the short CD dimer could be used for photocontrolled release and uptake of TSPP from solution.

Chapter 5 presents two alternative methods to achieve tunable binding. By metal complexation and partial protonation, defined states of ethylenediamine-tetraacetate- (EDTA-) tethered CD dimers have been accessed that differed in tether charge and flexibility. Also here a short CD dimer, with the EDTA tether directly coupled to the secondary rim of the CD cavities, and a long CD dimer, for which propyl spacers were used to couple the CD cavities to the EDTA moiety, have been studied. Calorimetric studies with charged porphyrin guests and the different states of the CD dimers indicated that both tether charge and flexibility strongly influenced the binding properties of the CD dimers, giving rise to large differences in binding affinity. Binding experiments with TSPP and the long EDTA-tethered CD dimer showed that attractive electrostatic interactions can lead to entropically more favorable binding as a consequence of more extensive desolvation of the complex formed. This resulted in a factor of 5 stronger complexation of the tetraanionic TSPP by the positively charged europium(III) complex of the longer CD dimer compared to the corresponding complexation by the negatively charged free ligand. No differences in binding affinity for the different forms of the short CD dimer were found, although also for this CD dimer trends in entropy and enthalpy values were observed indicative of (de)solvation effects. Binding experiments of the long EDTA-tethered CD dimer with the larger tetracationic *p-tert*-butylbenzyl-functionalized *p*-pyridylporphyrin (TBPYP) indicated that restricted tether flexibility can give rise to enthalpically less favorable binding due to a less effective cooperation between the two CD cavities of the CD dimer. TBPYP was bound a factor of 22 more strongly by the flexible

(negatively charged, mono-protonated) long CD dimer than the corresponding positively charged europium(III) complex. All forms of the short CD dimer were too short to effectively bind TBPYP in a divalent fashion.

In Chapter 6, multivalent binding in solution is correlated to multivalent binding at interfaces. The binding of a bis(adamantyl)-functionalized calix[4]arene guest by a CD dimer in solution, studied by calorimetry, has been compared to the corresponding binding of the guest at a CD self-assembled monolayer (SAM) on gold as studied by surface plasmon resonance spectroscopy. Both interactions were shown to be divalent; the enthalpy of binding for the guest-CD dimer interaction was twice that of a single adamantyl-CD interaction, and the interaction of the guest with the CD SAMs was stable towards rinsing with water, but could be disrupted by rinsing with (competing) CD solutions. The divalent binding of the guest at the CD interface gave an association constant of $\sim 1 \times 10^{10} \text{ M}^{-1}$, which was found to be three orders of magnitude stronger than the corresponding divalent binding of the guest to the CD dimer in solution. This difference in binding has been rationalized using a theoretical model, in which the divalent binding is interpreted as two consecutive intrinsic and independent monovalent binding events, i.e. an intermolecular interaction followed by an intramolecular binding event. The latter was accompanied by an effective concentration (C_{eff}) term, accounting for the increased probability of interaction, which governs the overall binding affinity. Modeling of C_{eff} for the intramolecular reactions revealed that at the CD SAMs, C_{eff} is over two orders of magnitude higher than in solution. The interaction of the divalent guest with the CD SAMs was sufficient to be applied in microcontact printing and dip-pen nanolithography for the creation of patterns of assemblies at the CD SAMs that were stable towards rinsing with water. Complete removal of patterns produced on hydroxyl-terminated layers upon rinsing with water indicated that the stability of the patterns on the CD SAMs was governed by specific host-guest interactions. The patterns on the CD SAMs were largely erased when washed with concentrated CD solutions, implying that the interactions are multivalent. With the use of dip-pen nanolithography, patterns of sub-100 nm resolution were created.

Chapter 7 describes CD monolayers on silicon oxide as an alternative interface for the complexation of multivalent guests. These monolayers enabled the visualization and study of multivalent CD host-guest interactions at interfaces with

fluorescence microscopy techniques. The monolayers were synthesized via a four-step synthesis route, leading to monolayers with a dense packing of CDs with their secondary side oriented to the solution. The CD monolayers on silicon oxide displayed all the characteristic features of the CD SAMs on gold. The binding constant of a bis(adamantyl)-functionalized fluorescent dye with CD monolayers on silicon oxide ($\sim 10^{10} \text{ M}^{-1}$) was of the same order as that of the divalent bis(adamantyl)-calix[4]arene with the CD SAMs on gold. With the use of microcontact printing and dip-pen nanolithography, patterns of fluorescent bis- and tetra(adamantyl)-functionalized dyes were created at the CD monolayers that were stable towards various rinsing procedures and could only be partly erased by rinsing with concentrated CD solutions. Patterns created on reference poly(ethylene glycol) monolayers were completely removed upon rinsing with water or buffer solutions, demonstrating the need for specific interactions to achieve stable patterns.

The results presented in this thesis illustrate the versatility of multivalency as a supramolecular tool in nanotechnology. The work on the tunable receptors demonstrates that, by controlling the extent of multivalency, it is possible to tune the interaction strength of an assembly, enabling externally controlled association and dissociation. The work performed on the CD monolayers shows that, in analogy with Nature, multivalency can be used for the formation of highly stable, yet reversible, assemblies at interfaces. Combined with lithographic techniques such as microcontact printing and dip-pen nanolithography this opens new approaches for the supramolecular patterning of interfaces. Taken together this thesis demonstrates the potential role of multivalency in molecular devices and supramolecular nanofabrication schemes.

Samenvatting

Dit proefschrift behandelt multivalente β -cyclodextrine- (CD-) gastheer-gast-interacties in oplossing en aan oppervlakken. In oplossing werd multivalentie gebruikt voor de ontwikkeling van sterk complexerende CD-dimeren. CD-dimeren met extern controleerbare complexeringseigenschappen werden verkregen door gebruik te maken van schakelbare eenheden die de twee CD-holtes met elkaar verbinden. Deze schakelbare eenheden maakten het mogelijk om met behulp van externe stimuli de relatieve oriëntatie van de twee CD-holtes van de CD-dimeren te controleren en daarmee de mate waarin gastmoleculen multivalent gecomplexeerd werden. Verschillende benaderingen voor de ontwikkeling van dergelijke schakelbare CD-dimeren staan beschreven in de hoofdstukken 3 t/m 5. Aan oppervlakken werden multivalente CD-gastheer-gast-interacties toegepast om gastmoleculen sterk en selectief te complexeren aan CD-monolagen. Deze CD-monolagen werden gebruikt als moleculaire printplaten, waarop met behulp van lithografische technieken patronen van multivalente, supramoleculaire complexen gecreëerd konden worden. Twee verschillende types moleculaire printplaten, gebaseerd op CD-monolagen op goud en glas, staan beschreven in de hoofdstukken 6 en 7.

In hoofdstuk 2 wordt multivalentie gedefinieerd en worden de karakteristieke eigenschappen van multivalente interacties beschreven. Een speciale sectie is gewijd aan multivalente CD-complexen. Er wordt duidelijk gemaakt dat de sterkte van multivalente interacties afhankelijk is van het aantal deelnemende individuele interacties en de sterkte daarvan. Daarnaast wordt getoond dat de stabiliteit van multivalente complexen sterk beïnvloed door de aanwezigheid van competitieve gastheren of gasten in oplossing. Deze aspecten van multivalentie vormen de basis voor het onderzoek beschreven in dit proefschrift en zijn in de hoofdstukken 3 t/m 7 op verschillende manieren benut om de stabiliteit van supramoleculaire systemen te controleren.

Hoofdstuk 3 behandelt twee dithienyletheen-gebrugde CD-dimeren die functioneren als receptormoleculen met lichtschakelbare bindingseigenschappen. De twee CD-dimeren verschillen qua koppeling van de CD-holtes aan de dithienyletheen-brug. Een kort CD-dimeer werd verkregen door directe koppeling van de secundaire zijdes van de CD-holtes met de dithienyletheen-eenheid. Een langer CD-dimeer werd

verkregen door gebruik te maken van een flexibele propylketen om de CD-holtes en de dithienyletheen-eenheid met elkaar te verbinden. Door bestraling met UV-licht was het mogelijk deze CD-dimeren te schakelen van een relatief flexibele open vorm naar een rigide gesloten vorm, waarbij de fotostationaire toestand voor beide CD-dimeren bestond uit 25 % van de open en 75 % van de gesloten vorm. De CD-dimeren konden volledig teruggeschakeld worden naar de open vorm door bestraling met zichtbaar licht ($\lambda > 460$ nm). De CD-dimeren toonden zelfs na herhaalde bestralingscycli geen tekenen van afbraak, hetgeen de uitstekende duurzaamheid van het schakelproces demonstreerde. Microcalorimetrie-studies met meso-tetrakis(4-sulfonatofenyl)-porfyrine (TSPP) als gastmolecuul toonden aan dat de bindingseigenschappen van de CD-dimeren afhankelijk waren van de toestand van de dithienyletheenbrug. Zo complexeerde de open vorm van het korte CD-dimeer TSPP 35 keer sterker dan de gesloten vorm. Op basis van de bindingsenthalpiën werd geconcludeerd dat de gesloten vorm van het korte CD-dimeer, in tegenstelling tot de open vorm, niet in staat was TSPP te complexeren in een effectieve, divalente wijze, waarbij beide CD-holtes volledig gebruikt worden voor het binden van het gastmolecuul. Computer-gemodelleerde complexen lieten zien dat de rigide gesloten dithienyletheen-eenheid de twee CD-holtes dusdanig van elkaar scheidt dat deze niet in staat zijn gezamenlijk TSPP te complexeren. De twee vormen van het langere CD-dimeer gaven geen verschillen in TSPP-bindingsaffiniteit. Voor zowel de open als de gesloten vorm werden bindingsconstanten gevonden gelijk aan die voor de complexering van TSPP door de open vorm van het korte CD-dimeer. De bindingsenthalpiën voor zowel de open als de gesloten vorm, beide twee keer de bindingsenthalpie gevonden voor de complexering van TSPP door niet-gemodificeerd CD, gaven aan dat beide vormen in staat zijn TSPP op een divalente wijze te complexeren. Computer-gemodelleerde complexen lieten zien dat de flexibele propylketens van het langere CD-dimeer in staat zijn de starheid, die het CD-dimeer wordt opgelegd in de gesloten vorm, te compenseren. Het verschil in bindingsaffiniteit tussen de open en gesloten vorm van het korte CD-dimeer maakte het mogelijk om, door middel van het schakelen met licht, gecontroleerd TSPP los te laten en op te nemen. Hierdoor werd het mogelijk extern de verhouding van gecomplexeerd en vrij TSPP in oplossing te reguleren.

Hoofdstuk 4 behandelt twee lichtschakelbare CD-dimeren met een langere bis(fenylthienyl)etheenbrug. De langere bis(fenylthienyl)etheenbrug is bestudeerd om een vollediger conversie van de open naar de gesloten vorm te bewerkstelligen en

om grotere verschillen in bindingseigenschappen tussen de open en gesloten vorm te verkrijgen in vergelijking met de dithienyletheen-gebrugde CD-dimeren uit hoofdstuk 3. Afgezien van de lichtschakelbare brug lijken deze CD-dimeren op de CD-dimeren beschreven in hoofdstuk 3; dat wil zeggen een kort CD-dimeer, waarbij de secundaire zijden van de CD-holtes direct gekoppeld zijn aan de bis(fenylthienyl)etheenbrug en een langer CD-dimeer, waarbij propylketens gebruikt zijn om de secundaire zijdes van de CD-holtes aan de lichtschakelbare eenheid te koppelen. UV-vis-spectroscopie toonde aan dat bestraling van deze CD-dimeren met UV-licht leidde tot een nagenoeg volledige omzetting van de open vormen naar de gesloten vormen, waarbij voor beide CD-dimeren de fotostationaire toestand bestond uit 8 % van de open en 92 % van de gesloten vorm. Bestraling met zichtbaar licht gaf een volledige conversie van de gesloten naar de open vorm. De bindingseigenschappen van de twee vormen van de CD-dimeren is bestudeerd met behulp van microcalorimetrie, waarbij TSPP als gastmolecuul gebruikt werd. Het korte CD-dimeer gaf het sterkste verschil in bindingsterkte, met een open vorm die TSPP een factor 8 sterker complexeerde dan de gesloten vorm. Het feit dat dit verschil in bindingssterkte relatief klein is in vergelijking met de verschillen gevonden voor het korte dithienyletheen-gebrugde CD-dimeer in hoofdstuk 3, was te wijten aan de relatief sterke bindingsaffiniteit van de gesloten vorm van het korte bis(fenylthienyl)etheen-gebrugde CD-dimeer voor TSPP. Op basis van de bindingsenthalpie voor de complexering van TSPP door het gesloten korte CD-dimeer (aanzienlijk sterker exotherm dan voor de complexering door niet-gemodificeerd CD) en CPK-modellen (die aantoonde dat de twee CD-holtes van het gesloten CD-dimeer niet konden samen werken in het complexeren van TSPP) werd geconcludeerd dat de grote hydrofobe bis(fenylthienyl)etheenbrug een bijdrage levert aan het bindingsproces. Dit werd bevestigd door de thermodynamische parameters gevonden voor de complexering van TSPP door het langere CD-dimeer. Deze toonden aan dat de gesloten vorm, ondanks de beperkte flexibiliteit van de brug tussen de twee CD-holtes, een sterkere, meer exotherme enthalpie-bijdrage had in de complexering van TSPP dan de open vorm. Met behulp van UV-vis-spectroscopie werd aangetoond dat het korte CD-dimeer gebruikt kon worden om TSPP los te laten en op te nemen door externe schakeling met licht.

Hoofdstuk 5 beschrijft twee alternatieve methoden om de bindingseigenschappen van CD-dimeren te controleren. Door middel van

metaalcomplexering en gedeeltelijke protonering werden een viertal gedefinieerde toestanden van ethyleendiaminetetraacetaat- (EDTA-) gebrugde CD-dimeren verkregen, die verschilden qua lading en flexibiliteit van de EDTA-brug. Ook hier werden een kort CD-dimeer, waarbij de secundaire zijde van de CD-holtes direct gekoppeld waren aan de EDTA-eenheid, en een lang CD-dimeer, waarbij gebruik werd gemaakt van propylketens om de secundaire zijdes van de CD-holtes met de EDTA-eenheid te verbinden, bestudeerd. Microcalorimetrie-studies met de verschillende toestanden van de CD-dimeren en geladen, op porfyriene-gebaseerde, gastmoleculen gaven aan dat zowel de lading als de flexibiliteit van de EDTA-brug de bindingseigenschappen van de CD-dimeren sterk beïnvloeden, met als gevolg sterke verschillen in bindingssterktes. Bindingsstudies met TSPP toonden aan dat attractieve interacties kunnen leiden tot entropisch gunstigere complexering als gevolg van een vollediger desolvatatie van het gevormde complex. Voor het lange CD-dimeer resulteerde dit een factor 5 sterkere binding van het tetra-anionische TSPP door het positief geladen europium(III)-complex in vergelijking met het negatief geladen vrije ligand van hetzelfde CD-dimeer. Het korte CD-dimeer gaf geen dussdanige verschillen in bindingssterkte, al werden ook voor dit CD-dimeer trends in entropie en enthalpie waargenomen die duiden op (de)solvatatie-effecten. Bindingsstudies met het lange EDTA-gebrugde CD-dimeer en de grotere tetrakationische *p*-tert-butylbenzyl-gefunctionaliseerde *p*-pyridylporfyriene (TBPYP) toonden aan dat beperking van de brugflexibiliteit kan leiden tot enthalpisch minder gunstige binding als gevolg van een minder effectieve samenwerking tussen de twee CD-holtes van het CD-dimeer in het complexeren van gastmoleculen. Zo bond het flexibele (negatief geladen, mono-geprotoneerde) lange CD-dimeer TBPYP 22 keer sterker dan het corresponderende positief geladen europium(III)-complex van het CD-dimeer. Geen van de vormen van het korte EDTA-gebrugde CD-dimeer bleek lang genoeg om TBPYP op een effectieve, divalente wijze te binden.

In hoofdstuk 6 worden multivalente interacties in oplossing vergeleken met multivalente interacties aan oppervlakken. De complexering van een bis(adamantyl)-gefunctionaliseerd calix[4]areen gastmolecuul door een CD-dimeer in oplossing (bestudeerd met behulp van microcalorimetrie) is vergeleken met de corresponderende complexering van het gastmolecuul aan een zelf-organiserende monolaag (SAM) van CD op goud (bestudeerd met behulp van oppervlakte-plasmonresonantie spectroscopie). Beide interacties waren divalent; de bindingsenthalpie voor

de CD-dimeer-gast interactie was twee keer de bindingsenthalpie gevonden voor de monovalente interactie van de gast met ongemodificeerd CD en de interactie van de gast met CD-SAMs was stabiel onder blootstelling aan grote hoeveelheden water, maar labiel wanneer blootgesteld aan competitieve, geconcentreerde CD-oplossingen. Voor de divalente binding van het gastmolecuul aan de CD-SAMs werd een bindingsconstante ($\sim 1 \times 10^{10} \text{ M}^{-1}$) gevonden die drie ordegrottes sterker was dan voor de corresponderende divalente interactie tussen het gastmolecuul en het CD-dimeer in oplossing. Dit verschil in bindingssterkte werd verklaard met behulp van een theoretisch model, waarin de divalente interactie werd opgedeeld in twee opeenvolgende, intrinsieke en onafhankelijke, monovalente interacties: een intermoleculaire gevolgd door een intramoleculaire interactie. Deze laatste werd afhankelijk verondersteld van een effectieve concentratie (C_{eff}) die het effect van toegenomen waarschijnlijkheid van interactie op de bindingssterkte meeneemt. Theoretische berekeningen van C_{eff} gaven aan dat deze voor CD-SAMs twee ordegrottes hoger is dan in oplossing. De binding van het divalente gastmolecuul aan de CD-SAMs bleek voldoende sterk om het gastmolecuul in microcontact-drukken en dip-pen-nanolithografie te kunnen toepassen om zo patronen van complexen op CD-SAMs te creëren die stabiel zijn tegen wassen met water. Het feit dat soortgelijke patronen op hydroxyl-getermineerde monolagen wel verwijderd konden worden door te wassen met water bevestigde dat de stabiliteit van de patronen bepaald werd door specifieke gastheer-gast-interacties. De patronen op de CD-SAMs konden alleen gedeeltelijk verwijderd worden door te wassen met geconcentreerde CD-oplossingen, wat aangaf dat de interacties multivalent waren. Met behulp van dip-pen-nanolithografie werden patronen met sub-100-nm-resolutie gecreëerd.

Hoofdstuk 7 beschrijft CD-monolagen op siliciumoxide als een alternatief oppervlak voor de complexering van multivalente gasten. Deze monolagen maken de studie en visualisatie van multivalente CD-gastheer-gast-interacties met behulp van fluorescentie-microscopie mogelijk. Een vier-stapssyntheseroute gaf dichtgepakte CD-monolagen, waarbij de secundaire zijde van de CD-holtes naar de oplossing gericht waren. Qua pakking en bindingseigenschappen waren deze CD-monolagen op siliciumoxide vergelijkbaar met de CD-SAMs op goud zoals beschreven in hoofdstuk 6. De bindingsconstante van een bis(adamantyl)-gefunctionaliseerd fluorescent kleurstofmolecuul en de CD-monolagen op siliciumoxide ($\sim 10^{10} \text{ M}^{-1}$) was van

dezelfde orde-grootte als die van het divalente bis(adamantyl)-gefunctionaliseerde calix[4]areen met de CD-SAMs op goud. Met behulp van microcontact-drukken en dip-pen-nanolithografie werden patronen van fluorescente bis- en tetrafunctionaliseerde kleurstofmoleculen gecreëerd die stabiel waren tegen verschillende wasprocedures en alleen gedeeltelijk verwijderd konden worden door te wassen met geconcentreerde CD-oplossingen. Patronen gemaakt op poly(ethyleenglycol)-monolagen konden geheel verwijderd worden door te wassen met water of bufferoplossingen, hetgeen aantoonde dat specifieke interacties noodzakelijk zijn voor het verkrijgen van stabiele patronen.

Het onderzoek beschreven in dit proefschrift illustreert de veelzijdigheid van multivalentie en de mogelijkheden voor praktische toepassing van multivalentie binnen de nanotechnologie. Het werk aan de schakelbare receptoren laat zien dat controle over de mate van multivalentie het mogelijk maakt de interactiesterkte van een complex te controleren, waardoor extern controleerbare associatie en dissociatie bewerkstelligd kan worden. Het werk aan de CD-monolagen toont dat, in navolging van natuurlijke interacties, multivalentie gebruikt kan worden voor de vorming van zeer stabiele, maar reversibele complexen aan oppervlakken. In combinatie met lithografische technieken, zoals microcontact-drukken en dip-pen-nanolithografie, biedt dit nieuwe mogelijkheden voor het supramoleculair patroneren van oppervlakken. Tezamen demonstreren deze studies de potentiële rol van multivalente interacties in moleculaire systemen en supramoleculaire nanofabricage.

Dankwoord

Met het schrijven van dit dankwoord leg ik mij erbij neer dat mijn promotieonderzoek nu dan toch echt tot een einde gekomen is. Het verschijnen van dit proefschrift vormt de afronding van vier bijzonder leerzame en plezierige jaren, waarin ik creatief onderzoek heb kunnen doen binnen een geweldige groep. Op deze plaats wil ik graag een aantal mensen bedanken die dit mogelijk gemaakt hebben.

Op de eerste plaats wil ik mijn promotor David Reinhoudt bedanken. David, jij bent degene die mij, na mijn afstuderen, de mogelijkheid gaf om in deze groep te promoveren en hebt me daarbij alle vrijheid gegeven die een promovendus zich kan wensen. Daarnaast heb je er altijd voor gezorgd dat het mij aan niets ontbrak; de researchfaciliteiten binnen MESA⁺ zijn nagenoeg onbeperkt, ik heb op diverse conferenties mijn werk mogen presenteren en door de (werk)besprekingen die we hadden kwam ik nooit zonder (wilde) ideeën te zitten. Ik heb veel respect voor de wijze waarop je, ondanks jouw drukke bestaan, toch altijd tijd kon vrijmaken voor zorgvuldige correcties en aanvullingen op mijn publicaties en proefschrift.

Met mijn copromotor en dagelijks begeleider Jurriaan Huskens heb ik het al net zo goed getroffen. Jurriaan, vanwege jouw welhaast alles-omvattende kennis keek ik al vrij snel tegen je op en na vier jaren, waarin je me ontzettend veel geleerd hebt op het gebied van fysische chemie, modelleren, het constructief aanpakken van onderzoek, rikken en weet ik al wat niet meer, ben ik bang dat het nog niet veel anders is. Naast het enthousiasme en geduld dat je voor mij had, dank ik je voor jouw spontane bulderende lach.

De kaft van dit proefschrift, met enkel mijn naam, verbloemt dat de inhoud veelal voortgekomen is uit samenwerkingen. Zonder de inbreng van de volgende personen was dit proefschrift niet hetzelfde geweest.

Voor de grootschalige synthese van de lichtschakelbare CD-dimeren, beschreven in de hoofdstukken 3 en 4, ben ik mijn ijverige HLO-studente Amela Juković zeer dankbaar. Bart Nelissen van de Universiteit Nijmegen dank ik voor zijn hulp bij de hoge-druk-reacties. Voor de spectroscopische metingen aan de lichtschakelbare CD-dimeren kon ik altijd terecht bij de groep van prof. Ben Feringa en dr. Jan van Esch. Ik heb de samenwerking met de Universiteit Groningen zeer gewaardeerd en ik wil in het bijzonder Linda Lucas, Jaap de Jong en Ralph Hania

bedanken. Zij zorgden dat ik altijd wel een plekje kon krijgen op de UV-vis-spectrofotometer en waren altijd bereid mijn lange e-mails met vragen over dithienylethenen te beantwoorden. SMCT's kristallenbakker en grafisch ontwerper Fijs van Leeuwen dank ik voor het medeontwerpen van een Chemistry-cover en voor het kweken van het dithienyletheenkristal, Huub Kooijman en Anthony Spek voor het oplossen van deze structuur.

Voor het onderzoek beschreven in hoofdstuk 5 heb ik mezelf wat synthese kunnen besparen door zeer kritisch de nalatenschap van oudgedienden Roberto Fiammengo en Jasper Michels te doorzoeken. Laatstgenoemde vormde de afgelopen vier jaar samen met Menno de Jong een welkome vraagbaak voor alles wat met CD-chemie te maken had. Mijn dank heren!

The work described in Chapter 6 is the result of fruitful collaborations with the group of prof. Rocco Ungaro and prof. Alessandro Casnati from the Università degli Studi di Parma and prof. Vancso's Materials Science Technology of Polymers group of the University of Twente. I thank Andrea Sartori and Susanna Del Ciotto for their synthetic contributions, and I am indebted to Barbara Dordi for the hours she spent behind the AFM. Thanks also to Holger Schönherr and Tommaso Auletta for the discussions concerning the work described in Chapter 6 and to the new CD-generation, Christiaan Bruinink, Olga Crespo, Manon Ludden and Christian Nijhuis, for the nice collaborations and discussions on the molecular printboard project.

Aan het onderzoek beschreven in Hoofdstuk 7 heeft al net zo'n bont genootschap gewerkt. HLO-student Hans Beijleveld was zo vriendelijk zijn afstudeerperiode te wijden aan de synthese van de adamantyl-getermineerde PPI-wedges. CT-student Jurjen ter Maat gebruikte zijn capita selecta voor een twee maanden durend proefabonnement SMCT en volbracht de synthese van de bis(adamantyl)-gefunctionaliseerde fluorescente wedges. Veel dank ben ik verschuldigd aan Steffen Onclin, die net als ik wel brood zag in de CD-monolagen op glas. Steffen, de tijd en moeite die jij hebt gestoken in de vele printexperimenten en het synthetiseren van de reactieve monolagen op siliciumoxide waardeer ik enorm. Henk-Jan van Manen dank ik voor mijn inwijding in de wereld van de confocale microscopie. I am grateful to Mária Péter who wrote the fluorescent "X" depicted in Chapter 7. Maria, with your enthusiasm it should not take long before the first full-color, fluorescent MESA⁺ logo is written. Voor het terugvinden van de minieme "X" was de hulp van de groep van prof. Niek van Hulst en diens microscopen

noodzakelijk en van één persoon in het bijzonder: Jacob Hoogenboom, de man die in staat is om samples met een vinger systematisch enkele tientallen nanometers te verschuiven.

I am grateful to Bart Jan Ravoo and Becky Zimmerman for carefully proofreading my Thesis. Becky, as a sign of gratitude, I will not cite your memory aid for when to use “-ly” here. Francesca Corbellini’s (critical) remarks and spiritual murmuring/singing during our imprisonment in room 1717 contributed to the quality of this thesis and made the long writing period an enjoyable time. Mille grazie.

Een speciaal woord van dank aan de mensen die dagelijks zorgden dat het onderzoek een beetje vlot kon verlopen. Mijn waardering voor de altijd vriendelijke en snelle amaneusele ondersteuning van Marcel de Bruine en Marc Brouwer, de welkome geel, danwel roze, gemarkeerde massapieken van Thieme Stevens en Roel Fokkens en de scansvretende NMR-spectra gemeten door Bianca Snellink-Ruël en Hannie Visser. Carla van der Ploeg en Izabel Katalanc dank ik voor de broodnodige eerste hulp bij administratieve zaken.

Partly responsible for the pleasure with which I faced the many oversized columns in my fume-hood is the good atmosphere within the SMCT group, and lab 2906 in particular. My dear colleagues and friends, it goes too far to list the names of all of you and it would not be correct to name only a few. I will leave with only good memories and will miss the daily laughs and weekly soccer games. Thank you all!

I thank my paranimfen Tommaso Auletta and Steffen Onclin for their friendship, their contributions to my thesis and their willingness to support me during my defense.

Tenslotte wil ik nog een drietal mensen bedanken die een speciale plaats innemen in mijn leven. Vader en moeder, ik dank jullie voor de onverminderde steun die jullie me tijdens al die jaren studie hebben gegeven, ondanks het feit dat de vervreemding voor jullie met de jaren groter werd. Ik ben bang dat dit proefschrift wat dat betreft niet veel zal verduidelijken, maar ik hoop dat jullie, net als ik, trots zullen zijn op de afronding hiervan. Lieve Jantsje, jij mag dan als laatste genoemd worden in dit dankwoord, jij staat voor mij boven alles en iedereen. Jij was de reden dat ik aan het einde van iedere dag met een glimlach naar huis terug ging en als het aan mij ligt houden we dat samen nog een aantal decennia zo vol.

Alart Mulder

curriculum vitae

Alart Mulder werd geboren op 15 september 1976 te Meppel. Na het behalen van zijn VWO-diploma aan de openbare scholengemeenschap “de Groene Driehoek” te Hoogeveen, begon hij in 1994 aan de studie chemische technologie aan de Universiteit Twente. In 1999 studeerde hij af binnen de vakgroep Supramoleculaire Chemie en Technologie onder leiding van prof. dr. ir. D. N. Reinhoudt. Zijn afstudeerwerk betrof de synthese van metaal-complexerende dendrimeren voor toepassing in radiofarmaceutica. Vanaf januari 2000 verrichtte hij zijn promotieonderzoek binnen dezelfde vakgroep onder de supervisie van prof. dr. ir. D. N. Reinhoudt en dr. ir J. Huskens. De resultaten van dit promotieonderzoek zijn beschreven in dit proefschrift. Vanaf 17 mei zal hij, onder leiding van prof. dr. R. Tampé, werkzaam zijn als post-doc aan het Institut für Biochemie van de Johann Wolfgang Goethe-Universität in Frankfurt am Main, Duitsland.